

Quantitative Modeling of Credit Derivatives

Yu Hang Kan

Submitted in partial fulfillment of the
requirements for the degree
of Doctor of Philosophy
in the Graduate School of Arts and Sciences

COLUMBIA UNIVERSITY

2011

©2011

Yu Hang Kan

All Rights Reserved

ABSTRACT

Quantitative Modeling of Credit Derivatives

Yu Hang Kan

The recent financial crisis has revealed major shortcomings in the existing approaches for modeling credit derivatives. This dissertation studies various issues related to the modeling of credit derivatives: hedging of portfolio credit derivatives, calibration of dynamic credit models, and modeling of credit default swap portfolios.

In the first part, we compare the performance of various hedging strategies for index collateralized debt obligation (CDO) tranches during the recent financial crisis. Our empirical analysis shows evidence for market incompleteness: a large proportion of risk in the CDO tranches appears to be unhedgeable. We also show that, unlike what is commonly assumed, dynamic models do not necessarily perform better than static models, nor do high-dimensional bottom-up models perform better than simpler top-down models. On the other hand, model-free regression-based hedging appears to be surprisingly effective when compared to other hedging strategies.

The second part is devoted to computational methods for constructing an arbitrage-free CDO pricing model compatible with observed CDO prices. This method makes use of an inversion formula for computing the aggregate default rate in a portfolio from expected tranche notionalss, and a quadratic programming method for recovering expected tranche notionalss from CDO spreads. Comparing this approach to other calibration methods, we find that model-dependent quantities such as the forward starting tranche spreads and jump-to-default ratios are quite sensitive to the

calibration method used, even within the same model class.

The last chapter of this dissertation focuses on statistical modeling of credit default swaps (CDSs). We undertake a systematic study of the univariate and multivariate properties of CDS spreads, using time series of the CDX Investment Grade index constituents from 2005 to 2009. We then propose a heavy-tailed multivariate time series model for CDS spreads that captures these properties. Our model can be used as a framework for measuring and managing the risk of CDS portfolios, and is shown to have better performance than the affine jump-diffusion or random walk models for predicting loss quantiles of various CDS portfolios.

Keywords: credit derivatives, credit default swaps, index default swaps, collateralized debt obligations, default intensity, pricing, hedging, inverse problem, model calibration, statistical modeling

Contents

List of Tables	vi
List of Figures	ix
Acknowledgments	xv
Chapter 1: Introduction	1
1.1 Credit derivatives	1
1.1.1 Commonly traded credit derivatives	3
1.1.2 Valuation and quotation	7
1.1.3 Economic benefits	8
1.2 Quantitative modeling of credit derivatives and the financial crisis	9
1.2.1 Risk management of portfolio credit derivatives	9
1.2.2 Implementation of dynamic credit models	11
1.2.3 Central clearing and statistical modeling of CDS	12
1.3 Comparison of strategies for hedging index CDO tranches	13
1.4 A non-parametric approach for recovering default intensities implied by CDO spreads	17
1.5 Statistical modeling of credit default swap portfolios	20
1.6 Publications	23

Chapter 2: Dynamic hedging of portfolio credit derivatives	24
2.1 Credit derivatives	27
2.1.1 Credit default swaps	28
2.1.2 Index default swap	29
2.1.3 Collateralized debt obligations	29
2.2 Data analysis	30
2.2.1 Co-movements in CDSs and CDO tranches	30
2.2.2 Impact of defaults on credit spreads	32
2.3 Models for portfolio credit derivatives	33
2.3.1 Gaussian copula model	34
2.3.2 Affine jump-diffusion model	35
2.3.3 Local intensity models	36
2.3.4 Bivariate spread-loss model	36
2.3.5 Calibration results	38
2.4 Hedging strategies	39
2.4.1 Delta hedging of single-name spread movements	39
2.4.2 Delta hedging of index spread movements	40
2.4.3 Delta and gamma hedging of index spread movements	42
2.4.4 Hedging parallel shifts in correlations	44
2.4.5 Hedging default risk	45
2.4.6 Variance minimization	46
2.4.7 Regression-based hedging	50
2.5 Empirical performance of hedging strategies	51
2.5.1 Does delta hedging work?	51
2.5.2 Does gamma hedging improve the performance?	52
2.5.3 Can hedging parallel shifts in correlations improve the performance?	53

2.5.4	Do dynamic models have better hedging performance than static models?	54
2.5.5	Do bottom-up models perform better than top-down models?	55
2.5.6	How does model-based hedging compare to regression-based hedging?	56
2.5.7	Performance on credit event dates	56
2.6	Conclusion	58
2.7	Variance-minimizing hedge and Galtchouk-Kunita-Watanabe decomposition	59
2.8	Derivation of the variance-minimizing hedge ratio	61
2.8.1	Proof of Proposition 2.1	61
2.8.2	Proof of Proposition 2.2	63
Chapter 3: Default intensities implied by CDO spreads: inversion formula and model calibration		66
3.1	An inversion formula for the local intensity function	69
3.1.1	Local intensity function	69
3.1.2	Expected tranche notional	71
3.1.3	Inversion formula and Markovian projection	72
3.2	Non-parametric estimation of the local intensity function	75
3.2.1	CDOs and expected tranche notional	76
3.2.2	Recovering expected tranche notional via quadratic programming	77
3.2.3	Numerical issues	79
3.2.4	Calibration algorithm for the local intensity function	80
3.2.5	Arbitrage opportunities when using base-correlation interpolation	81
3.3	Application to iTraxx tranches	83
3.3.1	Local intensity functions	84
3.3.2	Stability analysis	87
3.3.3	Marginal distributions and expected losses	87

3.3.4	Forward starting tranche spreads	89
3.3.5	Jump-to-default ratios	90
3.4	Local intensity function implied by credit portfolio loss models	90
3.4.1	Herbertsson model	92
3.4.2	Bivariate spread-loss model	92
3.4.3	Shot-noise model	94
3.4.4	Gaussian and Student-t copula models	95
3.4.5	Affine jump-diffusion model	97
3.5	Conclusion	98
3.6	Proofs	99
3.6.1	Proof of Property 3.1	99
3.6.2	Proof of Theorem 3.1	99
3.6.3	Proof of Proposition 3.1	100
3.6.4	Existence of arbitrage in the base correlation model	101
3.7	Matrix representation of constraints	103
3.7.1	Pricing constraints	103
3.7.2	Relations in Condition 3.1	106
3.8	Laplace transform of cumulative portfolio default intensity for shot-noise model . . .	108
Chapter 4: Statistical modeling of credit default swap portfolios		110
4.1	Data	114
4.2	Stylized properties of CDS spreads	117
4.2.1	Stationarity and unit root tests	117
4.2.2	Linear serial dependence	118
4.2.3	Heavy tails	120
4.2.4	Nonlinear serial dependence	121

4.2.5	Absence of correlation between spread returns and changes in spread volatility	122
4.2.6	Heavy-tailed conditional distributions	124
4.2.7	Positive serial dependence in extreme values	125
4.2.8	Co-movements in CDS spreads	129
4.2.9	Principal component analysis	132
4.2.10	Spread movements during credit events	136
4.3	Comparison with affine jump-diffusion models	139
4.3.1	A simulation study	139
4.3.2	Absence of serial dependence	141
4.3.3	Distributional properties of CDS spread returns	141
4.3.4	Co-movements in CDS spread returns	142
4.3.5	Principal components of CDS spread moves	142
4.3.6	Goodness-of-fit vs statistical properties	143
4.4	A heavy-tailed multivariate time series model for CDS spreads	144
4.4.1	A heavy-tailed multivariate AR-GARCH model	144
4.4.2	Parameter estimation	145
4.4.3	Reproducing stylized properties of CDS spreads	148
4.5	Application: estimating loss distributions for CDS portfolios	149
4.5.1	Models for CDS portfolios	150
4.5.2	Backtesting	153
4.6	Moment generating function for affine jump diffusion process	160
4.7	CDS spread simulation under affine jump-diffusion model	161
4.8	Estimation of the affine jump-diffusion model from CDS spread time series	163
Bibliography		168

List of Tables

2.1	Conditional correlations between daily spread returns of the index and tranche [10%, 15%] show evidence of a common heavy-tailed factor.	31
2.2	Daily spread returns on the next business day after Fannie Mae/Freddie Mac (8 September, 2008) and Lehman Brothers (16 September, 2008) credit events, normalized by unconditional sample standard deviations.	33
2.3	Relative calibration error (RMSE), as a percentage of market spreads.	38
2.4	Overview of hedging strategies.	52
2.5	Hedging tranches for gamma hedging strategy.	53
3.1	Upfront payments of 5-year iTraxx IG CDO tranches with 100bps periodic spread. Pricing method: one-factor Gaussian copula model with linearly interpolated base correlations. . . .	83
3.2	Calibrated CDO tranche spreads of 5Y iTraxx Europe IG Series 6 on 20 September 2006 and Series 9 on 25 March 2008. Quotes are given in bps except for equity tranches which are quoted as upfront in percent with 500bps periodic coupons.	85
3.3	Frobenius norm of the changes in the local intensity function with respect to 1% proportional increase in the CDO spreads. Data: 5Y iTraxx Europe IG S6 on 20 September 2006 and S9 on 25 March 2008.	87
3.4	Spreads of forward starting tranches which start in 1 year and mature 3 years afterwards. Data: 5Y iTraxx Europe IG S6 on 20 September 2006 and S9 on 25 March 2008.	89
3.5	Model uncertainty ratio of the forward starting tranche spreads.	90

3.6	Jump-to-default ratios computed from the calibrated local intensity functions. Data: 5Y iTraxx Europe IG S6 on 20 September 2006 and S9 on 25 March 2008.	91
3.7	Calibration of different models to 5Y iTraxx Europe IG Series 9 tranche spreads on 25 March 2008. Quotes are given in bps except for equity tranches which are quoted as upfront in percent with 500bps periodic coupons.	92
4.1	Percentiles of the daily profit-and-loss (percentage of the total portfolio notional value) of an equally weighted credit portfolio consisting of the 5-year CDS written on the constituents in CDX.NA.IG.12.	111
4.2	Distribution of obligors in terms of sectors, Standard and Poor's credit ratings and number of available daily observations.	115
4.3	Summary statistics of 5-year CDS spreads (daily observations).	116
4.4	Summary statistics of daily spread returns.	117
4.5	Number of obligors that reject the null hypothesis of Augmented Dickey-Fuller (ADF) test, reject the null hypothesis of Phillips-Peron (PP) test and cannot reject the null hypothesis of Kwiatkowski, Phillips, Schmidt and Shin (KPSS) test at 95% confidence level for (1) CDS spreads and (2) spread returns time series. CDS spreads and spread returns are observed at 1- and 5-day time interval.	118
4.6	Autocorrelation coefficients of 1, 5 and 10-day spread returns. Ljung-Box test statistics and p-values (in brackets) for 5, 10 and 20 lags.	119
4.7	Number of obligors that appear to have positive or negative slopes at 95% confidence level in the regression of realized volatility daily returns against CDS spread daily returns. Realized volatilities are computing using 5, 10, 20, 50-day rolling windows.	124
4.8	Average R^2 , across all sample obligors, of the OLS regression of realized volatility daily returns against CDS spread daily returns.	124
4.9	Percentage of variance that can be explained by the principal components. 112 obligors in 2005-07 period and 123 obligors in 2007-09 period. Data series: unconditional CDS spread daily returns.	133
4.10	Percentage of variance that can be explained by the principal components. 112 obligors in 2005-07 period and 123 obligors in 2007-09 period. Data series: conditional spread daily returns from ARMA-GARCH models.	133

4.11	BIC of the PC factors fitted to (1) normal, (2) Student t, (3) double exponential, (4) normal inverse Gaussian and (5) stable distribution. Lowest BIC among the distributions is indicated by *	135
4.12	The three largest values of the first principal component factor (common factor) in 2005-07 and 2007-09.	136
4.13	The three smallest values of the first principal component factor (common factor) in 2005-07 and 2007-09.	136
4.14	Highlights of credit events in 2008-09. From left to right: the event date or the next business day after the event; description of the events; the CDX.NA.IG series that the obligors belong to; first principal component factor values.	138
4.15	Percentage of variance that can be explained by the principal components. Data: simulated CDS speards based on affine jump-diffusion model.	143
4.16	Estimated parameters for the MAG model. Values in brackets are standard errors of the estimators.	148
4.17	Empirical exceedance probabilities: percentage of trading days which have losses larger than the 99% VaR. Portfolio type: protection sellers (short), protection buyers (long). Models: affine jump-diffusion model (AJD), random walk model (RW), heavy-tailed multivariate AR-GARCH model (MAG).	155
4.18	Test for accuracy of loss quantile estimation: percentage of portfolios that have less than 1 or more than 7 (resp. less than 1 or more than 6) exceedances in 2005-07 (resp. 2007-09), i.e. which reject the null hypothesis that the exceedance probability is equal to 1% under the Kupiec test at 95% confidence level.	155
4.19	Test for autocorrelated exceedances: percentage of portfolios which reject the null hypothesis that the exceedance sequence ($1_{\{L_t > VaR_t\}}$) is serially uncorrelated, by using the Ljung-Box test at 95% confidence level.	158
4.20	Average relative shortfall deviation (4.13) for CDS portfolios.	160
4.21	Test for accuracy of expected shortfall estimation: percentage of portfolios which reject the null hypothesis that expected shortfall residual (4.14) has zero mean at 95% confidence level. Data: 2005-09.	160

List of Figures

1.1	Outstanding notional value and gross market value of credit default swaps. Source: the Bank of International Settlements.	2
1.2	Cashflows of a credit default swap. Solid line represents the premium payment from the protection buyer and dashed line represents default payment from the protection seller. . . .	3
1.3	5-year CDS par spreads and CDS spread daily log return of MetLife.	4
1.4	Cashflows of an index default swap. Solid line represents the premium payment from the protection buyer and dashed line represents default payment from the protection seller. . . .	4
1.5	5-year index par spreads and index spread daily log return of CDX.NA.IG on-the-run series.	5
1.6	Standard CDO tranche subordination of the CDX North America Investment Graded index.	6
1.7	Cashflows of a CDO tranche. Solid line represents the premium payment from the protection buyer and dashed line represents default payment from the protection seller. L_t is the cumulative portfolio loss at default time and LGD stands for loss given default.	7
1.8	5-year par spreads and spread daily log return of CDX.NA.IG series 10 tranche [3%,7%]. . .	7
1.9	Evidence of heavy-tailed distribution and large co-movements of CDS spreads. Left: QQ-plot for 5-year CDS spread daily log return of MetLife. Right: 5-year CDS spread daily log return of MetLife vs First Energy.	13
2.1	Left: 5Y CDX.NA.IG.10 index and tranche [10%, 15%] spreads. Right: 5Y CDS spreads of IBM and Disney Corp. (DIS)	30

2.2	Tranche [10%, 15%] daily spread returns versus index daily spread returns and IBM CDS daily spread returns. Crosses represent data points where spread returns have the same signs (movements in the same direction), and circles represent data points where spread returns have opposite signs (movements in opposite directions).	32
2.3	Index spread-deltas. Data: CDX.NA.IG.S10 on 25 March 2008.	42
2.4	Values of gammas $\Gamma_{gc}^{[a,b]}(t)$ for [0%, 3%] and [3%, 7%] CDX tranches. Each point represents one day in the sample.	43
2.5	Jump-to-default ratios. Data: CDX.NA.IG.S10 on 25 March 2008. Ratios of Gaussian copula model and affine jump-diffusion model are computed by assuming IBM defaults.	46
2.6	Variance-minimization hedge ratios. Data: CDX.NA.IG.S10 on 25 March 2008.	50
2.7	Comparison among delta hedging strategies based on the Gaussian copula model.	52
2.8	Comparison among delta and gamma hedging strategies.	53
2.9	Comparison between delta hedging and the addition of hedging parallel shifts in compound correlations.	54
2.10	Comparison between delta hedging under the static Gaussian copula model and the dynamic affine jump-diffusion model.	55
2.11	Comparison of top-down and bottom-up hedging.	56
2.12	Comparison among top-down, bottom-up and regression-based hedging.	57
2.13	Comparison of strategies on the next business day after Fannie Mae/Freddie Mac (8 September 2008) and Lehman Brothers (16 September 2008) credit events.	57
3.1	Application of the inversion formula to recover the local intensity function.	68
3.2	Base correlations of one-factor Gaussian copula model. Data: 5Y iTraxx Europe IG S9 on 25 March 2008.	83
3.3	Local intensity functions implied from 5Y iTraxx Europe IG tranche spreads using the quadratic programming method (Algorithm 2) Left: S6 on 20 September 2006. Right: S9 on 25 March 2008.	85
3.4	Local intensity functions implied from 5Y iTraxx Europe IG tranche spreads using the a parametric model [60]. Left: S6 on 20 September 2006. Right: S9 on 25 March 2008.	86

3.5	Local intensity functions implied from 5Y iTraxx Europe IG tranche spreads using a non-parametric entropy minimization method [28]. Left: S6 on 20 September 2006. Right: S9 on 25 March 2008.	86
3.6	Marginal distribution at year 1 and year 4, truncated up to 20 defaults. Data: 5Y iTraxx Europe IG S9 on 25 March 2008.	88
3.7	Term structure of the differences in the expected loss $E(L_T) - E(L_{T-0.25})$. Data: 5Y iTraxx Europe IG S9 on 25 March 2008.	88
3.8	Local intensity functions implied by credit portfolio loss models. Data: 5Y iTraxx Europe IG S9 on 25 March 2008.	93
3.9	Change of the local intensity function implied by bivariate spread-loss model with respect to a small increase of the risk factor value Y_0 at time 0.	94
4.1	5-year CDS spreads (left) and daily spread returns (right) of Conoco Philips.	116
4.2	Sample autocorrelation function of daily spread returns in 2005-07 and 2007-09. Obligors: Conoco Philips, Eastman Chemical and First Energy . The 95% confidence interval bounds are computed under the hypothesis that the time series is a sequence of i.i.d. random variables.	119
4.3	Number of obligors whose spread returns have statistically significant positive and negative autocorrelations at each lag at 95% confidence level. The critical values for statistical testing is computed under the hypothesis that the time series is a sequence of i.i.d. random variables.	120
4.4	Quantile plots of 1-day spread returns of Conoco Philips vs normal distribution.	121
4.5	Hill estimators for the tail indices of CDS spread daily returns. The number observations for estimation is equal to 2.5% of the sample size.	121
4.6	Sample autocorrelation function of daily absolute spread returns in 2005-07 and 2007-09. Obligors: Conoco Philips, Eastman Chemical and First Energy . The 95% confidence interval bounds are computed under the hypothesis that the time series is a sequence of i.i.d. random variables.	122
4.7	Number of obligors whose absolute spread returns have statistically significant positive and negative autocorrelations at each lag at 95% confidence level. The critical values for statistical testing is computed under the hypothesis that the time series is a sequence of i.i.d. random variables.	123
4.8	Daily spread returns vs 20-day realized volatility returns of Conoco Philips.	124

4.9	Quantile plots of Conoco Philips conditional spread returns vs normal distribution.	125
4.10	Hill estimators for the tail indices of conditional spread returns from ARMA-GARCH models fitted to daily spread returns. The number observations for estimation is equal to 2.5% of the sample size.	126
4.11	Number of obligors whose 95% confidence interval for the Hill estimator contains α . Data series: conditional spread returns from ARMA-GARCH models.	126
4.12	Empirical extremograms for daily spread returns of Eastman Chemical in 2005-07 (top) and 2007-09 (bottom). For the left tail estimates (resp. right tail estimates), threshold a_m is equal to 5% (resp. 95%) quantile of the sample. Blue solid line is the 95% confidence bound constructed from randomly permuted data series. Blue dotted line is equal to 5%, which is the theoretical value for an independent series.	128
4.13	Number of obligors in which the 95% confidence intervals for the empirical extremograms do not contain zero. The confidence intervals are computed from asymptotic normality.	128
4.14	Jitter plot of cross-obligor correlations of daily spread returns.	129
4.15	Jitter plots of cross-obligor correlations coefficients in different rating categories of daily spread returns.	130
4.16	Jitter plots of cross-obligor correlations in different industrial sectors of daily spread returns. F: Financial, M: Materials, CS: Consumer Stable, U: Utilities, E: Energy, I: Industrial, CC: Consumer Cyclical, CT: Communication and Technology.	130
4.17	Estimators, \hat{p}^- and \hat{p}^+ , for the conditional probability of having a large CDS spread move in an obligor given that there is a large CDS spread move in other obligor. Each point represents the conditional tail probability for a pair of obligors. Blue dotted lines at 5% level represents the estimator value for independent series.	132
4.18	The first four principal component factors.	134
4.19	Loadings of the first three principal component factors.	134
4.20	Hill estimators for the tail indices of the PC factors. The number observations for estimation is equal to 2.5% of the sample size.	135
4.21	Jitter plots of daily spread returns normalized by the unconditional sample standard deviations (top) and the conditional daily spread returns from ARMA-GARCH models (bottom) during the credit events in Table 4.14. Each point represents the spread return/conditional spread return of an obligor on the corresponding event date.	138

4.22 Simulated time series of CDS spreads and daily spread returns from the affine jump-diffusion model.	140
4.23 Sample autocorrelation function for simulated daily spread returns and absolute spread returns from the affine jump-diffusion model.	141
4.24 Empirical extremograms for simulated daily spread returns from the affine jump-diffusion model. For the left tail estimates (resp. right tail estimates), threshold a_m is equal to 5% (resp. 95%) quantile of the sample. Blue line is the 95% confidence bound constructed from randomly permuted data series. Blue dotted line is equal to 5%, which is the theoretical value for an independent series.	141
4.25 Quantile plots (left) and Hill estimators for the tail indices (right) of simulated CDS spread return from the affine jump-diffusion model.	142
4.26 Left: Jitter plot of cross-obligor correlations. Right: Estimators, \hat{p}^- and \hat{p}^+ , for the conditional probability of having a large CDS spread move in an obligor given that there is a large CDS spread moves in other obligor. Each point represents the conditional tail probability between two obligors. Blue dotted lines at 5% level represents the estimator value for independent series. Data: Simulated spread returns from the affine jump-diffusion model.	143
4.27 Upper and lower bounds of the 95% confidence intervals for the degree of freedom estimators of V_t^i . Black dotted line represents the average of the degree of freedom estimators across obligors.	147
4.28 Sample autocorrelation function for simulated daily spread returns and absolute spread returns from the heavy-tailed multivariate AR-GARCH model (MAG).	149
4.29 Empirical extremograms for simulated daily spread returns from the heavy-tailed multivariate AR-GARCH model (MAG). For the left tail estimates (resp. right tail estimates), threshold a_m is equal to 5% (resp. 95%) quantile of the sample. Blue line is the 95% confidence bound constructed from randomly permuted data series. Blue dotted line is equal to 5%, which is the theoretical value for an independent series.	149
4.30 Quantile plots (left) and Hill estimators for the tail indices (right) of simulated CDS spread return from the heavy-tailed multivariate AR-GARCH model (MAG).	150
4.31 Left: Jitter plot of cross-obligor correlations. Right: Estimators, \hat{p}^- and \hat{p}^+ , for the conditional probability of having a large CDS spread move in an obligor given that there is a large move in the CDS spread of another obligor. Each point represents the conditional tail probability for a pair of obligors. Blue dotted lines at 5% level represents the estimator value for independent series. Data: Simulated spread returns from the heavy-tailed multivariate AR-GARCH model.	150

4.32 CDX.NA.IG on-the-run index and number of portfolios that have losses exceed 99% VaR in 2005-07. Portfolio types: protection sellers only (short), protection buyers only (long); half protection sellers half protection buyers (long-short).	157
4.33 CDX.NA.IG on-the-run index and number of portfolios that have losses exceed 99% VaR in 2007-09. Portfolio types: protection sellers only (short), protection buyers only (long); half protection sellers half protection buyers (long-short).	157
4.34 Daily P&L of a short-only, a long-only and a long-short portfolio, and the corresponding 99% VaR computed by the affine jump-diffusion model (AJD), the random walk model (RW) and the heavy-tailed multivariate AR-GARCH model (MAG) in 2008. Values are expressed as percentages of the total portfolio notional value.	158

Acknowledgments

First and foremost, I would like to thank my family, Norman, Shirley and Joseph, for their endless support and encouragement over the years, and my wife, Jessica, who has been sharing important moments of my life.

I wish to express my deepest gratitude to my advisor Professor Rama Cont for his guidance. This dissertation would not have been possible without his invaluable assistance, teaching and support.

I am grateful to have Professor Jussi Keppo and Professor Kristen Moore who introduce me the fascinating world of mathematical finance, and encourage me to pursue higher education in this area of study. I would also like to thank Professor Pierre Collin-Dufresne, Professor Richard Davis, Professor Emanuel Derman and Professor Xuedong He for their time to be my thesis committee, and all professors from IEOR Department for their teaching and advices over the years.

I would like to give special thanks to my friends, especially Bruce Wong, Kenneth Hui, David Mundorf, Gordon Pang, Ming Hu, Alfred Ma, Thiam Hui Lee, Romain Deguest and Johannes Ruf for their support and encouragement.

To my family

Chapter 1

Introduction

Credit derivatives, in particular credit default swaps (CDSs) and collateralized debt obligations (CDOs), played an important role in the recent financial crisis. In particular, the crisis revealed major shortcomings in the existing approaches for modeling and risk management these instruments and posed new challenges for modeling the risks associated with them. In this dissertation, we study various issues related to the modeling of credit derivatives: hedging of portfolio credit derivatives, calibration of dynamic credit models, and modeling of credit default swap portfolios.

This chapter gives an introduction to the credit derivatives market discusses various issues which motivated our study and summarizes the contributions of the thesis.

1.1 Credit derivatives

A credit derivative is similar to an insurance contract against the loss incurred in the case of “credit events” associated with a single or a pool of reference entities, which are referred to as “names” or “obligors”. A credit event, which is also called a default, that triggers the contractual payment is defined as any of the following:

- Bankruptcy: the risk that the reference entity will become bankrupt.

- Failure to pay: the risk that the reference entity will default on one of its obligations such as a bond or loan.
- Obligation acceleration: the risk that an obligation of the reference entity will be accelerated e.g. a bond will be declared immediately due and payable following a default.
- Repudiation or moratorium: the risk that the reference entity or a government will declare a moratorium over the reference entity's obligations.
- Restructuring: the risk that obligations of the reference entity will be restructured.

Unlike insurance contracts, investors do not have to hold the bonds to buy a credit derivative on the bonds, whereas with an insurance contract, insurance buyers need to have a direct economic exposure to the reference entities. Moreover, insurance contracts are mostly not traded, where credit derivatives are traded over the counter or via central counterparties.

Given the function for credit risk migration that favors hedgers and the built-in leverage that attracts speculators, size of the credit derivative market has grown enormously from late 1990s until the recent financial crisis. According to the survey data from the Bank of International Settlements¹, the total notional amount of credit default swaps increases from \$6.4 trillion in 2005 to \$58 trillion in 2008. After the financial crisis, it drops to \$33 trillion in 2010.

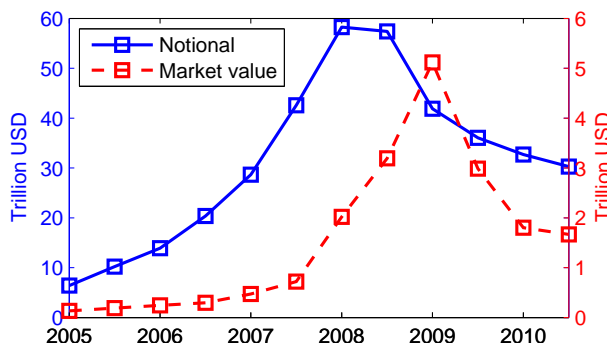


Figure 1.1: Outstanding notional value and gross market value of credit default swaps. Source: the Bank of International Settlements.

¹See <http://www.bis.org/statistics/derstats.htm>

1.1.1 Commonly traded credit derivatives

The most commonly traded credit derivatives are single-name credit default swaps (CDSs), index default swaps and collateralized debt obligations (CDOs). In the following, we describe the mechanism of the three credit derivatives. A mathematical formulation is presented in chapter 2 and more details can be found in [20].

Credit default swaps is a contract between two parties, a protection buyer and a protection seller, whereby the protection buyer is compensated for the loss generated by a credit event of a reference entity. In return the protection buyer pays a premium equal to an annual percentage of the notional to the protection seller (see Figure 1.2). The premium, quoted in basis points or percentage points of the notional, is called the *CDS spread*. This spread is paid periodically, typically quarterly, in arrears until either maturity is reached or default occurs. In practice, CDS is quoted in terms of its fair spread, or known as the *CDS par spread*, which is the premium rate that gives zero market value to both the protection buyer and seller.

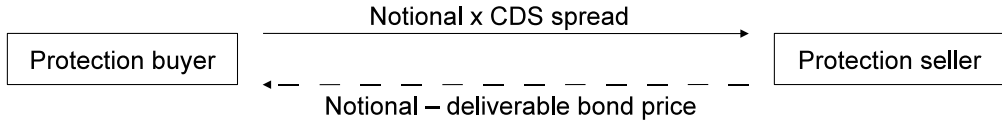


Figure 1.2: Cashflows of a credit default swap. Solid line represents the premium payment from the protection buyer and dashed line represents default payment from the protection seller.

There are various methods for settlement at default. In a cash settlement, the protection seller pays the protection buyer the face value of the reference asset minus its post-default market value. In a physical settlement, the protection buyer receives face value of the reference asset, but in turn must make physical delivery of the reference asset or a bond from a pool of eligible assets to the protection seller in exchange for par. In both cases, the post-default market value of the reference is typically determined by a dealer poll.

Figure 1.3 shows the 5-year CDS par spreads and the spread daily log returns of MetLife from 2005 to 2010. As we can see, the CDS spreads appear to be substantially more volatile during the

financial crisis from late 2007 to 2010.

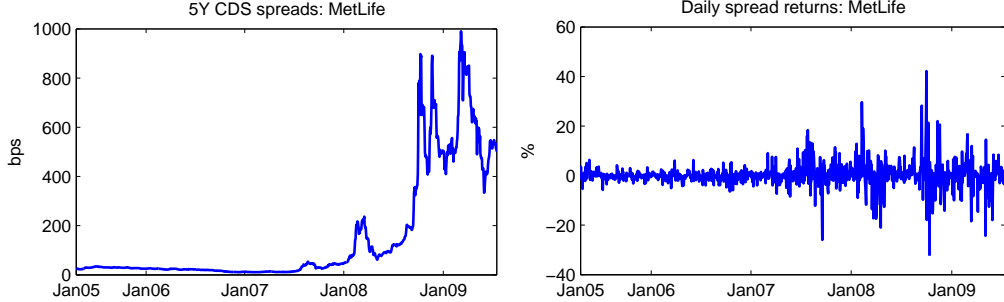


Figure 1.3: 5-year CDS par spreads and CDS spread daily log return of MetLife.

Index default swap, which is also known as CDS index, is a natural extension of single-name CDS, which insures against the cost of credit events arise from a portfolio of obligors. Similar to CDS, the protection buyer pays a quarterly premium, equal to an annual percentage of the remaining notional value of the portfolio, to the protection seller until either maturity is reached or all reference obligors have defaulted (see Figure 1.4). Upon an arrival of a credit event from the reference credit portfolio, the protection buyer delivers the bond of the defaulted obligor in return for a cash payment of par in the case of a physical settlement. In a cash settlement, the protection buyer receives the par minus the post-default market value of the bond. After that, the outstanding notional of the basket is reduced by the notional of the defaulted obligor. Index default swap is quoted in terms of its *index par spread*, which is the premium rate that sets the market value of the contract equal to zero. Economically, an index default swap can be thought of an equally weighted portfolio of CDSs.

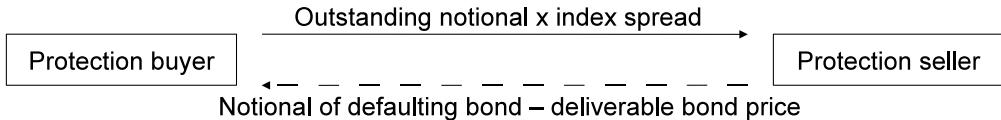


Figure 1.4: Cashflows of an index default swap. Solid line represents the premium payment from the protection buyer and dashed line represents default payment from the protection seller.

Commonly traded indices include the iTraxx Europe indices for European corporates and the

CDX North America indices for North American corporates. In particular, the iTraxx Investment Grade index and CDX Investment Grade index each represents an equally weighted basket of 125 CDSs. The index composition changes every half year and some obligors, typically those have been downgraded, will be replaced. The latest composition is called the on-the-run series, while other former compositions are called off-the-run series. The on-the-run series appears to have higher trading volume as investors switch to the new series. Figure 1.5 shows the 5-year on-the-run CDX Investment Graded index spreads from 2005 to 2010. Similar to the previous observations from CDS spreads in Figure 1.3, volatility of the CDX index spread increases significantly during the financial crisis.

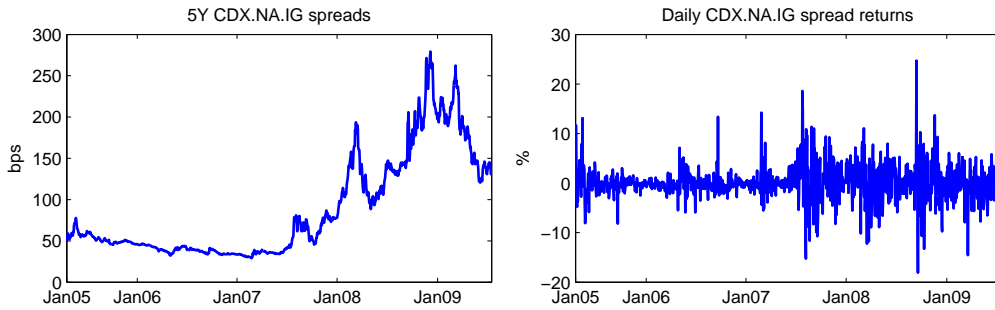


Figure 1.5: 5-year index par spreads and index spread daily log return of CDX.NA.IG on-the-run series.

Collateralized debt obligation (CDO) is a credit derivative that is also written on a portfolio of obligors. But unlike index default swaps, it only insures against part of the total losses generated from the credit events, which is defined by the level of subordination (tranche). We will focus on synthetic CDO where the underlying is a portfolio of CDSs, as opposed to an underlying of actual bonds. Figure 1.6 shows the standard subordination of CDX investment grade index CDOs.

Consider a CDO tranche with attachment-detachment interval $[a, b]$, i.e. the initial notional value of the tranche is $b - a$. The protection buyer of this tranche pays a quarterly premium, equal to an annual percentage of the remaining notional value of the tranche, to the protection seller until either maturity is reached or the cumulative loss on the underlying portfolio exceeds the detachment level b . Upon arrival of a credit event, if the cumulative loss on the underlying

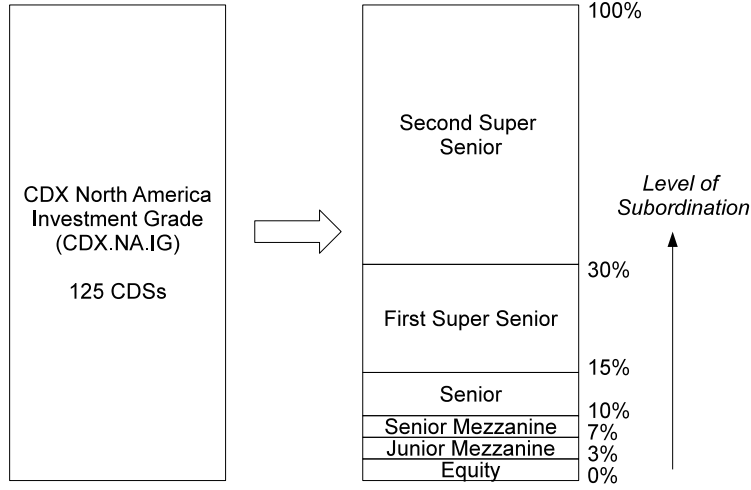


Figure 1.6: Standard CDO tranche subordination of the CDX North America Investment Graded index.

portfolio (including the loss from the latest credit event) is smaller than the attachment level a , no payment will be made by the protection seller. Otherwise, if the cumulative loss exceeds the attachment level a , the protection buyer will receive the loss given default of the defaulting obligor (par minus the deliverable bond price), or the cumulative portfolio loss in excess of the attachment level, whichever is smaller (see Figure 1.7). The total default payment received by the protection buyer is capped by the width of the tranche, $b - a$. The cumulative loss of the tranche $[a, b]$ can be expressed as

$$L_t^{[a,b]} = \max(L_t - a, 0) - \max(L_t - b, 0),$$

where L_t is the cumulative loss from the underlying portfolio at time t . Following the credit event, the remaining notional value of the tranche is reduced to $b - a - L_t^{[a,b]}$. Furthermore, the notional value of the most senior tranche, which has detachment level equal to 100% of the total notional value, is reduced by the recovery on the bond. This ensures that the sum of the remaining notional value of all tranches is equal to the remaining notional value of the whole portfolio. CDO tranches are also quoted in terms of their fair spreads, *CDO tranche par spreads*, which are the premium rates that set the tranche values equal to zero.

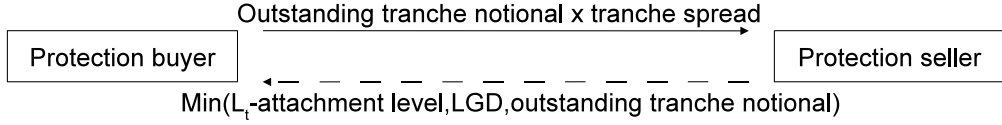


Figure 1.7: Cashflows of a CDO tranche. Solid line represents the premium payment from the protection buyer and dashed line represents default payment from the protection seller. L_t is the cumulative portfolio loss at default time and LGD stands for loss given default.

Figure 1.8 shows the 5-year par spreads and spread daily log returns of CDX Investment Graded index tranche [3%, 7%] in 2008. Observe that there is a sharp “jump” in the CDO spread in the middle of September 2008. This jump in fact happened on 15 September 2008 when Lehman Brothers filed for bankruptcy.

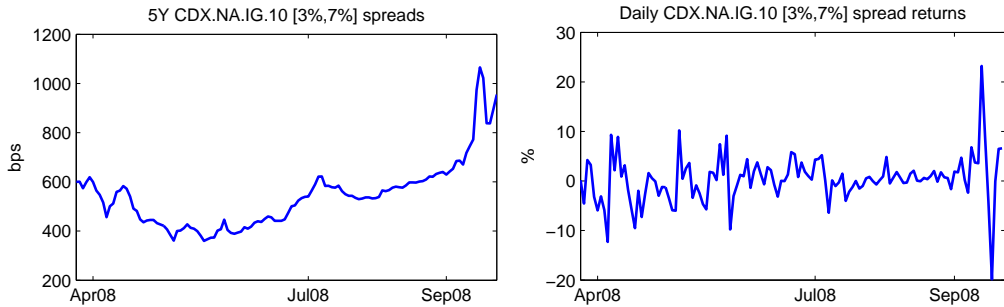


Figure 1.8: 5-year par spreads and spread daily log return of CDX.NA.IG series 10 tranche [3%,7%].

1.1.2 Valuation and quotation

For each of the above three credit derivatives, the stream of payments can be divided into default payments from the protection seller (default leg) and premium payments from the protection buyer (premium leg). Value of the credit derivative is then the difference between the present value of the default leg and the premium leg. For a protection seller who receives premiums,

$$\text{Protection seller value} = \text{Premium leg value} - \text{Default leg value},$$

and the corresponding protection buyer value is simply the negative of the protection seller value. In practice, the present value is evaluated under a risk-neutral probability measure determined by

the choice of pricing models. The par spread (par premium rate), which is usually quoted in the market, can be expressed as

$$\text{Par spread} = \frac{\text{Default leg value}}{\text{Premium leg value with premium rate} = 100\%}.$$

For simplicity, we will use the term *CDS spread* (*resp. index spread, CDO tranche spread*) interchangeably with *CDS par spread* (*resp. index par spread, CDO tranche par spread*), unless noted otherwise.

In 2009, major changes to credit derivative contracts and conventions have been made which is known as “the Big Bang”². CDSs, indices and CDO tranches are suggested to quote in terms of an upfront payment with a fixed periodic premium instead of a periodic spread with zero upfront payment. Nevertheless, most of our analysis will still be based on the old conventional par spreads because first, most historical prices are still recorded in terms of the par spreads, and second, since there is an one-to-one relationship between the two quotation conventions, studying of fair spreads (with zero upfront) can easily be transformed to those of the new conventional CDS upfront payments (with fixed periodic premium).

1.1.3 Economic benefits

In principle, credit derivatives should make the financial market more efficient and improve capital allocation. By using credit derivatives, financial institutions who provide the capital can reside the credit risk of the borrowers to a third party, who may be in a better position to bear the credit risk. In this case, financial institutions can make loans that they were not able to make previously and this can reduce the cost of capital for firms.

Moreover, credit derivative market appears to be a better forum for credit risk discovery than the bond market. Blanco, Brennan and Marsh [11] show that information on credit risk mostly flows from the CDS market to the bond market. This result may not be surprising as liquidity

²See http://www.markit.com/cds/announcements/resource/cds_big_bang.pdf for description of CDS Big Bang.

should be less of a factor in trading credit derivatives than the underlying bonds as actual bonds involve funding issues.

Finally, credit derivative market provides more investment opportunities. For example, even if we believe that the credit quality of a firm will deteriorate, it can be difficult to short sell the firm's bonds and loans. On the other hand, we can buy protection on the firm's debts by entering a credit derivative contract. When the credit quality gets worse but the firm has not defaulted yet, the value of our position as a protection buyer will increase due to the rise of the protection premium. If the firm eventually defaults, we will receive payment from the protection seller. In either case, we are benefiting from the deterioration of the firm's credit quality.

1.2 Quantitative modeling of credit derivatives and the financial crisis

Despite the contributions to market efficiency and credit risk assessment, the financial crisis in 2007-08 revealed various issues related to credit derivatives [94]. This dissertation is motivated by problems arising in the risk management of portfolio credit derivatives, implementation of dynamic credit models and statistical modeling of CDS portfolios.

1.2.1 Risk management of portfolio credit derivatives

The hedging benefit of credit derivatives should have made it possible for credit risk to be located with those institutions which can efficiently bear the risk. However, the recent financial crisis shows that many of those institutions, especially insurance companies that sell protections such as AIG, do not have the ability to absorb the credit risk that they have taken. As pointed out by Stulz [94], the benefit of credit risk hedging turns out to be illusory, or the risk is ultimately transferred to taxpayers. According to a report by the International Swaps and Derivatives Association [1], AIG had borrowed a total of almost \$128 billion by the end of 2008 from the Federal Reserve and the

Treasury:

- \$40 billion from a bridge loan designed to help the company continue operating while it sells off non-core assets.
- \$28 billion to purchase the collateralized debt obligations on which AIGFP had sold protection.
- \$20 billion of the \$22.5 billion allotted to purchase subprime mortgage backed securities in which AIG had invested as part of its securities lending program.
- \$40 billion capital investment through the TARP program.

The report also states that “*The acute liquidity crunch, triggered by AIG’s credit rating downgrade, that ultimately led to AIG’s bailout is attributable to AIG’s failure to assess the risks of MBS, CDOs and other mortgage market exposures.*”

In order to maintain the effectiveness of credit derivatives to protect investors from losses given defaults, it is important for those who are selling protections to have a sound risk management. In particular, a successful risk management can be achieved by having effective hedging strategies for credit derivatives, especially for the more complex derivatives such as CDO tranches. The Gaussian copula model [74] has been widely used for hedging such portfolio credit derivatives. In the model, the risk of a credit derivative is characterized in terms of sensitivities to shifts in risk factors [44, 85], and hedging practices have typically been based on such measures of sensitivity. However, the recent turmoil in the credit derivative market shows that these commonly used hedging approaches are inefficient.

In section 1.3, we discuss various approaches for hedging of portfolio credit derivatives and compare their performances during the crisis period. We also address various claims in the literature that have not been justified by using empirical data. Those include examinations of whether strategies using single-name CDSs perform better than hedges using the credit index, and whether

dynamic models provide better hedges than the static copula models. The analysis is based on the article [26], and the details are shown in chapter 2.

1.2.2 Implementation of dynamic credit models

While some of the credit derivatives are not liquidly traded, such as index CDO tranches with nonstandard attachment levels, valuation and risk assessment of those contracts have to be done by using credit models. The Gaussian copula model [74] has been the market standard for pricing and hedging portfolio credit derivatives, but it also faces heavy criticism regarding its static nature and the inability to generate arbitrage-free prices for nonstandard CDO tranches [25]. In chapter 3, we give an example of how such arbitrage opportunities can actually arise.

By knowing the deficiency of the static copula-based models, it then leads to the development of various dynamic credit models. One of the main obstacles in implementing and using these dynamic models is the availability of efficient calibration algorithms. Previous studies on calibration of dynamic models have mostly been based on black-box optimization procedures applied to non-convex least squares minimization problems. The lack of convexity entails that the convergence and stability of these methods are not guaranteed, casting doubts on the reproducibility of calibration results and their stability.

In section 1.4, we present a stable calibration method to recover the default intensity from a given set of CDO tranche spreads. The method makes use of a closed-form expression of the *local intensity function*, which is an analog to the Dupire [43] formula for the local volatility function, and a quadratic programming method to recover expected tranche notional from the CDO tranche spreads. We also show that this calibration method overcomes the stability and convergence problems that appear in other black-box calibration algorithms. The derivation is based on the article [25], and the details are shown in chapter 3.

1.2.3 Central clearing and statistical modeling of CDS

Many researchers have focused on problems caused by counterparty risk in arguing that credit derivatives made the financial crisis worse. In particular, credit derivatives lead to a huge network of exposures across financial institutions [29, 30]. If an institution fails, it can lead other institutions to fail as they experience losses on their exposures. Therefore, this web of exposures can lead to *systemic risk*. Credit derivatives arguably heighten this concern because the protection sellers may face sudden and substantial losses when defaults occur. The typical example is the bankruptcy of Lehman Brothers in September 2008, which then leads to concerns of the credit quality of various financial institutions afterwards.

A popular proposal for reducing systemic risk arising from over-the-counter trading of credit derivatives is to clear the transactions via central counterparties (CCPs) [18, 24, 42]. Given their important role as a bulwark against counterparty risk and contagion, CCPs need to use stringent risk management procedures to ensure their own financial stability, especially when a large clearing member defaults. In practice, margin requirements are used to absorb losses in the case of the default of a clearing member [63, 91]. Since the credit derivative prices are observed to be highly volatile, such margin requirements should cover losses which may arise from this price volatility. For example, Figure 1.9 shows that CDS spread returns exhibit two-sided heavy-tailed distribution and large co-movements. Therefore, computation of the margins should be based on a statistical model which accounts for such empirical properties of the credit derivative prices.

In section 1.5, we present a systematic study of the univariate and multivariate properties of CDS spreads, using time series of spreads for the constituents of the CDX Investment Grade index from 2005 to 2009. We then propose a heavy-tailed multivariate time series model that captures these properties, and which can be used as a framework for measuring and managing the risk of CDS portfolios. The model appears to provide accurate prediction of loss quantiles for a variety of CDS portfolios and performs well during the financial crisis. The analysis is based on the article [27], and the details are shown in chapter 4.

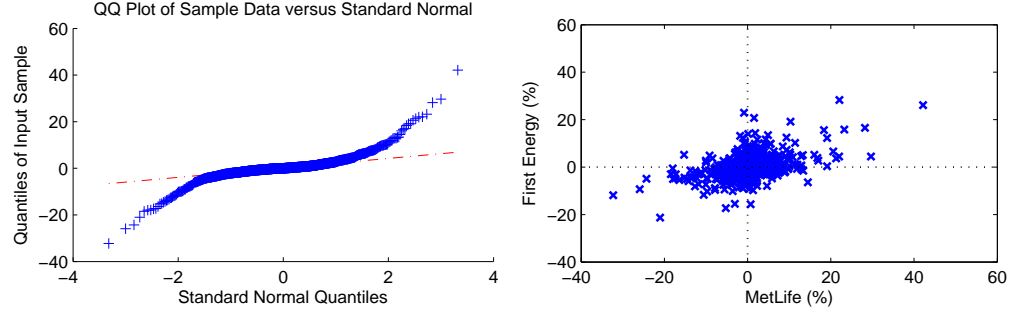


Figure 1.9: Evidence of heavy-tailed distribution and large co-movements of CDS spreads. Left: QQ-plot for 5-year CDS spread daily log return of MetLife. Right: 5-year CDS spread daily log return of MetLife vs First Energy.

1.3 Comparison of strategies for hedging index CDO tranches

The recent turmoil in financial market reveals inefficiency of the commonly used hedging approaches for portfolio credit derivatives, namely the sensitivity-based hedging methods under the Gaussian copula model [74]. One of the main criticisms is the lack of well-defined dynamics for the risk factors in such static models, which prevents any model-based assessment of hedging strategies. Knowing the deficiencies of copula-based hedging methods, alternatives have been proposed to tackle the problem of hedging (see, for example [8, 9, 44, 51, 53, 71]). However, these studies approach the problem from different, often incompatible, standpoints, and a systematic comparison of the resulting hedge ratios and the subsequent hedging performance has not been done in a realistic setting with market data. These studies often assume a complete market environment [8, 9, 71] which is indeed not realistic according to the experience of the credit derivative market turmoil, leading to questionable conclusion. On the other hand, some studies, such as [51, 53], acknowledge market incompleteness and approach the hedging problem by incorporating both spread risk and default risk. However, those analyses only focus on a particular model, and a comprehensive examination across different models and strategies has not been addressed. Needless to say, in order for such a comparison to be meaningful, the models need to be calibrated to the same data set. The very feasibility of this calibration is a serious (computational) constraint which excludes

many models discussed in the literature, leading us to focus on the class of tractable models.

In chapter 2, we assess the performance of hedging strategies for index CDO tranches derived under various model assumptions, which is motivated by previous studies indicating the impact of model uncertainty on hedging of derivative instruments [23, 39]. To our knowledge, this study is the first to compare a variety of models and hedging strategies under a realistic setting using historical data. Models that are considered include:

- *The Gaussian copula model* [74] is a static copula model in which the correlations between default arrivals are specified via a Gaussian copula function. In this model, the marginal distribution of the default time for each underlying obligor is calibrated to the corresponding CDS term structure. Then correlation parameters of the Gaussian copula function are fitted to the CDO tranche spreads. In practice, the common approach is to consider a one-factor Gaussian copula model with one correlation parameter and the CDO tranche spreads are expressed as different *implied correlations*. Therefore, CDO market is also known as correlation market [20].
- *The affine jump-diffusion model* is a multiname reduced-form model which is first introduced by Duffie and Gărleanu [41]. In this model, the default arrival times are modeled as Cox processes where the default intensity for each obligor is driven by affine jump-diffusion processes. Unlike the Gaussian copula model, this model is dynamic and the correlation structure is modeled through the loading of each default intensity on the common affine process.
- *The Herbertsson model* [60] is a simple Markovian portfolio default model where the credit portfolio loss is assumed to follow a finite-state continuous-time Markov process with a transition rate that depends on time and the loss level. The transition probability of the loss process has a semi-analytic expression which leads to an efficient calibration algorithm. However, such model does not incorporate spread volatility, meaning that it implies deterministic movements of the index and CDO tranche spreads between successive defaults.

- *The bivariate spread-loss model* [5] is an extension of the Herbertsson model where the portfolio default intensity is governed by the portfolio loss process itself and also an additional factor which drives spread volatility between defaults. This model, which is introduced by Arnsdorf and Halperin [5], is able to incorporate both spread and default risk.

Under the above modeling frameworks, we consider the following hedging strategies.

- *Delta hedging of spread risk* is the most common strategy for hedging CDO tranches. Investors use either the underlying CDSs or the index to protect against small movements in the CDO tranche values. However, this does not take into account of either changes in the implied correlations or large movements in the credit derivative values.
- *Gamma hedging of spread risk* is an extension of delta hedging which attempts to neutralize the convexity of change in the CDO tranche values with respect to shifts in CDS spreads. This strategy involves trading of other CDO tranches.
- *Hedging of implied correlation movements* can be achieved by trading other CDO tranches. However, implied correlations do not necessarily move in parallel and the performance of such strategy is questionable.
- *Hedging of default risk* is carried out by entering position in the underlying CDS or the index according to the *jump-to-default ratio*, which is defined as the change in the CDO tranche value over the change in the CDS or index value with respect to a constituent default.
- *Quadratic hedging* is the strategy that minimizes the quadratic hedging error under the risk-neutral pricing measure. In the case of a Markovian model, such as the Herbertsson model and the bivariate spread-loss model, there is an analytical expression for the optimal hedge ratio.
- *Regression-based hedging* estimates the optimal hedge ratios by regressing the changes in CDO tranche values against the changes of the index values based on historical data. Unlike

quadratic hedging which is computed under the risk-neutral probability measure, the regression approach incorporates the statistical (real-world) relationship between the CDO tranches and the underlying index.

By using the CDX.NA.IG data in 2008, we compare the performance of the above strategies for hedging index CDO tranches. The performance is measured in terms of the reduction in magnitude and volatility of the daily profit-and-loss. Our empirical analysis shows evidence for market incompleteness: a large proportion of risk in the CDO tranches appears to be unhedgeable. This suggests that market completeness is by no means an acceptable approximation, and toy models [9, 71] which assume a complete market may fail to provide useful insight for issues related to hedging of CDO tranches. We also show that, unlike what is commonly assumed [8], dynamic models do not necessarily perform better than static models, nor do high-dimensional bottom-up models perform better than simpler top-down models. When it comes to hedging, top-down and regression-based hedging provide significantly better results during the crisis than bottom-up hedging with single-name CDS contracts. This leads us to question the need for computationally costly dynamic bottom-up models instead of the top-down models for hedging portfolio credit derivatives. Model-free regression-based hedging appears to be more effective than other hedging strategies. This suggests that incorporating the statistical behavior of credit spreads is an important criterion for a successful hedging strategy. Our empirical study also reveals that while significantly large moves, “jumps”, do occur in CDS, index, and CDO tranche spreads, where these jumps do not necessarily occur on the default dates of index constituents, an observation which shows the insufficiency of some recently proposed portfolio credit risk models [53].

Our empirical study has left out some of the practical considerations such as (il)liquidity of CDS contracts, higher transaction costs for trading CDSs than for the index, and higher computational costs for the bottom-up multiname models than for the top-down aggregate loss models into account. If we take these aspects into account in addition to our backtesting analysis, it would tilt the comparison even more in favor of top-down/index hedging as opposed to hedging with single-name

CDSs.

1.4 A non-parametric approach for recovering default intensities implied by CDO spreads

The inadequacy of the Gaussian copula model and its various extensions for pricing and hedging is emphasized by the recent turmoil in the credit derivative market. In particular, those static models are not able to price path-dependent derivatives such as forward starting CDO tranches, and pricing non-standard CDO tranches based on implied correlations interpolation yields static arbitrage opportunities (see [25]). It then leads to the development of various dynamic models for portfolio credit risk.

One of the main obstacles in implementing and using these dynamic models has been the availability of efficient calibration algorithms. Previous studies on dynamic models have mostly been based on black-box optimization procedures applied to non-convex least squares minimization problems (for example [5, 45, 54, 60]). The lack of convexity entails that the convergence and stability of these methods are not guaranteed, casting doubts on the reproducibility of calibration results and their stability.

Recovering implied default rates from market data is by nature an ill-posed problem. Although the actual default rate may depend on the past market history, it has been argued [28, 31, 93] that the information contained in CDO tranche spreads can be used at best to recover the *local intensity function*, $a(.,.)$, which is defined as the conditional expectation of the portfolio default intensity given the loss level:

$$a(t, i) := E^{\mathbb{Q}}[\lambda_t | N_{t-} = i, \mathcal{F}_0],$$

where \mathbb{Q} is a risk-neutral pricing measure, N_t is the number of underlying defaults happened by time t , (λ_t) is the (portfolio default) intensity for the counting process (N_t) , and \mathcal{F}_0 represents the

information observed today (time 0). The local intensity function is analogous to the local volatility function introduced by Dupire [43] for equity derivatives. It summarizes all information available from CDO tranche spreads on the marginal loss distributions of the credit portfolio.

In chapter 3, we derive a simple computational method for constructing an arbitrage-free CDO pricing model in terms of the local intensity function which matches a prespecified set of CDO tranche spreads. Our method can overcome the convergence problem arises from black-box optimization and it is carried out in two steps. In the first step, we recover the so-called *expected tranche notionals*, which are essentially the expected put payoffs:

$$P(T, K) := E^{\mathbb{Q}}[(K - L_T)^+ | \mathcal{F}_0],$$

with different maturity T and strike K . We show that a set of arbitrage-free expected notionals can be obtained from the market CDO tranche spreads by solving a quadratic programming problem. Linear constraints in the optimization represent the no-arbitrage conditions and the consistency with respect to the market CDO tranche spreads. We then solve for the set of arbitrage-free expected tranche notionals that is “closest” to a set of reference expected tranche notionals in terms of their sum of the squared differences. The reference values can represent a “prior” view on the market, which can also be computed from a reference model such as the Gaussian copula model.

In the second step, values of the local intensity function are obtained by using an analytical inversion formula:

$$a(T, i) = \begin{cases} \frac{-\partial_T P(T, \delta)}{P(T, \delta)}, & i = 0, \\ \frac{-\nabla_K \partial_T P(T, i\delta)}{\nabla_K^2 P(T, (i-1)\delta)}, & i = 1, \dots, n-1, \\ 0, & i = n, \end{cases}$$

where n is the total number of obligors in the underlying portfolio, δ is the loss given default that is assumed to be constant, $\partial_T P(T, \delta)$ is the partial derivative with respect to maturity, and

$\nabla_K P(T, i\delta) = P(T, (i+1)\delta) - P(T, i\delta)$ is the forward difference of the function in strike. Application of this formula is justified by an existence theorem, which states that if the local intensity function is bounded, there exists a Markovian point process (M_t) with intensity $(a(t, M_{t-}))$ such that the marginal distributions of this Markovian point process match the given set of expected tranche notinals. Details of the theorem are presented in chapter 3.

Since the calibration method only requires to solve a quadratic programming problem and make use of an analytical formula, convergence and uniqueness of the resulting default intensity are guaranteed. Moreover, we show that this method is significantly more stable with respect to shifts in the market CDO tranche spreads than the parametric method introduced by Herbertsson [60]. Unlike the calibration algorithm introduced by Cont and Minca [28], our method has the advantage of requiring only relatively simple mathematical techniques.

Comparing this approach to other calibration methods using iTraxx Europe index CDO spreads, we find that model-dependent quantities such as the forward starting tranche spreads and jump-to-default ratios are quite sensitive to the calibration method used, while the default intensities maintain a good match to the CDO market spreads. This illustrates clearly the ill-posedness of the calibration problem, and also demonstrates that uncertainty due to the choice of the calibration method can have a large impact on both pricing and hedging of credit derivatives.

Since the local intensity function can be defined for a wide range of credit portfolio models, it also provides a common basis for model comparison. By comparing the local intensity functions implied by different credit portfolio models, we find that apparently different models, such as static Student-t copula models [70] and reduced-form affine jump-diffusion models [41, 83], lead to similar marginal loss distributions and tranche spreads. This suggests that market CDO prices alone are insufficient to discriminate between these model classes.

Our results emphasize the importance of model uncertainty when addressing the pricing and hedging of portfolio credit derivatives and call for more research in this direction.

1.5 Statistical modeling of credit default swap portfolios

The recent financial crisis illustrates that investors in credit derivatives can experience substantial losses even in absence of any defaults. The risk associated with such volatility in market values is mainly due to the change of credit quality of the underlying obligors, which is reflected in their credit spreads. This *spread risk*, overlooked in the first generation of default risk models [16, 25, 28, 60, 67, 68, 80], turned out to be the major risk faced by investors in credit derivatives.

In our opinion, a realistic model for CDS spreads should (at least) be capable of explaining the empirical properties that are observed in the historical data. However most existing default risk models have focused on analytical tractability rather than statistical properties of credit spreads [41, 49, 83], and spread dynamics implied by these models do not necessarily correspond to observed dynamics of spreads. This may result in poor performance of these models for hedging and risk management [26].

Modeling of spread risk is also important for calculating the margin requirements for centrally cleared credit derivatives. Regulatory reform in the light of 2008 crisis has moved CDS trading from over-the-counter bilateral trading to clearing houses. The consistent computation of such margin requirements requires a multivariate model for (co-)movements in CDS spreads.

As shown by Collin-Dufresne, Goldstein and Martin [21], credit spread changes are principally driven by supply/demand fluctuations that are independent from factors traditionally considered in credit risk modeling. This observations suggests that direct stochastic modeling of CDS spread returns is more effective than trying to explain spread movements in terms of other economic variables. This is the approach we adopt here: in chapter 4, we first undertake a systematic study of the univariate and multivariate properties of CDS spreads. By using the CDS time series of CDX investment grade index constituents in 2005-09, we observe the following statistical properties:

- CDS spread returns can be modeled as stationary processes with positive autocorrelations, positive serial correlations in extreme values, conditional heteroscedasticity and two-sided

heavy tails.

- Large co-movements are observed in the CDS spread series, indicating the presence of heavy-tailed common factors. However, these large co-movements are not necessarily linked to credit events.
- Correlations across obligors of CDS spread returns increase substantially in 2007-09.
- Principal component analysis suggests that the main contribution to the variance of CDS spread returns comes from idiosyncratic jumps.
- Credit events do not necessarily lead to large upward moves in the CDS spreads.

These properties can serve as a guideline to check whether a credit model is valid for modeling CDS spreads. In particular, we show that the affine jump-diffusion model [41, 49, 83] fails to reproduce the serial dependence and the two-sided heavy-tailed distribution for CDS spread returns. Moreover, the affine jump-diffusion model estimated by a Markov Chain Monte Carlo method [49] overestimates the probability of having large co-movements in the CDS spreads. While previous studies, such as [6, 49], show that the affine jump-diffusion model fits well to the CDS and CDO tranche spread time series, our results illustrate that goodness-of-fit does not necessarily lead to the desired statistical properties.

Recognizing insufficiency of the affine jump-diffusion model, we propose a heavy-tailed multivariate AR-GARCH model (MAG model) for CDS spread returns. In this model, the CDS spread returns are modeled as AR(1)-GARCH(1,1) processes:

$$\begin{aligned} r_t^i &= C^i + \phi^i r_{t-1}^i + \epsilon_t^i, \\ \epsilon_t^i &= \sigma_t^i Z_t^i, \end{aligned}$$

where the index i represents the reference obligor i , (r_t^i) is the CDS spread daily returns, (Z_t^i) is an i.i.d. sequence, and σ_t^i is the conditional volatility which follows

$$(\sigma_t^i)^2 = K^i + G^i (\sigma_{t-1}^i)^2 + A^i (\epsilon_{t-1}^i)^2,$$

where $K^i > 0$, $G^i \geq 0$, $A^i \geq 0$, $G^i + A^i < 1$. We assume that the i.i.d. sequence (Z_t^i) follows a heavy-tailed distribution

$$Z_t^i = a^i V_t^0 + b^i V_t^i,$$

where (V_t^0) and (V_t^1, \dots, V_t^n) are i.i.d. sequences which follow a Student t distribution with degree of freedom ν^0 and a multivariate Student t distribution with degree of freedom ν respectively. Notice that Z_t^i is a weighted sum of two Student t distributed variables with possibly different degrees of freedom. By using a quasi maximum likelihood method to estimate the model parameters, we show that this model is able to reproduce the observed statistical properties of CDS spreads as well as their multivariate dependence structures adequately.

In the final section of chapter 4, we compare the MAG model to the affine jump-diffusion model and a random walk model introduced by Saita [91] in terms of predicting loss quantiles of various examples of CDS portfolios. Loss quantiles for CDS portfolios is important in practice since it underlies the risk measurement for the portfolios and is used for the determination of margin requirements for the clearing of CDS contracts by central counterparties. In particular, we compute the 99% quantile of the daily loss, which corresponds to the 99% 1-day Value-at-Risk (VaR), and compare these quantile levels to the realized daily losses.

We first use the Kupiec test [65] to examine whether the exceedance probability, the probability that the realized loss is larger than the VaR estimate, is significantly different from 1%. According to our backtest, the MAG model gives the fewest number of portfolios whose exceedance probability is significantly different from the target 1%. The random walk model appears to perform better than the affine jump diffusion model in 2005-07, but the two models are comparable in 2007-09.

We then investigate the timing of exceedances and check whether the exceedances exhibit autocorrelations by using the Ljung-Box test on the exceedance sequence $(1_{\{L_t > VaR_t\}})$ for each portfolio where L_t is the portfolio loss at time t and VaR_t is the VaR estimate. We find that the random walk model gives positively autocorrelated exceedances, especially in late 2008 when a series of

market shocks was triggered by Lehman Brother’s bankruptcy. This reveals that random walk model is inadequate for predicting loss quantiles in difficult market condition. On the other hand, the MAG model gives the fewest number of portfolios that have autocorrelated exceedances.

Finally, we examine whether the sample expected shortfall is statistically different from the model expected shortfall. We follow McNeil, Frey and Embrechts [79] and compute the confidence intervals for the sample expected shortfall by using the bootstrap method [46, 79]. Our results show that the MAG model gives the best performance, which has the fewest number of portfolios that can reject the hypothesis that the sample expected shortfall is different from the model expected shortfall.

Overall, our heavy-tailed multivariate AR-GARCH model compares favorable to the affine jump-diffusion model [41] and the random walk model [91], while it provides more accurate prediction for the quantiles of the loss distribution of a wide variety of CDS portfolios.

1.6 Publications

- Rama Cont, Romain Deguest and Yu Hang Kan. Default intensities implied by CDO spreads: inversion formula and model calibration. *SIAM Journal on Financial Mathematics*, 1:555–585, 2010.
- Rama Cont and Yu Hang Kan. Dynamic hedging of portfolio credit derivatives. *SIAM Journal on Financial Mathematics*, 2:112–140, 2011.
- Rama Cont and Yu Hang Kan. Statistical modeling of credit default swap portfolios. Working paper, Columbia University, 2011.
- Yu Hang Kan and Claus Pedersen. The impact of margin interest on the valuation of credit default swaps. Working paper, 2011.

Chapter 2

Dynamic hedging of portfolio credit derivatives

Static factor models, in particular the Gaussian copula model [74], have been widely used for hedging portfolio credit derivatives such as collateralized debt obligations (CDOs). In such models, the risk of a CDO tranche is characterized in terms of sensitivities to shifts in risk factors [44, 85]. Accordingly, hedging practices have typically been based on such measures of sensitivity. The most common hedging approach has been to “delta hedge” spread fluctuations using credit default swaps (CDSs).

However, the recent turmoil in credit derivatives markets shows that these commonly used hedging approaches are inefficient. One of the main criticisms has been the lack of well-defined dynamics for the risk factors in such static models, which prevents any model-based assessment of hedging strategies. In particular, delta hedging of spread risk is loosely justified using a Black-Scholes analogy which does not necessarily hold, and the corresponding hedge ratios, the spread-deltas, are in fact computed from a static model without spread risk. Indeed, delta hedging of spread risk is not deduced from any theory of derivative replication. Furthermore, delta hedging of spread risk ignores default risk and jumps in the spreads, which appeared to be critical for risk management

during the difficult market environment in 2008. Although gamma hedging can improve performance slightly, it is not sufficient to solve these issues. Finally, the common approach to price portfolio credit derivatives using copula-based models does not guarantee the absence of arbitrage. Cont, Deguest, and Kan [25] show that pricing CDO tranches based on linear interpolation of the base correlations in a one-factor Gaussian copula model can lead to static arbitrage.

Given the deficiencies of copula-based hedging methods, alternatives have been proposed to tackle the problem of hedging portfolio credit derivatives. Durand and Jouanin [44] describe common hedging practices for credit derivatives and correctly point out the inconsistency between most of the pricing models, where the sole risk is in the occurrence of defaults, and delta hedging strategies, where the trader seeks to protect his/her portfolio against small movements in CDS spreads. Bielecki, Jeanblanc, and Rutkowski [9] show that, in a bottom- up hazard process framework driven by a Brownian motion, perfect replication is possible by continuously trading a sufficient number of liquid CDS contracts. Bielecki, Crépey, and Jeanblanc [8] discuss hedging performance in bottom-up and top-down models using simulation but do not comment on the performance of such strategies in a real market setting.

Laurent, Cousin, and Fermanian [71] study hedging of synthetic CDO tranches in a local intensity framework without spread risk, and show that CDO tranches can then be replicated by a self-financing portfolio consisting of the index default swap and a risk-free bond. However, as we will show in section 2.2, spread fluctuation is a major source of risk even in the absence of defaults, so failure to incorporate spread risk can lead to unrealistic conclusions.

Using a more realistic approach which acknowledges market incompleteness and incorporates both spread risk and default contagion, Frey and Backhaus [51] observe significant differences between the sensitivity-based hedging strategies computed in the Gaussian copula framework and the dynamic hedging strategies derived in their setup. They also show that variance-minimization hedging provides a model-based endogenous interpolation between the hedging against spread risk and default risk.

Giesecke, Goldberg, and Ding [53] discuss an alternative hedging approach based on a self-exciting process for portfolio defaults and compare the hedging performance for equity CDO tranches in September 2008 with a Gaussian copula model.

The hedging methods in these studies approach the problem from different, often incompatible, standpoints, and a systematic comparison of the resulting hedge ratios and the subsequent hedging performance has not been done in a realistic setting with market data. Needless to say, in order for such a comparison to be meaningful, the models need to be calibrated to the same data set. The very feasibility of this calibration is a serious (computational) constraint which excludes many models discussed in the literature, leading us to focus on the class of tractable models.

Motivated by previous studies indicating the impact of model uncertainty on the pricing and hedging derivative instruments [23], our objective is to assess the performance of hedging strategies of index CDO tranches derived under various model assumptions. We compare the performance of different dynamic hedging strategies across a range of models including the Gaussian copula model, a multiname reduced-form model introduced by Duffie and Gărleanu [41], a Markovian portfolio default model [60], and a two-factor model with spread and default risk [5]. Strategies considered include delta hedging of spread risk, hedging of default risk, variance minimization (quadratic hedging), and regression-based hedging.

In particular we shall attempt to address some important questions which have been left unanswered by previous studies:

- How did various hedging strategies for CDOs perform during major credit events in 2008?
- Do complete market models provide the right insight for hedging credit derivatives?
- How good are delta hedging strategies for CDO tranches?
- Does gamma hedging improve hedging performance?
- Do hedge ratios based on jump-to-default fare better than sensitivity-based hedge ratios?

- Are dynamic models better for hedging than static models?
- Do hedging strategies using single-name CDSs perform better than hedges using the index?
- Are bottom-up models more suitable for hedging than top-down models?

This chapter is structured as follows. Section 2.1 describes the cash flow structure of credit default swaps, index default swaps, and index CDO tranches. Section 2.2 presents the dataset used for the empirical analysis and describes some important statistical features of the CDO and CDS markets. Section 2.3 introduces the models under consideration and discusses procedures used for parameter calibration. Section 2.4 discusses the hedging strategies under consideration. Section 2.5 compares the performance of different strategies for the hedging of index tranches in 2008. Section 2.6 summarizes our main findings and discusses some implications.

2.1 Credit derivatives

A credit derivative is a financial instrument whose payoff depends on the losses due to defaults of the reference obligors (debt instruments). A portfolio credit derivative is a credit derivative whose payoffs depend on default losses in a reference portfolio of obligors. We will consider here index credit derivatives, for which the underlying portfolio is an equally weighted portfolio, such as the CDX or iTraxx indices. Typically, the payoffs depend only on the aggregate loss due to defaults in the index, not on the identity of the defaulting firm.

Consider an equally weighted portfolio consisting of n obligors, and assume for simplicity a constant recovery rate R (typically assumed to be 40%) and deterministic interest rates. Let τ_i be the default time of obligor i . The portfolio loss (in fraction of total notional value) at time t is equal to

$$L_t = \frac{1-R}{n} \sum_{i=1}^n 1_{\tau_i \leq t} = \frac{1-R}{n} N_t,$$

where N_t is the number of defaults by time t . The portfolio loss (L_t) is modeled as a stochastic process on a (filtered) probability space $(\Omega, \mathcal{F}, (\mathcal{F}_t), \mathbb{Q})$, where Ω is the set of market scenarios, (\mathcal{F}_t) represents the flow of information, and \mathbb{Q} is a risk-neutral probability measure representing the market pricing rule.

We will consider the three most commonly traded credit derivatives: credit default swaps (CDSs), index default swaps (index), and collateralized debt obligations (CDOs). All three derivatives are swap contracts between two parties, a protection buyer and a protection seller, whereby the protection buyer is compensated for the loss generated by the default of a reference obligor (CDS) or defaults from a pool of obligors (index and CDO). In return, the protection buyer pays a premium to the protection seller. A more detailed description of these products can be found in [28, 51, 76].

2.1.1 Credit default swaps

Consider a reference obligor i and its corresponding CDS contract initiated at time 0 with unit notional and payment dates $T_1 < T_2 < \dots < T_M$, where $T = T_M$ is the maturity date. Assume that the default payments are made on the next payment date¹, then if obligor i defaults between time T_{m-1} and T_m , the default payment at time T_m is equal to $1 - R$. On the other hand, if obligor i has not defaulted yet at time T_m , the protection seller will receive a premium payment $s_0^i(T_m - T_{m-1})$, where s_0^i is the CDS spread that has been determined at the inception.

The par CDS spread s_t^i quoted in the market at date t is defined as the value of the spread which sets the present values of the default leg and the premium leg equal. The mark-to-market value of a protection seller's position at time t is equal to the difference between the net present values of the two legs:

$$V_t^i = (s_0^i - s_t^i) \sum_{T_m > t} B(t, T_m)(T_m - T_{m-1})\mathbb{Q}(\tau_i > T_m | \mathcal{F}_t), \quad (2.1)$$

¹The default payment is sometimes assumed to be made immediately after the default. Nevertheless, the choice of payment schedule has negligible effects on our analysis in this chapter.

where $B(t, T_m)$ is the discount factor from time t to T_m . In what follows we will refer to the value of the protection seller's position as the mark-to-market value, and we will use $\mathbf{s}_t^{cds} = (s_t^1, \dots, s_t^n)$ to denote the vector of constituent CDS spreads and $\mathbf{D}_t = (1_{\tau_1 \leq t}, \dots, 1_{\tau_n \leq t})$ to denote the vector of default indicators at time t .

2.1.2 Index default swap

Index default swaps are now commonly traded on various credit indices such as iTraxx and CDX series which are equally weighted indices of CDSs. In an index default swap transaction initiated at time 0, a protection seller agrees to pay all default losses in the index in return for a fixed periodic spread s_0^{idx} paid on the total notional of obligors remaining in the index.

The index default swap par spread s_t^{idx} quoted in the market at time t is defined as the value of the spread which balances the present values of the default leg and the premium leg. The mark-to-market value of a protection seller's position at time t is equal to the difference between the two legs, which can be expressed as

$$V_t^{idx} = \left(s_0^{idx} - s_t^{idx} \right) \sum_{T_m > t} B(t, T_m) (T_m - T_{m-1}) E^{\mathbb{Q}} \left[1 - \frac{N_{T_m}}{n} \middle| \mathcal{F}_t \right]. \quad (2.2)$$

Here, we assume that the outstanding notional value is calculated at payment dates².

2.1.3 Collateralized debt obligations

Consider a tranche defined by an interval $[a, b]$, $0 \leq a < b \leq 1$, for the portfolio loss normalized by the total notional value of the underlying portfolio. We call a (resp., b) the attachment (resp., detachment) point of the tranche. A synthetic CDO tranche swap is a bilateral contract in which the protection seller agrees to pay all portfolio loss within the interval $[a, b]$ in return for a periodic spread $s_0^{[a,b]}$, which is determined at inception $t = 0$, on the remaining tranche notional value.

²A more precise valuation would consider the average outstanding notional value over the time period between the payment dates [15], but the approximation above has negligible effects on our analysis.

The par tranche spread $s_t^{[a,b]}$ quoted in the market at time t is defined as the spread which sets the present values of the default leg and the premium leg to be equal. The mark-to-market value of a protection seller's position (normalized by the total tranche notional value) at time t is equal to the difference between the two legs, which can be expressed as

$$V_t^{[a,b]} = \left(s_0^{[a,b]} - s_t^{[a,b]} \right) \sum_{T_m > t} \frac{B(t, T_m)}{b-a} (T_m - T_{m-1}) E^{\mathbb{Q}} \left[(b - L_{T_m})^+ - (a - L_{T_m})^+ \middle| \mathcal{F}_t \right]. \quad (2.3)$$

2.2 Data analysis

Our dataset contains the 5-year CDX North America Investment Grade Series 10 (CDX) index spreads; the standard tranche spreads with attachment/detachment points 0%, 3%, 7%, 10%, 15%, 30%, 100%; and the constituent 5-year CDS spreads, all obtained from Bloomberg. The time series runs from 25 March, 2008 until 25 September, 2008. Figure 2.1 illustrates the time series of the index, tranche [10%, 15%], CDS of IBM and Disney Corp.

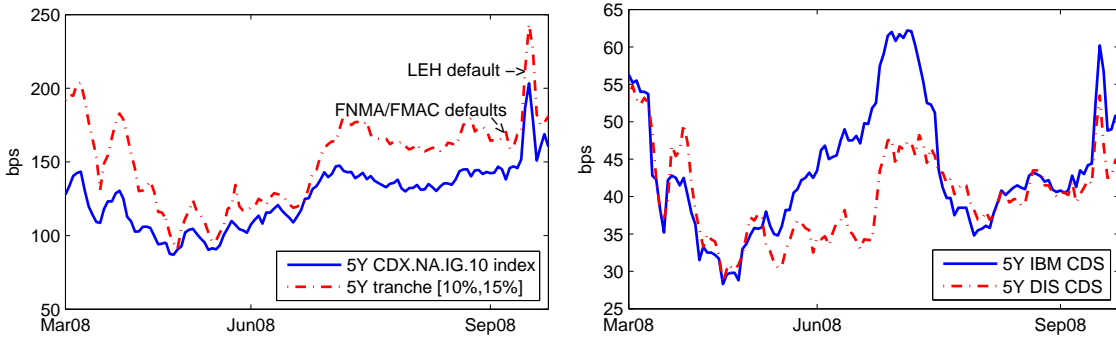


Figure 2.1: Left: 5Y CDX.NA.IG.10 index and tranche [10%, 15%] spreads. Right: 5Y CDS spreads of IBM and Disney Corp. (DIS)

2.2.1 Co-movements in CDSs and CDO tranches

A CDO hedging strategy should be based on a good understanding of the relation between the profit and loss (P&L) of the hedging instruments, namely the CDSs and the index, and that of the target instruments, the CDO tranches. Given that the P&L is driven mainly by the changes in spreads,

this requires a correct representation of co-movements in the credit spreads. Figure 2.2 shows the tranche [10%, 15%] daily spread returns against the index and IBM CDS daily spread returns. The crosses and circles represent the data points where spread returns of the two credit derivatives move in the same and opposite directions, respectively. Here we use IBM CDS and the [10%, 15%] tranche data for illustration, but similar results are obtained by looking at other constituent CDSs and tranches. From the figure, we can immediately observe two important properties:

1. CDS/Index spreads tend to move *together* with the tranche spreads when the movements are *large*.
2. In many cases, CDS/Index spreads and tranche spreads move in *opposite* directions, especially when the movements are *small*.

Large co-movements of the spreads, or common jumps, can be explained by the exposures of the credit derivatives to common risk factors which undergo large movements. This phenomenon can be seen more clearly in Table 2.1, which shows that the correlation between the index and tranche spread returns increases substantially if we condition on larger observations.

From a hedging perspective, frequent opposite movements between the CDS/index and the tranche spreads can lead to serious problems, because most hedging strategies imply positive hedge ratios with respect to the CDSs or the index. When the values of the hedging instruments and the tranche move in opposite directions, those strategies may fail to reduce the exposure of the tranche positions or, more seriously, can substantially amplify the overall exposure. As we will see in our empirical study in section 2.5, this problem frequently arises in common hedging strategies.

Index spread return	Unconditional	> 8%	> 5%	> 1%	< -1%	< -5%	< -8%
Correlation	0.63	0.82	0.82	0.60	0.68	0.71	0.81
Observations	126	4	12	52	43	11	6

Table 2.1: Conditional correlations between daily spread returns of the index and tranche [10%, 15%] show evidence of a common heavy-tailed factor.

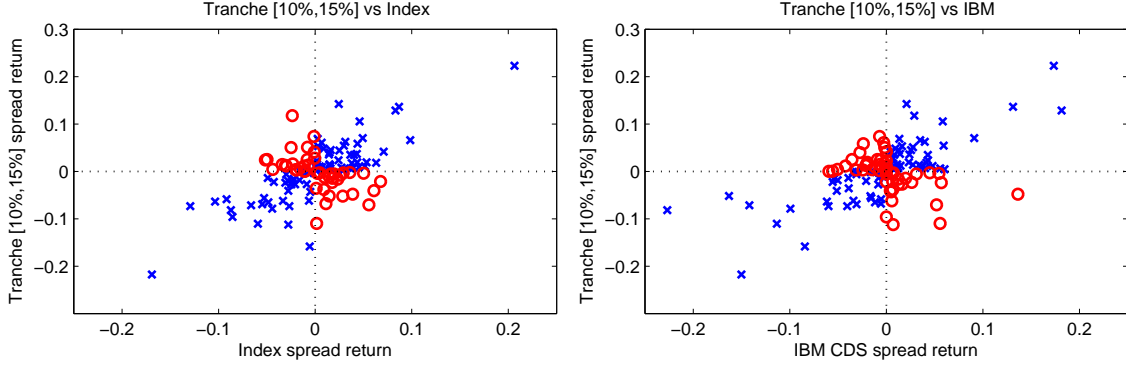


Figure 2.2: Tranche [10%, 15%] daily spread returns versus index daily spread returns and IBM CDS daily spread returns. Crosses represent data points where spread returns have the same signs (movements in the same direction), and circles represent data points where spread returns have opposite signs (movements in opposite directions).

2.2.2 Impact of defaults on credit spreads

Our sample period covers several important credit events: the takeover of Fannie Mae and Freddie Mac, which led to losses in the CDX, and the bankruptcy of Lehman Brothers, which led to a significant shock to the market.

During the sample period, Fannie Mae and Freddie Mac were taken over by the U.S. government on 7 September, 2008, which generated a credit event in the CDX reference portfolio. According to Bloomberg, the recovery rates of the 5-year senior CDS contracts of Fannie Mae and Freddie Mac were 92% and 94%, respectively, which will be used to determine the losses in our empirical study. On the other hand, although Lehman Brothers is *not* a reference obligor in the CDX, Figure 2.1 shows that there is considerable upward movement of the spreads on the next business day after Lehman Brothers announced bankruptcy.

Table 2.2 shows the daily spread returns on the next business day after Fannie Mae/Freddie Mac and Lehman Brothers credit events in units of sample standard deviation. Interestingly, we observe that the IBM, the index, and the super senior tranche [30%, 100%] spreads *decrease* on the next business day after Fannie Mae/Freddie Mac were taken over. Although the spreads of other tranches do increase, the magnitudes of these changes are rather small, less than 0.5 standard

deviations.

On the other hand, we *do* observe jumps in CDX spreads, but not necessarily on the dates corresponding to constituent defaults. The typical example is on 16 September, 2008 when Lehman Brothers filed for bankruptcy. Although Lehman Brothers is not a constituent of the CDX, the IBM, index, and tranche spreads increase by as much as 4.9 standard deviations, which are substantial upward moves and can be attributed to jumps.

These observations have two important implications. First, they show that jumps in the spreads are not necessarily tied to defaults in the underlying portfolio, as is the case in Markovian contagion models [5, 60] and self-exciting models [48, 53], where jumps occur only on portfolio default dates. Jumps may be caused by information external to the portfolio, such as macroeconomic events, of which the Lehman credit event is an example. Second, jump sizes at default dates appear to depend on the severity of the events, with lower recovery rate implying fewer or no upward jumps in the spreads. This suggests that models with constant jumps in the default intensity at each default are insufficient for capturing the impact of defaults on the spread movements: this impact should depend on the severity of loss in the given default, as suggested in [53]. We note that this may be difficult in practice, since recovery rates are usually not observable immediately after default and can be determined only after liquidation.

	IBM	Index	0%-3%	3%-7%	7%-10%	10%-15%	15%-30%	30%-100%
8-Sep-08	-0.66	-1.10	0.16	0.05	0.04	0.44	0.02	-0.06
16-Sep-08	3.23	4.55	3.51	4.92	4.45	3.91	4.14	4.05

Table 2.2: Daily spread returns on the next business day after Fannie Mae/Freddie Mac (8 September, 2008) and Lehman Brothers (16 September, 2008) credit events, normalized by unconditional sample standard deviations.

2.3 Models for portfolio credit derivatives

We will consider four different modeling approaches in our analysis: the one-factor Gaussian copula model [74], a bottom-up affine jump- diffusion model [41], a local intensity model [25, 28, 60, 77, 93],

and a top-down bivariate spread-loss model [5].

2.3.1 Gaussian copula model

The one-factor Gaussian copula model [74] is a standard market reference for pricing CDO tranches, in which the default times are constructed as

$$\tau_i = F_i^{-1}(\Phi(\rho M_0 + \sqrt{1 - \rho^2} M_i)),$$

where M_0, M_i are independent standard normal random variables, $\Phi(\cdot)$ is the standard normal distribution function, F_i is the marginal distribution of τ_i , and ρ is a correlation parameter. The distribution function $F_i(\cdot)$ is calibrated to the single-name CDS spreads by assuming a constant hazard rate.³ Then, we fit one correlation to each tranche, which is a situation known as compound correlations. If multiple correlations give the same tranche spread, we will choose the smallest one.

There are two reasons why we consider compound correlations instead of the base correlations [75] for calibration. As noted by Morgan and Mortensen [82], we found that computing the spread-deltas while keeping base correlations fixed can lead to a negative sensitivity of a tranche with respect to a change in the CDS spreads. Therefore, even if the CDS and the tranche spreads move in the same direction, especially when the movement is large, the negative spread-deltas will have the wrong sign and give poor hedging results. Second, unlike the Black-Scholes implied volatility, which is in a one-to-one correspondence to the vanilla options prices, base correlations are not guaranteed to exist. For instance, we were not able to calibrate the base correlation for 15% strike on many of the dates in our sample.

In order to express the hedging positions in later sections, it is convenient to write the mark-to-market values of the credit derivatives as functions of the modeling variables. Given the CDS spreads $\mathbf{s}_t^{cds} = \mathbf{s}^{cds} = (s^1, \dots, s^n)$, the default indicators $\mathbf{D}_t = \mathbf{D}$, and the set of compound correlations $\rho_t = \rho$, we write the mark-to-market values of CDS i , the index, and a tranche $[a, b]$ at time t

³The hazard rate term structure is usually assumed to be piecewise constant. Since we consider only CDS with one maturity for each obligor, it reduces to a constant hazard rate.

computed under the Gaussian copula model as $V_{gc}^i(t, s^i)$, $V_{gc}^{idx}(t, \mathbf{s}^{cds}, \boldsymbol{\rho}, \mathbf{D})$ and $V_{gc}^{[a,b]}(t, \mathbf{s}^{cds}, \boldsymbol{\rho}, \mathbf{D})$ respectively.

2.3.2 Affine jump-diffusion model

Various dynamic reduced-form models have been proposed to overcome some of the shortcomings of static copula-based models. An example of such a model used in industry is the affine jump-diffusion model introduced by Duffie and Gârleanu [41]. In this model the default time τ_i of an obligor i is modeled as a random time with a stochastic intensity (λ_t^i) given by

$$\lambda_t^i = X_t^i + a^i X_t^0, \quad (2.4)$$

where the idiosyncratic risk factors (X_t^1, \dots, X_t^n) and the common (macro) risk factor (X_t^0) are independent affine jump-diffusion processes

$$dX_t^i = \kappa(\theta - X_t^i)dt + \sigma \sqrt{X_t^i} dW_t^i + dJ_t^i,$$

where (W_t^i) are standard Brownian motions and (J_t^i) are compound Poisson process with exponentially distributed jump sizes. The conditional survival probability is then given by

$$\mathbb{Q}(\tau_i > T | \mathcal{F}_t) = E^{\mathbb{Q}} \left[\exp(- \int_t^T \lambda_u^i du) \middle| \mathcal{F}_t \right].$$

We will denote by $\mathbf{X}_t = (X_t^0, X_t^1, \dots, X_t^n)$ the risk factor values at time t . In order to calibrate the model, we follow the algorithm proposed by Eckner [45]. The tractability of this model relies on the conditional independence assumption of the default processes and also an analytical formula for the characteristic function of the affine jump-diffusion process. We refer readers to [41, 45] for the details of the calibration procedure.

Since $(\mathbf{X}_t, \mathbf{D}_t)$ is a Markov process, given the values $\mathbf{X}_t = \mathbf{X} = (X^0, X^1, \dots, X^n)$ and the default indicators $\mathbf{D}_t = \mathbf{D}$, we can write the mark-to-market values of CDS i , the index, and a tranche $[a, b]$ at time t computed under the affine jump-diffusion model as $V_{af}^i(t, X^0, X^i)$, $V_{af}^{idx}(t, \mathbf{X}, \mathbf{D})$ and $V_{af}^{[a,b]}(t, \mathbf{X}, \mathbf{D})$ respectively. The mark-to-market values are computed as given in (2.1), (2.2) and (2.3).

2.3.3 Local intensity models

Local intensity models [25, 28, 60, 77, 93] are top-down models in which the number of defaults N_t in a reference portfolio is modeled as a Markov point process with an intensity $\lambda_t = f(t, N_{t-})$: the portfolio default intensity is a (positive) function of time and the number of defaulted obligors.

We consider the following parametrization of the local intensity function, introduced by Herbertsson [60]:

$$\lambda_t = (n - N_{t-}) \sum_{k=0}^{N_{t-}} b_k, \quad (2.5)$$

where $\{b_k\}$ are the parameters. The interpretation of (2.5) is that the portfolio default intensity jumps by an amount b_k when the k th default happens. There is no sign restriction on $\{b_k\}$ as long as the portfolio default intensity remains positive. As in [60] we parametrize $\{b_k\}$ as

$$b_k = \begin{cases} b^{(1)} & 1 \leq k < \mu_1, \\ b^{(2)} & \mu_1 \leq k < \mu_2, \\ \vdots & \\ b^{(I)} & \mu_{I-1} \leq k < \mu_I = n, \end{cases} \quad (2.6)$$

where $1, \mu_1, \dots, \mu_I$ is a partition of $\{1, \dots, n\}$ which includes the attachment points of the tranches. The local intensity model is a Markovian top-down model in which the only risk factor is the loss process. Therefore we can express the mark-to-market values of the index and a tranche $[a, b]$ at date t computed as functions $V_{lo}^{idx}(t, N)$ and $V_{lo}^{[a,b]}(t, N)$ of the number of defaults and time.

2.3.4 Bivariate spread-loss model

One major shortcoming of the local intensity model is that spreads have piecewise-deterministic dynamics - i.e., no “volatility” - between defaults. As we have seen in Figure 2.1, credit derivative positions fluctuate substantially in value even in the absence of defaults in the underlying credit portfolio, so a hedging strategy based on the jump-to-default ratio may lead to poor performance.

A more realistic picture is given by a two-factor top-down model [5, 77] which accounts for both default risk and spread volatility by allowing the portfolio default intensity to depend on the number of defaults and a factor driving spread volatility:

$$\lambda_t = F(t, N_{t-}, Y_t).$$

Arnsdorff and Halperin [5] model the number of default N_t in a reference portfolio as a point process which has a (portfolio default) intensity (λ_t) that follows

$$\lambda_t = e^{Y_t} (n - N_{t-}) \sum_{k=0}^{N_{t-}} b_k, \quad (2.7)$$

where $\{b_k\}$ are parameters and the second factor (Y_t) generates spread volatility between default dates which follows an Ornstein-Uhlenbeck process

$$dY_t = -\kappa Y_t dt + \sigma dW_t,$$

where (W_t) is a standard Brownian motion. Notice that the parameters $\{b_k\}$ will provide enough degrees of freedom to fit the CDO tranche spreads on a given date, so the remaining parameters (κ, σ) are estimated from time series of tranche spreads as follows:

- On the first sample day: Set $Y_0 = 0$, $\kappa = 0.3$, and $\sigma = 0.7$ and calibrate $\{b_k\}$ to index and tranche spreads on day 1.
- On the j th sample day:
 1. Fix $\{b_k\}$ as those calibrated on day $j - 1$.
 2. Calibrate Y_0 , κ , and σ by minimizing the mean square pricing error of day $j - 10, j - 9, \dots, j$.
 3. Calibrate $\{b_k\}$ to the index and the tranche spreads on day j .

Since (N_t, Y_t) is a Markov process, given the values $N_t = N$ and $Y_t = Y$, we can write the mark-to-market values of the index and a tranche $[a, b]$ at time t computed under the bivariate spread-loss model as functions $V_{bi}^{idx}(t, Y, N)$ and $V_{bi}^{[a,b]}(t, Y, N)$ of the state variables.

2.3.5 Calibration results

All models are calibrated to the same market data using a 40% recovery rate. Table 2.3 shows the root mean square calibration error (RMSE). Since we calibrate the Gaussian copula model to each tranche with a different correlation (compound correlations), it by design gives good fits to the tranche spreads. The discrepancy of CDS spreads is due to the adjustment to match the index spreads. Top-down models are amendable to calibration to the market data as well. The RMSE are well within 2% for all tranches and around 5% for the CDS and the index. On the other hand, the Duffie-Gărleanu affine jump-diffusion does not calibrate market data as well as the top-down models. The CDS and the tranche spreads have RMSE at about 10%, which is still reasonable, but the fit to the index spread has RMSE larger than 20%, which is a poor fit. This is due to the fact that its calibration involves a high dimensional nonlinear optimization problem which is not guaranteed to converge. Therefore, we will consider only a hedging strategy using the single-name CDS as the hedging instruments in the affine jump-diffusion framework, so that the poor calibration to the index will not affect our analysis significantly. Note that, for all models under consideration, we have experienced a poor fit to the super senior tranche [30%, 100%], even with the Gaussian copula model. Since poor calibration leads to inaccurate computation of the mark-to-market values and the hedge ratios, we will omit the [30%, 100%] tranche in what follows.

Model	CDS	Index	0%-3%	3%-7%	7%-10%	10%-15%	15%-30%
Gaussian copula	6.04	0.00	0.00	0.18	0.05	0.00	0.00
affine jump-diffusion	14.53	21.67	14.56	5.05	10.40	13.91	6.17
Local intensity	-	6.29	1.60	0.95	0.46	0.34	1.71
Bivariate spread-loss	-	6.67	1.67	1.02	0.42	0.39	1.79

Table 2.3: Relative calibration error (RMSE), as a percentage of market spreads.

2.4 Hedging strategies

Our objective is to hedge a position in a tranche $[a, b]$ using the constituent CDSs and the index, and sometimes with an additional tranche $[l, u]$. We will now introduce different dynamic hedging strategies that aim to achieve this task.

We assume a continuously rebalancing framework and let (ϕ_t^i) , (ϕ_t^{idx}) and $(\phi_t^{[l,u]})$ be predictable processes which denote the hedging positions in CDS i , the index, and a tranche $[l, u]$, respectively. In addition, we will use the same notation as in section 2.3 to represent the mark-to-market values of the credit derivatives computed under different models. All hedging strategies are implemented using daily rebalancing.

2.4.1 Delta hedging of single-name spread movements

The most common approach for hedging CDO tranches is to hedge against small changes in the single-name CDS spreads [44, 85]. In practice, traders usually consider delta hedging under the Gaussian copula model where the corresponding hedging position in CDS i is known as the *spread-delta*:

$$\phi_t^i = \frac{\delta_{s^i} V_{gc}^{[a,b]}(t, \mathbf{s}_{t-}^{cds}, \boldsymbol{\rho}_{t-}, \mathbf{D}_{t-})}{\delta_{s^i} V_{gc}^i(t, \mathbf{s}_{t-}^i)}, \quad (2.8)$$

where

$$\begin{aligned} \delta_{s^i} V_{gc}^{[a,b]}(t, \mathbf{s}^{cds}, \boldsymbol{\rho}, \mathbf{D}) &= V_{gc}^{[a,b]}(t, \mathbf{s}^{cds} + \mathbf{e}_i, \boldsymbol{\rho}, \mathbf{D}) - V_{gc}^{[a,b]}(t, \mathbf{s}^{cds}, \boldsymbol{\rho}, \mathbf{D}), \\ \delta_{s^i} V_{gc}^i(t, s^i) &= V_{gc}^i(t, s^i + 1bp) - V_{gc}^i(t, s^i) \end{aligned}$$

are the change in values of a tranche $[a, b]$ and CDS i with respect to an increase in the CDS spread of obligor i by 1 basis point, while the correlations and other CDS spreads remain unchanged. $\mathbf{e}_i \in \mathbb{R}^n$ is a vector with all entries equal to 0 except for the i th entry equal to 1 basis point.

In order to compute the spread-deltas, we first calibrate the one-factor Gaussian copula model [74] to the market CDS and the tranche spreads as described in section ???. After that, we perturb

the CDS spread of, say, obligor i by 1 basis point while keeping all other CDS spreads and the correlations unchanged. Then, we *recalibrate* the hazard rate function of obligor i and compute the new values for CDS i and the tranche. The spread-delta defined by (2.8) is the ratio of the change in the tranche value to the change in the CDS value.

The main drawback of implementing the spread-deltas (2.8) is the absence of well-defined dynamics for the single-name CDS spreads in the Gaussian copula framework. On the other hand, we can consider delta hedging under the dynamic affine jump-diffusion model [41]. Hedging moves in the single-name CDS spreads is then equivalent to hedging against changes in the idiosyncratic risk factor. The corresponding position in CDS i is equal to

$$\phi_t^i = \frac{\partial_{X^i} V_{af}^{[a,b]}(t, \mathbf{X}_{t-}, \mathbf{D}_{t-})}{\partial_{X^i} V_{af}^i(t, X_{t-}^0, X_{t-}^i)}, \quad (2.9)$$

where $\partial_{X^i} V_{af}^{[a,b]}(t, \mathbf{X}, \mathbf{D})$ and $\partial_{X^i} V_{af}^i(t, X^0, X^i)$ are the partial derivatives with respect to X^i which can be approximated by finite differences. Note that one of the main differences between the hedge ratio (2.9) and the spread-delta (2.8) is that there is no recalibration involved when computing (2.9) under the affine jump-diffusion model.

2.4.2 Delta hedging of index spread movements

In section 2.2.1, we observe that the CDS and the tranche spreads appear to be driven by some common risk factors. Therefore, we may argue that it is also important to hedge against *global* movements in the CDS spreads. We use the Gaussian copula model and enter positions in the index to neutralize the *index spread-delta*:

$$\phi_t^{idx} = \frac{\Delta_{gc}^{[a,b]}(t)}{\Delta_{gc}^{idx}(t)}, \quad (2.10)$$

where

$$\begin{aligned} \Delta_{gc}^{[a,b]}(t) &= V_{gc}^{[a,b]}(t, \mathbf{s}_{t-}^{cds} + \mathbf{e}, \boldsymbol{\rho}_{t-}, \mathbf{D}_{t-}) - V_{gc}^{[a,b]}(t, \mathbf{s}_{t-}^{cds}, \boldsymbol{\rho}_{t-}, \mathbf{D}_{t-}), \\ \Delta_{gc}^{idx}(t) &= V_{gc}^{idx}(t, \mathbf{s}_{t-}^{cds} + \mathbf{e}, \mathbf{D}_{t-}) - V_{gc}^{idx}(t, \mathbf{s}_{t-}^{cds}, \mathbf{D}_{t-}), \end{aligned}$$

and $\mathbf{e} \in \mathbb{R}^n$ is a vector with all entries equal to 1 basis point. Notice that $\Delta_{gc}^{[a,b]}(t)$ and $\Delta_{gc}^{idx}(t)$ are the changes of a tranche $[a, b]$ and the index values with respect to a parallel shift in all CDS spreads by 1 basis point while keeping the correlations unchanged. Computation of the index spread-delta is the same as for the spread-deltas, except that we need to shift all CDS spreads by 1 basis point.

This strategy also has the advantage of being cost-effective. Unlike delta hedging individual CDS fluctuations, which requires rebalancing multiple hedging positions, this strategy only requires adjusting the position in the index.

If we consider the CDS/index spreads and the correlations as the market inputs, which is analogous to the stock price and implied volatility moves in equity derivatives markets, the index spread-delta (2.10) can also be computed by models other than the Gaussian copula model. The procedure is similar to the case described above in which we first calibrate the models to the CDS/index spreads and the correlations. Then, we recalibrate the models to the perturbed CDS/index spreads while keeping the correlations unchanged. The index spread-delta is the ratio of the change in tranche value over the change in the index value.

Figure 2.3 shows the index spread-deltas (2.10) computed under different models. Interestingly, we observe that the index spread-deltas are very similar across the models, except those for tranches [7%, 10%] and [10%, 15%] computed from the affine jump-diffusion model. In fact, this discrepancy is due only to the fact that the affine jump-diffusion model does not calibrate well to the market data.

The similarity of the index spread-deltas across the models implies that there is no point in using a more sophisticated model if its only use is to delta hedge spread risk. The standard one-factor Gaussian copula model would be sufficient to carry out this strategy. Indeed, a more meaningful hedging strategy for the dynamic models is to hedge against the underlying risk factors specified in the modeling framework, taking into account the dynamics of these factors and their correlations.

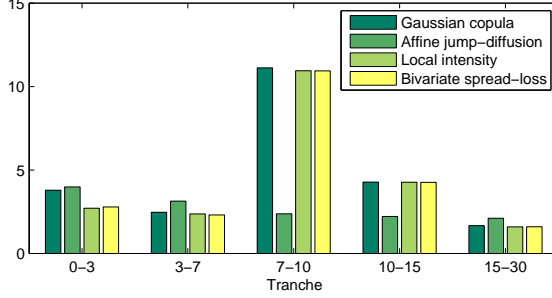


Figure 2.3: Index spread-deltas. Data: CDX.NA.IG.S10 on 25 March 2008.

2.4.3 Delta and gamma hedging of index spread movements

By analogy with gamma hedging of equity derivatives, one may consider hedging the second-order changes in the tranche values due to fluctuations in the CDS spreads. We consider positions in the index and a tranche $[l, u]$ such that

$$\begin{aligned}\Delta_{gc}^{[a,b]}(t) &= \phi_t^{[l,u]} \Delta_{gc}^{[l,u]}(t) + \phi_t^{idx} \Delta_{gc}^{idx}(t), \\ \Gamma_{gc}^{[a,b]}(t) &= \phi_t^{[l,u]} \Gamma_{gc}^{[l,u]}(t) + \phi_t^{idx} \Gamma_{gc}^{idx}(t),\end{aligned}$$

where

$$\begin{aligned}\Gamma_{gc}^{[a,b]}(t) &= V_{gc}^{[a,b]}(t, \mathbf{s}_{t-}^{cds} + \mathbf{e}, \boldsymbol{\rho}_{t-}, \mathbf{D}_{t-}) - 2V_{gc}^{[a,b]}(t, \mathbf{s}_{t-}^{cds}, \boldsymbol{\rho}_t, \mathbf{D}_{t-}) + V_{gc}^{[a,b]}(t, \mathbf{s}_{t-}^{cds} - \mathbf{e}, \boldsymbol{\rho}_{t-}, \mathbf{D}_{t-}) \\ \Gamma_{gc}^{idx}(t) &= V_{gc}^{idx}(t, \mathbf{s}_{t-}^{cds} + \mathbf{e}, \mathbf{D}_{t-}) - 2V_{gc}^{idx}(t, \mathbf{s}_{t-}^{cds}, \mathbf{D}_{t-}) + V_{gc}^{idx}(t, \mathbf{s}_{t-}^{cds} - \mathbf{e}, \mathbf{D}_{t-})\end{aligned}\quad (2.12)$$

are the *gammas* of a tranche $[a, b]$ and the index, or equivalently the second-order finite differences in the values with respect to 1 basis point shifting of all CDS spreads. Solving for the hedge ratios, we have

$$\phi_t^{idx} = \frac{\Delta_{gc}^{[a,b]}(t) \Gamma_{gc}^{[l,u]}(t) - \Delta_{gc}^{[l,u]}(t) \Gamma_{gc}^{[a,b]}(t)}{\Delta_{gc}^{idx}(t) \Gamma_{gc}^{[l,u]}(t) - \Delta_{gc}^{[l,u]}(t) \Gamma_{gc}^{idx}(t)}, \quad (2.13)$$

$$\phi_t^{[l,u]} = \frac{\Delta_{gc}^{[a,b]}(t) \Gamma_{gc}^{idx}(t) - \Delta_{gc}^{idx}(t) \Gamma_{gc}^{[a,b]}(t)}{\Delta_{gc}^{[l,u]}(t) \Gamma_{gc}^{idx}(t) - \Delta_{gc}^{idx}(t) \Gamma_{gc}^{[l,u]}(t)}. \quad (2.14)$$

Note that we can also delta hedge against movements in the single-name CDS spreads in the case of gamma hedging. However, we need to solve an ill-conditioned linear system which may lead

to unstable hedge ratios. Moreover, as we will see in section 2.5, the main component of changes in the single-name CDS spreads is a parallel move which is already reflected in the index spread. Thus, the inclusion of single-name CDS corresponds to hedging higher-order principal components, which have a smaller impact on the variance of the portfolio. Therefore, we do not include single-name CDS hedges in our gamma hedging analysis.

Unlike the situation in a Black-Scholes model, where the gamma of a call or put option is always positive and the gamma of a long position in a call or put option can be neutralized by shorting another call or put option, such simple relations fail to hold in the Gaussian copula framework for CDO tranches. Figure 2.4 shows the gammas of tranches [0%,3%] and [3%, 7%] computed for various days in the sample. Observe that the gammas can be positive or negative, even for the equity tranche. Moreover, the gammas of the two tranches do not have any clear relationship, in the sense that they do not always have the same sign. These results also suggest that the empirical performance of gamma hedging may depend on the choice of the hedging tranches, so we will consider below different choices of tranches as hedging instruments.

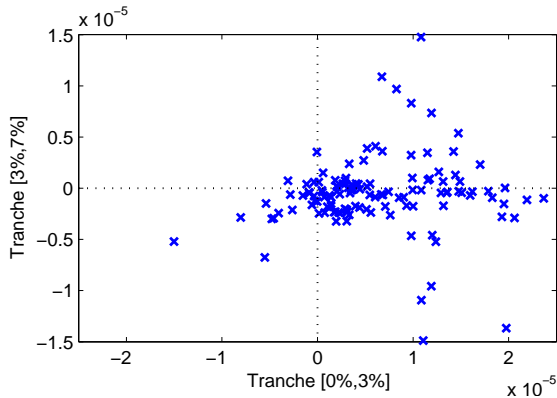


Figure 2.4: Values of gammas $\Gamma_{gc}^{[a,b]}(t)$ for [0%,3%] and [3%, 7%] CDX tranches. Each point represents one day in the sample.

2.4.4 Hedging parallel shifts in correlations

In addition to hedging against changes in spreads, by analogy with “vega” hedging in the Black-Scholes model, one can argue that it is also important to manage the risk of the fluctuation in another parameter of the Gaussian copula model, the implied correlation. We will consider scenarios where all (compound) correlations shift by the same magnitude.

A joint hedge with respect to small changes in spreads and correlation then requires to enter positions in the CDSs and a tranche $[l, u]$ such that

$$\begin{aligned}\delta_{s^i} V_{gc}^{[a,b]}(t, \mathbf{s}_{t-}^{cds}, \boldsymbol{\rho}_{t-}, \mathbf{D}_{t-}) &= \phi_t^{[l,u]} \delta_{s^i} V_{gc}^{[l,u]}(t, \mathbf{s}_{t-}^{cds}, \boldsymbol{\rho}_{t-}, \mathbf{D}_{t-}) + \phi_t^i \delta_{s^i} V_{gc}^i(t, s_{t-}^i), \quad i = 1, \dots, n, \\ \delta_\rho V_{gc}^{[a,b]}(t, \mathbf{s}_{t-}^{cds}, \boldsymbol{\rho}_{t-}, \mathbf{D}_{t-}) &= \phi_t^{[l,u]} \delta_\rho V_{gc}^{[l,u]}(t, \mathbf{s}_{t-}^{cds}, \boldsymbol{\rho}_{t-}, \mathbf{D}_{t-}),\end{aligned}$$

where

$$\delta_\rho V_{gc}^{[a,b]}(t, \mathbf{s}^{cds}, \boldsymbol{\rho}, \mathbf{D}) = V_{gc}^{[a,b]}(t, \mathbf{s}^{cds}, \boldsymbol{\rho} + 0.1\%, \mathbf{D}) - V_{gc}^{[a,b]}(t, \mathbf{s}^{cds}, \boldsymbol{\rho}, \mathbf{D})$$

is the change in the tranche value with respect to an increase in all compound correlations by 0.1%. Since the index is insensitive to the correlations, we must consider another tranche as a hedging instrument. Solving for the hedge ratios, we have

$$\begin{aligned}\phi_t^{[l,u]} &= \frac{\delta_\rho V_{gc}^{[a,b]}(t, \mathbf{s}_{t-}^{cds}, \boldsymbol{\rho}_{t-}, \mathbf{D}_{t-})}{\delta_\rho V_{gc}^{[l,u]}(t, \mathbf{s}_{t-}^{cds}, \boldsymbol{\rho}_{t-}, \mathbf{D}_{t-})}, \\ \phi_t^i &= \frac{1}{\delta_{s^i} V_{gc}^i(t, s_{t-}^i) \delta_\rho V_{gc}^{[l,u]}(t, \mathbf{s}_{t-}^{cds}, \boldsymbol{\rho}_{t-}, \mathbf{D}_{t-})} \left(\delta_{s^i} V_{gc}^{[a,b]}(t, \mathbf{s}_{t-}^{cds}, \boldsymbol{\rho}_{t-}, \mathbf{D}_{t-}) \delta_\rho V_{gc}^{[l,u]}(t, \mathbf{s}_{t-}^{cds}, \boldsymbol{\rho}_{t-}, \mathbf{D}_{t-}) \right. \\ &\quad \left. - \delta_\rho V_{gc}^{[a,b]}(t, \mathbf{s}_{t-}^{cds}, \boldsymbol{\rho}_{t-}, \mathbf{D}_{t-}) \delta_{s^i} V_{gc}^{[l,u]}(t, \mathbf{s}_{t-}^{cds}, \boldsymbol{\rho}_{t-}, \mathbf{D}_{t-}) \right).\end{aligned}$$

Note that this strategy does not take into account the *co-movements* in the index and in correlations. This is simply a first-order sensitivity-based hedge against moves in the CDS spreads and the correlation movements.

2.4.5 Hedging default risk

Although the common hedging practice is to protect against CDS spread fluctuations, the occurrence of defaults is also a major source of risk of a CDO tranche. The natural strategy to hedge against constituent defaults is to enter positions in the CDS or the index according to the *jump-to-default ratio*, which is defined as the ratio of the change in the tranche value over the change in the index (or CDS) value with respect to one additional default.

Since the top-down models, such as the local intensity model, focus on the next-to-default rather than the default of a specific obligor, there is only one jump-to-default ratio to be consider, which is equal to

$$\phi_t^{idx} = \frac{V_{lo}^{[a,b]}(t, N_{t-} + 1) - V_{lo}^{[a,b]}(t, N_{t-})}{V_{lo}^{idx}(t, N_{t-} + 1) - V_{lo}^{idx}(t, N_{t-})}. \quad (2.15)$$

The jump-to-default ratio under the bivariate spread-loss model is defined in the same manner.

On the other hand, since the bottom-up models specify the default probabilities of each obligor, there are n possible jump-to-default ratios to be considered. For the Gaussian copula model, the jump-to-default ratio corresponding to obligor i , using the index as the hedging instrument, is equal to

$$\phi_t^{idx} = \frac{V_{gc}^{[a,b]}(t, \mathbf{s}_{t-}^{cds}, \boldsymbol{\rho}_{t-}, \mathbf{D}_{t-} + \mathbf{u}_i) - V_{gc}^{[a,b]}(t, \mathbf{s}_{t-}^{cds}, \boldsymbol{\rho}_{t-}, \mathbf{D}_{t-})}{V_{gc}^{idx}(t, \mathbf{s}_{t-}^{cds}, \mathbf{D}_{t-} + \mathbf{u}_i) - V_{gc}^{idx}(t, \mathbf{s}_{t-}^{cds}, \mathbf{D}_{t-})}, \quad (2.16)$$

where $\mathbf{u}_i \in \mathbb{R}^n$ is a vector with all entries equal to 0 except for the i th entry equal to 1. We can define the jump-to-default ratio for the affine jump-diffusion model in the same manner.

Figure 2.5 shows the jump-to-default ratios computed from different models using the index as the hedging instrument as in (2.15) and (2.16). For the bottom-up models, the ratios are computed in the scenario where IBM defaults. Unlike the index spread-deltas, the jump-to- default ratios are substantially different across models. This implies that hedging against occurrence of default is also exposed to substantial model risk, because the jump-to-default ratio, which is computed by assuming the occurrence of one additional default, depends on the credit portfolio loss dynamic in

the modeling framework. Although each model is calibrated to the same CDS, index, and CDO market data, those credit derivatives provide information only on the *marginal distribution* of the loss process at some fixed times. Therefore, the dynamic of the loss process cannot be uniquely determined by the market data, and thus the jump-to-default ratios are substantially different across models.

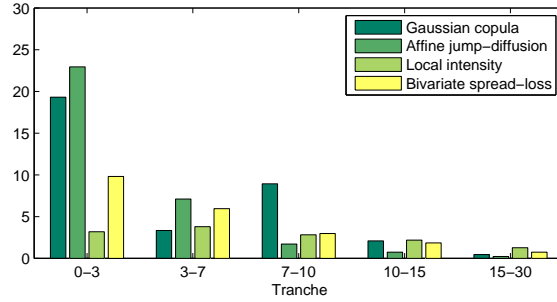


Figure 2.5: Jump-to-default ratios. Data: CDX.NA.IG.S10 on 25 March 2008. Ratios of Gaussian copula model and affine jump-diffusion model are computed by assuming IBM defaults.

2.4.6 Variance minimization

When spread risk and default risk are considered simultaneously, we are in an incomplete market setting, and hedging strategies in this setting need to be determined by an optimality criterion which takes both spread risk and default risk into account. A well-known approach to hedging in incomplete markets is the variance-minimizing strategy, introduced by Föllmer and Sondermann [50]. Unlike many other approaches to hedging in incomplete markets, it has been shown that this approach actually leads to analytically tractable hedging strategies [33, 51].

Definition 2.1. Let H be a square-integrable contingent claim at maturity T , and (X_t) be the discounted price process of the hedging instrument which is a square-integrable martingale under \mathbb{Q} . Let \mathcal{S} the set of admissible self-financing strategies with $E^{\mathbb{Q}} \left[\left(\int_0^T \phi_t dX_t \right)^2 \right] < \infty$. A variance-minimizing strategy is a choice of initial capital c and a self-financing trading strategy $(\phi_t) \in \mathcal{S}$

which minimizes the quadratic hedging error:

$$\inf_{c \in \mathbb{R}, (\phi_t) \in \mathcal{S}} E^{\mathbb{Q}} \left[\left(c + \int_0^T \phi_t dX_t - H \right)^2 \right]. \quad (2.17)$$

The variance (2.17) is computed under the risk-neutral probability measure \mathbb{Q} , because the models are calibrated to the observed credit spreads which only provide information on the risk factor dynamics under the risk-neutral measure. If we want to minimize the hedging error under the real-world measure, we will need a statistical model. One example is the regression-based hedging strategy in section 2.4.7.

Föllmer and Sondermann [50] characterize the variance-minimizing strategy in terms of a Galtchouk-Kunita-Watanabe projection of the claim on the set of replicable payoffs (see section 2.7). One nice property of the variance-minimizing strategy is that it coincides with the self-financing hedging strategy, which replicates the contingent claim in a complete market. Furthermore, in many Markovian models with jumps, the variance-minimizing hedge ratios can be explicitly computed [33, 51, 84]. The justification for this approach, which is not specific to credit derivatives, is discussed in [33, 51] from a methodological standpoint.

We will show that these variance-minimizing hedge ratios can be explicitly computed for the local intensity model and the bivariate spread-loss model. Our analysis will omit the Gaussian copula model and the affine jump-diffusion model. The reason is that since the Gaussian copula model defines the marginal distribution of the portfolio losses only at fixed times, there is no intrinsic dynamic for the loss process. For the affine jump-diffusion model, the computation requires inverting a high dimensional matrix (125×125) which is numerically unstable.

2.4.6.1 Local intensity model

Laurent, Cousin, and Fermanian [71] show that the local intensity framework generates a complete market in the sense that we can replicate the payoff of a tranche $[a, b]$ by means of a self-financing

portfolio with positions in the index default swap and a numeraire. The hedge ratio in the replication strategy then coincides with the variance-minimizing hedge ratio, which is equal to the jump-to-default ratio.

Proposition 2.1. *Consider a local intensity model in which the portfolio default intensity (λ_t) under the risk-neutral measure \mathbb{Q} has the form $\lambda_t = f(t, N_{t-})$ for some positive function $f(., .) > 0$. Let $V_{lo}^{idx}(t, N)$ and $V_{lo}^{[a,b]}(t, N)$ be the mark-to-market values of the index and a tranche $[a, b]$ at time t given N number of defaults which satisfy:*

- For $N = 0, \dots, n$, the functions $t \mapsto V_{lo}^{idx}(t, N)$ and $t \mapsto V_{lo}^{[a,b]}(t, N)$ belong to $C^1([0, T])$.
- $|V_{lo}^{idx}(t, N+1) - V_{lo}^{idx}(t, N)| > 0$ for all $t \in [0, T], N = 0, \dots, n-1$.

Then, the variance-minimizing hedge defined in Definition 2.1 for a tranche $[a, b]$ using the index as the only hedging instrument is given by

$$\phi_t = \frac{V_{lo}^{[a,b]}(t, N_{t-} + 1) - V_{lo}^{[a,b]}(t, N_{t-})}{V_{lo}^{idx}(t, N_{t-} + 1) - V_{lo}^{idx}(t, N_{t-})}. \quad (2.18)$$

The second condition in Proposition 2.1 implies that the index default swap value is always sensitive to defaults in the underlying portfolio. The proof of this proposition is shown in section 2.8.1.

2.4.6.2 Bivariate spread-loss model

In the bivariate spread-loss model, the portfolio default intensity is driven by the loss process (L_t) and a diffusion process (Y_t). Since we consider the index as the only hedging instrument, the market is incomplete in this two-factor framework. We use variance minimization to compute a trade-off between default risk and spread risk, as follows.

Proposition 2.2. *Consider the bivariate spread-loss model [5] in which the portfolio default intensity (λ_t) under the risk-neutral measure \mathbb{Q} follows (2.7). Let $V_{bi}^{idx}(t, Y, N)$ and $V_{bi}^{[a,b]}(t, Y, N)$ be the*

values of the index and a tranche $[a, b]$ at time t given N number of defaults and risk factor value Y which satisfy:

- For $N = 0, \dots, n$, the functions $(t, Y) \mapsto V_{bi}^{idx}(t, Y, N)$ and $(t, Y) \mapsto V_{bi}^{[a,b]}(t, Y, N)$ belong to $C^{1,2}([0, T] \times \mathbb{R})$.
- $[\partial_Y V_{bi}^{idx}(t, Y, N)]^2 + [\delta_N V_{bi}^{idx}(t, Y, N)]^2 \lambda > 0$ for all $t \in [0, T]$, $Y \in \mathbb{R}$, $N = 0, \dots, n - 1$.
- $E^{\mathbb{Q}} \left[\int_0^T \left(\partial_Y V_{bi}^{[a,b]}(t, Y_{t-}, N_{t-}) \right)^2 dt \right] < \infty$

where $\lambda = (n - N) \sum_{k=0}^N b_k$, $\partial_Y V_{bi}(t, Y, N)$ is the partial derivative with respect to Y and $\delta_N V_{bi}(t, Y, N) = V_{bi}(t, Y, N+1) - V_{bi}(t, Y, N)$ is the change of value with respect to one additional default. Then, the variance-minimizing hedge defined in Definition 2.1 for a tranche $[a, b]$ using the index as the only hedging instrument is given by

$$\phi_t = \frac{\partial_Y V_{bi}^{[a,b]}(t, Y_{t-}, N_{t-}) \partial_Y V_{bi}^{idx}(t, Y_{t-}, N_{t-}) \sigma^2 + \delta_N V_{bi}^{[a,b]}(t, Y_{t-}, N_{t-}) \delta_N V_{bi}^{idx}(t, Y_{t-}, N_{t-}) \lambda_t}{[\partial_Y V_{bi}^{idx}(t, Y_{t-}, N_{t-}) \sigma]^2 + [\delta_N V_{bi}^{idx}(t, Y_{t-}, N_{t-})]^2 \lambda_t} \quad (2.19)$$

The second condition in Proposition 2.2 implies that the index default swap is always sensitive to either the change of the risk factor (Y_t) or defaults in the underlying portfolio. The third condition is an integrability condition to ensure that the optimal hedging portfolio has finite variance. The proof of this proposition is shown in section 2.8.2.

Unlike the case of the local intensity model, the variance-minimizing hedge ratio for the bivariate spread-loss model involves not only the jump-to-default values but also the partial derivatives of the values with respect to the additional risk factor (Y_t). This reflects the fact that variance-minimization hedging is a strategy that takes both default risk and spread risk into account.

Figure 2.6 shows the variance-minimizing hedge ratios of the local intensity model and the bivariate spread-loss model. Similar to the case of comparing the jump-to-default ratios, the variance-minimizing hedge ratios are substantially different across the models, especially for the junior tranches. The reason for the differences is the same as the case for the jump-to-default ratios:

from (2.18) and (2.19), we can see that the variance-minimizing hedge ratio is a model-dependent quantity.

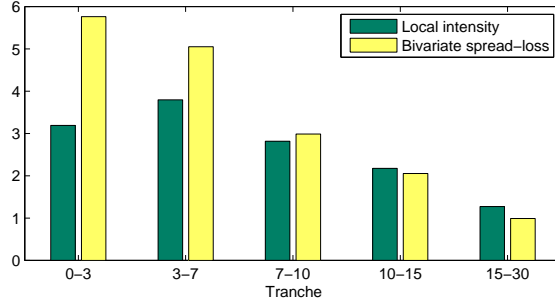


Figure 2.6: Variance-minimization hedge ratios. Data: CDX.NA.IG.S10 on 25 March 2008.

2.4.7 Regression-based hedging

One drawback of hedging strategies based on pricing models is that it is not clear how well the models can capture the dynamics of the credit spreads under the real-world measure, which is an important issue for hedging in practice. We now discuss a model-free, regression-based hedging strategy based on the observed dynamics of the credit spreads.

Consider a simple regression model relating the daily changes in the index and tranche values:

$$\delta V_{t_j}^{[a,b]} = \alpha^{[a,b]} + \beta^{[a,b]} \delta V_t^{idx} + \epsilon_j,$$

where $\delta V_{t_j} := V_{t_j} - V_{t_{j-1}}$ is the daily change of value from time t_{j-1} to t_j . $\alpha^{[a,b]}$ and $\beta^{[a,b]}$ can be estimated by the ordinary least squares regression over a rolling window. Choosing the hedging position in the index default swap as

$$\hat{\beta}_t^{[a,b]} := \frac{\sum_{t_j \leq t} (\delta V_{t_j}^{idx} - \overline{\delta V_t^{idx}})(\delta V_{t_j}^{[a,b]} - \overline{\delta V_t^{[a,b]}})}{\sum_{t_j \leq t} (\delta V_{t_j}^{idx} - \overline{\delta V_t^{idx}})^2} \quad (2.20)$$

yields a model-free hedging strategy which we call the *regression-based hedge*. Here $\overline{\delta V_t}$ is the average of daily P&L on $[0, t]$ and $\hat{\beta}_t^{[a,b]}$ is the estimate of $\beta^{[a,b]}$ using observations over the period $[0, t]$.

The main advantages of this strategy are its ability to directly capture the actual dynamics of co-movements in credit spreads and its simplicity.

2.5 Empirical performance of hedging strategies

We now present an empirical assessment of the performance of the eight hedging strategies described in section 2.4 using the dataset in section 2.2. Table 2.4 summarizes all the strategies that will be considered. Note that we will consider two choices of hedging tranches for gamma hedging where the details will be presented in the following subsections.

We consider the hedging of the protection seller's position on a CDX tranche, initiated on the first day of the sample period. On each day, we calibrate the models to the market data, as stated in section 2.4, and compute the corresponding hedging positions. A successful strategy should (substantially) reduce dispersion of the P&L distribution with respect to an unhedged position. Here, we use the following metrics to assess the reduction in magnitude and volatility of the daily P&L:

$$\text{Relative hedging error} = \left| \frac{\text{Average daily P\&L of hedged position}}{\text{Average daily P\&L of unhedged tranche position}} \right|,$$

$$\text{Residual volatility} = \frac{\text{Daily P\&L volatility of hedged position}}{\text{Daily P\&L volatility of unhedged tranche position}}.$$

Note that the two ratios should be close to 0 for a good hedging strategy.

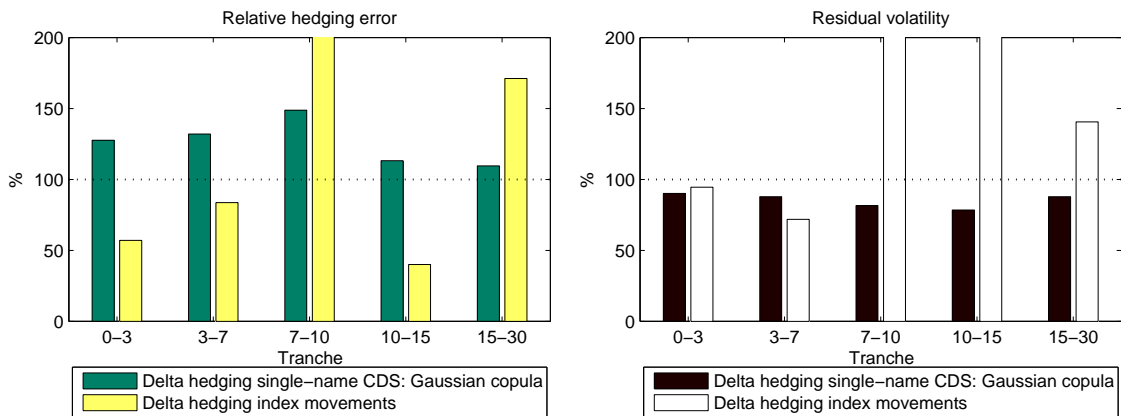
2.5.1 Does delta hedging work?

Our first analysis is to check whether the commonly criticized delta hedging strategies under the Gaussian copula model work. In Figure 2.7, we see that delta hedging does not work well. Indeed, the only effective strategy is a delta hedge against index movements, which reduces the absolute exposures of tranches [0%, 3%], [3%, 7%], and [10%, 15%]. On the other hand, delta hedging against single-name CDS movements fails to reduce absolute exposures. In terms of reduction in P&L volatility, delta hedging of single name CDS movements results in a consistent reduction of

Strategy	Underlying risk	Model	Type	Nature
1	Single-name CDS fluctuation	Gaussian copula	Bottom-up	Static
2	Global CDS/index fluctuation	Gaussian copula	Bottom-up	Static
3	1st and 2nd order global CDS fluctuation	Gaussian copula	Bottom-up	Static
4	Single-name CDS fluctuation + correlations shifts	Gaussian copula	Bottom-up	Static
5	Single-name CDS fluctuation	Affine jump-diffusion	Bottom-up	Dynamic
6	Default risk	Local intensity	Top-down	Dynamic
7	Variance minimization (risk-neutral measure)	Bivariate spread-loss	Top-down	Dynamic
8	Variance minimization (statistical measure)	Ordinary least squares regression	Statistical	-

Table 2.4: Overview of hedging strategies.

volatility across all tranches, while delta hedging index movements fails to do so for the three most senior tranches.

**Figure 2.7:** Comparison among delta hedging strategies based on the Gaussian copula model.

2.5.2 Does gamma hedging improve the performance?

In order to examine whether gamma hedging can improve performance, we consider two different choices of tranches as the hedging instruments, as illustrated in Table 2.5.

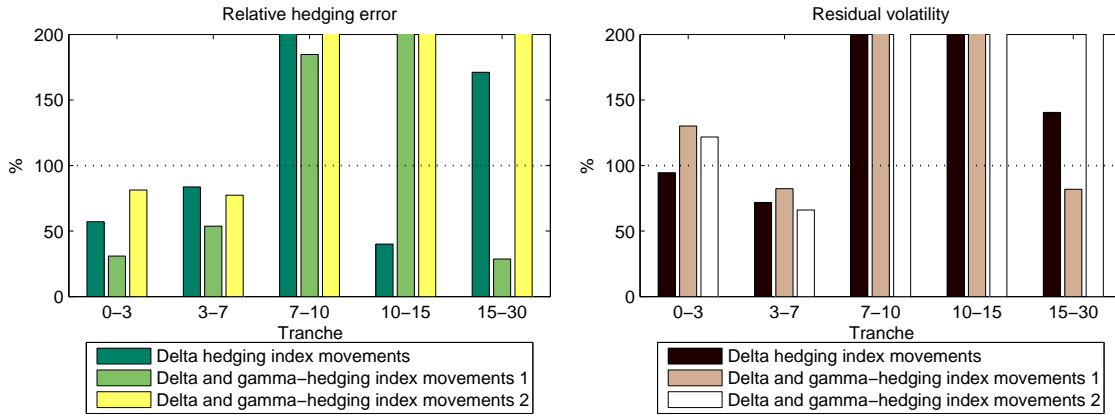
Hedging tranches in Case 1 are chosen such that they give the best performance in our sample in terms of the relative hedging errors, and those in Case 2 are chosen as a comparison with

Tranche being hedged	0%-3%	3%-7%	7%-10%	10%-15%	15%-30%
Hedging tranche: Case 1	7%-10%	7%-10%	10%-15%	15%-30%	10%-15%
Hedging tranche: Case 2	15%-30%	15%-30%	15%-30%	7%-10%	7%-10%

Table 2.5: Hedging tranches for gamma hedging strategy.

Case 1. Figure 2.8 shows that gamma hedging can help reduce the hedging error for the [0%,3%], [3%,7%], and [15%,30%] tranches and reduce the P&L volatility for the tranches [3%,7%] and [15%,30%]. However, gamma hedging worsens the hedging performance in all other cases. Moreover, its performance is very sensitive to the choice of hedging tranches.

In summary, we conclude that gamma hedging, while very sensitive to the choice of hedging instruments, does not necessarily perform well. Indeed, observations in section 2.2.1 suggest that the appropriate correction to delta hedging is not the second-order sensitivity with respect to the CDS spread movements but a correction taking into account jumps in spreads. This situation also arises in other contexts when jump risk is present [33].

**Figure 2.8:** Comparison among delta and gamma hedging strategies.

2.5.3 Can hedging parallel shifts in correlations improve the performance?

As shown in Figure 2.9, immunizing the portfolio against parallel shifts in the (implied) correlation does not improve performance: for almost all tranches neither the hedging error nor the P&L volatility is reduced. This suggests that the (observed) changes in the compound correlations are

typically not parallel. Hedging performance may be improved if we consider other scenarios for changes in the correlations.

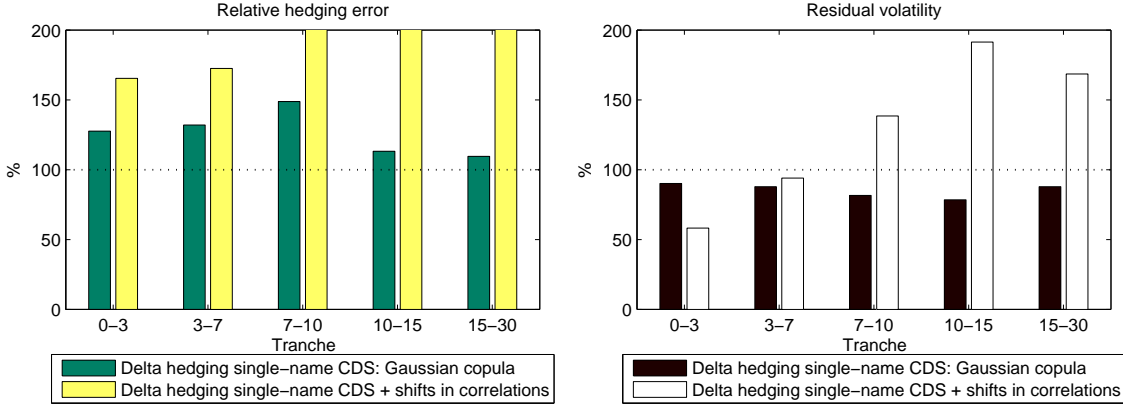


Figure 2.9: Comparison between delta hedging and the addition of hedging parallel shifts in compound correlations.

2.5.4 Do dynamic models have better hedging performance than static models?

Copula- based factor models have faced a lot of criticism for their insufficiency for hedging, and one popular explanation is that this is due to their static nature. In order to verify this claim, we compare the hedging performance of delta hedging under the static Gaussian copula model and under the dynamic affine jump-diffusion model [41].

Interestingly, the hedging error and the reduction in volatility ratios in Figure 2.10 do not provide any evidence that dynamic models perform better than this simple static model. Although the dynamic model successfully reduces the hedging error for tranches [10%,15%] and [15%, 30%], it amplifies the hedging error significantly for the two most junior tranches. Moreover, the residual volatilities from the dynamic model are larger than those from the static model for tranches [7%, 10%], [10%, 15%], and [15%, 30%].

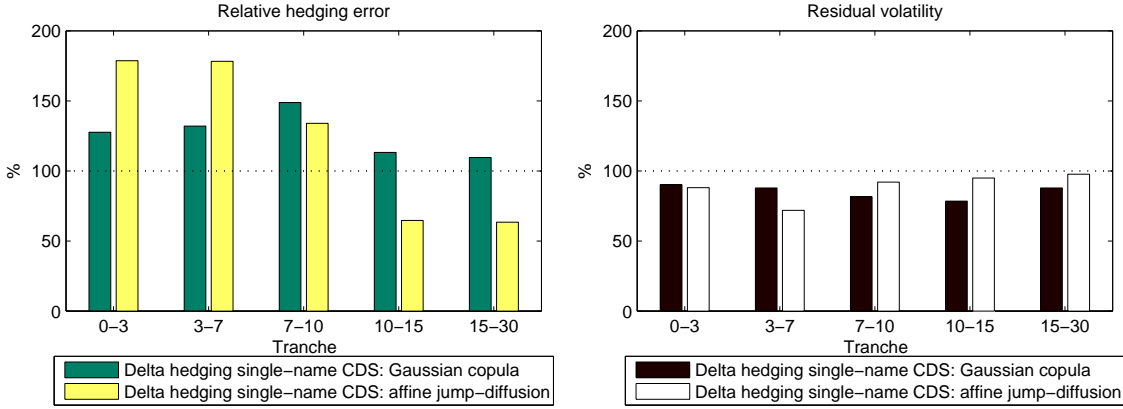


Figure 2.10: Comparison between delta hedging under the static Gaussian copula model and the dynamic affine jump-diffusion model.

2.5.5 Do bottom-up models perform better than top-down models?

Although top-down models are more flexible for calibration, it has been suggested that they may be inadequate for hedging [8]. However, this claim has not been backed by any empirical evidence: we will attempt to verify whether there is indeed an advantage in using bottom-up models for hedging.

Figure 2.11 compares the performance of various strategies based on bottom-up models, delta hedging based on the Gaussian copula model and the affine jump-diffusion model, versus the top-down strategies, hedging default risk based on the local intensity model and variance minimization based on the bivariate spread-loss model. First, we observe that the reduction of volatility is similar across the strategies, which does not provide much information to distinguish them. By comparing the hedging error, we find that the top-down models perform better than the bottom-up models for the three junior tranches, [0%,3%], [3%,7%], and [7%,10%], while bottom-up models fare better for the other two senior tranches.

Overall, there is no strong evidence that hedging based on the bottom-up models must perform better than that based on the top-down models. This observation contradicts the statements of Bielecki, Crépey, and Jeanblanc [8], who compare bottom-up and top-down hedging based on simulation. Although bottom-up models provide additional degrees of freedom, the effectiveness

of a hedging strategy is not about goodness of fit but depends on how well the model can predict short-term co-movements of the target instrument and the hedging instruments. From our results it appears that existing bottom-up models do a poor job at predicting such short-term co-movements.

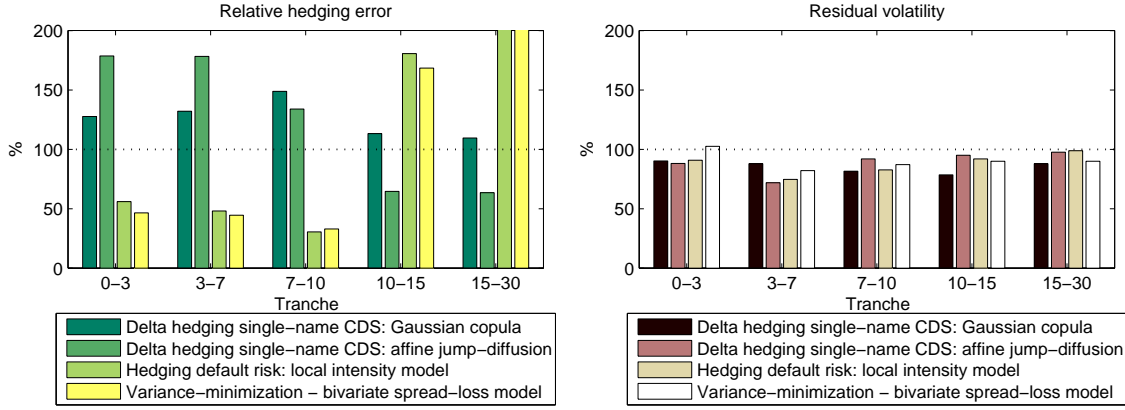


Figure 2.11: Comparison of top-down and bottom-up hedging.

2.5.6 How does model-based hedging compare to regression-based hedging?

Given the simplicity and intuitiveness of regression-based hedging, it is interesting to examine how well it performs relative to the model-based strategies. In Figure 2.12, we observe that regression-based hedging performs well across all tranches, consistently reducing both the hedging error and the daily P&L volatility. In particular, it reduces the volatilities for all tranches more than do the model-based strategies which are theoretically “optimal” in the respective models. This suggests that model misspecification is nonnegligible in all the models considered above.

2.5.7 Performance on credit event dates

Of particular interest is the performance of the hedging strategies on the next business day after the Lehman Brothers and Fannie Mae/ Freddie Mac credit events. Figure 2.13 shows the hedging error on the next business days after the credit events under various hedging strategies. During the Lehman Brothers event, we observe that the top-down and regression-based hedging outperform the

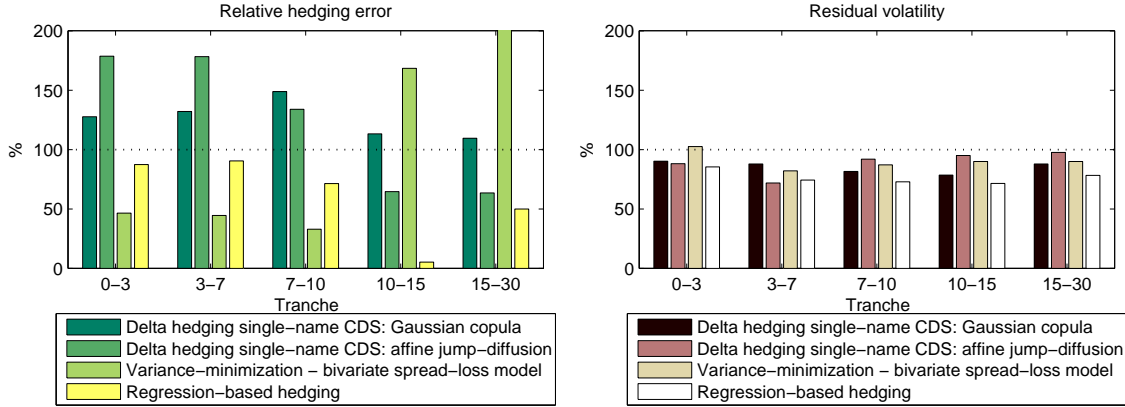


Figure 2.12: Comparison among top-down, bottom-up and regression-based hedging.

bottom-up hedging for all tranches. In particular, variance minimization based on the two-factor top-down model provides the best hedge for most tranches. This suggests that a macro event is better captured by top-down hedging.

On the other hand, all strategies failed to reduce the P&L during the Fannie Mae and Freddie Mac credit event, because, as we saw in section 2.2, the market happened to have anticipated the event, and there are no significant movements in the spreads. In particular, we observe a negative change in the CDS and index spreads, which leads to an increase in the overall exposure when we try to hedge the tranche positions with positive hedge ratios.

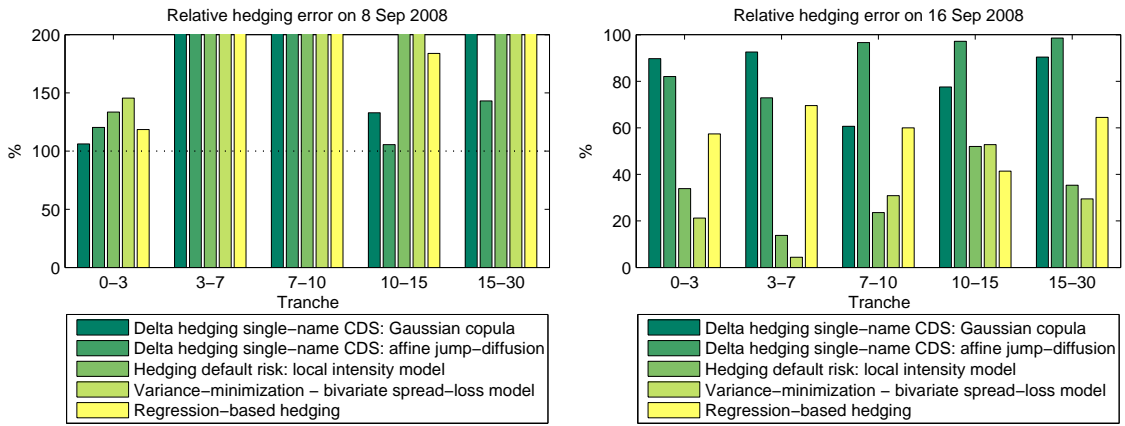


Figure 2.13: Comparison of strategies on the next business day after Fannie Mae/Freddie Mac (8 September 2008) and Lehman Brothers (16 September 2008) credit events.

2.6 Conclusion

We have presented theoretical and empirical comparison of a wide range of hedging strategies for portfolio credit derivatives, with a detailed analysis of the hedging of index CDO tranches. By comparing the performance of these strategies in 2008, our analysis reveals several interesting features:

- Our analysis reveals a large proportion of unhedgeable risk in CDO tranches. This suggests that market completeness is by no means an acceptable approximation, and toy models which assume a complete market may fail to provide useful insight for issues related to hedging of CDO tranches.
- Delta hedging of CDO tranche positions based on the Gaussian copula model is not effective.
- Although gamma hedging can improve the performance for certain tranches, its effectiveness is very sensitive to the choice of hedging instruments and is inconsistent across tranches.
- We do not find strong evidence that the Duffie and Ga  leanu [41] bottom-up dynamic model performs better than the static Gaussian copula model when it comes to delta hedging with credit default swaps.
- Moreover, bottom-up models ([41] and [74]) do not appear to perform consistently better than top-down models ([5] and [60]), in contrast to what has been asserted (without justification) in the literature [8]. In fact, during the period around the Lehman Brothers default, hedging strategies based on top-down models performed substantially better than those based on bottom-up models. This leads us to question the need for computationally costly dynamic bottom-up models instead of the top- down models for hedging portfolio credit derivatives.
- Model-free regression-based hedging appears to be surprisingly effective when compared to other hedging strategies. This suggests - not surprisingly - that incorporating the statistical behavior of credit spreads is an important criterion for a successful hedging strategy.

- We find evidence for common jumps, or large co-movements, in spreads. However, index and tranche spreads did not appear to have upward jumps at the default dates of index constituents. This observation goes against models, such as Markovian contagion models [5, 60] and self-exciting models [53], in which jumps in spreads occur only at constituent default dates. Jumps in spreads may also arise from unexpected events not necessarily related to defaults inside the portfolio.

We have left out many practically important considerations, such as liquidity, transaction costs, and computational issues, when assessing hedging performance. The (*il*)*liquidity* of CDS contracts leads to questions of feasibility of hedging strategies which require frequent rebalancing of positions in single-name CDS. *Transaction costs* - as reflected, for instance, in bid-ask spreads - are known to be higher for single-name CDS contracts than for the index, and taking them into account would favor top-down/index hedging strategies as opposed to hedging with single-name CDS, which requires rebalancing more than a hundred single- name CDS positions. Finally, computational costs are much lower for the top-down models, especially when it comes to calibration: various fast calibration methods have been proposed for top-down models [5, 25, 28, 77], whereas parameter calibration, especially if it needs to be done on a periodic basis, remains nontrivial for bottom-up models [45]. Therefore it should be clear that taking these aspects into account would tilt the comparison even more in favor of top-down/index hedging as opposed to hedging with single-name CDS.

2.7 Variance-minimizing hedge and Galtchouk-Kunita-Watanabe decomposition

Our work in this section is similar to the earlier work by Frey and Backhaus [51]. We first define the *gain process* for the index and tranches. Let $P^{idx}(T_m)$ be the net payment received from an index default swap contract at time T_m which is bounded by definition. The mark-to-market value

of an index default swap at time t is equal to

$$V_t^{idx} = \sum_{T_m > t} B(t, T_m) E^{\mathbb{Q}}[P^{idx}(T_m) | \mathcal{F}_t].$$

We define the discounted value process as

$$\tilde{V}_t^{idx} := B(0, t) V^{idx}(t).$$

Then, the gain process is defined as the present value of all cash-flows:

$$G_t^{idx} = \sum_{T_m \leq t} B(0, T_m) P^{idx}(T_m) + \tilde{V}_t^{idx} = E^{\mathbb{Q}} \left[\sum_{T_m > 0} B(0, T_m) P^{idx}(T_m) \middle| \mathcal{F}_t \right], \quad (2.21)$$

where (G_t^{idx}) is a square-integrable (bounded) martingale under \mathbb{Q} . Similarly, we can derive the expression for the gain process of a $[a, b]$ tranche $(G_t^{[a,b]})$ which is also a square-integrable (bounded) martingale under \mathbb{Q} .

Consider the variance minimization setting in Definition 2.1. Our goal is to hedge a tranche $[a, b]$ using the index default swap. Although we consider a terminal payoff H at maturity in Definition 2.1, the results in [84] allow us to replace the conditional expected value of the terminal payoff $E^{\mathbb{Q}}[H | \mathcal{F}_t]$ by the gain process value $G_t^{[a,b]}$. Let (ϕ_t) be the variance-minimizing hedging strategy which represents positions in the index default swap. Then, it can be shown that (see [50]) (ϕ_t) satisfies the Galtchouk-Kunita-Watanabe decomposition

$$G_t^{[a,b]} = G_0^{[a,b]} + \int_0^t \phi_s dG_s^{idx} + Z_t, \quad (2.22)$$

where the process $(Z_t G_t^{idx})$ is a martingale under \mathbb{Q} . Therefore, the variance-minimizing strategy satisfies

$$d\langle G^{[a,b]}, G^{idx} \rangle_t = \phi_t d\langle G^{idx} \rangle_t, \quad 0 \leq t \leq T, \quad (2.23)$$

where $(\langle G \rangle_t)$ denotes the unique predictable process with $\langle G \rangle_0 = 0$ and right-continuous increasing paths such that $(G_t^2 - \langle G \rangle_t)$ is a martingale under \mathbb{Q} .

Remark 2.1. Instead of variance minimization in Definition 2.1, Föllmer and Sondermann [50] introduce a stronger optimality condition which is known as risk-minimization. However, since the gain processes of the index and CDO tranches are bounded martingales under \mathbb{Q} , the trading strategies are the same under the two optimal criteria.

2.8 Derivation of the variance-minimizing hedge ratio

The key to computing the variance-minimizing hedge under a particular model is to express (G_t^{idx}) and $(G_t^{[a,b]})$ as stochastic integrals, use the Ito isometry formula for these stochastic integrals, then solve (2.23) (see, e.g., [33]). In particular, Frey and Backhaus [51] show the derivation for the *convex counterparty risk model*, and our following computations are similar to those in [51].

2.8.1 Proof of Proposition 2.1

Let (U_t) be a deterministic counting process which jumps by 1 at payment dates, i.e. $U_{T_m} - U_{T_{m-1}} = 1$ for all $m = 1, \dots, M$. Using Ito's lemma, the dynamic of the discounted value process under \mathbb{Q} for the index follows

$$d\tilde{V}_{lo}^{idx}(t, N_{t-}) = \frac{\partial}{\partial t}\tilde{V}_{lo}^{idx}(t, N_{t-})dt + \delta_N \tilde{V}_{lo}^{idx}(t, N_{t-})dN_t - B(0, t)P^{idx}(t)dU_t,$$

where $P^{idx}(t)$ is the net payment received at time t . Using Ito's lemma again and from (2.21), dynamic of the gain process under \mathbb{Q} for the index follows

$$\begin{aligned} dG_{lo}^{idx}(t) &= B(0, t)P^{idx}(t)dU_t + d\tilde{V}_{lo}^{idx}(t, N_{t-}) \\ &= \frac{\partial}{\partial t}\tilde{V}_{lo}^{idx}(t, N_{t-})dt + \delta_N \tilde{V}_{lo}^{idx}(t, N_{t-})dN_t \\ &= \left(\frac{\partial}{\partial t}\tilde{V}_{lo}^{idx}(t, N_{t-}) + \delta_N \tilde{V}_{lo}^{idx}(t, N_{t-})\lambda_t \right) dt + \delta_N \tilde{V}_{lo}^{idx}(t, N_{t-})dN_t^c \\ &= \delta_N \tilde{V}_{lo}^{idx}(t, N_{t-})dN_t^c, \end{aligned}$$

where $(N_t^c) = (N_t - \int_0^t \lambda_s ds)$ is the compensated version of (N_t) . The last equality comes from the fact that $(G_{lo}^{idx}(t))$ is a martingale under \mathbb{Q} . Similar, the gain process of a tranche $[a, b]$ under \mathbb{Q}

follows

$$dG_{lo}^{[a,b]}(t) = \delta_N \tilde{V}_{lo}^{[a,b]}(t, N_{t-}) dN_t^c.$$

We now compute the compensators involved in (2.23) and obtain

$$\begin{aligned} \phi_t &= \frac{\delta_N \tilde{V}_{lo}^{[a,b]}(t, N_{t-}) \delta_N \tilde{V}_{lo}^{idx}(t, N_{t-}) \lambda_t}{(\delta_N \tilde{V}_{lo}^{idx}(t, N_{t-}))^2 \lambda_t} \\ &= \frac{B(0, t) \delta_N V_{lo}^{[a,b]}(t, N_{t-})}{B(0, t) \delta_N V_{lo}^{idx}(t, N_{t-})} \\ &= \frac{V_{lo}^{[a,b]}(t, N_{t-} + 1) - V_{lo}^{[a,b]}(t, N_{t-})}{V_{lo}^{idx}(t, N_{t-} + 1) - V_{lo}^{idx}(t, N_{t-})}. \end{aligned}$$

Then, we want to show that the hedging portfolio by implementing the above strategy has finite variance, i.e. $E^{\mathbb{Q}} \left[\int_0^T \phi_t dG_{lo}^{idx}(t) \right]^2 < \infty$, and it is sufficient to show that $E^{\mathbb{Q}} \left[\int_0^T \phi_t^2 d\langle G_{lo}^{idx} \rangle_t \right] < \infty$. Since all the cash flows of tranche $[a, b]$ are bounded, there exists a $K > 0$ such that $|V_{lo}^{[a,b]}(t, N)| \leq K/2$ for all $t \in [0, T]$, $N = 0, \dots, n$, which implies that $|\delta_N V_{lo}^{[a,b]}(t, N)| \leq K$ for all $t \in [0, T]$, $N = 0, \dots, n$. Consider

$$\begin{aligned} E^{\mathbb{Q}} \left[\int_0^T \phi_t^2 d\langle G_{lo}^{idx} \rangle_t \right] &= E^{\mathbb{Q}} \left[\int_0^T \left(\frac{\delta_N V_{lo}^{[a,b]}(t, N_{t-})}{\delta_N V_{lo}^{idx}(t, N_{t-})} \right)^2 \left(\delta_N \tilde{V}_{lo}^{idx}(t, N_{t-}) \right)^2 \lambda_t dt \right] \\ &\leq E^{\mathbb{Q}} \left[\int_0^T \left(\delta_N V_{lo}^{[a,b]}(t, N_{t-}) \right)^2 \lambda_t dt \right] \\ &\leq K^2 E^{\mathbb{Q}} \left[\int_0^T \lambda_t dt \right] \\ &\leq K^2 n < \infty, \end{aligned}$$

which gives the desired result.

Note that if we implement this hedging strategy, we have

$$dG_{lo}^{[a,b]}(t) = \phi_t dG_{lo}^{idx}(t).$$

The tranche is perfectly hedged in this case, which is consistent with the results of [71].

2.8.2 Proof of Proposition 2.2

Defining the deterministic counting process (U_t) as in section 2.8.1 and applying Ito's lemma, the dynamic of the discounted value process for the index becomes

$$\begin{aligned} d\tilde{V}_{bi}^{idx}(t, Y_{t-}, N_{t-}) &= \frac{\partial}{\partial t}\tilde{V}_{bi}^{idx}(t, Y_{t-}, N_{t-})dt + \frac{\partial}{\partial Y}\tilde{V}_{bi}^{idx}(t, Y_{t-}, N_{t-})dY_t \\ &\quad + \frac{1}{2}\frac{\partial^2}{\partial Y^2}\tilde{V}_{bi}^{idx}(t, Y_{t-}, N_{t-})\sigma^2dt + \delta_N\tilde{V}_{bi}^{idx}(t, Y_{t-}, N_{t-})dN_t - B(0, t)P^{idx}(t)dU_t, \end{aligned}$$

where $P^{idx}(t)$ is the net payment received at time t . Then, using Ito's lemma again and from (2.21), dynamic of the gain process for the index follows

$$\begin{aligned} dG_{bi}^{idx}(t) &= B(0, t)P^{idx}(t)dU_t + d\tilde{V}_{bi}^{idx}(t, Y_{t-}, N_{t-}) \\ &= \frac{\partial}{\partial t}\tilde{V}_{bi}^{idx}(t, Y_{t-}, N_{t-})dt + \frac{\partial}{\partial Y}\tilde{V}_{bi}^{idx}(t, Y_{t-}, N_{t-})dY_t \\ &\quad + \frac{1}{2}\frac{\partial^2}{\partial Y^2}\tilde{V}_{bi}^{idx}(t, Y_{t-}, N_{t-})\sigma^2dt + \delta_N\tilde{V}_{bi}^{idx}(t, Y_{t-}, N_{t-})dN_t \\ &= \left(\frac{\partial}{\partial t}\tilde{V}_{bi}^{idx}(t, Y_{t-}, N_{t-}) - \frac{\partial}{\partial Y}\tilde{V}_{bi}^{idx}(t, Y_{t-}, N_{t-})\kappa Y_t \right. \\ &\quad \left. + \frac{1}{2}\frac{\partial^2}{\partial Y^2}\tilde{V}_{bi}^{idx}(t, Y_{t-}, N_{t-})\sigma^2 + \delta_N\tilde{V}_{bi}^{idx}(t, Y_{t-}, N_{t-})\lambda_t \right) dt \\ &\quad + \frac{\partial}{\partial Y}\tilde{V}_{bi}^{idx}(t, Y_{t-}, N_{t-})\sigma dW_t + \delta_N\tilde{V}_{bi}^{idx}(t, Y_{t-}, N_{t-})dN_t^c \\ &= \frac{\partial}{\partial Y}\tilde{V}_{bi}^{idx}(t, Y_{t-}, N_{t-})\sigma dW_t + \delta_N\tilde{V}_{bi}^{idx}(t, Y_{t-}, N_{t-})dN_t^c. \end{aligned}$$

Similarly, the gain process of a tranche $[a, b]$ follows

$$dG_{bi}^{[a,b]}(t) = \frac{\partial}{\partial Y}\tilde{V}_{bi}^{[a,b]}(t, Y_{t-}, N_{t-})\sigma dW_t + \delta_N\tilde{V}_{bi}^{[a,b]}(t, Y_{t-}, N_{t-})dN_t^c.$$

We can now compute the compensators of $(G_{bi}^{[a,b]}(t))$ and $(G_{bi}^{idx}(t))$ and use (2.23) to compute (ϕ_t) which gives (2.19).

Let us now show that the hedging portfolio based on (2.19) has finite variance. Consider the

following:

$$\begin{aligned}
& E^{\mathbb{Q}} \left[\int_0^T \phi_t d\langle G_{bi}^{idx} \rangle_t \right] \\
= & E^{\mathbb{Q}} \left[\int_0^T \left[\partial_Y \tilde{V}_{bi}^{[a,b]}(t, Y_{t-}, N_{t-}) \partial_Y \tilde{V}_{bi}^{idx}(t, Y_{t-}, N_{t-}) \sigma^2 \right. \right. \\
& \quad \left. \left. + \delta_N \tilde{V}_{bi}^{[a,b]}(t, Y_{t-}, N_{t-}) \delta_N \tilde{V}_{bi}^{idx}(t, Y_{t-}, N_{t-}) \lambda_t \right]^2 \right. \\
& \quad \times \frac{1}{(\partial_Y \tilde{V}_{bi}^{idx}(t, Y_{t-}, N_{t-}) \sigma)^2 + (\delta_N \tilde{V}_{bi}^{idx}(t, Y_{t-}, N_{t-}))^2 \lambda_t} dt \Bigg] \\
\leq & E^{\mathbb{Q}} \left[\int_0^T \left[\partial_Y V_{bi}^{[a,b]}(t, Y_{t-}, N_{t-}) \partial_Y V_{bi}^{idx}(t, Y_{t-}, N_{t-}) \sigma^2 \right. \right. \\
& \quad \left. \left. + \delta_N V_{bi}^{[a,b]}(t, Y_{t-}, N_{t-}) \delta_N V_{bi}^{idx}(t, Y_{t-}, N_{t-}) \lambda_t \right]^2 \right. \\
& \quad \times \frac{1}{(\partial_Y V_{bi}^{idx}(t, Y_{t-}, N_{t-}) \sigma)^2 + (\delta_N V_{bi}^{idx}(t, Y_{t-}, N_{t-}))^2 \lambda_t} dt \Bigg] \\
\leq & 2E^{\mathbb{Q}} \left[\int_0^T \frac{\left[\partial_Y V_{bi}^{[a,b]}(t, Y_{t-}, N_{t-}) \partial_Y V_{bi}^{idx}(t, Y_{t-}, N_{t-}) \sigma^2 \right]^2}{(\partial_Y V_{bi}^{idx}(t, Y_{t-}, N_{t-}) \sigma)^2 + (\delta_N V_{bi}^{idx}(t, Y_{t-}, N_{t-}))^2 \lambda_t} dt \right] \\
& + 2E^{\mathbb{Q}} \left[\int_0^T \frac{\left[\delta_N V_{bi}^{[a,b]}(t, Y_{t-}, N_{t-}) \delta_N V_{bi}^{idx}(t, Y_{t-}, N_{t-}) \lambda_t \right]^2}{(\partial_Y V_{bi}^{idx}(t, Y_{t-}, N_{t-}) \sigma)^2 + (\delta_N V_{bi}^{idx}(t, Y_{t-}, N_{t-}))^2 \lambda_t} dt \right].
\end{aligned}$$

Consider the first term. For a fixed time t , the integrand is equal to zero if $\partial_Y V_{bi}^{idx}(t, Y_{t-}, N_{t-}) = 0$.

If $\partial_Y V_{bi}^{idx}(t, Y_{t-}, N_{t-}) \neq 0$, we have

$$\frac{\left[\partial_Y V_{bi}^{[a,b]}(t, Y_{t-}, N_{t-}) \partial_Y V_{bi}^{idx}(t, Y_{t-}, N_{t-}) \sigma^2 \right]^2}{(\partial_Y V_{bi}^{idx}(t, Y_{t-}, N_{t-}) \sigma)^2 + (\delta_N V_{bi}^{idx}(t, Y_{t-}, N_{t-}))^2 \lambda_t} \leq \left[\partial_Y V_{bi}^{[a,b]}(t, Y_{t-}, N_{t-}) \sigma \right]^2.$$

For the second expectation, for a fixed time t , the integrand is equal to zero if $\delta_N V_{bi}^{idx}(t, Y_{t-}, N_{t-}) \lambda_t = 0$. Otherwise, we have

$$\frac{\left[\delta_N V_{bi}^{[a,b]}(t, Y_{t-}, N_{t-}) \delta_N V_{bi}^{idx}(t, Y_{t-}, N_{t-}) \lambda_t \right]^2}{(\partial_Y V_{bi}^{idx}(t, Y_{t-}, N_{t-}) \sigma)^2 + (\delta_N V_{bi}^{idx}(t, Y_{t-}, N_{t-}))^2 \lambda_t} \leq \left(\delta_N V_{bi}^{[a,b]}(t, Y_{t-}, N_{t-}) \right)^2 \lambda_t.$$

Using the fact that $\delta_N V_{bi}^{[a,b]}(t, Y, N)$ is bounded, we obtain

$$\begin{aligned} E^{\mathbb{Q}} \left[\int_0^T \phi_t d\langle G_b^{idx} i \rangle_t \right] &\leq 2E^{\mathbb{Q}} \left[\int_0^T \left[\partial_Y V_{bi}^{[a,b]}(t, Y_{t-}, N_{t-}) \sigma \right]^2 + \left(\delta_N V_{bi}^{[a,b]}(t, Y_{t-}, N_{t-}) \right)^2 \lambda_t dt \right] \\ &\leq 2\sigma^2 E^{\mathbb{Q}} \left[\int_0^T \left(\partial_Y V_{bi}^{[a,b]}(t, Y_{t-}, N_{t-}) \right)^2 dt \right] + 2K^2 n < \infty. \end{aligned}$$

Therefore, $E^{\mathbb{Q}} \left[\int_0^T \phi_t dG_b^{idx}(t) \right]^2 < \infty$.

Chapter 3

Default intensities implied by CDO spreads: inversion formula and model calibration

The inadequacy of widely used static factor models, such as the Gaussian copula model and its various extensions, for pricing and hedging portfolio credit derivatives, as emphasized by the recent turmoil in credit derivatives markets, has led to the development of various dynamic models for portfolio credit risk.

One of the main obstacles in implementing and using these dynamic models has been the availability of efficient calibration algorithms. Once models are calibrated to market data, they can be compared in terms of pricing and hedging performance. Previous studies on dynamic models have mostly been based on black-box optimization procedures applied to nonconvex least squares minimization problems. The lack of convexity entails that the convergence and stability of these methods are not guaranteed, casting doubts on the reproducibility of calibration results and their stability.

Recovering implied default rates from market data is by nature an ill-posed problem. Although the actual default rate (intensity) may depend on the past market history, it has been argued [28, 31, 93] that the information contained in collateralized debt obligation (CDO) tranche spreads

can be used at best to recover the *local intensity function*, defined as the conditional expectation of the portfolio default intensity given the loss level. The local intensity function is analogous to the local volatility function introduced by Dupire [43] for equity derivatives. It summarizes all information available from CDO tranche spreads on the marginal loss distributions of the portfolio and provides a common basis to compare different models.

Herbertsson [60] and Lopatin and Misirpashaev [77] have used parametric methods to recover local intensity functions from CDO data. Laurent, Cousin, and Fermanian [71] propose an implied tree method for reconstructing the local intensity function. Reformulating the calibration of default intensity as a stochastic control problem, Cont and Minca [28] proposed a stable nonparametric approach based on relative entropy minimization for recovering the local intensity function.

We propose in this chapter an alternative, and simpler, approach based on an analytical inversion formula for the local intensity function, which is analogous to the Dupire formula in diffusion models [43]. This formula allows us to compute the local intensity function of a portfolio from its expected tranche notionalss. This yields a simple computational method for constructing an arbitrage-free CDO pricing model which matches a prespecified set of tranche spreads.

Together with a quadratic programming method for recovering expected tranche notionalss from CDO spreads, our inversion formula leads to an efficient nonparametric method for calibrating CDO pricing models. In a first step, we extract the expected tranche notionalss from the CDO spreads by solving a quadratic minimization problem under linear constraints. Next, the default intensity is computed from the expected tranche notionalss using the inversion formula. Unlike the calibration methods introduced in [28, 60], our method requires only relatively simple mathematical techniques.

Comparing this approach to other calibration methods using iTraxx Europe index CDO spreads, we find that model-dependent quantities such as the forward starting tranche spreads and jump-to-default ratios are quite sensitive to the calibration method used, even within the same model class. On the other hand, comparing the local intensity functions implied by different credit portfolio

models reveals that apparently different models, such as static Student-t copula models and reduced-form affine jump-diffusion models, lead to similar marginal loss distributions and tranche spreads.

Figure 3.1 gives an overview of this chapter, and the details are structured as follows. Section 3.1 derives our main results concerning the existence and expression of the local intensity function given the expected tranche notional. Section 3.2 proposes a nonparametric method to recover the local intensity function from the CDO market data. Section 3.3 compares this calibration method with the parametric approach introduced by Herbertsson [60] and the entropy minimization algorithm proposed by Cont and Minca [28]. Section 3.4 compares the local intensities implied by various credit portfolio loss models. Section 3.5 summarizes our main findings and discusses some implications. Proofs are presented in section 3.6.

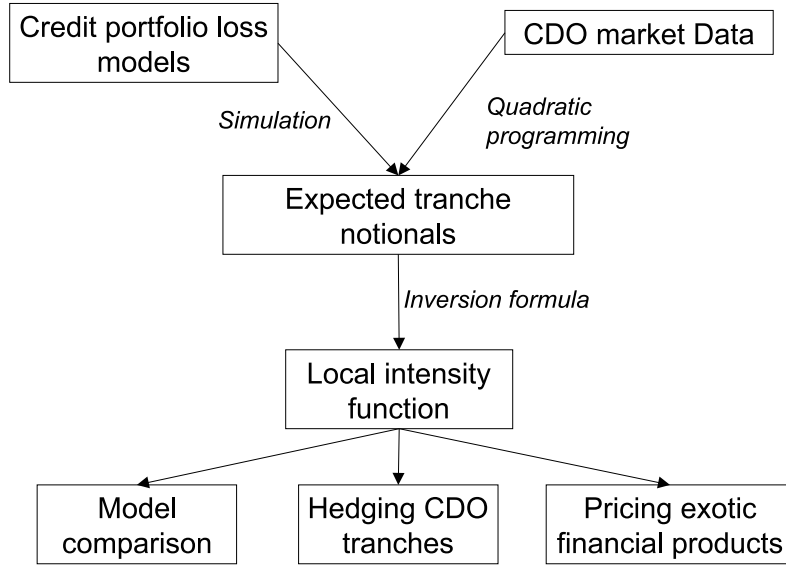


Figure 3.1: Application of the inversion formula to recover the local intensity function.

3.1 An inversion formula for the local intensity function

In this section, we first introduce the notions of effective intensity, local intensity function, and expected tranche notional. Then, we present two theorems that are related to the inversion formula of the local intensity function. Those theorems are the key results for computing the local intensity function implied by a credit portfolio loss model or the expected tranche notional obtained from the market data.

3.1.1 Local intensity function

We model credit events using a filtered probability space $(\Omega, \mathcal{F}, (\mathcal{F}_t)_{t \in [0, T^*]}, \mathbb{Q})$ where Ω is the set of market scenarios, the filtration $(\mathcal{F}_t)_{t \in [0, T^*]}$ represents the flow of information up to a terminal date T^* , and \mathbb{Q} is a probability measure representing the market pricing rule (pricing measure).

Consider an equally weighted credit portfolio (index) consisting of n names. Our main interest is the aggregate portfolio loss due to defaults, modeled as

$$L_t = \delta N_t, \quad (3.1)$$

where (N_t) is a point process representing the number of defaults and δ is the loss at each default, assumed to be constant. Without loss of generality, we set $N_0 = 0$ and assume that the timing of default events is independent of the interest rates. We assume the existence of a (risk-neutral) default intensity.

Assumption 3.1. *The point process (N_t) admits an intensity: there exists a non-negative \mathcal{F}_t -predictable process (λ_t) such that for all $t \in [0, T^*]$,*

$$\int_0^t \lambda_s ds < \infty \quad \mathbb{Q} - a.s.$$

The portfolio default intensity can be seen as the conditional probability per unit time of the next default:

$$\lambda_t = \lim_{\Delta t \rightarrow 0} \frac{1}{\Delta t} \mathbb{Q}(N_{t-+\Delta t} - N_{t-} = 1 | \mathcal{F}_{t-}).$$

It is characterized by the fact that, for any nonnegative \mathcal{F}_t -predictable process (C_t)

$$E^{\mathbb{Q}} \left[\int_0^{T^*} C_s dN_s \right] = E^{\mathbb{Q}} \left[\int_0^{T^*} C_s \lambda_s ds \right].$$

In general can be path-dependent i.e. it may depend on the entire market history. However, as shown in , one can construct a Markovian pricing model whose marginal distributions mimick those of (L_t) . The intensity of this Markovian projection is called the *effective default intensity* .

In general, (λ_t) can be path dependent; i.e., it may depend on the entire market history. However, as shown in [28, 31], one can construct a Markovian pricing model whose marginal distributions mimic those of (L_t) . The intensity (λ_t^{eff}) of this Markovian projection is called *the effective default intensity* [28].

Definition 3.1 (Local intensity function).

Consider a loss process satisfying Assumption 3.1 with

$$\forall t \in (0, T^*], \quad E^{\mathbb{Q}}[\lambda_t | \mathcal{F}_0] < \infty.$$

The local intensity function $a : (0, T^*] \times \{0, 1, \dots, n\} \mapsto \mathbb{R}_+$ at time 0 is defined as

$$a(t, i) := E^{\mathbb{Q}}[\lambda_t | N_{t-} = i, \mathcal{F}_0]. \quad (3.2)$$

If $\mathbb{Q}(N_{t-} = i | \mathcal{F}_0) = 0$, we set $a(t, i) = 0$ by convention.

We call $\lambda_t^{\text{eff}} := a(t, N_{t-})$ the effective intensity of the loss process: it is the best estimate for the default intensity given the portfolio loss level. $a(t, i)$ may also be viewed as a forward default rate for the portfolio given that i defaults have occurred in the portfolio [93]. Similarly to the local volatility function in diffusion models [43], the local intensity function summarizes all the necessary

information to price non-path-dependent portfolio credit derivatives: for any point process (N_t) that satisfies Assumption 3.1, there exists a Markovian point process (\tilde{N}_t) with transition rate $a(t, \tilde{N}_{t-})$ such that (N_t) and (\tilde{N}_t) have the same marginal distributions at all dates $t \in [0, T^*]$ [31]. Moreover, given the local intensity function, the marginal distribution can be computed by solving the forward Kolmogorov equations [93].

Given that the information content of market prices can be summarized in the local intensity function, various calibration methods have been proposed in the recent literature for recovering the local intensity function from CDO tranche spreads. Examples include parametric methods introduced by Herbertsson [60] and Lopatin and Misirpashaev [77] and a nonparametric entropy minimization algorithm proposed by Cont and Minca [28]. In section 3.2, we will introduce a novel nonparametric calibration method which makes use of the inversion formula that will be shown later in this section.

As the local intensity function can be defined for a wide range of credit portfolio loss processes, it provides a common basis to compare models defined in different manners. We will further study this aspect in section 3.4.

3.1.2 Expected tranche notinals

Consider the equity tranche of a synthetic CDO with detachment point K . The expected remaining notional value of this equity tranche at time $T > t$ is equal to

$$P_t(T, K) := E^{\mathbb{Q}}[(K - L_T)^+ | \mathcal{F}_t].$$

We follow the notation in [31] and call this quantity the *expected tranche notional* with maturity T and strike K . For simplicity, we will fix the observation time at 0 in the remainder of the chapter and drop the subscript t in the notation of the expected tranche notials. Expected tranche notials verify the following static arbitrage constraints (a proof is given in section 3.6).

Property 3.1 (Static arbitrage constraints).

- (a) $P(T, K) \geq 0,$
- (b) $P(T, 0) = 0,$
- (c) $P(0, K) = K,$
- (d) $K \mapsto P(T, K)$ is convex,
- (e) $P(T_2, K_1) - P(T_1, K_1) \geq P(T_2, K_2) - P(T_1, K_2)$ for any $T_1 \leq T_2, K_1 \leq K_2,$
- (f) $K \mapsto P(T, K)$ is continuous and piecewise linear on $[(i-1)\delta, i\delta], i = 1, \dots, n.$

Cont and Săvescu [31] show that the expected tranche notional can be computed directly from the local intensity function by solving a system of forward differential equations: for $T \in (0, T^*]$, $i = 1, \dots, n,$

$$\partial_T P(T, i\delta) = -a(T, 0)P(T, \delta) - \sum_{k=1}^{i-1} a(T, k)\nabla_K^2 P(T, (k-1)\delta), \quad (3.3)$$

with initial condition $P(0, i\delta) = i\delta,$

where ∇_K is the forward difference operator in strike:

$$\nabla_K F(T, i\delta) := F(T, (i+1)\delta) - F(T, i\delta)$$

for any function $F : [0, T^*] \times \{i\delta : i = 0, \dots, n-1\} \mapsto \mathbb{R}$. In fact, the forward equations (3.3) is a result of the forward Kolmogorov equations with the identities

$$\mathbb{Q}(L_T = i\delta | \mathcal{F}_0) = \begin{cases} \frac{P(T, \delta)}{\delta}, & i = 0, \\ \frac{\nabla_K^2 P(T, (i-1)\delta)}{\delta}, & i = 1, \dots, n-1. \end{cases} \quad (3.4)$$

3.1.3 Inversion formula and Markovian projection

To compute the local intensity function implied by a credit portfolio loss model, Theorem 3.1 shows that we can first compute the expected tranche notional under the model assumption and then convert them into a local intensity function using an inversion formula. This approach avoids computing the conditional expectation of the default intensity (λ_t), which can be a difficult task.

Theorem 3.1 (Inversion formula).

Consider a portfolio loss process $L_t = \delta N_t$ where the point process (N_t) verifies Assumption 3.1 and

$$\forall T \in (0, T^*], \quad E^{\mathbb{Q}}[\lambda_T | \mathcal{F}_0] < \infty.$$

The local intensity function (3.2) is given by

$$a(T, i) = E^{\mathbb{Q}}[\lambda_T | N_{T^-} = i, \mathcal{F}_0] = \begin{cases} \frac{-\partial_T P(T, \delta)}{P(T, \delta)}, & i = 0, \\ \frac{-\nabla_K \partial_T P(T, i\delta)}{\nabla_K^2 P(T, (i-1)\delta)}, & i = 1, \dots, n-1, \\ 0, & i = n, \end{cases} \quad (3.5)$$

for all $T \in (0, T^*]$, where $P(T, i\delta) = E^{\mathbb{Q}}[(i\delta - L_T)^+ | \mathcal{F}_0]$ is the expected tranche notional.

The proof is given in section 3.6.

In a practical situation, the default intensity (λ_t) is unobservable, but, if sufficiently many tranche spreads are quoted, expected tranche notionals can be recovered from market data. We will present a nonparametric method to recover the expected tranche notionals from the tranche spreads in section 3.2. Given such a set of values of expected tranche notionals, Theorem 3.2 shows that we can construct a Markovian loss process with an intensity in the form of (3.5) consistent with these values. This result, which is analogous to the Dupire formula for local volatility [43], is particularly useful when we want to recover a local intensity function from either the market data or a model that does not satisfy Assumption 3.1, such as the static factor models.

Theorem 3.2 (Local intensity function implied by expected tranche notionals).

Let $\{P(T, i\delta)\}_{T \in [0, T^*], i=0, \dots, n}$ be a (complete) set of expected tranche notionals verifying Property 3.1 and define the function $a : (0, T^*] \times \{0, 1, \dots, n\}$ by

$$a(T, i) = \begin{cases} \frac{-\partial_T P(T, \delta)}{P(T, \delta)}, & i = 0, \\ \frac{-\nabla_K \partial_T P(T, i\delta)}{\nabla_K^2 P(T, (i-1)\delta)}, & i = 1, \dots, n-1, \\ 0, & i = n, \end{cases} \quad (3.6)$$

for all $T \in (0, T^*]$. If $a(., .)$ is bounded, there exists a Markovian point process (M_t) with intensity $\gamma_t = a(t, M_{t-})$ defined on some probability space $(\Omega_0, \mathcal{G}, (\mathcal{G}_t), \mathbb{Q}_0)$ such that

$$\forall T \in [0, T^*], \quad \forall i \in \{0, \dots, n\}, \quad P(T, i\delta) = E^{\mathbb{Q}_0}[(i\delta - \delta M_T)^+ | \mathcal{G}_0].$$

If in addition

$$\nabla_K \partial_T P(T, i\delta) < 0, \quad (3.7)$$

the intensity function $a(T, i)$ is strictly positive for all $i < n$.

Proof. Property 3.1 entails that the function $a(., .)$ defined in the theorem is non-negative. Consider a standard Poisson process (N_t) constructed on a probability space $(\Omega_0, \mathcal{G}, (\mathcal{G}_t), \mathbb{P})$. Denote by $\tau_1 < \tau_2 < \dots$ the jump times of (N_t) and set $M_t = N_{t \wedge \tau_n}$. (\mathcal{G}_t) is the filtration generated by (M_t) . Define now the non-negative predictable process

$$\gamma_t := a(t, M_{t-}).$$

Since the function $a(., .)$ is assumed to be bounded, we know that for all $t \in [0, T^*]$

$$\int_0^t \gamma_s ds < \infty \quad \mathbb{P} - a.s.$$

We now apply the change of measure theorem for point processes [14, Theorem T3, Ch. VI Sec 2], and define a new probability measure \mathbb{Q}_0 by

$$\frac{d\mathbb{Q}_0}{d\mathbb{P}} \Big|_{\mathcal{G}_t} = \exp \left(\int_0^t (1 - \gamma_s) ds \right) \prod_{\tau_j < t} \gamma_{\tau_j}.$$

Under \mathbb{Q}_0 , (M_t) is a Markovian point process with intensity (γ_t) .

As shown in [31], the function $u(T, i) = E^{\mathbb{Q}_0}[(i\delta - \delta M_T)^+ | \mathcal{G}_0]$ is a solution of (3.3). On the other hand, substituting $\{a(T, i)\}_{T \in [0, T^*], i=0, \dots, n}$ into the forward equations (3.3) shows that the expected tranche notional $\{P(T, i\delta)\}_{T \in [0, T^*], i=0, \dots, n}$ solve (3.3). The boundedness of $a(., .)$ entails that the linear system of ODEs (3.3) has a unique solution, so

$$P(T, i\delta) = E^{\mathbb{Q}_0}[(i\delta - \delta M_T)^+ | \mathcal{G}_0]$$

for all $T \in [0, T^*]$, $i = 0, \dots, n$.

Finally, under (3.7), the positivity of $a(T, i)$ is immediate from (3.6). \square

Formula (3.5) is analogous to the Dupire formula [43], which expresses the local volatility as a function of the call prices:

$$\sigma^2(T, K) = \frac{2}{K^2} \frac{\partial_T C(T, K)}{\partial_K^2 C(T, K)}, \quad T \geq 0, K \geq 0,$$

where $C(T, K)$ is the call price with maturity T and strike K . In the diffusion framework, asset prices take values in $[0, \infty)$, which leads to a marginal probability density defined on $[0, \infty)$. This explains why a continuum of call prices in both strike and maturity is required to recover the local volatility function. On the other hand, since we model the portfolio loss as a point process with finite state space $(i\delta)_{i=0, \dots, n}$, we require only a set of expected tranche notional values with n strikes equal to the possible loss levels to recover the local intensity function.

Schönbucher [93] shows a similar formula expressed in terms of the marginal distribution:

$$a(T, i) = \frac{-\sum_{k=0}^i \partial_T \mathbb{Q}(L_T = i\delta | \mathcal{F}_0)}{\mathbb{Q}(L_T = i\delta | \mathcal{F}_0)}, \quad i = 0, \dots, n-1, \quad T \in (0, T^*]. \quad (3.8)$$

However, formula (3.5) appears to have an important advantage over (3.8). As we will discuss in section 3.2, the value of a CDO tranche can be expressed as a linear combination of a *small* set of expected tranche notional values. In this case, recovering the expected tranche notional values from the CDO market data can be achieved efficiently and the results can be used to compute the local intensity function using formula (3.5). However, this procedure will become more difficult if we consider the marginal distribution because we need the marginal distribution at all loss levels to express the CDO mark-to-market values.

3.2 Non-parametric estimation of the local intensity function

We now present a non-parametric method for recovering the local intensity function from CDO tranche spreads. The idea is to first extract the expected tranche notional values from the CDO market

data using a nonparametric approach and then compute the local intensity function by using formula (3.5), based on the results in Theorem 3.2.

We briefly recall the structure of index CDO tranches and their relationship with the expected tranche notional [26] and introduce a quadratic programming method to recover expected tranche notional from the CDO market data. Subsequently, we will outline the calibration algorithm for the local intensity function. We show that, unlike our proposed method, which yields an arbitrage-free pricing model, base-correlation interpolation does not guarantee the absence of arbitrage.

3.2.1 CDOs and expected tranche notional

Consider a CDO tranche defined by an interval $[a, b]$, $0 \leq a < b \leq 1$. a and b are called, respectively, the attachment and detachment points of the tranche and expressed in percentage of the total notional value. A synthetic CDO tranche swap is a bilateral contract in which the protection seller agrees to pay all portfolio loss within the interval $[a, b]$ in exchange for a periodic spread $s^{[a,b]}$ on the remaining notional value and an upfront payment $U^{[a,b]}$ on the initial notional value $b - a$.

Assume that the tranche is inception at time 0, and the spread $s^{[a,b]}$ and the upfront payment $U^{[a,b]}$ are given such that the mark-to-market value of the tranche is equal to zero. Then, we have¹

$$\begin{aligned} U^{[a,b]}(b-a) &= \sum_{j=1}^m D(0, t_j) [P(t_j, a) - P(t_j, b) - P(t_{j-1}, a) + P(t_{j-1}, b)] \\ &\quad - s^{[a,b]} \sum_{t_j > 0} D(0, t_j) (t_j - t_{j-1}) [P(t_j, b) - P(t_j, a)], \end{aligned} \tag{3.9}$$

where $D(0, t_j)$ is the discount factor from time t_j to 0, and $0 = t_0 < t_1 < \dots < t_m$ are the payment times, where the last payment time t_m corresponds to the expiration time. Notice that equality (3.9) is linear in the expected tranche notional with strikes equal to the attachment and detachment points and maturities equal to the payment times.

¹Expression (3.9) is slightly different for the most senior tranche. Please see section 3.7 for details.

3.2.2 Recovering expected tranche notional via quadratic programming

Assume that at time 0 we observe the spreads and upfront payments of CDO tranches $[\kappa_{i-1}, \kappa_i]$ for $i = 1, \dots, I$. Without loss of generality, we assume $I \leq n$ ² and denote the payment times $0 = t_0 < t_1 < \dots < t_m$ with expiration time t_m ³.

Our goal is to recover a local intensity function from the CDO market data using the results in Theorem 3.2. For computational purposes, we approximate the derivatives in formula (3.5) by finite differences and therefore consider expected tranche notional with maturities on a discrete time grid. In particular, we focus on the set of expected tranche notional $\{P(t_j, i\delta)\}_{j=0, \dots, m; i=1, \dots, n}$, which is represented in vector-form:

$$\mathbf{p} = [P(t_0, \delta), \dots, P(t_0, n\delta), \dots, P(t_m, \delta), \dots, P(t_m, n\delta)]^T \in \mathbb{R}^{n(m+1)}.$$

By definition, $\{P(t_j, i\delta)\}_{j=0, \dots, m; i=1, \dots, n}$ has to satisfy Property 3.1. In order to apply Theorem 3.2, the function defined by (3.5) has to be bounded, which means that the denominator of formula (3.5) has to be strictly positive. Moreover, we impose additional condition (3.7) to ensure that the local intensity function is strictly positive. Taking all constraints into account, $\{P(t_j, i\delta)\}_{j=0, \dots, m; i=1, \dots, n}$ must verify the following conditions.

Condition 3.1.

- (a) $P(t_j, \delta) > 0, j = 1, \dots, m,$
- (b) $\nabla_K^2 P(t_j, (i-1)\delta) > 0, j = 1, \dots, m, i = 1, \dots, n-1,$
- (c) $\nabla_K P(t_{j-1}, i\delta) > \nabla_K P(t_j, i\delta), j = 1, \dots, m, i = 0, \dots, n-1.$

Since the relations in Condition 3.1 are linear in the expected tranche notional, they can be written in matrix-form (see section 3.7):

$$\mathbf{B}\mathbf{p} < \mathbf{0}, \quad (3.10)$$

²It is natural to assume that the number of tranches I is less than the number of names n in the reference portfolio.

³Our formulation can be easily extended to CDO tranches with multiple expirations, but it will not be further discussed in this chapter.

where \mathbf{B} is a $2nm \times n(m + 1)$ matrix.

In order to be consistent with the CDO market data, the expected tranche notional must satisfy (3.9) for each tranche. Although (3.9) may involve expected tranche notional with strikes not equal to the multiples of δ (because attachment and detachment points may not be multiples of δ), Property 3.1(f) shows that we can always compute an expected tranche notional by linearly interpolating its neighbors which have strikes equal to the multiples of δ . Therefore, we can express (3.9) in terms of $\{P(t_j, i\delta)\}_{j=0,\dots,m; i=1,\dots,n}$. Writing this in matrix-form (see section 3.7), we have

$$\mathbf{A}\mathbf{p} = \mathbf{b}, \quad (3.11)$$

where $\mathbf{b} \in \mathbb{R}^I$, \mathbf{A} is an $I \times n(m + 1)$ matrix, and both depend on the CDO market data and the discount factors. Thus, calibrating a set of expected tranche notional that satisfies Condition 3.1 and is consistent with the CDO data is equivalent to finding a solution of the linear system (3.10)-(3.11). However, this system has either no or infinitely many solutions.

Proposition 3.1. *Given the CDO market data, there are either no or infinitely many sets of expected tranche notional with maturities $t_0 < \dots < t_m$ and strikes $\delta < \dots < n\delta$ which satisfy (3.10)-(3.11).*

In order to pinpoint a unique set of expected tranche notional, we consider a convex optimization problem under constraints (3.10)-(3.11). Consider a convex function $f : \mathbb{R}_+^{n(m+1)} \mapsto \mathbb{R}$, we calibrate the expected tranche notional by solving

$$\min_{\mathbf{p}} f(\mathbf{p}) \text{ subject to } \mathbf{A}\mathbf{p} = \mathbf{b}, \quad \mathbf{B}\mathbf{p} \leq -\mathbf{e}. \quad (3.12)$$

Here, we replace the strict inequalities in (3.10) by inequalities with an error vector $\mathbf{e} > 0$ that can be chosen arbitrarily. In fact, if (3.10)-(3.11) has a solution, then we can always pick \mathbf{e} such that (3.12) is feasible. If there exists a set of expected tranche notional \mathbf{p} that satisfies Condition 3.1 and is consistent with the CDO market data, solving (3.12) gives us a unique solution. In

particular, we propose a selection criterion:

$$f(\mathbf{p}) = \sum_{j=0}^m \sum_{i=1}^n w_{ij} \left(P(t_j, i\delta) - \tilde{P}(t_j, i\delta) \right)^2, \quad (3.13)$$

where $(w_{ij})_{j=0,\dots,m-1; i=1,\dots,n-1}$ are weights, and $\{\tilde{P}(t_j, i\delta)\}_{j=0,\dots,m; i=1,\dots,n-1}$ is a reference set of expected tranche notional. Using this objective function, we can impose a “prior” view by choosing the reference expected tranche notional, e.g. the reference expected tranche notional can be computed from a particular credit model. Furthermore, (3.12) reduces to a quadratic programming problem which can be solved efficiently [12, 95].

3.2.3 Numerical issues

Notice that CDO tranche payments are typically made every quarter. In this case, the expected tranche notional $\{P(t_j, i\delta)\}_{j=0,\dots,m; i=1,\dots,n}$ obtained by solving (3.12) are sparsely spaced in maturity. In order to obtain a finer set of expected tranche notional, a simple method is to linearly interpolate $\{P(t_j, i\delta)\}_{j=0,\dots,m; i=1,\dots,n}$ across maturities. This guarantees that the finer set will also satisfy Condition 3.1. However, this method will give extremely large values to the local intensity function for short maturities and may lead to computational instability. The reason is the following.

Assume that we are interested in computing the expected tranche notional $P(T_j, i\delta)$ for $j = 0, \dots, q, i = 1, \dots, n$, on the finer time grid $(T_j)_{j=0,\dots,q}$ which includes the payment times $(t_j)_{j=0,\dots,m}$. For $i > 0$, we compute $P(T_1, i\delta)$ and $P(T_2, i\delta)$ where $T_1 < T_2 < t_1$ by linearly interpolating the values $P(t_0, i\delta)$ and $P(t_1, i\delta)$. Then, the local intensity function computed from (3.5) is equal to

$$a(T_1, i) = \frac{(-\nabla_K P(T_2, i\delta) + \nabla_K P(T_1, i\delta)) / (T_2 - T_1)}{\nabla_K^2 P(T_1, (i-1)\delta)},$$

where we approximate the partial derivatives by finite differences. Since we compute $P(T_2, i\delta)$ and $P(T_1, i\delta)$ by linear interpolation, the numerator of $a(T_1, i)$ is strictly positive and has the same value for any $T_1 < T_2 < t_1$. On the other hand, if T_1 is close to 0, the denominator $\nabla_K^2 P(T_1, (i-1)\delta)$ is also close to 0 because $K \mapsto P(0, K)$ is linear. Therefore, $a(T_1, i)$ becomes extremely large when T_1 is small.

To overcome this problem, we propose the following method.

Algorithm 1 Maturity interpolation of expected tranche notionalss

1. Construct an arbitrage-free set $\{P(t_j, i\delta)\}_{j=0, \dots, m; i=0, \dots, n}$ of expected tranche notionalss by solving (3.12).
 2. Fix an integer r such that $n \leq r < q$ and $0 = T_0 < T_1 < \dots < T_r < t_1$. Arbitrarily set a positive but sufficiently small value for the local intensity function at times $(T_j)_{j=0, \dots, r-1}$ such that $\nabla_K P(T_r, i\delta) > \nabla_K P(t_1, i\delta)$ for all i .
 3. Compute the expected tranche notionalss for maturities $(T_j)_{j=0, \dots, r}$ using forward equations (3.3). Note that the set of expected tranche notionalss at the maturity T_r , $\{P(T_r, i\delta)\}_{i=0, \dots, n}$, automatically satisfies the strict convexity constraint in Condition 3.1(b).
 4. Linearly interpolate expected tranche notionalss in maturity starting from maturity T_r .
-

Since the linear interpolation starts from maturity T_r and $\{P(T_r, i\delta)\}_{i=0, \dots, n}$ satisfies the strict convexity constraint in Condition 3.1(b), the denominator in the local intensity function formula (3.5) is strictly positive at maturity T_r . Therefore, having extremely large values for the local intensity function at short maturities is avoided.

Remark 3.1. *The purpose of Algorithm 1 is to compute the expected tranche notionalss on a finer time grid, but not to build a complete set of expected tranche notionalss. In particular, if $T \mapsto P(T, i\delta)$ is piecewise linear, it will no longer be differentiable at certain points. If one is interested in recovering a complete set of expected tranche notionalss and apply Theorem 3.2, all necessary conditions must be verified carefully.*

3.2.4 Calibration algorithm for the local intensity function

The above considerations lead to the following algorithm for computing a local intensity function from a discrete set of CDO tranche spreads:

Algorithm 2 Quadratic programming calibration for the local intensity function

1. Compute matrices \mathbf{A} and \mathbf{b} in (3.11) according to the CDO market data, and matrix \mathbf{B} in (3.10) according to Condition 3.1. (See section 3.7)
 2. Solve quadratic programming problem (3.12) with objective function (3.13) and obtain a set of expected tranche notional which is consistent with the CDO market data.
 3. Apply Algorithm 1 to obtain expected tranche notional on a finer time grid if desired.
 4. Convert the calibrated expected tranche notional into a local intensity function using formula (3.5).
-

3.2.5 Arbitrage opportunities when using base-correlation interpolation

To price non-standard CDO tranches, or equivalently expected tranche notional, it is common to use the base-correlation interpolation method under the Gaussian copula framework. For example, if we want to price tranches [5%, 6%] and [6%, 7%] of the iTraxx investment grade (IG) portfolio, we first calibrate the one-factor Gaussian copula model [74] to the standard tranches, and obtain the base correlations [75] at the standard strikes 3%, 6%, 9%, 12% and 22%. Then, we interpolate the base correlations for other strikes, say 5% and 7% in this example. After that, we compute the expected tranche notional at strikes 5% and 7% using the two different base correlations obtained by interpolation and price the corresponding CDO tranches. However, we show that this method does not guarantee absence of arbitrage.

Figure 3.2 shows the base correlations of the one-factor Gaussian copula model calibrated to the iTraxx data in Table 3.2. By linearly interpolating the base correlations, we compute the upfront payments of nonstandard tranches [5%, 6%] and [6%, 7%] with a fixed periodic spread 100bps in Table 3.1. At first glance, we can see that the upfront payment of the more senior tranche [6%, 7%] is larger than the upfront payment of tranche [5%, 6%]. To show that it leads to an arbitrage opportunity, we take the following positions:

- Buy protection on tranche [5%, 6%],

- Sell protection on tranche [6%, 7%].

At inception time t_0 , the cash flow of our positions is equal to the difference of the upfront payments:

$$(879.3 \text{ bps} - 819.5 \text{ bps})(1\%) = 0.598 \text{ bps},$$

which is strictly positive.

At payment time t_j , the net premium received from our positions, $\text{Prem}(t_j)$, is equal to

$$\begin{aligned} \text{Prem}(t_j) &= 100 \text{ bps}(t_j - t_{j-1}) [(7\% - L_{t_j})^+ - (6\% - L_{t_j})^+] \\ &\quad - 100 \text{ bps}(t_j - t_{j-1}) [(6\% - L_{t_j})^+ - (5\% - L_{t_j})^+] \\ &= 100 \text{ bps}(t_j - t_{j-1}) [(5\% - L_{t_j})^+ - 2(6\% - L_{t_j})^+ + (7\% - L_{t_j})^+], \end{aligned}$$

which is positive, due to the fact that $K \mapsto (K - L)^+$ is a convex function. Therefore, the value of the premium leg at expiration time t_m is positive and equal to

$$\text{Value of premium leg at expiration} = \sum_{j=1}^m D(t_j, t_m)^{-1} \text{Prem}(t_j) \geq 0,$$

where $D(t_j, t_m)$ is the risk-free zero coupon bond price at time t_j with maturity t_m .

On the other hand, at payment time t_j , the net default payment received from the positions, $\text{Def}(t_j)$, is equal to

$$\begin{aligned} \text{Def}(t_j) &= [(5\% - L_{t_j})^+ - 2(6\% - L_{t_j})^+ + (7\% - L_{t_j})^+] \\ &\quad - [(5\% - L_{t_{j-1}})^+ - 2(6\% - L_{t_{j-1}})^+ + (7\% - L_{t_{j-1}})^+], \end{aligned}$$

and the value of the default leg at expiration time t_m is equal to

$$\text{Value of default leg at expiration} = \sum_{j=1}^m D(t_j, t_m)^{-1} \text{Def}(t_j).$$

In section 3.6.4, we show that the value of the default leg is also positive. Therefore, our total payoff (sum of premium leg and default leg) at expiration is positive. Recall that at the inception

of the tranches at time t_0 , we received a strictly positive cash flow. As a result, our trading strategy shows an arbitrage opportunity.

In contrast to our method in Algorithm 2, this example illustrates that interpolation of base correlation can result in arbitrage opportunities.

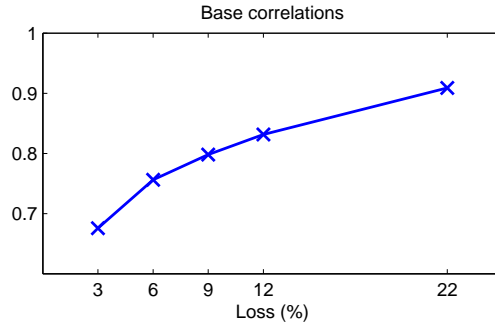


Figure 3.2: Base correlations of one-factor Gaussian copula model. Data: 5Y iTraxx Europe IG S9 on 25 March 2008.

Tranche	5% - 6%	6% - 7%
Upfront payment	819.5 bps	879.3 bps

Table 3.1: Upfront payments of 5-year iTraxx IG CDO tranches with 100bps periodic spread. Pricing method: one-factor Gaussian copula model with linearly interpolated base correlations.

3.3 Application to iTraxx tranches

In this section, we illustrate the calibration method introduced in section 3.2 by using the iTraxx data. We refer to this calibration method as the *quadratic programming method* (QP). The weights in the objective function (3.13) are chosen to be proportional to the reference expected tranche notional which are computed from a flat local intensity function equal to 1. In addition, we compare our results to two alternative calibration methods:

- **A parametric method.**

Herbertsson [60] specifies the local intensity function in the parametric form

$$a(t, i) = (n - i) \sum_{k=0}^i b_k, \quad (3.14)$$

where the parameters b_0, \dots, b_n are constants. This model states that the local intensity function is constant except when defaults occur. There is no sign restriction on b_k as long as the local intensity function remains nonnegative. To recover the parameters from the CDO spreads, we minimize the sum across observed tranches of squared differences between model and market CDO spreads using a gradient-based algorithm. Note that this objective function is not convex; hence the gradient-based algorithm may not necessarily yield a global minimum, and the minimum need not be unique.

- **Entropy minimization algorithm.**

Cont and Minca [28] introduced a non-parametric method for recovering the local intensity function as the solution of a relative entropy minimization problem

$$\inf_{\mathbb{Q} \in \Lambda} \mathbb{E}^{\mathbb{Q}_0} \left[\frac{d\mathbb{Q}}{d\mathbb{Q}_0} \ln \left(\frac{d\mathbb{Q}}{d\mathbb{Q}_0} \right) \right]$$

subject to calibration constraints (3.9). \mathbb{Q}_0 denotes the law of a prior Markovian point process, and Λ is the set of laws of Markovian point processes, equivalent to \mathbb{Q}_0 . To implement this algorithm, we choose as prior measure the law of a standard Poisson process stopped at n .

These three methods are applied to the 5-year iTraxx Europe Investment Grade Index CDO tranche spreads on 20 September 2006 and 25 March 2008, a portfolio consisting of 125 names. The recovery rate is assumed to be $R = 40\%$. Table 3.2 shows the result of the calibration.

3.3.1 Local intensity functions

Figures 3.3 to 3.5 show local intensity functions implied from iTraxx CDO spreads using the three different approaches presented above on two different dates: 20 Sept 2006 and 25 March 2008. These local intensity functions exhibit qualitatively similar features, but the value they imply for

	0% - 3%	3% - 6%	6% - 9%	9% - 12%	12% - 22%	22% - 100%
20-Sep-06						
Market bid	11.8%	53.8	14.0	5.8	2.1	0.8
Market ask	12.0%	55.3	15.5	6.8	2.9	1.3
QP	11.9%	54.6	14.8	6.3	2.5	1.0
Parametric	11.9%	54.5	14.8	6.3	2.5	1.1
Entropy Min	11.9%	54.5	14.8	6.3	2.5	1.1
25-Mar-08						
Market bid	37.7%	441.6	270.2	174.4	97.4	42.8
Market ask	39.7%	466.6	290.2	189.4	110.7	46.9
QP	38.4%	451.9	279.0	181.1	103.2	44.3
Parametric	38.7%	454.1	280.2	181.9	104.1	44.8
Entropy Min	38.6%	453.3	279.5	181.2	103.4	44.6

Table 3.2: Calibrated CDO tranche spreads of 5Y iTraxx Europe IG Series 6 on 20 September 2006 and Series 9 on 25 March 2008. Quotes are given in bps except for equity tranches which are quoted as upfront in percent with 500bps periodic coupons.

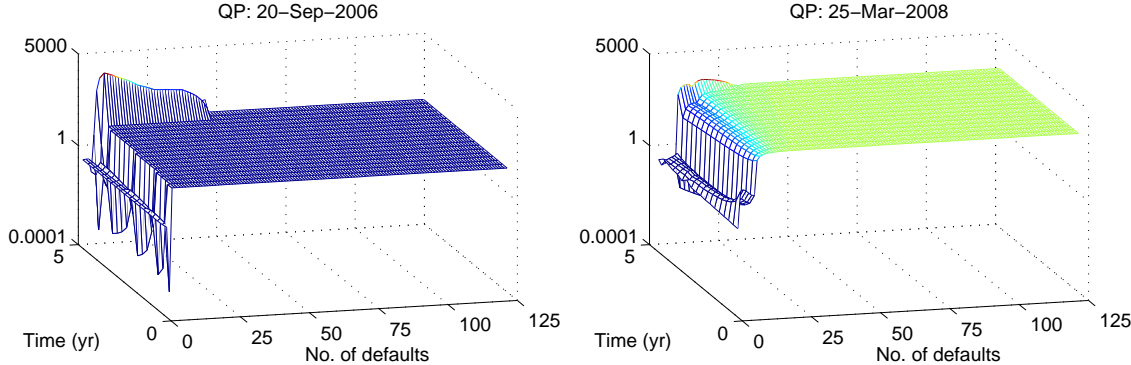


Figure 3.3: Local intensity functions implied from 5Y iTraxx Europe IG tranche spreads using the quadratic programming method (Algorithm 2) Left: S6 on 20 September 2006. Right: S9 on 25 March 2008.

the default intensity can be quite different. Also, for each calibration method, we observe that the general shape of the local intensity function calibrated to the 2006 dataset is similar to the one calibrated to the 2008 dataset.

For the quadratic programming method (Figure 3.3), we observe that at any fixed time, the local intensity functions stay at a low level when the number of defaults is small but sharply increases around 5 defaults: this sharp increase signals the onset of contagion. After that, the local intensity functions stay almost flat at a high level when the number of defaults is larger than 5. The term

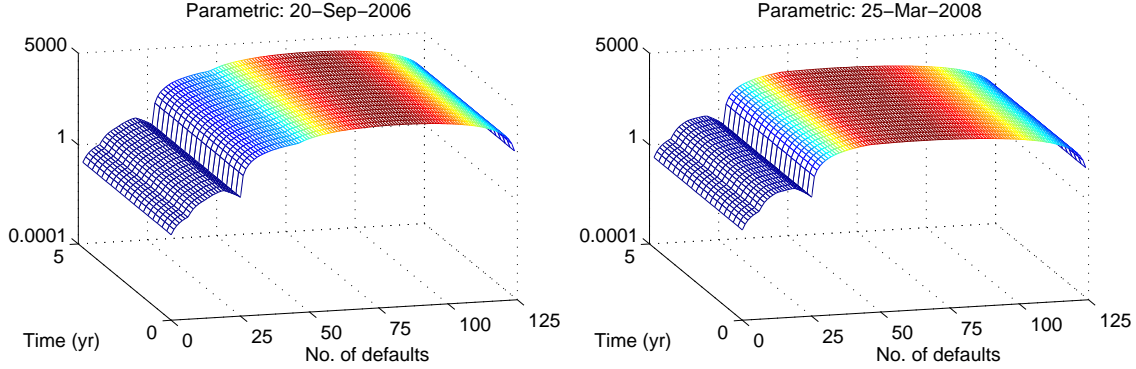


Figure 3.4: Local intensity functions implied from 5Y iTraxx Europe IG tranche spreads using a parametric model [60]. Left: S6 on 20 September 2006. Right: S9 on 25 March 2008.

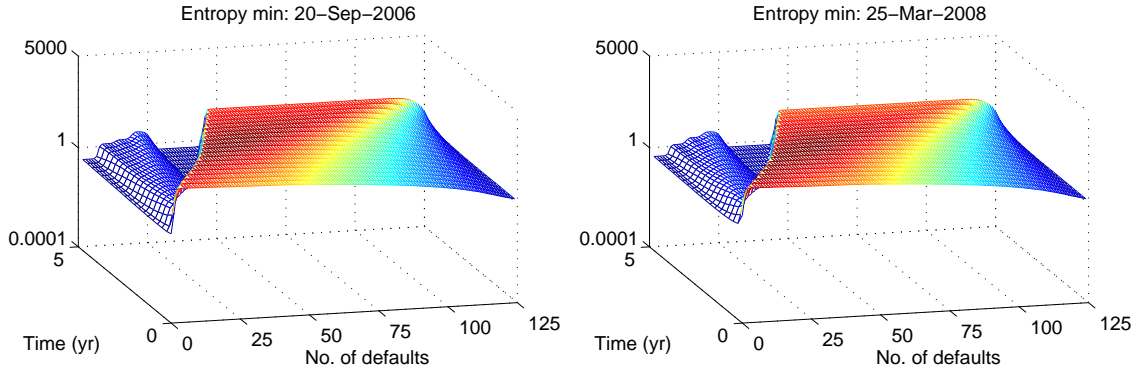


Figure 3.5: Local intensity functions implied from 5Y iTraxx Europe IG tranche spreads using a nonparametric entropy minimization method [28]. Left: S6 on 20 September 2006. Right: S9 on 25 March 2008.

structure is relatively flat in all examples.

The parametric approach (Figure 3.4) yields, by construction, smoother local intensity functions. When the loss is large, unlike the local intensity functions obtained via quadratic programming, the parametric local intensity functions decrease gradually towards zero as the number of defaults increases. Interestingly, this feature is also observed in the local intensity functions obtained with the nonparametric entropy minimization algorithm (Figure 3.5), but the decrease is much faster for short times than the parametric model. Furthermore, the maximum attained value of the local intensity function obtained via entropy minimization algorithm is substantially lower than both the

parametric and quadratic programming methods.

3.3.2 Stability analysis

A crucial property of a calibration method is its stability with respect to the inputs. To examine the stability of the various calibration methods considered above, we apply a 1% proportional shift to all CDO market spreads, recalibrate the local intensity function to the shifted CDO spreads, and measure the magnitude of the changes using the Frobenius norm:

$$\left(\sum_{i=0}^n \sum_{j=0}^q |a(T_j, i) - \hat{a}(T_j, i)|^2 \right)^{1/2},$$

where $\{a(T_j, i)\}$ and $\{\hat{a}(T_j, i)\}$ are, respectively, the local intensity functions calibrated to the original and perturbed CDO tranche spreads. The smaller the value of this norm, the more stable is the method. From Table 3.3, we observe that the entropy minimization algorithm is substantially more stable than the other two methods with respect to a change in the inputs, while the parametric approach is the most unstable one among the three. This result is in line with findings in similar studies using equity derivatives [32].

	QP	Parametric	Entropy Min
20-Sep-06	56.2	32116.2	2.0×10^{-2}
25-Mar-08	673.2	728.3	2.0×10^{-1}

Table 3.3: Frobenius norm of the changes in the local intensity function with respect to 1% proportional increase in the CDO spreads. Data: 5Y iTraxx Europe IG S6 on 20 September 2006 and S9 on 25 March 2008.

3.3.3 Marginal distributions and expected losses

Figure 3.6 shows the marginal distribution of the default process on 25 March 2008. We see that the marginal distributions are similar across the three calibration methods at year 1, but have more significant differences for longer time at year 4. This suggests that pricing non-path-dependent

credit derivatives is more sensitive to the choice of the calibration method used to recover the local intensity function for longer maturities.

Another important quantity that we study is the expected portfolio loss. Figure 3.7 shows the differences of the expected losses in a quarterly basis, i.e. $E(L_T) - E(L_{T-0.25})$. Observe that the differences in the expected losses are almost flat for all calibration methods when time is smaller than 2 years. When time increases, the difference of the expected loss computed from the parametric method increases gradually. On the other hand, the other two calibration methods give similar differences of the expected loss along time, except a sharp increase at year 5 for the quadratic programming method.

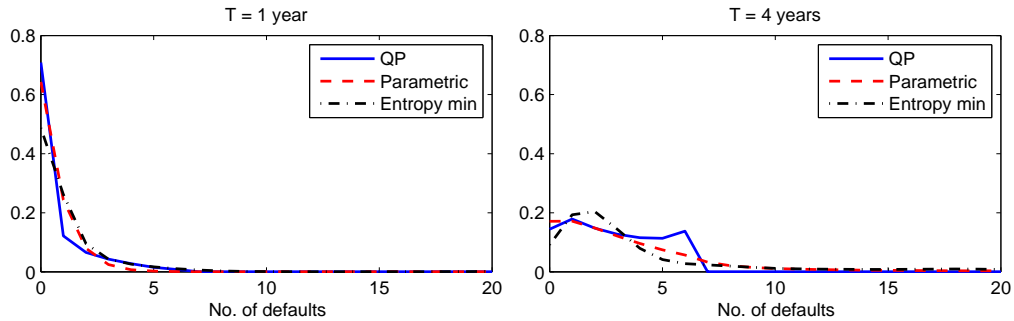


Figure 3.6: Marginal distribution at year 1 and year 4, truncated up to 20 defaults. Data: 5Y iTraxx Europe IG S9 on 25 March 2008.

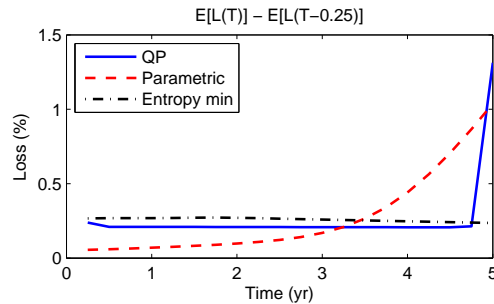


Figure 3.7: Term structure of the differences in the expected loss $E(L_T) - E(L_{T-0.25})$. Data: 5Y iTraxx Europe IG S9 on 25 March 2008.

3.3.4 Forward starting tranche spreads

Forward starting tranches provide protection against tranche losses in a pre-specified future period $[t, T]$. The distinguishing feature is that default occurring prior to the starting date do not affect the subordination of the tranche. In particular, a forward tranche with attachment-detachment interval $[a, b]$ can be valued as the forward value of a tranche with adjusted interval $[a', b']$ where $a' = \min(1, a + L_t)$ and $b' = \min(1, b + L_t)$. This dependence of the payoff on the loss makes the forward tranche path dependent.

Table 3.4 shows the spreads of forward starting tranches which start in 1 year and mature 3 years later. As we can see, the forward tranche spreads are significantly different across the calibration methods. Table 3.5 shows the model uncertainty ratio [23], which is defined as

$$\text{Model uncertainty ratio} = \frac{s^{max} - s^{min}}{s^{ave}},$$

where s^{max} , s^{min} and s^{ave} are the maximum, minimum and average forward spreads respectively across the calibration methods. Notice that the ratio is larger than 90% for all tranches except for the equity tranche. This reveals a serious problem because, even if we price exotic credit derivatives in the same modeling framework (local intensity framework in this case), there is substantial uncertainty in pricing exotic credit derivatives due to the choice of calibration method.

	20 September 2006			25 March 2008		
	QP	Parametric	Entropy Min	QP	Parametric	Entropy Min
0% - 3%	12.05	12.25	14.26	53.46	36.92	65.92
3% - 6%	2.72	17.89	33.62	93.79	290.65	482.23
6% - 9%	2.46	3.18	7.46	92.46	142.25	236.22
9% - 12%	2.21	0.79	4.14	91.45	63.45	170.80
12% - 22%	1.59	0.36	4.03	89.36	34.49	165.59
22% - 100%	0.03	0.15	0.69	37.99	13.38	27.60

Table 3.4: Spreads of forward starting tranches which start in 1 year and mature 3 years afterwards. Data: 5Y iTraxx Europe IG S6 on 20 September 2006 and S9 on 25 March 2008.

	0% - 3%	3% - 6%	6% - 9%	9% - 12%	12% - 22%	22% - 100%
20-Sep-06	17%	171%	115%	141%	184%	226%
25-Mar-08	56%	134%	92%	99%	136%	93%

Table 3.5: Model uncertainty ratio of the forward starting tranche spreads.

3.3.5 Jump-to-default ratios

In the local intensity framework, the market is complete and the self-financing strategy to replicate the payoff of a CDO tranche involves trading the underlying index default swap. The corresponding hedge ratio, which is known as the *jump-to-default ratio*, is defined by:

$$\frac{v^{[a,b]}(t, N_t + 1) - v^{[a,b]}(t, N_t)}{v^{index}(t, N_t + 1) - v^{index}(t, N_t)}$$

where $v^{[a,b]}(t, m)$ and $v^{index}(t, m)$ denote the mark-to-market values per unit notional of tranche $[a, b]$ and the index default swap respectively, conditional on m defaults being occurred by time t . More details on this subject can be found in [26, 71].

Table 3.6 shows the jump-to-default ratios computed from the local intensities in section 3.3.1. Interestingly, we observe that the jump-to-default ratios generated by the quadratic programming and the entropy minimization methods are quite similar. However, substantial differences are observed when comparing to the parametric method. This implies that uncertainty due to the choice of the calibration method not only affects the pricing of credit derivatives, as we have shown in section 3.3.4, but may also have a large impact on hedging strategies for portfolio credit derivatives [26].

3.4 Local intensity function implied by credit portfolio loss models

Market practice has been to calibrate credit portfolio models to market observations of index spreads and index tranche spreads and use the resulting parameters to price non-standard or illiquid products. As observed in section 3.3, even in a local intensity model, the marginal distributions for the portfolio loss generated by the model can vary substantially depending on the calibration

	20 September 2006			25 March 2008		
	QP	Parametric	Entropy Min	QP	Parametric	Entropy Min
0% - 3%	6.29	20.97	6.32	1.03	3.62	1.60
3% - 6%	2.12	5.16	3.51	1.69	3.31	2.33
6%- 9%	1.63	2.00	2.23	1.68	2.65	2.15
9% - 12%	1.52	1.02	1.72	1.68	2.08	1.97
12% - 22%	1.47	0.48	1.39	1.68	1.48	1.76
22% - 100%	0.67	0.22	0.61	0.81	0.66	0.75

Table 3.6: Jump-to-default ratios computed from the calibrated local intensity functions. Data: 5Y iTraxx Europe IG S6 on 20 September 2006 and S9 on 25 March 2008.

methods. This raises the question whether there is also a substantial difference of loss distributions across different models, when these models are calibrated to the same market data.

We compare the local intensity functions implied by six different models: Herbertsson model [60], bivariate spread-loss model [5], shot-noise model [52], one-factor Gaussian copula model [74], one-factor Student-t copula model [70] and a bottom-up affine jump-diffusion model [41, 83, 45]. The first three are top-down models, which means that the portfolio default intensity is directly specified. The one-factor Gaussian and Student-t copula models are bottom-up static factor models, and the affine jump-diffusion model is a dynamic bottom-up model.

All models are calibrated to the iTraxx Europe IG Series 9 CDO data on 25 March 2008. Table 3.7 shows the calibration results. The Gaussian and Student-t copula models are calibrated using the base-correlation method [75]. Except for the shot-noise model and the affine jump-diffusion model, all models yield tranche spreads well within the bid-ask intervals.

In order to compute the local intensity functions, we first compute the expected tranche notional for each model. For the dynamic models, we apply Theorem 3.1 and convert the expected tranche notional into local intensity functions based on formula (3.5). For the copula models we compute the implied portfolio default intensity using Theorem 3.2: the local intensity function is computed using (3.6). The local intensity functions are shown in Figure 3.8.

	0% - 3%	3% - 6%	6%- 9%	9% - 12%	12% - 22%	22% - 100%
25-Mar-08						
Market bid	37.7%	441.6	270.2	174.4	97.4	42.8
Market ask	39.7%	466.6	290.2	189.4	110.7	46.9
Bivariate spread-loss	38.7%	454.1	280.2	181.9	104.1	44.8
Shot-noise	43.8%	463.5	219.5	159.9	128.0	40.7
Gaussian Copula	38.7%	454.1	280.2	181.9	104.1	43.3
Student-t Copula	38.7%	454.1	280.2	181.9	104.1	44.9
Affine jump-diffusion	48.2%	493.0	244.8	186.5	154.4	37.2

Table 3.7: Calibration of different models to 5Y iTraxx Europe IG Series 9 tranche spreads on 25 March 2008. Quotes are given in bps except for equity tranches which are quoted as upfront in percent with 500bps periodic coupons.

3.4.1 Herbertsson model

In section 3.3, we have presented the parametric model introduced by Herbertsson [60], in which the portfolio default intensity has the functional form (3.14). Since the portfolio default intensity only depends on the credit portfolio loss level, this is one of the “simplest” models in a sense that the effective default intensity (λ_t^{eff}) is the same as the portfolio default intensity (λ_t). It can serve as a benchmark to compare with other models.

3.4.2 Bivariate spread-loss model

Arnsdorff and Halperin [5] introduce the bivariate spread-loss model in which the portfolio default intensity not only depends on the loss process but also on a mean-reverting diffusion process (Y_t) which generates spread volatility. The portfolio default intensity is given by

$$\lambda_t = Y_t F(N_t),$$

where F is called the contagion function. The factor (Y_t) generates spread volatility between default dates and follows

$$d \ln Y_t = \kappa (b - \ln Y_t) dt + \sigma dW_t,$$

where (W_t) is a standard Brownian motion.

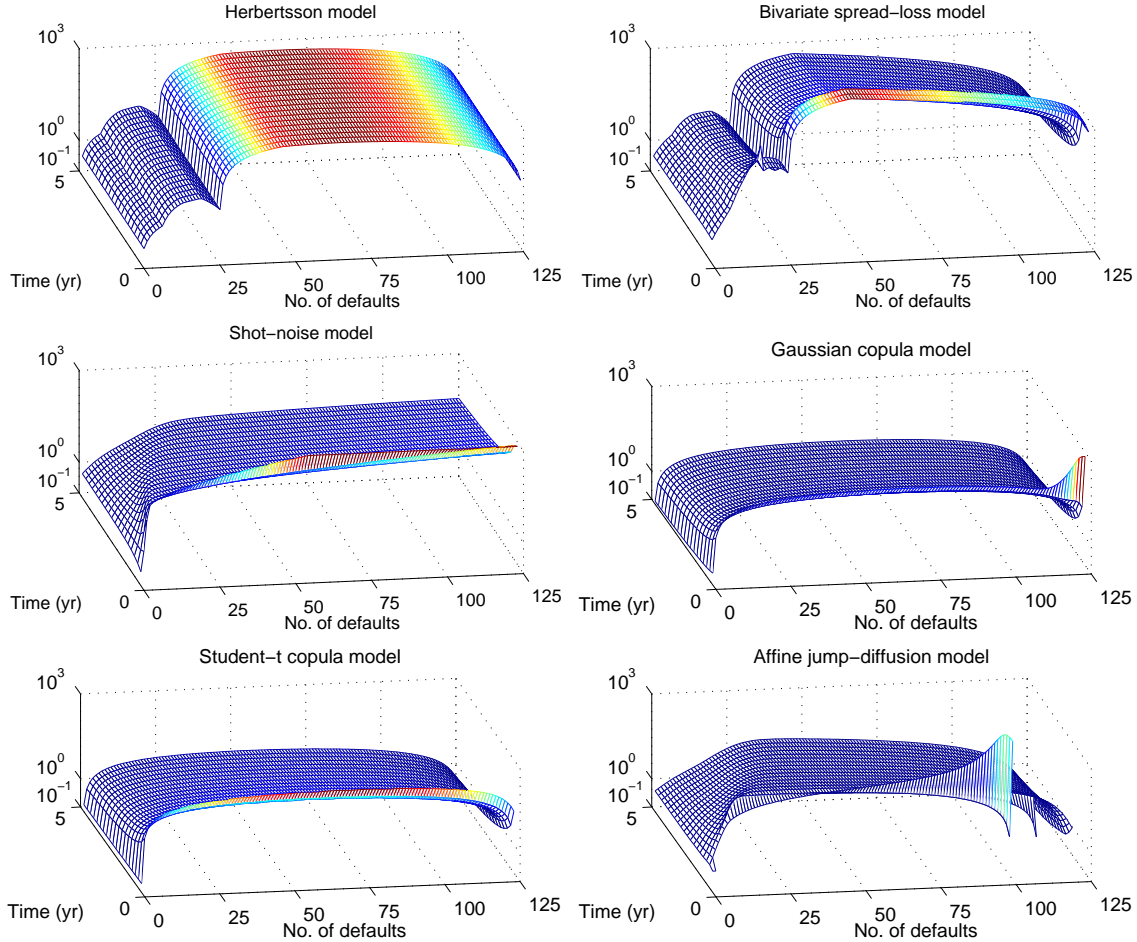


Figure 3.8: Local intensity functions implied by credit portfolio loss models. Data: 5Y iTraxx Europe IG S9 on 25 March 2008.

From Figure 3.8, we observe that the local intensity functions obtained from the bivariate spread-loss model and Herbertsson's parametric model are similar. The reason is that Arnsdorff and Halperin parameterize the contagion function F in the same way as Herbertsson specifies the local intensity function.

Another interesting feature to investigate is how the local intensity function changes with respect to the initial value of the risk factor Y_0 . In Figure 3.9, we show the time evolution of the difference of the local intensity function $a(t, i)$ calibrated with two different risk factors Y_0 . We represent only this difference for $i = 0$ and $i = 5$ and observe that a change in the risk factor will mostly affect

the local intensity function at short times. This observation is consistent with the fact that, since the risk factor is specified as mean reverting, it will revert back to its average in the long run and give similar local intensity functions for longer times.

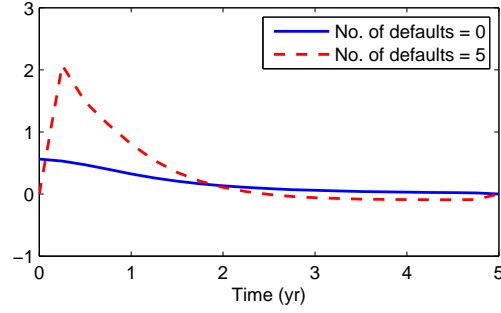


Figure 3.9: Change of the local intensity function implied by bivariate spread-loss model with respect to a small increase of the risk factor value Y_0 at time 0.

3.4.3 Shot-noise model

In order to better capture the possibility of extreme events, Gaspar and Schmidt [52] propose the shot-noise model in which the portfolio default intensity has the form

$$\lambda_t = \eta_t + J_t,$$

where (η_t) is a continuous affine process

$$d\eta_t = \kappa(b - \eta_t)dt + \sigma\sqrt{\eta_t}dW_t$$

with (W_t) a standard Brownian motion, and (J_t) is a non-Gaussian Ornstein-Uhlenbeck process which represents the shot-noise:

$$J_t = \sum_{\tau_i \leq t} Y_i e^{-\alpha(t-\tau_i)}$$

where $\tau_i, i = 1, 2, \dots$ are the jump times of a Poisson process and $Y_i, i = 1, 2, \dots$ are independent and identically distributed variables independent of the τ_i . We assume here Y_i to have an exponential

distribution. Under this setting, they provide a semianalytical expression for the local intensity function:

$$a(T, k) = \frac{\frac{\partial^k}{\partial \theta^k} \Big|_{\theta=-1} \frac{\partial}{\partial T} \frac{1}{\theta} S(\theta, T)}{\frac{\partial^k}{\partial \theta^k} \Big|_{\theta=-1} S(\theta, T)} \quad (3.15)$$

where $S(\theta, T)$ is the Laplace transform of the cumulative portfolio default intensity

$$S(\theta, T) = E^{\mathbb{Q}} \left[e^{\theta \int_0^T \lambda_s ds} \middle| \mathcal{F}_0 \right], \quad \theta < 0$$

which has a closed-form expression (see section 3.8). However, formula (3.15) is of little use for computing the local intensity function for a typical credit portfolio which consists of more than 100 names, we have to (numerically) differentiate $S(\theta, T)$ with respect to θ more than 100 times, which yields an unstable result. This example illustrates the difficulty of computing the local intensity function, even with a semianalytical formula. On the other hand, we can easily overcome this problem by using the inversion formula (3.5).

In Figure 3.8, we see that the local intensity function implied by the shot-noise model first increases sharply when the number of defaults is small and then slowly increases when the number of defaults gets larger. This is consistent with the argument given by Gaspar and Schmidt [52]: since the default intensity (λ_t) is not observed, the loss level (L_t) is used as a statistic to estimate the default intensity. If the loss increases, it is more likely that the default intensity is high. Therefore, it leads to an increasing local intensity function in the loss level.

3.4.4 Gaussian and Student-t copula models

Because of its tractability, the one-factor Gaussian copula model has been the financial industry benchmark despite some well-known drawbacks. The Student-t copula model, which embeds the Gaussian copula model as a limit when the degree of freedom goes to infinity, is widely used as well. More precisely, given a family of marginal default time distributions $(F_i, i = 1, \dots, n)$, the joint

distribution of the default times τ_i is modeled by first defining latent factors

$$X_i = S \left(\rho Z_0 + \sqrt{1 - \rho^2} Z_i \right), \text{ with } S = \begin{cases} 1 & \text{for Gaussian copula} \\ \sqrt{\frac{\nu}{V}} & \text{for Student-t copula} \end{cases}$$

where $Z_0, Z_i \sim \mathcal{N}(0, 1)$, $V \sim \chi_\nu^2$ are independent variables, and then defining the default times by

$$\tau_i = F_i^{-1}(F_{X_i}(X_i)),$$

where $F_{X_i}(\cdot)$ denotes the distribution of X_i . We refer readers to [70] for details.

To study the local intensity function implied by these two bottom-up models, we first calibrate them using the base-correlation method [75]. Then, we study the local intensity function corresponding to different base correlations. Notice that these two models are static, which means that there is no default intensity defined in this framework: we are in effect representing the expected tranche notional in these models in terms of an equivalent local intensity function, which then enables to compare these static models with dynamic models presented above.

Figure 3.8 shows the local intensity functions implied by the two copula models with base correlations corresponding to tranche [6%, 9%]. Observe that the main difference between the two local intensity functions is that for the Gaussian copula model, there is a sharp increase for short times when the number of defaults is larger than 100. Other than that, both local intensity functions appear to have a smooth dome shape. This relatively restricted form of local intensity function can explain why a single correlation cannot fit the full set of CDO tranche spreads and why we usually observe a base-correlation skew. Also, since the Student-t copula embeds the Gaussian copula as a limit, it is not surprising that the local intensity functions implied by the two models are similar in general shape. This also suggests that the additional degree of freedom in the Student-t copula is still not able to generate a flexible enough local intensity function to match the full set of CDO market data.

3.4.5 Affine jump-diffusion model

Many “bottom-up” reduced form models [41, 45, 83, 92] based on diffusive or jump-diffusion dynamics for default intensities have been proposed for pricing portfolio credit derivatives. Most of these models are built in the “doubly stochastic” framework by specifying the default intensities for each name in the portfolio. A prominent example, which lends itself to implementation, is the model proposed by Duffie and Gârleanu [41] where the default intensities follow correlated affine jump-diffusion processes. We consider the extension of this model considered in Mortensen [83] here. The default intensity for name i is represented as

$$\lambda_{i,t} = X_t^i + a_i X_t^0,$$

where a_1, \dots, a_n are parameters, and $(X_t^i), i = 0, \dots, n$, are independent affine jump-diffusions with

$$dX_t^i = \kappa_i(b_i - X_t^i)dt + \sigma_i \sqrt{X_t^i} dW_t^i + dJ_t^i,$$

where $(W_t^i), i = 0, \dots, n$, are independent Brownian motions and $(J_t^i), i = 0, \dots, n$, are independent compound Poisson processes with exponentially distributed jumps. This general specification is theoretically appealing, but the calibration to 125 individual CDS spreads and 6 tranche spreads of a CDO involves the solution to a nonlinear optimization problem in dimension 881: 125 factor loadings, 126 initial risk factor values and 630 parameters for the risk factor dynamics. Eckner [45] proposes a parsimonious version of this model, which we will adopt here.

Interestingly, Figure 3.8 shows that the local intensity function implied by the affine jump-diffusion model [45] is similar to the one implied by the one-factor Student-t copula model. This is a surprising result because the two modeling frameworks are fundamentally different: one is dynamic, while the other one is static.

3.5 Conclusion

We have proposed a simple and efficient calibration method for recovering the default intensity of a portfolio from CDO spreads. Our method is based on two ingredients: a nonparametric method based on quadratic programming for recovering expected tranche notionals from CDO spreads, and an inversion formula for computing the local intensity function from the expected tranche notionals. This method is shown to be much more stable, with respect to changes in inputs, than the commonly used nonlinear least squares method based on parametric models (see, e.g. [60]). Contrarily to the base-correlation method, our method yields an arbitrage-free model.

Comparing our calibration algorithm to a parametric calibration method [60] and to a nonparametric entropy minimization method [28] using iTraxx Europe index CDO spreads, we observe that these different calibration methods lead to quite different values of default intensity while maintaining a good match to the observations: this illustrates clearly the ill-posedness of the calibration problem. We also find that model-dependent quantities such as forward starting tranche spreads and jump-to-default ratios are quite sensitive to the calibration method used, even within the same model class.

On the other hand, comparing the local intensity functions implied by different credit portfolio models reveals that apparently different models, such as static Student-t copula models and reduced-form affine jump-diffusion models, lead to similar marginal loss distributions and tranche spreads. Thus, market prices alone are insufficient to discriminate between these model classes.

These results emphasize the importance of model uncertainty when addressing the pricing and hedging of portfolio credit derivatives and call for more research in this direction.

3.6 Proofs

3.6.1 Proof of Property 3.1

Property 3.1(a)-(c) are immediate results from the definition. Since the payoff function $(K - L_T)^+$ is convex in K and taking expectation of the payoff function preserves convexity, Property 3.1(d) holds. Since (L_t) is an increasing process, we know that for $T_1 \leq T_2$, $K_1 \leq K_2$

$$(K_1 - L_{T_2})^+ - (K_1 - L_{T_1})^+ \geq (K_2 - L_{T_2})^+ - (K_2 - L_{T_1})^+.$$

Taking the expectation on both sides, we obtain Property 3.1(e).

For Property 3.1(f), consider $K \in [(i-1)\delta, i\delta]$ for any $i \in \{1, \dots, n\}$ and $T \in [0, T^*]$. From the definition of $P(T, K)$, we have

$$P(T, K) = E^{\mathbb{Q}}[(K - L_T)^+ | \mathcal{F}_0] = \sum_{k=0}^{i-1} (K - k\delta) \mathbb{Q}(L_T = k\delta | \mathcal{F}_0), \quad (3.16)$$

which shows immediately that $K \mapsto P(T, K)$ is linear on $[(i-1)\delta, i\delta]$ and that $K \mapsto P(T, K)$ is a continuous function.

3.6.2 Proof of Theorem 3.1

Since $E^{\mathbb{Q}}[\lambda_T | \mathcal{F}_0] < \infty$ for all $T \in (0, T^*]$, the local intensity function defined by (3.2) satisfies $a(T, i) < \infty$ for all T and i . Therefore the forward equations (3.3) hold and have the solution $P(T, i\delta) = E^{\mathbb{Q}}[(i\delta - L_T)^+ | \mathcal{F}_0]$. By rewriting (3.3) in matrix-form for $T \in (0, T^*]$, we have

$$\mathbf{P}' = -\mathbf{M}\mathbf{a}, \quad (3.17)$$

where $\mathbf{P}' = [\partial_T P(T, \delta), \dots, \partial_T P(T, n\delta)]^T$, $\mathbf{a} = [a(T, 0), \dots, a(T, n-1)]^T$, and \mathbf{M} is a n -by- n lower triangular matrix with entries

$$\begin{aligned} \mathbf{M}(i, 1) &= P(T, \delta), \\ \mathbf{M}(i, j) &= \nabla_K^2 P(T, (j-2)\delta), \quad j = 2, \dots, i, \end{aligned}$$

for $i = 1, \dots, n$ and $\mathbf{M}(i, j) = 0$ otherwise. From (3.4), we know that:

$$\begin{aligned}\mathbf{M}(i, 1) &= \delta \mathbb{Q}(N_T = 0 | \mathcal{F}_0), \\ \mathbf{M}(i, j) &= \delta \mathbb{Q}(N_T = j - 1 | \mathcal{F}_0) \quad j = 2, \dots, i,\end{aligned}$$

for $i = 1, \dots, n$. Let $\mathcal{K} \subseteq \{0, \dots, n - 1\}$ be the set of integers k such that $\mathbb{Q}(N_T = k | \mathcal{F}_0) = 0$. We know that the $(k + 1)^{th}$ column of \mathbf{M} is equal to zero for all $k \in \mathcal{K}$, and this implies that $\partial_T P(T, k\delta) = \partial_T P(T, (k - 1)\delta)$. Moreover, in order to respect the convention given in the definition of the local intensity function (3.2), for all $k \in \mathcal{K}$, we have $a(T, k) = 0$.

Now, let $\widetilde{\mathbf{M}}$ be the $(n - |\mathcal{K}|) \times (n - |\mathcal{K}|)$ matrix resulting from the elimination of the $(k + 1)^{th}$ row and column in \mathbf{M} for all $k \in \mathcal{K}$. $\widetilde{\mathbf{M}}$ is a lower triangular matrix with $\widetilde{\mathbf{M}}(i, j) > 0$ for all i and $j \leq i$, and therefore it is invertible. Since for all $k \in \mathcal{K}$, we have set $a(T, k) = 0$ and noticed that $\partial_T P(T, k\delta) = \partial_T P(T, (k - 1)\delta)$, we can rewrite the linear system (3.17) as

$$\widetilde{\mathbf{P}}' = -\widetilde{\mathbf{M}}\widetilde{\mathbf{a}}, \quad (3.18)$$

where $\widetilde{\mathbf{P}}'$ and $\widetilde{\mathbf{a}}$ are $(n - |\mathcal{K}|)$ -vectors which result from the elimination of the $(k + 1)^{th}$ entries of \mathbf{P}' and \mathbf{a} respectively for all $k \in \mathcal{K}$. Multiplying both sides of (3.18) by $\widetilde{\mathbf{M}}^{-1}$, we have

$$\widetilde{\mathbf{a}} = -\widetilde{\mathbf{M}}^{-1}\widetilde{\mathbf{P}}'. \quad (3.19)$$

Therefore, the local intensity function $a(\cdot, \cdot)$ is uniquely determined by the set of expected tranche notamentals via (3.19). By the Gaussian elimination method, it is easy to check that (3.19) is equivalent to expression (3.5). Therefore, the local intensity function must have the form given in (3.5).

3.6.3 Proof of Proposition 3.1

Assume there exists a vector $\mathbf{p} \in \mathbb{R}^{n(m+1)}$ that satisfies (3.10)-(3.11). Using the fact that $\text{rank}(\mathbf{A}) \leq I < n(m + 1)$, we know from the rank-nullity theorem that there exists a non-zero $\mathbf{y} \in \mathbb{R}^{n(m+1)}$ such that

$$\mathbf{A}\mathbf{y} = \mathbf{0}.$$

Then, we choose the smallest $\mu_0 < 0$ and largest $\mu_1 > 0$ such that

$$\mathbf{B}(\mathbf{p} + \mu_0 \mathbf{y}) \leq \mathbf{0}, \quad \mathbf{B}(\mathbf{p} + \mu_1 \mathbf{y}) \leq \mathbf{0}.$$

Then, for any $\mu \in (\mu_0, \mu_1)$, we have

$$\mathbf{B}(\mathbf{p} + \mu \mathbf{y}) < \mathbf{0}.$$

Therefore, the vector $\mathbf{p} + \mu \mathbf{y}$ also satisfies constraints (3.10)-(3.11) for all $\mu \in (\mu_0, \mu_1)$; i.e. there are infinitely many solutions for the system (3.10)-(3.11).

3.6.4 Existence of arbitrage in the base correlation model

To show that the total default payments received from our trading strategy in section 3.2.5 is positive, we consider different scenarios at the last payment time, or equivalently the expiration time, t_m .

- For $L_{t_{m-1}} \leq 5\%$, we are only possible to receive a default payment at the expiration time t_m .

Then, we have

$$\begin{aligned} & \text{Value of default leg at expiration} \\ = & (5\% - L_{t_m})^+ - 2(6\% - L_{t_m})^+ + (7\% - L_{t_m})^+ \\ & - (5\% - L_{t_{m-1}})^+ + 2(6\% - L_{t_{m-1}})^+ - (7\% - L_{t_{m-1}})^+ \\ = & \begin{cases} 0, & \text{if } L_{t_m} \leq 5\% \\ L_{t_m} - 5\%, & \text{if } 5\% < L_{t_m} \leq 6\% \\ 7\% - L_{t_m}, & \text{if } 6\% < L_{t_m} \leq 7\% \\ 0, & \text{if } 7\% < L_{t_m} \end{cases} \\ \geq & 0. \end{aligned}$$

- For $5\% < L_{t_{m-1}} \leq 6\%$, we would have received certain amount of default payments before time t_m from tranche $[5\%, 6\%]$. Taking the reinvestment of those received payments at risk-free rate into account, we know that the total value of the received payments at time t_m is

greater than $L_{t_{m-1}} - 5\%$. Then, we have

$$\begin{aligned}
 & \text{Value of default leg at expiration} \\
 & \geq (L_{t_{m-1}} - 5\%) \\
 & \quad - 2(6\% - L_{t_m})^+ + (7\% - L_{t_m})^+ \\
 & \quad + 2(6\% - L_{t_{m-1}})^+ - (7\% - L_{t_{m-1}})^+ \\
 & = \begin{cases} L_{t_m} - 5\%, & \text{if } L_{t_m} \leq 6\% \\ 7\% - L_{t_m}, & \text{if } 6\% < L_{t_m} \leq 7\% \\ 0, & \text{if } 7\% < L_{t_m} \end{cases} \\
 & \geq 0.
 \end{aligned}$$

- For $6\% < L_{t_{m-1}} \leq 7\%$, we would have:

- received default payments from tranche $[5\%, 6\%]$ before time t_m , with value greater than 1% at time t_m ,
- paid default payments for tranche $[6\%, 7\%]$ before time t_m , with value greater than $L_{t_{m-1}} - 6\%$ at time t_m .

Since we would have received all default payments from tranche $[5\%, 6\%]$ before paying any default payments for tranche $[6\%, 7\%]$, the difference in timing of the reinvestment tells us that the total net value of default payments received before time t_m is greater than $7\% - L_{t_{m-1}}$.

Then, we have

$$\begin{aligned}
 & \text{value of default leg at expiration} \\
 & \geq (7\% - L_{t_{m-1}}) + (7\% - L_{t_m})^+ - (7\% - L_{t_{m-1}})^+ \\
 & = (7\% - L_{t_m})^+ \geq 0.
 \end{aligned}$$

- For $7\% < L_{t_{m-1}}$, all possible default payments have been made before time t_m , and we would have:

- received default payments from tranche [5%, 6%], with value greater than 1% at time t_m
- paid default payments for tranche [6%, 7%], with value greater than 1% at time t_m .

Again, since we would have received all default payments from tranche [5%, 6%] before paying any default payments for tranche [6%, 7%], the total net value of default payments received before time t_m is greater than 0.

Therefore, the value of the default leg at expiration is positive.

3.7 Matrix representation of constraints

Recall that we write the expected tranche notional in vector-form:

$$\mathbf{p} = [P(t_0, \delta), \dots, P(t_0, n\delta), \dots, P(t_m, \delta), \dots, P(t_m, n\delta)]^T \in \mathbb{R}^{n(m+1)}.$$

Since $t_0 = 0$ and $N_0 = 0$, we must have $P(t_0, i\delta) = i\delta$ for all i .

3.7.1 Pricing constraints

Assume that there are I CDO tranches $[\kappa_{i-1}, \kappa_i]$, $i = 1, \dots, I$, written on the reference portfolio with $\kappa_0 = 0$ and $\kappa_I = 1$. Denoting $0 = t_0 < t_1 < \dots < t_m$ the payment dates of the CDO tranches, we can rewrite (3.9) for each tranche and obtain the following linear pricing constraints:

- For each of the mezzanine tranches $[\kappa_{i-1}, \kappa_i]$, $i = 2, \dots, I - 1$, without upfront payment, we

have

$$\begin{aligned}
0 &= \sum_{j=1}^m D(0, t_j) [(1 + s^{[\kappa_{i-1}, \kappa_i]} \Delta t_j) P(t_j, \kappa_i) - (1 + s^{[\kappa_{i-1}, \kappa_i]} \Delta t_j) P(t_j, \kappa_{i-1}) \\
&\quad - P(t_{j-1}, \kappa_i) + P(t_{j-1}, \kappa_{i-1})] \\
&= D(0, t_1) P(t_0, \kappa_{i-1}) - D(0, t_1) P(t_0, \kappa_i) \\
&\quad - \sum_{j=1}^{m-1} [D(0, t_j) (1 + s^{[\kappa_{i-1}, \kappa_i]} \Delta t_j) - D(0, t_{j+1})] P(t_j, \kappa_{i-1}) \\
&\quad + \sum_{j=1}^{m-1} [D(0, t_j) (1 + s^{[\kappa_{i-1}, \kappa_i]} \Delta t_j) - D(0, t_{j+1})] P(t_j, \kappa_i) \\
&\quad - D(0, t_m) (1 + s^{[\kappa_{i-1}, \kappa_i]} \Delta t_m) P(t_m, \kappa_{i-1}) + D(0, t_m) (1 + s^{[\kappa_{i-1}, \kappa_i]} \Delta t_m) P(t_m, \kappa_i).
\end{aligned}$$

where $\Delta t_j = t_j - t_{j-1}$.

- For the most senior tranche $[\kappa_{I-1}, \kappa_I]$ with $\kappa_{I-1} < n\delta$, each default in the portfolio will reduce the notional value by $\frac{1}{n} - \delta$. In this case, the expected remaining notional value of tranche $[\kappa_{I-1}, \kappa_I]$ at payment time t_j is equal to

$$\begin{aligned}
&E^{\mathbb{Q}} \left[(1 - L_{t_j}) - (\kappa_{I-1} - L_{t_j})^+ - \left(\frac{1}{n} - \delta \right) N_{t_j} \right] \\
&= E^{\mathbb{Q}} \left[\left(1 - \frac{N_{t_j}}{n} \right) - (\kappa_{I-1} - L_{t_j})^+ \right] \\
&= \frac{1}{n\delta} P(t_j, n\delta) - P(t_j, \kappa_{I-1}).
\end{aligned}$$

Taking this into account, we have a slightly different equality for the most senior tranche:

$$\begin{aligned}
0 &= D(0, t_1) P(t_0, \kappa_{I-1}) - D(0, t_1) P(t_0, n\delta) \\
&\quad - \sum_{j=1}^{m-1} [D(0, t_j) (1 + s^{[\kappa_{I-1}, \kappa_I]} \Delta t_j) - D(0, t_{j+1})] P(t_j, \kappa_{I-1}) \\
&\quad + \sum_{j=1}^{m-1} \left[D(0, t_j) \left(1 + \frac{s^{[\kappa_{I-1}, \kappa_I]} \Delta t_j}{n\delta} \right) - D(0, t_{j+1}) \right] P(t_j, n\delta) \\
&\quad - D(0, t_m) (1 + s^{[\kappa_{I-1}, \kappa_I]} \Delta t_m) P(t_m, \kappa_{I-1}) \\
&\quad + D(0, t_m) \left(1 + \frac{s^{[\kappa_{I-1}, \kappa_I]} \Delta t_m}{n\delta} \right) P(t_m, n\delta).
\end{aligned}$$

- For the equity tranche $[\kappa_0, \kappa_1]$ with an upfront payment $U^{[\kappa_0, \kappa_1]}$, we have

$$\begin{aligned} -U^{[\kappa_0, \kappa_1]} \kappa_1 &= -D(0, t_1)P(t_0, \kappa_1) \\ &\quad + \sum_{j=1}^{m-1} [D(0, t_j)(1 + s^{[\kappa_0, \kappa_1]} \Delta t_j) - D(0, t_{j+1})]P(t_j, \kappa_1) \\ &\quad + D(0, t_m)(1 + s^{[\kappa_0, \kappa_1]} \Delta t_m)P(t_m, \kappa_1). \end{aligned}$$

One may notice that the attachment/detachment points $(\kappa_i)_{i=1,\dots,I}$ of the CDO tranches are not necessary multiples of δ ; i.e. the existence of k such that $\kappa_i = k \delta$ is not guaranteed. Nonetheless, Property 3.1 gives us the piecewise linearity of $P(T, .)$ on each $(i\delta, (i+1)\delta)$, and therefore we can write

$$\mathbf{p}_\kappa = \mathbf{A}_1 \mathbf{p},$$

where

$$\mathbf{p}_\kappa = [P(t_0, \kappa_1), \dots, P(t_0, \kappa_{I-1}), P(t_0, n\delta), \dots, P(t_m, \kappa_1), \dots, P(t_m, \kappa_{I-1}), P(t_m, n\delta)]^T,$$

which is a $I(m+1) \times 1$ vector and matrix \mathbf{A}_1 is a linear interpolation operator equal to

$$\mathbf{A}_1 = \begin{bmatrix} \tilde{\mathbf{A}}_1 & & & \\ & \ddots & & \\ & & \ddots & \\ & & & \tilde{\mathbf{A}}_1 \end{bmatrix}_{I(m+1) \times n(m+1)},$$

where the non-zero entries of $\tilde{\mathbf{A}}_1 \in \mathbb{R}^{I \times n}$ are

$$\begin{aligned} \tilde{\mathbf{A}}_1(i, \lfloor \frac{\kappa_i}{\delta} \rfloor) &= -\frac{\kappa_i}{\delta} + (\lfloor \frac{\kappa_i}{\delta} \rfloor + 1), \quad i = 1, \dots, I-1, \\ \tilde{\mathbf{A}}_1(i, \lfloor \frac{\kappa_i}{\delta} \rfloor + 1) &= \frac{\kappa_i}{\delta} - \lfloor \frac{\kappa_i}{\delta} \rfloor, \quad i = 1, \dots, I-1, \\ \tilde{\mathbf{A}}_1(I, n) &= 1. \end{aligned}$$

Then, since each pricing constraint is linear in \mathbf{p}_κ and the transformation from \mathbf{p} to \mathbf{p}_κ is linear as well, it is easy to see that

$$\mathbf{A}_2 \mathbf{A}_1 \mathbf{p} = \mathbf{b},$$

where

$$\mathbf{b} = \begin{bmatrix} -U^{[\kappa_0, \kappa_1]} \kappa_1 & 0 & \cdots & 0 \end{bmatrix}^T \in \mathbb{R}^I,$$

and the non-zero entries of $\mathbf{A}_2 \in \mathbb{R}^{I \times I(m+1)}$ are

$$\mathbf{A}_2(1, 1) = -D(0, t_1),$$

$$\mathbf{A}_2(1, Ij + 1) = D(0, t_j)(1 + s^{[\kappa_0, \kappa_1]} \Delta t_j) - D(0, t_{j+1}), \quad j = 1, \dots, m-1,$$

$$\mathbf{A}_2(1, Im + 1) = D(0, t_m)(1 + s^{[\kappa_0, \kappa_1]} \Delta t_m),$$

for $i = 2, \dots, I-1$,

$$\mathbf{A}_2(i, i-1) = D(0, t_1),$$

$$\mathbf{A}_2(i, i) = -D(0, t_1),$$

$$\mathbf{A}_2(i, Ij + i-1) = -D(0, t_j)(1 + s^{[\kappa_{i-1}, \kappa_i]} \Delta t_j) + D(0, t_{j+1}), \quad j = 1, \dots, m-1,$$

$$\mathbf{A}_2(i, Ij + i) = D(0, t_j)(1 + s^{[\kappa_{i-1}, \kappa_i]} \Delta t_j) - D(0, t_{j+1}), \quad j = 1, \dots, m-1,$$

$$\mathbf{A}_2(i, Im + i-1) = -D(0, t_m)(1 + s^{[\kappa_{i-1}, \kappa_i]} \Delta t_m),$$

$$\mathbf{A}_2(i, Im + i) = D(0, t_m)(1 + s^{[\kappa_{i-1}, \kappa_i]} \Delta t_m),$$

and,

$$\mathbf{A}_2(I, I-1) = D(0, t_1),$$

$$\mathbf{A}_2(I, I) = -D(0, t_1),$$

$$\mathbf{A}_2(I, Ij + I-1) = -D(0, t_j)(1 + s^{[\kappa_{I-1}, \kappa_I]} \Delta t_j) + D(0, t_{j+1}), \quad j = 1, \dots, m-1,$$

$$\mathbf{A}_2(I, Ij + I) = D(0, t_j) \left(1 + \frac{s^{[\kappa_{I-1}, \kappa_I]} \Delta t_j}{n\delta} \right) - D(0, t_{j+1}), \quad j = 1, \dots, m-1,$$

$$\mathbf{A}_2(I, I(m+1)-1) = -D(0, t_m)(1 + s^{[\kappa_{I-1}, \kappa_I]} \Delta t_m),$$

$$\mathbf{A}_2(I, I(m+1)) = D(0, t_m) \left(1 + \frac{s^{[\kappa_{I-1}, \kappa_I]} \Delta t_m}{n\delta} \right).$$

3.7.2 Relations in Condition 3.1

The strict positivity constraints in Condition 3.1(a) can be written as

$$\mathbf{B}_0 \mathbf{p} < \mathbf{0},$$

where,

$$\mathbf{B}_0 = \left[\begin{array}{ccc|ccc|ccc|ccc|ccc} 0 & \cdots & 0 & -1 & 0 & \cdots & \cdots & \cdots & \cdots & \cdots & \cdots & 0 \\ 0 & \cdots & 0 & 0 & \cdots & 0 & -1 & 0 & \cdots & \cdots & \cdots & 0 \\ \vdots & \vdots \\ 0 & 0 & 0 & 0 & \cdots & & \cdots & \cdots & -1 & 0 & \cdots & \cdots & 0 \\ 0 & \cdots & 0 & 0 & \cdots & & \cdots & \cdots & \cdots & \cdots & -1 & 0 & \cdots \end{array} \right],$$

which is a $m \times n(m+1)$ matrix. The strict convexity constraints in Condition 3.1(b) can be written as

$$\mathbf{B}_1 \mathbf{p} < \mathbf{0},$$

where,

$$\mathbf{B}_1 = \left[\begin{array}{ccc|c} 0 & \cdots & 0 & \tilde{\mathbf{B}}_1 \\ \vdots & \vdots & & \ddots \\ 0 & \cdots & 0 & \tilde{\mathbf{B}}_1 \end{array} \right]_{(n-1)m \times n(m+1)},$$

$$\tilde{\mathbf{B}}_1 = \left[\begin{array}{cccc} 2 & -1 & 0 & \cdots \\ -1 & 2 & -1 & 0 & \cdots \\ & \ddots & \ddots & \ddots & \ddots \\ & & 0 & -1 & 2 & -1 \end{array} \right]_{(n-1) \times n}.$$

Finally, Condition 3.1(c) can be written as

$$\mathbf{B}_2 \mathbf{B}_3 \mathbf{p} < \mathbf{0},$$

where,

$$\mathbf{B}_2 = \begin{bmatrix} \tilde{B}_2 & & \\ & \ddots & \\ & & \tilde{B}_2 \end{bmatrix}_{nm \times nm} \quad \text{with} \quad \tilde{\mathbf{B}}_2 = \begin{bmatrix} 1 & 0 & & & \\ -1 & 1 & \ddots & & \\ 0 & -1 & \ddots & & \\ \ddots & \ddots & \ddots & 0 & \\ & 0 & -1 & 1 \end{bmatrix}_{n \times n},$$

and

$$\mathbf{B}_3 = \left[\begin{array}{cccc|cccc|c|ccccc} -1 & 0 & \dots & 0 & 1 & 0 & \dots & 0 & \dots & 0 & \dots & 0 & 0 & \dots & 0 \\ 0 & -1 & \ddots & 0 & 0 & 1 & \ddots & 0 & \dots & \dots & \dots & \dots & \dots & \dots & 0 \\ & \ddots & & & & \ddots & & & \vdots & \ddots & \ddots & \vdots & \ddots & \ddots & \vdots \\ & \vdots & & & \vdots & & \dots & & \vdots & \vdots & -1 & 0 & \vdots & 1 & 0 \\ 0 & \dots & 0 & 0 & \dots & 0 & \dots & 0 & \dots & 0 & \dots & 0 & 0 & \dots & 0 & 1 \end{array} \right].$$

which is a $nm \times n(m+1)$ matrix.

In summary, we can represent all strict inequality constraints conditions in matrix form:

$$\mathbf{B}\mathbf{p} < \mathbf{0},$$

where,

$$\mathbf{B} = \begin{bmatrix} \mathbf{B}_0 \\ \mathbf{B}_1 \\ \mathbf{B}_2 \mathbf{B}_3 \end{bmatrix}_{2nm \times n(m+1)}.$$

3.8 Laplace transform of cumulative portfolio default intensity for shot-noise model

Recall that the portfolio default intensity for the shot-noise model is equal to

$$\lambda_t = \eta_t + J_t,$$

where (η_t) and (J_t) are independent. Therefore,

$$S(\theta, T) = E^{\mathbb{Q}} \left[e^{\theta \int_0^T \lambda_t dt} \middle| \mathcal{F}_0 \right] = E^{\mathbb{Q}} \left[e^{\theta \int_0^T \eta_t dt} \middle| \mathcal{F}_0 \right] E^{\mathbb{Q}} \left[e^{\theta \int_0^T J_t dt} \middle| \mathcal{F}_0 \right].$$

Since (η_t) is an affine process, we have

$$E^{\mathbb{Q}} \left[e^{\theta \int_0^T \eta_t dt} \middle| \mathcal{F}_0 \right] = e^{A(\theta, T) + B(\theta, T)\eta_0},$$

where

$$A(\theta, T) = -\frac{2\kappa b}{\sigma^2} \ln \left(\frac{c + de^{-\gamma T}}{c + d} \right) + \frac{\kappa b T}{c}, \quad B(\theta, T) = \frac{1 - e^{-\gamma t}}{c + de^{-\gamma T}}$$

with

$$\gamma = \sqrt{\kappa^2 - 2\sigma^2\theta}, \quad c = (\kappa + \gamma)/2\theta, \quad d = (-\kappa + \gamma)/2\theta.$$

Since (J_t) is an Ornstein-Uhlenbeck process, we know that

$$E^{\mathbb{Q}} \left[e^{\theta \int_0^T J_t dt} \middle| \mathcal{F}_0 \right] = e^{C(\theta, T) + D(\theta, T)J_0},$$

where

$$C(\theta, T) = l \left(\int_0^T \psi \left(\frac{\theta}{\alpha} (1 - e^{\alpha(s-T)}) \right) ds - T \right), \quad D(\theta, T) = \frac{\theta}{\alpha} (1 - e^{-\alpha T})$$

with $\psi(u) := E^{\mathbb{Q}}[e^{uY_1}]$ is the Laplace transform of Y_1 and l is the intensity of the underlying Poisson process. If Y_1 is exponentially distributed with mean μ , then

$$C(\theta, T) = \frac{l\mu}{1 - \theta\mu} \left[\theta T - \frac{1}{\mu} \ln(1 - \theta\mu(1 - e^{-\alpha T})) \right].$$

Chapter 4

Statistical modeling of credit default swap portfolios

The first generation of credit risk models has primarily focused on the modeling of *default risk*, either by modeling the capital structure of firms [80] or through reduced-form models for 'hazard rates' and default probabilities [16, 25, 35, 28, 53, 60, 67, 69]. However, during the recent financial crisis, investors in credit derivatives experienced substantial losses even in absence of any defaults in the portfolios underlying these contracts. Volatility in market values of credit-sensitive instruments in absence of defaults is mainly due to the change of credit quality of the underlying obligors, which is reflected in their credit spreads. This *spread risk* turns out to be the major risk faced by investors in credit derivatives.

Consider for instance the CDX.NA.IG index, an equally weighted portfolio of 125 5-year credit default swaps (CDS) (see section 4.1). Assume that the protection premium of each CDS is equal to 100bps. If the recovery rate for each CDS is equal to 40%, which is a standard assumption for pricing credit derivatives, default of a single obligor will generate a loss of $0.6/125 = 0.48\%$ of the total portfolio notional value. In an investment grade index, such a default is a rare event:

8 defaults have been observed in the CDX.NA.IG since 2003¹. Table 4.1 shows that this loss is equivalent to the loss generated by a change in the CDS spreads which corresponds to the 99th percentile of daily changes, an event which occurs more than twice a year! This example shows that, at least for investment grade credit portfolios, spread risk is at least as important as default risk, if not more. Not surprisingly, credit risk models which did not accurately capture spread risk performed poorly during the recent crisis [26].

Period	Percentile of daily P&L								
	1%	5%	10%	30%	50%	70%	90%	95%	99%
2005-09	-0.431%	-0.206%	-0.103%	-0.015%	0.000%	0.011%	0.084%	0.192%	0.459%
2005-07	-0.070%	-0.031%	-0.020%	-0.004%	0.003%	0.008%	0.020%	0.026%	0.049%
2007-09	-0.700%	-0.297%	-0.207%	-0.071%	-0.011%	0.038%	0.202%	0.313%	0.542%

Table 4.1: Percentiles of the daily profit-and-loss (percentage of the total portfolio notional value) of an equally weighted credit portfolio consisting of the 5-year CDS written on the constituents in CDX.NA.IG.12.

The importance of spread risk calls for a better understanding of variations in credit spreads and models which accurately reflect the characteristics of these variations. The empirical literature shows that credit spreads have particular statistical features which need to be incorporated in a model for spread risk [3, 4, 11, 21, 88]. Collin-Dufresne et al [21], Blanco, Brennan and Marsh [11] and Alexander and Kaeck [2] explore the determinants of credit spreads and their relation with other economic variables. Rahman [88] and Almer, Heidorn and Schmaltz [3] study empirical properties of credit spreads for financial obligors; Rahman [88] proposed a multivariate DCC-GARCH model for credit spreads.

As argued by Blanco, Brennan and Marsh [11], the CDS market has become the main forum for credit risk price discovery. This work contributes to the previous empirical literature by undertaking a systematic study of the relationship between CDS spreads and credit yield credit spreads. In particular, CDS prices appear to be better integrated with firm-specific variables in the short run, and both CDS and bond markets equally reflect those factors in the long run.

The risk management of credit sensitive instruments calls for models which are capable of ad-

¹This includes both on-the-run and off-the-run series.

equately reproducing the statistical properties of CDS spreads. Any default risk model implies some dynamics for credit spreads, but most existing default risk models have focused on analytical tractability rather than statistical properties of (CDS) spreads, and spread dynamics implied by these models do not necessarily correspond to observed dynamics of spreads. This results in poor performance of these models for hedging and risk management [26]. Another context which requires joint statistical modeling of CDS spreads is the risk management of CDS clearinghouses. Regulatory reform in the light of the 2008 crisis has moved CDS trading from over-the-counter bilateral trading to central clearing. Central counterparties require a deposit (initial margin) from clearing participants, based on the risk of their CDS portfolios [24]. The consistent computation of such margin requirements requires a multivariate model for (co-)movements in CDS spreads.

As shown by Collin-Dufresne et al [21], credit spread changes are principally driven by supply/demand fluctuations that are independent from factors traditionally considered in credit risk modeling and standard proxies for liquidity. This observations suggests that direct stochastic modeling of CDS spread returns is more effective than trying to explain spread movements in terms of other economic variables. This is the approach we adopt here: we propose, in the second part of this chapter, a heavy-tailed multivariate time series model for the dynamics of CDS spreads which reflects the observed empirical properties of CDS spreads yet is easy to estimate and use. We compare our model with previously proposed –random walk and affine jump-diffusion– models and show that the model adequately predicts the distribution of losses for a variety of CDS portfolios with long and short positions, making it a useful tool for the risk management of CDS portfolios.

In this chapter, we undertake a systematic study of univariate and multivariate properties of CDS spread returns in (Section 4.2). Based on these observations, we propose a multivariate time series model which is suitable for measuring and managing the risk of CDS portfolios. Below is a summary of the main contributions of our study.

- The study of statistical properties of CDS spreads for CDX index constituents in the period 2005-09 reveals that:

- CDS spread returns can be modeled as stationary processes with positive autocorrelations, positive serial correlations in extreme values, conditional heteroscedasticity and two-sided heavy tails.
 - Large co-movements are observed in the CDS spread series, indicating the presence of heavy-tailed common factors; these large co-movements are not necessarily linked to credit events.
 - Correlations across obligors of CDS spread returns increase substantially in 2007-09.
 - Principal component analysis suggests that the main contribution to the variance of CDS spread returns comes from idiosyncratic jumps.
 - Credit events do not necessarily lead to large upward moves in the CDS spreads.
- Section 4.3 shows that commonly used affine jump-diffusion models [41, 49] are not able to match the observed serial dependence properties and the two-sided heavy-tailed distributions of CDS spread returns and tend to overestimate the probability of having (large) co-movements in the CDS spreads.
 - In section 4.4, we propose a heavy-tailed multivariate time series model for CDS spread returns and show that this model is able to reproduce the observed statistical properties of CDS spread returns as well as their dependence structures adequately. We also propose a quasi maximum likelihood estimation method for the model.
 - In section 4.5, we show that the heavy-tailed multivariate model compares favorable to the affine jump-diffusion model [41] and a random walk model [91]: it provides more accurate prediction for the loss quantiles of a wide variety of CDS portfolios, in 2005-07 and also during the market turmoil of late 2008.

4.1 Data

We consider daily observations of the 5-year CDS par spreads (or CDS spreads for simplicity) from 4 April 2005 to 17 July 2009, where the reference obligors belong to Markit CDX North America Investment Grade Series 12 portfolio (CDX.NA.IG.12). CDS with other maturities such as 1, 3, 7, and 10 years are sometimes available but less liquidly traded. Table 4.2 shows the distribution of the obligors in terms of industrial sectors, credit ratings and number of available observations. There are a total of 125 obligors in the CDX.NA.IG.12 portfolio which can be divided into eight industrial sectors as defined by Markit. The largest sector is the consumer cyclical sector which contains 29 obligors and the smallest is the materials sector which contains 6 obligors. As of 5 December 2009, all obligors are investment grade except for the CIT Group Inc whose S&P long-term local currency issuer rating is equal to D. Indeed, CIT Group Inc has been removed from CDX.NA.IG.12 on 3 November 2009 due to default.

Our sample covers the period before and during the subprime crisis. For each obligor whose data are available for the full sample period, it contains a total of 1109 daily observations. The data set spans the period 2005-2009 and spans a reasonably long period to provide a meaningful basis for the statistical analysis of CDS spreads

The CDS spread (log-)return over a time interval Δt (equal to 1 or 5 days) is defined as

$$r_t = \ln(s_t / s_{t-\Delta t})$$

where s_t is the CDS spread observed at time t . Figure 4.1 shows the CDS spreads and the daily spread returns of Conoco Philips. The behavior of the CDS spreads can be clearly divided into two regimes: before and after the onset of the subprime crisis in 2007. In particular, the CDS spreads are substantially larger and more volatile after 2007. Therefore, our analysis will focus on two sample periods:

1. Pre-subprime period (2005-07): 4 April 2005 to 30 June 2007

Sector	No. of obligors
Financial	23
Materials	6
Consumer Stable	13
Utilities	8
Energy	8
Industrial	21
Consumer Cyclical	29
Communications and Technology	17

S&P rating as of 5-Dec-2009	No. of obligors
AA- to AA+	5
A- to A+	42
BBB- to BBB+	73
BB- to BB+	4
D	1

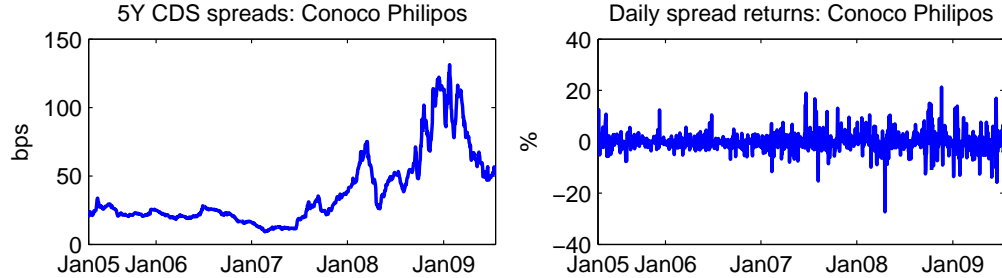
Available no. of sample days	No. of obligors
> 1000	115
800 - 1000	3
500 - 800	6
300 - 500	1

Table 4.2: Distribution of obligors in terms of sectors, Standard and Poor's credit ratings and number of available daily observations.

2. Subprime crisis (2007-09): 1 July 2007 to 17 July 2009

We consider obligors whose available CDS history exceeds 50 days, which leaves us with 121 obligors for analysis for 2005-2007. In the 2007-09 period, all obligors have more than 50 sample days.

Table 4.3 and 4.4 show the summary statistics of the CDS spreads and the spread returns respectively. We choose to present one obligor in each sector to demonstrate our observations. The summary statistics confirm our earlier observations that the CDS spreads and spread returns are significantly more volatile in 2007-09. For instance, the daily standard deviation of spread returns of MetLife in 2007-09 is twice its value in 2005-07. One interesting observation is that, the sample skewness of spread returns in 2007-09 is generally smaller and closer to 0. Moreover, although the spread returns appear to be leptokurtic in both periods, the sample kurtosis is generally smaller in 2007-09.

**Figure 4.1:** 5-year CDS spreads (left) and daily spread returns (right) of Conoco Philips.

Obligor	Period	Conoco Phillips	Eastman Chemical	First Energy	HP	JC Penny	MetLife	Motorola	Pfizer
Rating Sector		A Energy	BBB Materials	BBB Utilities	A Com Tech	BB C. Cyclical	A- Financial	BB+ Industrial	AA C. Stable
Mean (bps)	2005-09	38.02	65.79	63.97	34.71	156.04	151.12	137.84	25.52
	2005-07	20.16	49.46	37.34	21.39	69.02	20.86	30.41	7.13
	2007-09	57.17	83.32	92.54	49.01	249.40	290.88	253.10	45.26
Stddev (bps)	2005-09	26.79	35.40	40.77	22.42	140.06	229.35	159.10	28.97
	2005-07	5.19	7.59	12.41	10.11	33.05	7.11	9.03	2.76
	2007-09	27.37	44.09	41.28	23.19	150.53	266.99	163.47	31.29
Skewness	2005-09	1.46	2.05	1.23	1.31	1.69	1.75	1.40	1.71
	2005-07	-0.34	0.28	-0.42	0.84	1.64	-0.03	0.51	0.53
	2007-09	0.77	1.04	0.54	0.86	1.00	0.72	0.53	0.90
Kurtosis	2005-09	4.38	6.65	3.96	4.80	5.38	4.86	4.13	5.26
	2005-07	2.39	2.20	2.05	3.66	5.65	1.65	2.62	1.58
	2007-09	2.69	3.06	2.75	3.68	3.24	2.21	2.76	3.07
Max (bps)	2005-09	131.27	227.02	206.60	134.80	701.04	989.99	682.17	127.27
	2005-07	33.77	70.75	65.80	57.18	222.00	34.58	53.69	12.33
	2007-09	131.27	227.02	206.60	134.80	701.04	989.99	682.17	127.27
Min (bps)	2005-09	9.23	32.56	12.51	7.75	35.95	10.68	14.14	3.80
	2005-07	9.23	35.74	12.51	7.75	35.95	10.68	14.14	3.80
	2007-09	17.95	32.56	23.16	13.55	53.30	14.04	33.87	6.52

Table 4.3: Summary statistics of 5-year CDS spreads (daily observations).

Obligor	Period	Conoco Phillips	Eastman Chemical	First Energy	HP	JC Penny	MetLife	Motorola	Pfizer
Mean (%)	2005-09	0.08	0.04	0.08	0.04	0.00	0.27	0.16	0.13
	2005-07	-0.02	-0.01	-0.14	-0.14	-0.24	-0.10	-0.03	-0.11
	2007-09	0.19	0.10	0.32	0.23	0.26	0.67	0.36	0.39
Stdev (%)	2005-09	3.70	4.14	3.75	3.83	4.43	4.86	4.27	3.88
	2005-07	2.72	2.87	2.39	2.84	3.52	2.03	3.62	3.63
	2007-09	4.52	5.17	4.79	4.65	5.23	6.65	4.86	4.11
Skewness	2005-09	0.16	1.28	1.24	0.13	0.91	0.66	1.76	1.35
	2005-07	1.22	1.96	1.78	0.44	3.04	0.40	3.04	0.34
	2007-09	-0.15	0.98	0.88	-0.04	0.08	0.36	1.07	2.06
Kurtosis	2005-09	10.08	17.81	13.46	9.04	17.55	16.36	21.58	12.41
	2005-07	11.05	16.16	17.71	9.01	51.69	7.14	24.78	8.75
	2007-09	7.87	13.54	9.18	7.26	7.60	9.50	18.45	14.15
Max (%)	2005-09	21.32	43.89	28.29	21.01	44.08	42.15	41.55	31.23
	2005-07	19.00	25.58	20.73	15.14	44.08	10.86	32.17	22.04
	2007-09	21.32	43.89	28.29	21.01	28.36	42.15	41.55	31.23
Min (%)	2005-09	-27.32	-20.54	-21.27	-22.94	-26.72	-32.28	-33.51	-18.75
	2005-07	-11.65	-8.74	-9.72	-16.27	-20.49	-8.43	-14.62	-18.75
	2007-09	-27.32	-20.54	-21.27	-22.94	-26.72	-32.28	-33.51	-13.05

Table 4.4: Summary statistics of daily spread returns.

4.2 Stylized properties of CDS spreads

4.2.1 Stationarity and unit root tests

Property 4.1 (Stationarity of CDS spread returns). *CDS spread returns appear to be stationary, whereas CDS spreads themselves are not.*

We consider three tests for stationarity: (1) Augmented Dickey-Fuller (ADF) test [40, 59], (2) Phillips-Perron (PP) test [87] and (3) Kwiatkowski, Phillips, Schmidt and Shin (KPSS) test [66]. For ADF test and PP test, the null hypothesis assumes the time series has a unit root. KPSS test is an inverse of the PP test in which the null hypothesis assumes that the time series does not have a unit root. From Table 4.5, we observe that the spread returns of almost all obligors reject the null hypothesis of ADF and PP tests and cannot reject the null hypothesis of KPSS test. On the other hand, CDS spread series of only a small number of obligors can reject the null hypothesis of ADF and PP and cannot reject the null hypothesis of KPSS. This suggests that our statistical analysis should focus on CDS spread returns which appear to be stationary.

CDS spreads					
Tests and decisions	1-day		5-day		
	2005-07	2007-09	2005-07	2007-09	
Reject H_0^{adf}	45	52	35	24	
Reject H_0^{pp}	48	43	45	46	
Cannot reject H_0^{kpss}	5	1	32	16	
Total number of obligors	121	125	118	125	

CDS spread log returns					
Tests and decisions	1-day		5-day		
	2005-07	2007-09	2005-07	2007-09	
ADF: Reject H_0	121	125	115	125	
Philips-Perron: Reject H_0	121	125	118	125	
KPSS: Cannot reject H_0	121	118	117	125	
Total number of obligors	121	125	118	125	

Table 4.5: Number of obligors that reject the null hypothesis of Augmented Dickey-Fuller (ADF) test, reject the null hypothesis of Phillips-Peron (PP) test and cannot reject the null hypothesis of Kwiatkowski, Phillips, Schmidt and Shin (KPSS) test at 95% confidence level for (1) CDS spreads and (2) spread returns time series. CDS spreads and spread returns are observed at 1- and 5-day time interval.

4.2.2 Linear serial dependence

Property 4.2 (Autocorrelation). *CDS spread returns exhibit positive autocorrelations at 1 to 3 days, especially during the crisis period 2007-09. The autocorrelations diminish when the observation interval increases.*

Linear autocorrelations of asset returns are often insignificant except for very small intraday time scales [22]. However, Figure 4.2 shows that daily spread returns exhibit positive autocorrelation for small time lags. Illiquidity may be one cause for the presence of positive autocorrelations.

Table 4.6 shows that the positive autocorrelations appear to diminish when the observation interval increases. In particular, while we can reject the null hypothesis of Ljung-Box test for all daily spread return series, we can no longer reject the test in many cases for 5-day and 10-day spread returns at 95% level. Our result is further supported by Figure 4.3 which shows the number of obligors that have significant autocorrelation coefficients at different time lags. Partial autocorrelations also exhibit similar features but they will not be shown this chapter.

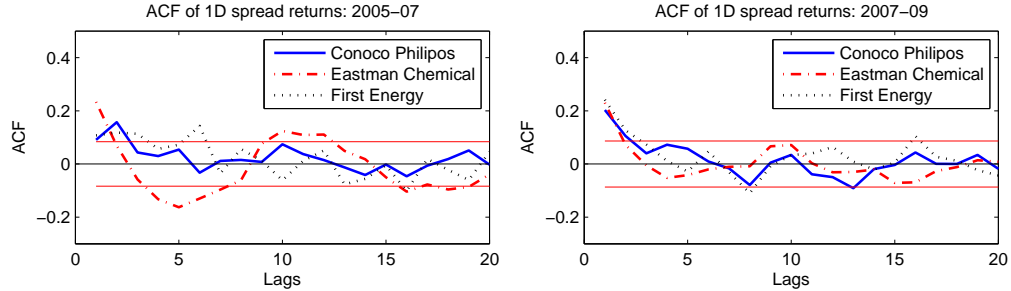


Figure 4.2: Sample autocorrelation function of daily spread returns in 2005-07 and 2007-09. Obligors: Conoco Philips, Eastman Chemical and First Energy . The 95% confidence interval bounds are computed under the hypothesis that the time series is a sequence of i.i.d. random variables.

	Obs (day)	ACF (lags)						Ljung-Box test		
		1	2	3	4	5	10	Q(5)	Q(10)	Q(20)
2005-07										
Conoco Philips	1	0.09	0.16	0.04	0.03	0.05	0.07	22.30 (0.00)	26.40 (0.00)	31.49 (0.05)
	5	-0.08	0.19	-0.12	0.06	-0.10	0.02	8.42 (0.13)	10.56 (0.39)	26.16 (0.16)
	10	0.13	-0.11	0.01	-0.07	-0.04	-0.21	2.22 (0.82)	19.46 (0.03)	27.10 (0.13)
Eastman Chemical	1	0.23	0.07	-0.06	-0.13	-0.16	0.12	61.46 (0.00)	91.31 (0.00)	129.26 (0.00)
	5	-0.36	0.28	-0.20	-0.01	-0.06	0.02	29.53 (0.00)	31.65 (0.00)	47.80 (0.00)
	10	0.00	-0.16	-0.11	-0.06	0.05	0.21	2.76 (0.74)	12.18 (0.27)	21.41 (0.37)
First Energy	1	0.11	0.12	0.11	0.06	0.07	-0.06	27.09 (0.00)	43.90 (0.00)	60.84 (0.00)
	5	0.41	0.04	-0.15	-0.16	-0.15	0.17	28.50 (0.00)	44.06 (0.00)	66.17 (0.00)
	10	0.14	-0.23	-0.30	-0.18	0.21	-0.13	15.25 (0.01)	25.81 (0.00)	32.18 (0.04)
2007-09										
Conoco Philips	1	0.20	0.11	0.04	0.07	0.06	0.03	33.61 (0.00)	37.86 (0.00)	46.65 (0.00)
	5	0.19	-0.11	-0.07	0.04	-0.03	-0.08	6.00 (0.31)	8.89 (0.54)	24.45 (0.22)
	10	-0.11	0.02	0.00	-0.08	-0.15	-0.19	2.40 (0.79)	12.22 (0.27)	23.82 (0.25)
Eastman Chemical	1	0.23	0.07	-0.01	-0.05	-0.04	0.07	33.71 (0.00)	39.24 (0.00)	46.57 (0.00)
	5	0.09	0.00	-0.06	-0.05	0.04	-0.10	1.58 (0.90)	5.58 (0.85)	15.22 (0.76)
	10	-0.08	-0.05	0.14	0.03	-0.13	0.02	2.63 (0.76)	6.65 (0.76)	12.88 (0.88)
First Energy	1	0.24	0.13	0.07	0.01	-0.03	0.03	43.39 (0.00)	52.37 (0.00)	63.66 (0.00)
	5	0.03	-0.09	0.20	-0.11	-0.16	-0.05	9.64 (0.09)	15.34 (0.12)	21.83 (0.35)
	10	0.00	-0.01	-0.09	-0.15	-0.16	-0.10	3.30 (0.65)	7.25 (0.70)	21.30 (0.38)

Table 4.6: Autocorrelation coefficients of 1, 5 and 10-day spread returns. Ljung-Box test statistics and p-values (in brackets) for 5, 10 and 20 lags.

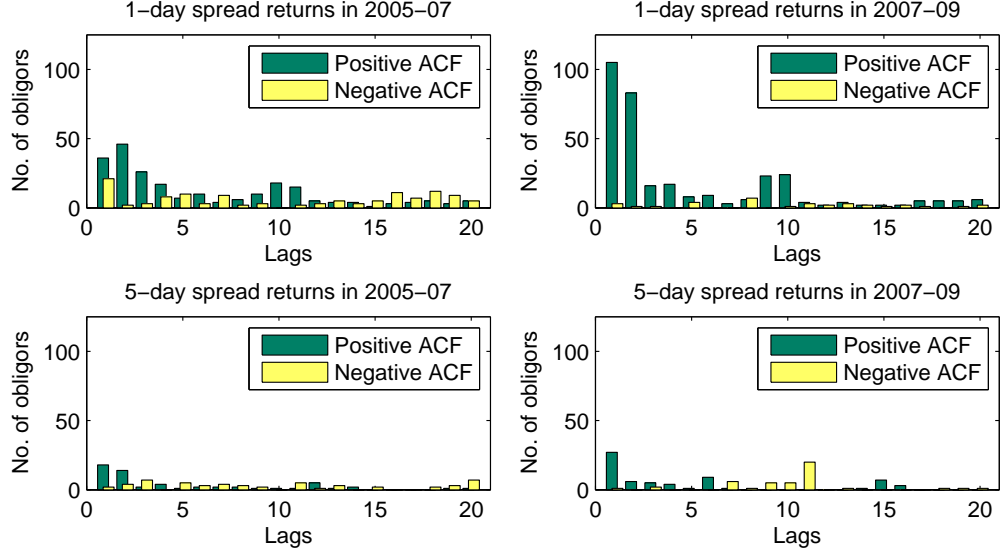


Figure 4.3: Number of obligors whose spread returns have statistically significant positive and negative autocorrelations at each lag at 95% confidence level. The critical values for statistical testing is computed under the hypothesis that the time series is a sequence of i.i.d. random variables.

4.2.3 Heavy tails

As early as the 1960s, Mandelbrot [22, 78] pointed out the insufficiency of the normal distribution for modeling the marginal distribution of asset returns and their heavy-tailed character. We observe similar features in CDS spreads:

Property 4.3 (Heavy-tailed distribution). *CDS spread returns appear to have two-sided heavy tails. In 2005-07, daily spread returns have heavier right tails which have tail indices in the range of $2 \sim 4$, and lighter left tails which have tail indices in the range of $3 \sim 6$. In 2007-09, CDS spread daily return tails are symmetric and have tail indices in the range of $3 \sim 6$.*

The heavy-tailed character of CDS spread returns can be clearly seen from the quantile plots in Figure 4.4 and the Hill estimators [61] for the tail indices in Figure 4.5. Since both left and right tails appear to be heavier than those implied by the normal distribution, models which only allow upward jumps, such as affine-jump diffusion models [41] and non-Gaussian Ornstein-Uhlenbeck models with

positive jumps [17] may not be sufficient to explain the two-sided heavy-tailed distribution.

We observe that almost all obligors have tail indices are larger than 2, which suggests that the spread returns have finite variances. Hypothesis testing on tail indices is complicated by the fact that spread returns are autocorrelated: we will perform a more detailed analysis below for conditional spread returns.

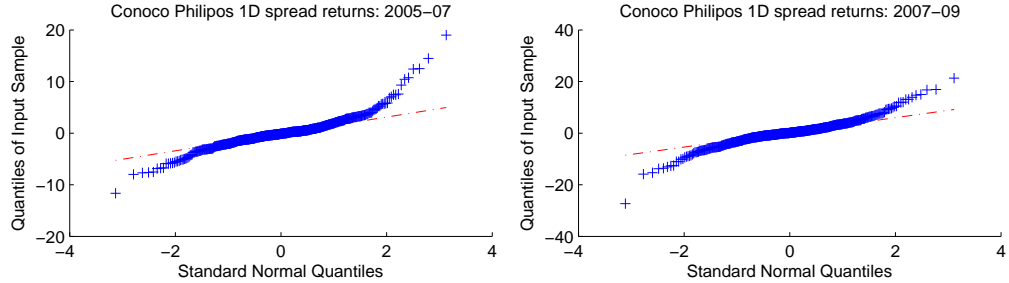


Figure 4.4: Quantile plots of 1-day spread returns of Conoco Philips vs normal distribution.

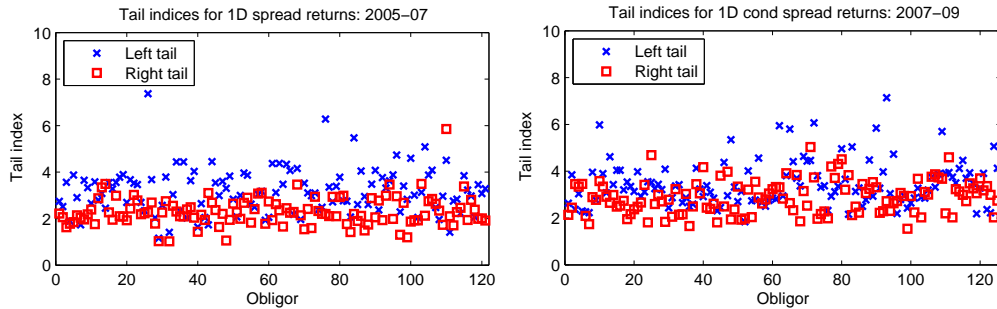


Figure 4.5: Hill estimators for the tail indices of CDS spread daily returns. The number observations for estimation is equal to 2.5% of the sample size.

4.2.4 Nonlinear serial dependence

Property 4.4 (Volatility clustering in CDS spreads). *Daily spread returns exhibit volatility clustering and conditional heteroscedasticity. In particular, absolute values of CDS spread returns exhibit significant positive autocorrelation.*

This effect, illustrated in Figure 4.6 and Figure 4.7, is a quantitative signature of volatility clustering: large price variations are more likely to be followed by large price variations.

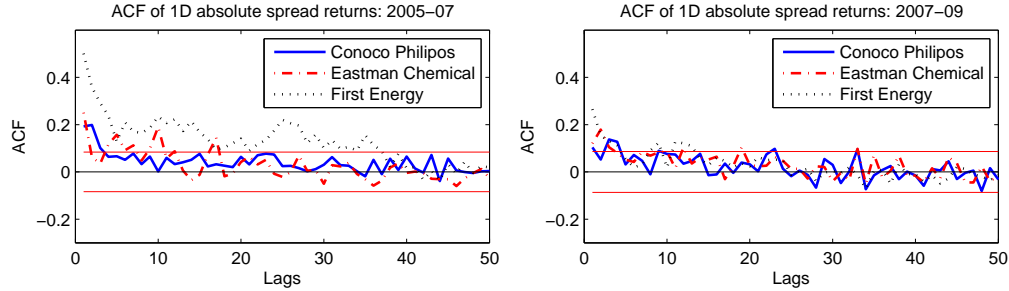


Figure 4.6: Sample autocorrelation function of daily absolute spread returns in 2005–07 and 2007–09. Obligors: Conoco Philips, Eastman Chemical and First Energy . The 95% confidence interval bounds are computed under the hypothesis that the time series is a sequence of i.i.d. random variables.

We further investigate this property by performing the White test [96] on the CDS spread returns. For the daily spread returns, most of the obligors, 83 out of 121 in 2005–07 and 75 out of 125 in 2007–09, reject the null hypothesis that the residual variance is constant at 95% confidence level. On the other hand, for 5-day spread returns, only a relatively small number of obligors, 50 out of 118 in 2005–07 and 20 out of 125 in 2007–09, reject the null hypothesis.

This property is traditionally modeled using ARMA-GARCH models [13, 47]. Thus, we estimate an ARMA-GARCH model with i.i.d. Student-t innovations for 1-day and 5-day spread returns by using maximum likelihood. Orders of the models are chosen based on Akaike information criterion (AIC). For the daily spread returns, most obligors, 105 out of 121 in 2005–07 and 119 out of 125 in 2007–09, have at last one statistically significant GARCH coefficients at 95% level. On the other hand, for the 5-day spread returns, there are 74 out of 118 obligors in 2005–07 and 36 out of 125 obligors in 2007–09 have statistically significant GARCH coefficients at 95% level, which is significantly less than the case for the daily spread returns.

4.2.5 Absence of correlation between spread returns and changes in spread volatility

Property 4.5. *No significant correlation is observed between spread return and moves in (realized) volatility of spreads.*

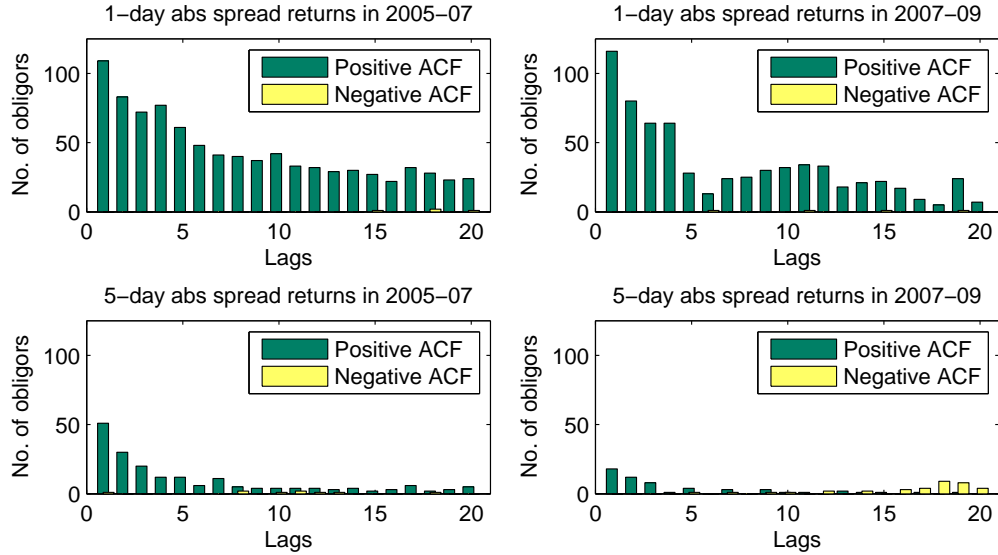


Figure 4.7: Number of obligors whose absolute spread returns have statistically significant positive and negative autocorrelations at each lag at 95% confidence level. The critical values for statistical testing is computed under the hypothesis that the time series is a sequence of i.i.d. random variables.

Figure 4.8 shows that, for Conoco Philips, there is no significant linear relationship between the daily returns of the 20-day realized spread volatility and the CDS spread daily returns. Then for each obligor, we regress the realized volatility returns with different rolling windows against the spread returns and check whether the regression models have positive slopes. Table 4.7 shows that, for short rolling windows, only less than half of the obligors give positive slopes in the OLS regression at 95% confidence level. Although more obligors give positive slopes when the rolling window gets larger, Table 4.8 shows that the relationship between returns of the realized volatilities and the CDS spread returns is not linear, as the R^2 of the OLS regression is extremely small.

This property shows that asymmetric conditional volatility model such as GJR model [56] is not necessary for modeling the CDS spreads.

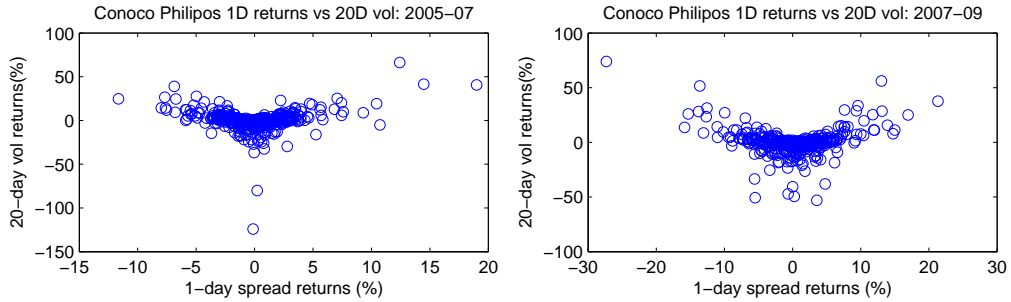


Figure 4.8: Daily spread returns vs 20-day realized volatility returns of Conoco Philips.

Period	Slope	Realized volatilities			
		rolling window (in days)	5	10	20
2005-07	Positive	49	62	73	80
	Negative	11	9	12	13
2007-09	Positive	32	52	67	81
	Negative	1	4	7	9

Table 4.7: Number of obligors that appear to have positive or negative slopes at 95% confidence level in the regression of realized volatility daily returns against CDS spread daily returns. Realized volatilities are computing using 5, 10, 20, 50-day rolling windows.

Period	Realized volatilities			
	rolling window (in days)			
	5	10	20	50
2005-07	0.016	0.031	0.043	0.062
2007-09	0.007	0.013	0.021	0.033

Table 4.8: Average R^2 , across all sample obligors, of the OLS regression of realized volatility daily returns against CDS spread daily returns.

4.2.6 Heavy-tailed conditional distributions

Heavy tails in unconditional distributions of spread returns can be due to the conditional heteroskedasticity observed above. So it is natural to investigate whether heavy tails persist after we correct for this heteroskedasticity. We estimate an ARMA-GARCH model as described in section 4.2.4 and study the resulting standardized residuals, the *conditional spread returns*.

Property 4.6 (Heavy-tailed conditional distribution). *Even after accounting for heteroskedasticity*

and volatility clustering using an ARMA-GARCH model, the conditional distribution (of residuals) exhibits heavy tails. In 2005-07, conditional spread returns have heavier right tails with tail indices in the range of $2 \sim 4$ and lighter left tails with tail indices in the range of $3 \sim 6$. In 2007-09, conditional spread return tails are symmetric with tail indices in the range of $3 \sim 5$. We cannot reject the null hypothesis that the conditional spread returns have tail indices larger than or equal to 2, which suggests that conditional spread returns have finite variance.

Although the heavy tails of the spread returns are partly contributed from conditional heteroscedasticity, quantile plots in Figure 4.9 and the Hill estimators for tail indices in Figure 4.10 show that the conditional spread returns also exhibit heavy tails. We estimate the confidence intervals for the tail indices using the asymptotic normality of the Hill estimators under i.i.d. assumptions for conditional spread returns [57]. From Figure 4.11, we observe that almost none of the confidence intervals contains the value 1, and most intervals contain values larger than or equal to 2. This suggests that the conditional spread returns have finite variances.

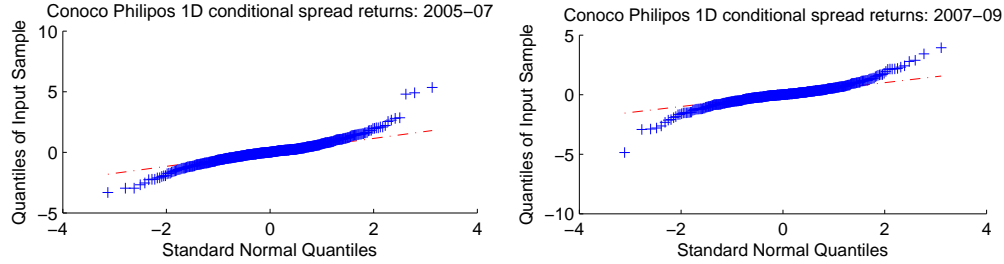


Figure 4.9: Quantile plots of Conoco Philips conditional spread returns vs normal distribution.

4.2.7 Positive serial dependence in extreme values

Property 4.7. *Extreme CDS spread returns exhibit positive serial dependence, especially for large upward movements and small time lags at 1 or 2 days.*

Given the presence of heavy tails, it is interesting to see whether extreme moves in CDS spreads are isolated occurrences or whether they exhibit any serial dependence. In order to examine the

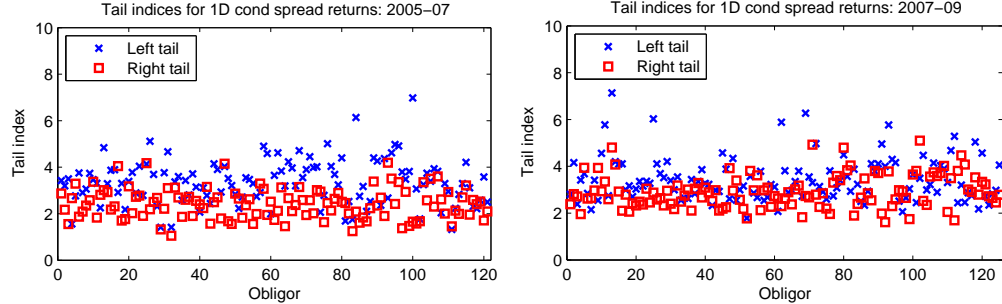


Figure 4.10: Hill estimators for the tail indices of conditional spread returns from ARMA-GARCH models fitted to daily spread returns. The number observations for estimation is equal to 2.5% of the sample size.

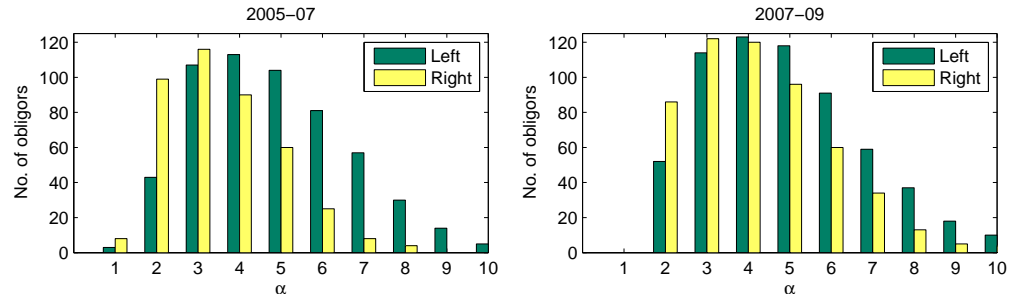


Figure 4.11: Number of obligors whose 95% confidence interval for the Hill estimator contains α . Data series: conditional spread returns from ARMA-GARCH models.

serial dependence of extreme values, Davis and Mikosch [36] introduce the *extremogram*, in the framework of multivariate regularly varying processes (see Resnick [89] for definitions).

Let $(X_t)_{t=0,1,\dots}$ be a (strictly) stationary and regularly varying process with tail index α . Consider a sequence of “high quantiles” $a_m \rightarrow \infty$ as $m \rightarrow \infty$ such that the probability that an observation exceeds a_m is of order $1/m$: $P(|X_0| > a_m) \sim m^{-1}$. Davis and Mikosch [36] define the (right tail) *extremogram* $(\rho^+(k), k \geq 1)$ of X as, in the case $P(X_0 > a_m) > 0$, as

$$\rho^+(k) = \lim_{m \rightarrow \infty} P(X_k > a_m | X_0 > a_m) = \lim_{m \rightarrow \infty} \frac{P(X_0 > a_m, X_k > a_m)}{P(X_0 > a_m)}$$

$\rho^+(k) \in [0, 1]$ behaves intuitively as a “tail autocorrelation” function: a large positive value of $\rho^+(k)$ indicates serial dependence in the large values X . Similarly, the left tail extremogram $(\rho^-(k), k \geq 1)$ is defined as

$$\rho^-(k) = \lim_{m \rightarrow \infty} P(X_k < -a_m | X_0 < -a_m) = \lim_{m \rightarrow \infty} \frac{P(X_0 < -a_m, X_k < -a_m)}{P(X_0 < -a_m)}.$$

These extremograms may be estimated by their empirical counterparts:

$$\hat{\rho}^+(h) = \frac{\sum_{t=1}^{n-h} 1_{X_t > a_m, X_{t+h} > a_m}}{\sum_{t=1}^n 1_{X_t > a_m}}, \quad \hat{\rho}^-(h) = \frac{\sum_{t=1}^{n-h} 1_{X_t < -a_m, X_{t+h} < -a_m}}{\sum_{t=1}^n 1_{X_t < -a_m}}, \quad (4.1)$$

where n is the number of samples, and (a_m) is chosen such that $P(|X_0| > a_m) \sim m^{-1}$, $m \rightarrow \infty$ and $m/n = o(1)$. (4.1) are called the *empirical extremograms*.

We choose the threshold a_m to be the 95% (resp. 5%) quantile for the right (resp. left) tail extremograms. We construct the confidence bound in the empirical extremogram via a bootstrap method: we randomly permute the time series and compute an empirical extremogram for each shuffled sample. At each lag, we use the 95% percentile across the simulated empirical extremogram values to be the 95% confidence bound. We refer readers to [37] for details on computing the confidence bound by using bootstrap method.

Figure 4.12 shows the empirical extremograms (4.1) for the daily spread return of Eastman Chemical. The empirical extremogram appears to be significantly larger than the 95% confidence bounds for 1 day. As shown by Davis and Mikosch [36], this may come from the autocorrelation and conditional heteroscedasticity, which we have observed in section 4.2.2 and section 4.2.4.

Davis and Mikosch [36] also show that, under certain conditions, the empirical extremogram (4.1) follows a multivariate normal distribution asymptotically:

$$\sqrt{n/m} [\hat{\rho}^+(i) - \rho^+(i)]_{i=1,\dots,h} \xrightarrow{d} N(0, F\Sigma F'),$$

where F and Σ are matrices which depend on the law of (X_t) . We refer readers to [36] for details of this central limit theorem. Using this asymptotic normality, we construct confidence intervals for the empirical extremograms. Figure 4.13 shows the number of obligors whose 95% confidence intervals do not contain zero, i.e. the corresponding empirical extremogram value is significantly positive. In both periods, more than half of the obligors appear to be serially dependent for large upward movements at small lags (1 and 2 days). On the other hand, serial dependence of large downward movements is not as common.

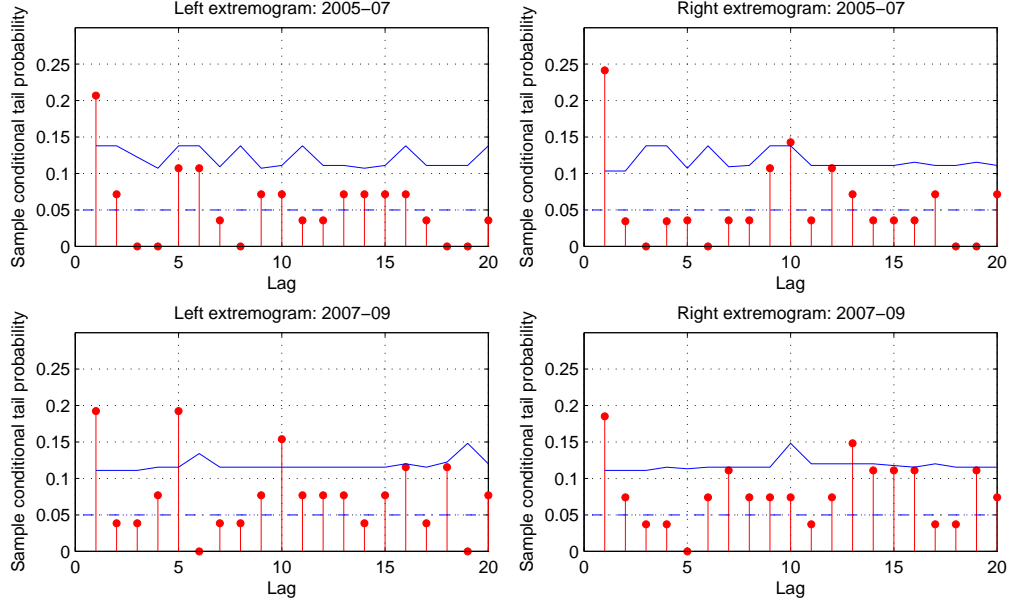


Figure 4.12: Empirical extremograms for daily spread returns of Eastman Chemical in 2005-07 (top) and 2007-09 (bottom). For the left tail estimates (resp. right tail estimates), threshold a_m is equal to 5% (resp. 95%) quantile of the sample. Blue solid line is the 95% confidence bound constructed from randomly permuted data series. Blue dotted line is equal to 5%, which is the theoretical value for an independent series.

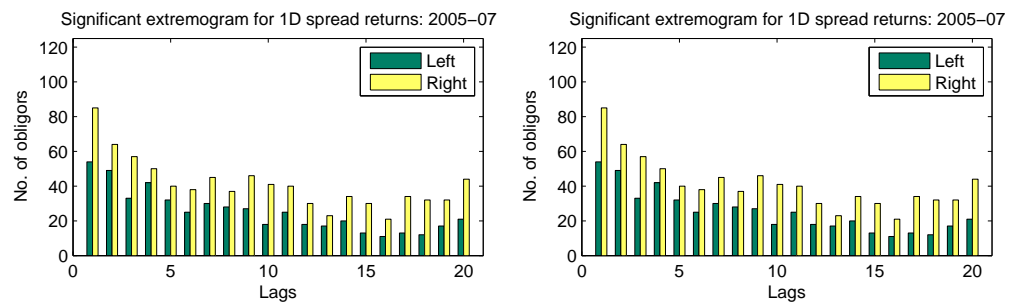


Figure 4.13: Number of obligors in which the 95% confidence intervals for the empirical extremograms do not contain zero. The confidence intervals are computed from asymptotic normality.

4.2.8 Co-movements in CDS spreads

Study of co-movements in CDS spreads provides strong evidence for dependence across obligors of CDS spread returns. Small co-movements may be studies using Pearson correlation coefficients, while large co-movements tend to display different dependence patterns and are better characterized using tail dependence coefficients[36, 89].

Property 4.8. *Cross-obligor correlations of CDS spread returns increase substantially from the range of $0.0 \sim 0.2$ in 2005–07 to the range of $0.3 \sim 0.5$ in 2007–09. Correlations are similar within each industrial sector and rating category.*

To display patterns observed in the correlation coefficients, we plot all the sample correlation coefficients in Figure 4.14 for each sample period. The cross-obligor correlations of spread returns have increased substantially during the subprime crisis. This suggests that after the series of bankruptcies and economic crisis since 2007, investors expect the shifting in credit quality, which can be represented by the changes of the CDS spreads to be more correlated across obligors.

If two obligors belong to the same group, e.g. rating category and industrial sector, it is common to expect that they are subjected to similar risk factors. Therefore, we may expect a higher correlation in spread returns between two obligors in the same group than two obligors in different groups. However, we do not observe this in Figure 4.15 and 4.16. This implies that a factor model for CDS spreads with rating or industry specific factors may not be necessary.

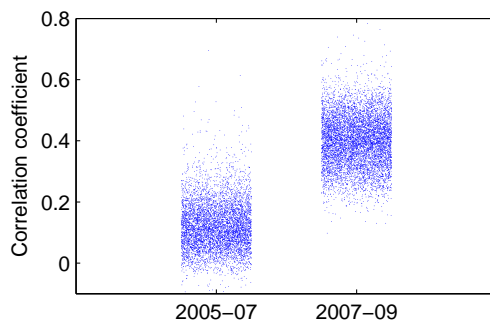


Figure 4.14: Jitter plot of cross-obligor correlations of daily spread returns.

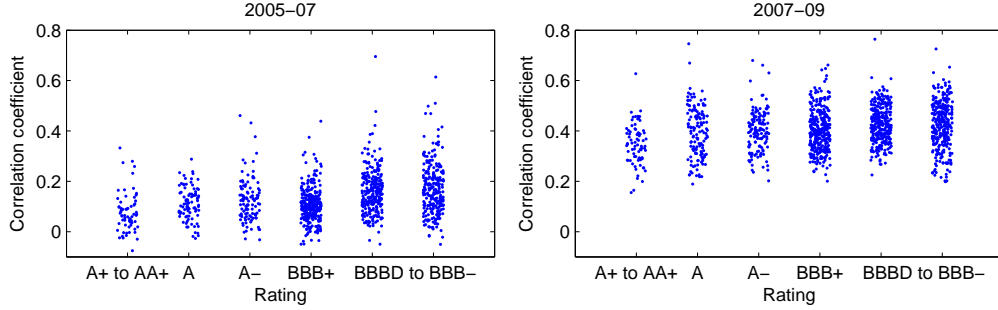


Figure 4.15: Jitter plots of cross-obligor correlations coefficients in different rating categories of daily spread returns.

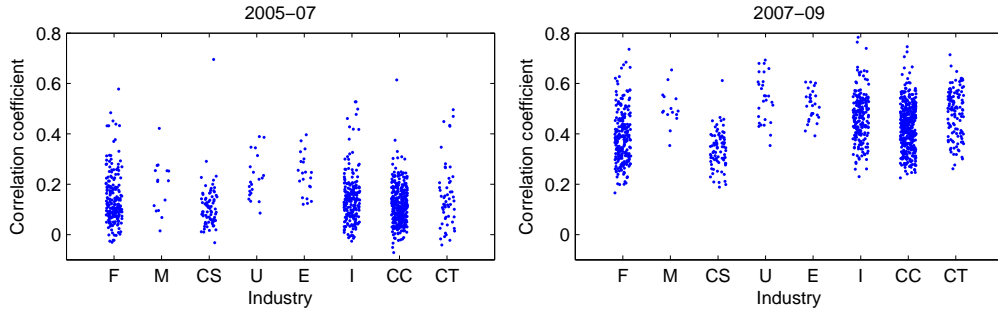


Figure 4.16: Jitter plots of cross-obligor correlations in different industrial sectors of daily spread returns. F: Financial, M: Materials, CS: Consumer Stable, U: Utilities, E: Energy, I: Industrial, CC: Consumer Cyclical, CT: Communication and Technology.

Property 4.9. *CDS spreads appear to have large co-movements. Upward co-movements are common in both 2005-07 and 2007-09, while downward co-movements are more common in 2007-09 than in 2005-07.*

In order to study whether the CDS spreads have large co-movements, we consider the conditional right tail probability $P(r_t^j > q^j | r_t^i > q^i)$ where (r_t^i, r_t^j) are the spread returns for obligor i and j at time t and (q^i, q^j) are some large constants. Similarly, we can consider the conditional left tail probability to study downward common jumps. We say the CDS spreads of obligor i and j are asymptotically independent if this probability is close to 0.

In Figure 4.17, we compute the natural estimators for the conditional left and right tail proba-

bilities

$$\hat{p}^- = \frac{\sum_t 1_{r_t^i < h^i, r_t^j < h^j}}{\sum_t 1_{r_t^i < h^i}}, \quad \hat{p}^+ = \frac{\sum_t 1_{r_t^i > q^i, r_t^j > q^j}}{\sum_t 1_{r_t^i > q^i}} \quad (4.2)$$

where h^i and q^i are chosen to be the 5% and 95% quantile of obligor i 's daily spread returns respectively. Observe that for many cases, the conditional probabilities are significantly different from the independence case, especially in 2007-09.

In order to perform a more robust inference on the large co-movements, we follow Coles, Hefernan and Tawn [19] and study the right tail dependence measure

$$\chi = \lim_{u \rightarrow \infty} \frac{2 \ln(P(U^j > u))}{\ln(P(U^i > u, U^j > u))} - 1 \quad (4.3)$$

where U^i is the Fréchet transformation of the spread return for obligor i . Values of $\chi > 0$, $\chi = 0$ and $\chi < 0$ correspond respectively to when the spread returns of the two obligors are positively associated in extremes, independent and negatively associated respectively. Under a broad set of conditions [72, 73] the following estimator of χ

$$\hat{\chi} = 2/\hat{\alpha} - 1$$

is consistent, where $\hat{\alpha}$ is the Hill estimator for the random variable $Z = \min(U^i, U^j)$. A similar analysis can be performed for the left tail dependence measure (see [62, Ch 7.2.]).

At 95% confidence level, we find that about 73% of the obligor pairs reject the hypothesis that $\chi = 0$ for large upward co-movements in both 2005-07 and 2007-09. On the other hand, 92% of the obligor pairs reject that $\chi = 0$ for large downward co-movements in 2007-09 and there is 38% in 2005-07. This shows strong evidence that CDS spreads exhibit large co-movements, especially for upward jumps. On the other hand, downward co-movements are more common in the subprime crisis period. Note that the results on testing large co-movements for the conditional spread returns from ARMA-GARCH models are similar and we will not further discuss in this section.

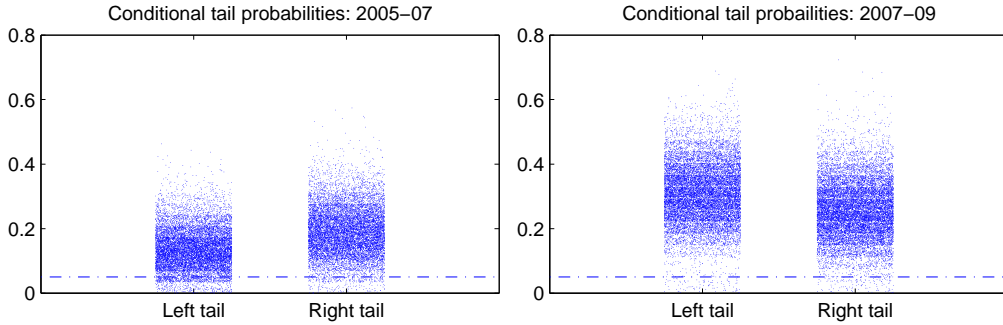


Figure 4.17: Estimators, \hat{p}^- and \hat{p}^+ , for the conditional probability of having a large CDS spread move in an obligor given that there is a large CDS spread move in other obligor. Each point represents the conditional tail probability for a pair of obligors. Blue dotted lines at 5% level represents the estimator value for independent series.

4.2.9 Principal component analysis

Principal component analysis (PCA) provides insights into the co-movements of CDS spreads.

Property 4.10.

- *The first principal component represents parallel moves in the CDS spreads and accounts for 12% (resp. 40%) of the daily variance of CDS spreads in 2005-07 (resp. 2007-09).*
- *The main contribution to the variance comes from large idiosyncratic moves (“jumps”).*

Table 4.9 shows the CDS spread return variance explained by the principal component factors. Notice that a relatively large number of factors is needed to explain substantial amount of the variance. This suggests that the main contribution of the variance comes from idiosyncratic variation, especially in 2005-07. In fact, these observations also hold for conditional spread returns, which are shown in Table 4.10.

Since our modeling approach in section 4.4 will involve specification of the condition spread returns, we will focus on it (instead of the unconditional one) in the remaining of this section. Nevertheless, we find that the conclusion drawn from the conditional spread return is very similar to the unconditional one. From Figure 4.18 and 4.19 we observe that the first factor loadings are all

positive and the magnitudes are similar across the obligors. This shows that the main driver of the underlying risk is roughly equal to an equally weighted CDS portfolio which can be approximated by the credit indices such as CDX. Figure 4.18 shows some obvious spikes in the factor time series especially in 2005-07. While the spikes are mostly from the second and higher order factors, it suggests that some extreme moves are due to idiosyncratic risk.

Period		No. of Principal Components							
		1	2	3	4	5	25	80	90
2005-07	% Explained	12.1%	5.3%	4.3%	3.8%	3.0%	1.1%	0.3%	0.2%
	% Cumulative	12.1%	17.4%	21.7%	25.5%	28.5%	61.3%	93.8%	96.3%
2007-09	% Explained	40.1%	3.6%	2.7%	2.3%	2.0%	0.7%	0.2%	0.2%
	% Cumulative	40.1%	43.7%	46.5%	48.8%	50.7%	71.1%	93.7%	95.8%

Table 4.9: Percentage of variance that can be explained by the principal components. 112 obligors in 2005-07 period and 123 obligors in 2007-09 period. Data series: unconditional CDS spread daily returns.

Period		Principal Component							
		1	2	3	4	5	25	80	90
2005-07	% Explained	12.1%	3.2%	2.9%	2.6%	2.1%	1.1%	0.4%	0.3%
	% Cumulative	12.1%	15.2%	18.2%	20.7%	22.8%	52.4%	90.9%	94.5%
2007-09	% Explained	37.3%	2.6%	1.8%	1.7%	1.6%	0.8%	0.3%	0.2%
	% Cumulative	37.3%	39.9%	41.8%	43.4%	45.0%	65.3%	92.0%	94.6%

Table 4.10: Percentage of variance that can be explained by the principal components. 112 obligors in 2005-07 period and 123 obligors in 2007-09 period. Data series: conditional spread daily returns from ARMA-GARCH models.

Property 4.11 (PC factor distribution). *PC factors appear to have heavy tails with tail indices are in the range of $2 \sim 5$ for the first few factors and increase to the range of $4 \sim 10$ for the last few factors. The distribution of the first four PC factors are well represented by a Student-t distribution.*

Figure 4.20 shows the tail indices for the PC factors. In both periods, we observe that the 95% confidence intervals of all tail index estimators contain values equal to or larger than 2, which implies that the PC factors have finite variances.

According to the Bayesian information criteria (BIC) shown in Table 4.11, Student t distribution appears to be the best fit for the first few factors in both periods. On the other hand,

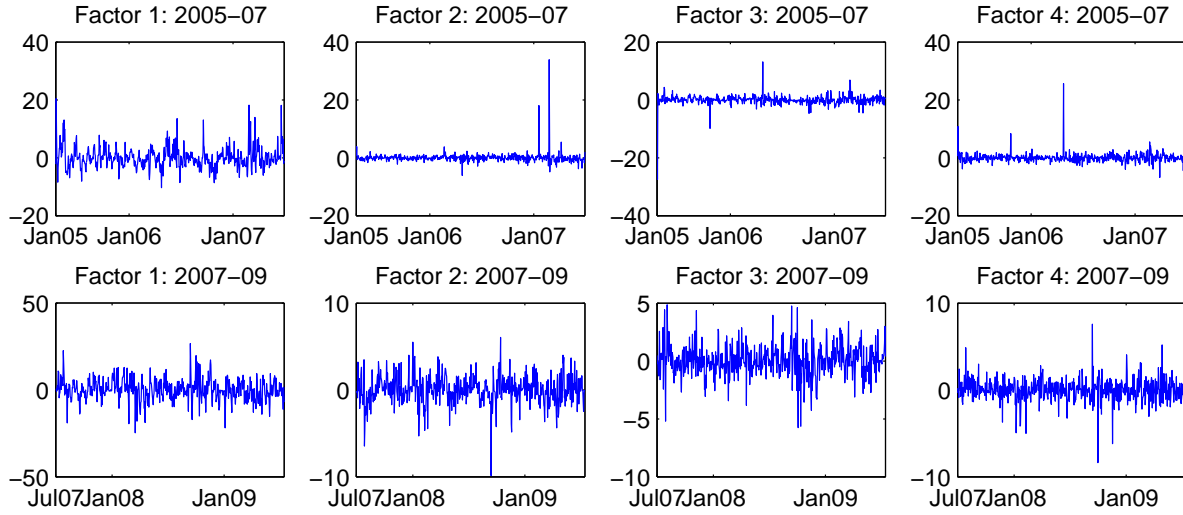


Figure 4.18: The first four principal component factors.

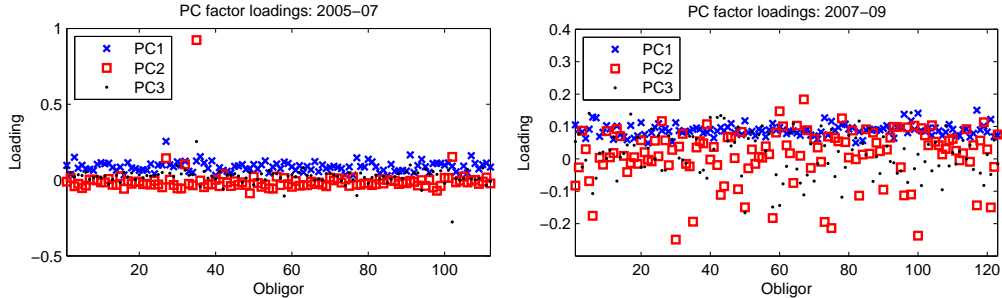


Figure 4.19: Loadings of the first three principal component factors.

normal distribution provides the worst fit while the first few factors appear to have heavy-tailed distributions.

Property 4.12 (Large moves in the first principal component). *Jumps in the first principal component are not only related to credit events, but also related to other market information such as changes in interest rates and economic outlook.*

We investigate the causes of jumps in the first PC factor, which sequentially cause large co-movements in the CDS spreads. In particular, we look at the financial market on the day when the first PC factor exhibits large moves. Table 4.12 and 4.13 show the headlines of New York Times when the first PC factor has its largest and smallest moves. From the descriptions of the market

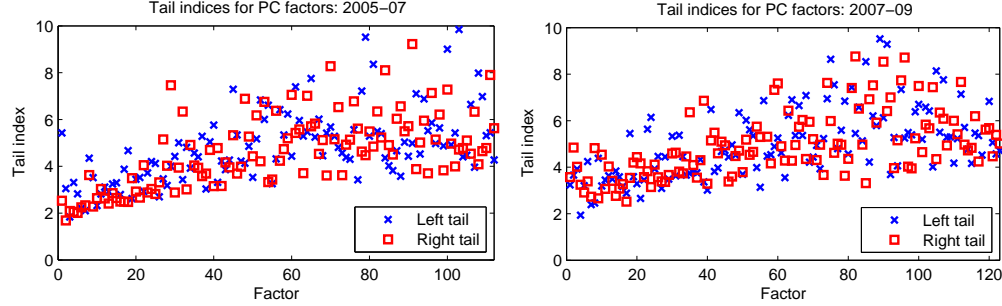


Figure 4.20: Hill estimators for the tail indices of the PC factors. The number observations for estimation is equal to 2.5% of the sample size.

PC factor	Normal	Student t	Double Exp	NIG	Stable
<i>2005-07</i>					
1	1498	1359*	1369	1359*	1372
2	2225	1390	1499	1431	1388*
3	1839	1350*	1418	1374	1356
4	1740	1300*	1338	1316	1311
5	1559	1370*	1399	1381	1379
<i>2007-09</i>					
1	1523	1495*	1512	1501	1506
2	1497	1449*	1453	1452	1466
3	1501	1461*	1477	1465	1476
4	1518	1417*	1430	1425	1425
5	1463	1366*	1370	1370	1380

Table 4.11: BIC of the PC factors fitted to (1) normal, (2) Student t, (3) double exponential, (4) normal inverse Gaussian and (5) stable distribution. Lowest BIC among the distributions is indicated by *.

conditions, we observe that the large moves are related to, not only credit events, such as Lehman bankruptcy on 15 September 2008 and the collapse of two Bear Stearns hedge funds on 20 June 2007, but also other market information, such as changes in interest rates on 18 March 2008 and economic outlook on 15 April 2005 and 15 October 2008.

While some of the previous works have focused on jumps in the CDS spreads when credit events occur [48], our results show that it is not sufficient to explain the common jumps in the CDS spreads. Moreover, as we will show in section 4.2.10, the first PC factor does not exhibit large movements during some of the important credit events such as Federal bailout of Fannie Mae and Freddie Mac and bankruptcy of General Motors. This leads to the question whether CDS spreads will in fact have significant movements during credit events, which will be further explored in the

next section.

Period	PC factor 1	Date	New York Times headlines
2005-07	5.96	15-Apr-05	“Stocks plunge to lowest point since election. I.B.M. earning a factor. Market slump continues amid uncertainty over economy’s growth.”
	5.09	20-Jun-07	“Bear Stearns staves off collapse of two hedge funds. Several lenders pull back from a larger liquidation, for now.”
	4.36	20-Jun-06	“Timber becomes tool in effort to cut estate tax.”
2007-09	4.45	15-Sep-08	“Bids to halt financial crisis reshape landscape of Wall Street: Merrill is sold; Failing to find buyer, Lehman set to file for bankruptcy.”
	3.62	26-Jul-07	“Global stock markets tumble amid deepening credit fears.”
	3.52	15-Oct-08	“After big rally, grim outlook still looms on profits and jobs.”

Table 4.12: The three largest values of the first principal component factor (common factor) in 2005-07 and 2007-09.

Period	PC factor 1	Date	New York Times headlines
2005-07	-2.49	21-Mar-07	“Fed weighs words about its next move. (The central bank left the overnight Federal funds rate at 5.25 percent, a level unchanged since last June.)”
	-2.30	26-Apr-06	“Second thoughts in Congress on oil tax breaks. New political pressure over record profits as gas prices soar.”
	-2.27	28-Nov-05	“U.S. Declines a chance to criticize Yuan policy.”
2007-09	-4.53	18-Mar-08	“Fed trims rates sharply, sending the markets up. Cut 3/4 of a point is less than expected signs of split on policy at Central Bank.”
	-3.33	24-Mar-08	“JP Morgan in negotiations to raise Bear Stearns bid. Price per share would quintuple to \$10 to appease firm’s shareholders.”
	-3.24	6-Jan-09	“Automakers fear a new normal of low sales. As prices rise, some see \$2 gas.”

Table 4.13: The three smallest values of the first principal component factor (common factor) in 2005-07 and 2007-09.

4.2.10 Spread movements during credit events

Property 4.13. *CDS spreads do not necessarily experience upward jumps during credit events.*

We study the spread returns during the credit events in 2008-09 shown in Table 4.14. On each event dates, we study two versions of “normalized” spread returns in Figure 4.21:

- Unconditional normalization: Daily spread returns normalized by the sample standard deviation computed from the data in 2007-09.
- Conditional normalization: Conditional spread returns from ARMA-GARCH fitted to the daily spread returns in 2007-09.

Notice that the patterns between the unconditional normalized spread returns and the conditional spread returns are similar during all credit events. On 15 September 2008 (Lehman bankruptcy) and 29 September 2008 (sale of Wachovia banking operations to Citigroup), most CDS spreads increase substantially. On the other hand, on 8 September 2008 (Federal bailout of Fannie Mae and Freddie Mac) and 1 July 2009 (General motors bankruptcy), most CDS spreads decrease substantially. In general, we have no evidence that the CDS spreads will move in a particular direction during the credit events. Our observations are consistent with Cont and Kan [26] who study index tranche spreads on credit event dates and find no strong evidence that the index tranche spreads must have upward jumps during credit events.

One explanation of the absence of large changes in the CDS spreads during credit events is that the market has already anticipated the events which no longer appear as “shocks” to the investors. Indeed, Guo, Jarrow and Lin [58] distinguish the *recorded* default date which is defined as the actual announcement date of default, from the *economic* default date which is defined as the first date when the market prices the firms debt as if it has defaulted. An interesting topic will be on examining the changes of CDS spreads during the economic default dates vs the recorded default dates and we will leave it for future research.

Date	Event	CDX.NA.IG	PC factor 1
14-Jan-08	BoA agreed to purchase Countrywide Financial	-	0.15
17-Mar-08	JPMorgan agreed to purchase Bear Stearns	-	0.39
1-Jul-08	BoA acquired Countrywide Financial	-	0.80
8-Sep-08	Federal takeover of Fannie Mae and Freddie Mac	S1-10	-2.15
15-Sep-08	Lehman Brothers filed for bankruptcy	-	4.45
17-Sep-08	Federal bailout of AIG	-	-0.69
26-Sep-08	Washington Mutual filed for bankruptcy	S1-10	0.26
29-Sep-08	Wachovia sold banking operations to Citigroup	-	0.86
3-Oct-08	Wells Fargo agreed to purchase Wachovia	-	-0.98
8-Dec-08	Tribune Company filed for bankruptcy	S6	-1.59
31-Mar-09	Idearc Inc filed for bankruptcy	S1-7	-0.35
29-May-09	Visteon Corporation filed for bankruptcy	S1	-1.14
1-Jun-09	General Motors filed for bankruptcy	-	-2.21
7-Jul-09	LEAR Corporation filed for bankruptcy	S4	0.19

Table 4.14: Highlights of credit events in 2008-09. From left to right: the event date or the next business day after the event; description of the events; the CDX.NA.IG series that the obligors belong to; first principal component factor values.

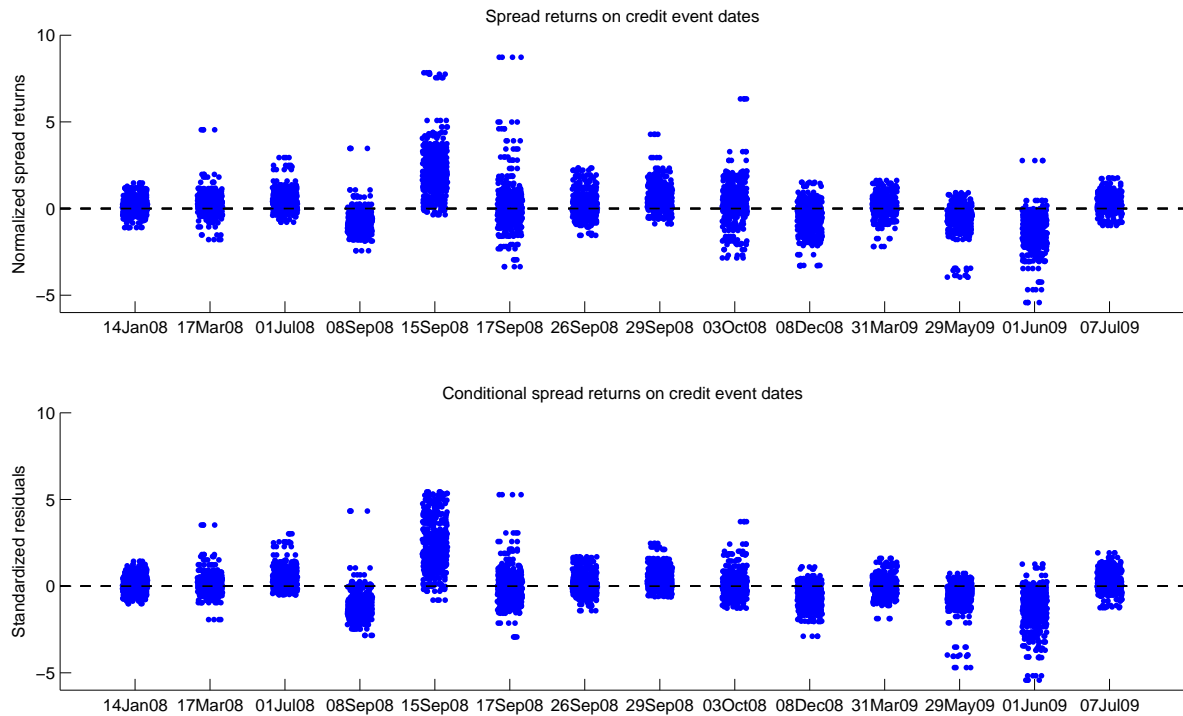


Figure 4.21: Jitter plots of daily spread returns normalized by the unconditional sample standard deviations (top) and the conditional daily spread returns from ARMA-GARCH models (bottom) during the credit events in Table 4.14. Each point represents the spread return/conditional spread return of an obligor on the corresponding event date.

4.3 Comparison with affine jump-diffusion models

Affine jump-diffusion models [41, 83] are reduced-form models for default risk in which the default time of an obligor i is modeled as a random time with intensity

$$\lambda_t^i = X_t^i + a^i X_t^0 \quad (4.4)$$

where $(X_t^k), k = 0, i$ are independent affine jump-diffusion processes whose dynamics under a pricing measure \mathbb{Q} is given by

$$dX_t^k = (\kappa_0^k + \kappa_1^{k,\mathbb{Q}} X_t^k)dt + \sigma^k \sqrt{X_t^k} dW_t^{k,\mathbb{Q}} + dJ_t^k \quad (4.5)$$

where $(W_t^{k,\mathbb{Q}})$ is a standard Brownian motion and (J_t^k) is a compound poisson process with jump intensity $\ell^{k,\mathbb{Q}}$ and jump sizes are exponentially distributed with mean $\mu^{k,\mathbb{Q}}$ under a risk-neutral pricing measure \mathbb{Q} . Choosing an affine risk premium as in [49], the risk-neutral intensity under the real-world statistical measure \mathbb{P} is given by

$$\text{Under } \mathbb{P}: \quad dX_t^k = (\kappa_0^k + \kappa_1^{k,\mathbb{P}} X_t^k)dt + \sigma^k \sqrt{X_t^k} dW_t^{k,\mathbb{P}} + dJ_t^k. \quad (4.6)$$

where $(W_t^{k,\mathbb{P}})$ is a standard Brownian motion under \mathbb{P} and (J_t^k) is now a compound Poisson process with jump intensity $\ell^{k,\mathbb{P}}$ and jump sizes are exponentially distributed with mean $\mu^{k,\mathbb{P}}$ under \mathbb{P} .

This model has been widely used in the literature such as pricing and hedging credit derivatives [41, 83, 45, 49, 17, 10], modeling default correlations [41, 83], portfolio selection [55] and counter-party risk modeling [34]. The main advantage of this model is having a closed-form expression for the default probability (see Appendix 4.6 and [68]). However, no work has been done to justify the use of affine jump-diffusion model in terms of the empirical properties of CDS spreads.

4.3.1 A simulation study

We simulate time series of 5-year CDS spreads under the affine jump-diffusion model and study their statistical properties. We use parameters estimated by Feldhütter [49] for CDX.NA.IG.6 CDS

and CDO tranche spreads from 30 March 2006 to 30 September 2006 using a Markov Chain Monte Carlo method (MCMC). Parameters for (X_t^0) are equal to

$$\begin{aligned} & (\kappa_0^0, \kappa_1^{0,\mathbb{Q}}, \sigma^0, \ell^{0,\mathbb{Q}}, \mu^{0,\mathbb{Q}}, \kappa_1^{0,\mathbb{P}}, \ell^{0,\mathbb{P}}, \mu^{0,\mathbb{P}}) \\ & = (1.59 \times 10^{-5}, 0.46, 3.66 \times 10^{-2}, 3.18 \times 10^{-3}, 1.23, 0.44, 3.37 \times 10^{-3}, 0.0023) \end{aligned}$$

and parameters for (X_t^i) are equal to

$$\begin{aligned} \kappa_1^{i,\mathbb{Q}} &= \kappa_1^{0,\mathbb{Q}}, \quad \kappa_1^{i,\mathbb{P}} = \kappa_1^{0,\mathbb{P}}, \quad \sigma^i = \sqrt{a^i} \sigma^0, \quad \mu^{i,\mathbb{Q}} = \mu^{0,\mathbb{Q}}, \quad \mu^{i,\mathbb{P}} = \mu^{0,\mathbb{P}}, \\ w &= \frac{a^i \kappa_0^0}{a^i \kappa_0^0 + \kappa_0^i} = \frac{\ell^{0,\mathbb{Q}}}{\ell^{0,\mathbb{Q}} + \ell^{i,\mathbb{Q}}} = \frac{\ell^{0,\mathbb{P}}}{\ell^{0,\mathbb{P}} + \ell^{i,\mathbb{P}}} = 0.9742, \end{aligned}$$

and a^i is equal to the CDS spread of obligor i on 30 March 2006 divided by the average CDS spreads among all obligors on the same day². For each CDX.NA.IG.6 obligor, we simulate 1000 daily observations of 5-year CDS spreads. Appendix 4.7 describes our simulation method based on Euler scheme.

Figure 4.22 shows a simulated time series of 5-year CDS spread and the corresponding daily spread returns. As we can see, there is an upward jump in the spread return on about day 610 which is contributed by the Poisson jump component in the default intensity (4.4).

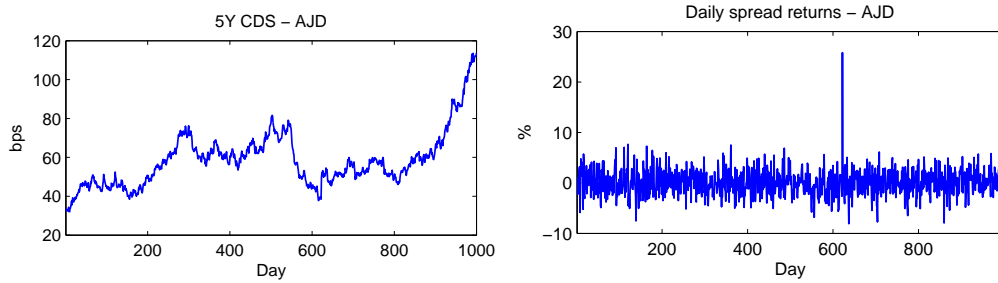


Figure 4.22: Simulated time series of CDS spreads and daily spread returns from the affine jump-diffusion model.

²Each parameter is set to be the median of the estimated distribution by MCMC in [49].

4.3.2 Absence of serial dependence

Figure 4.23 and 4.24 show no significant serial correlations in the simulated spread returns. This illustrates that the simple “volatility term”, $\sigma\sqrt{X_t^i}$, in the affine jump-diffusion process (4.6) is insufficient to produce the volatility clustering feature observed in the empirical data. For extreme values, the affine jump-diffusion model also underestimates the dependence where the extremograms are less than 0.1 at all lags comparing to the empirical values of $0.1 \sim 0.3$ in Figure 4.12.

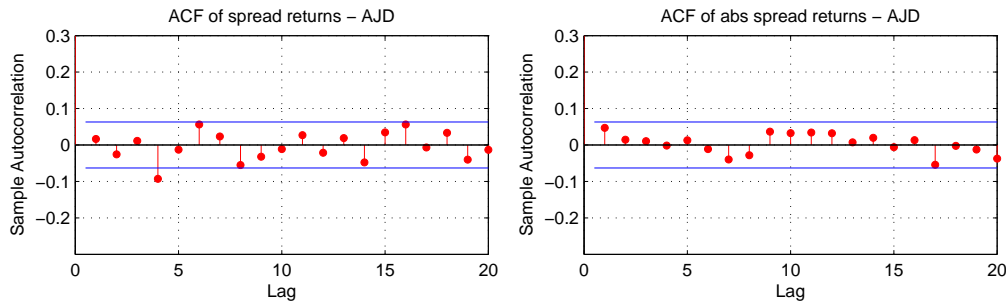


Figure 4.23: Sample autocorrelation function for simulated daily spread returns and absolute spread returns from the affine jump-diffusion model.

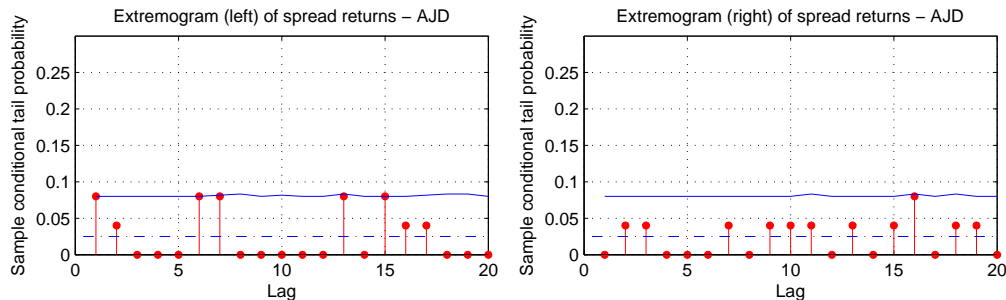


Figure 4.24: Empirical extremograms for simulated daily spread returns from the affine jump-diffusion model. For the left tail estimates (resp. right tail estimates), threshold a_m is equal to 5% (resp. 95%) quantile of the sample. Blue line is the 95% confidence bound constructed from randomly permuted data series. Blue dotted line is equal to 5%, which is the theoretical value for an independent series.

4.3.3 Distributional properties of CDS spread returns

Quantile plots in Figure 4.25 show that distribution of the simulated spread returns appear to be very close to the normal distribution except for occasional outliers in the right tail, resulting

from upward jumps, as observed in Figure 4.22. More generally, we observe that the right tail indices are similar to the empirical observations which are in the range of $3 \sim 5$. However, the model substantially underestimates the left tail: left tail indices appear to be in the range of $5 \sim 7$. This shows that the AJD model does not produce the type of two-sided heavy-tailed distributions observed for spread returns, and underestimates the left tails of these returns.

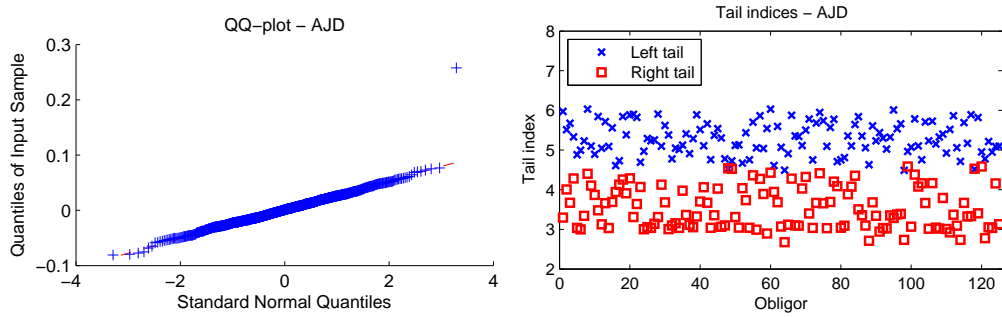


Figure 4.25: Quantile plots (left) and Hill estimators for the tail indices (right) of simulated CDS spread return from the affine jump-diffusion model.

4.3.4 Co-movements in CDS spread returns

Figure 4.26 shows that the affine jump-diffusion model, which is estimated by a MCMC method [49], significantly overestimates the probability of having co-movements in the CDS spreads. Comparing to the empirical observations in Figure 4.14 and Figure 4.17, the cross-obligor correlations and the probabilities of large co-movements are substantially higher than those from the historical data.

4.3.5 Principal components of CDS spread moves

Table 4.15 shows that the first PC factor of the simulated spread returns explains more than 93% of the variance, which is significantly larger than the empirical case.

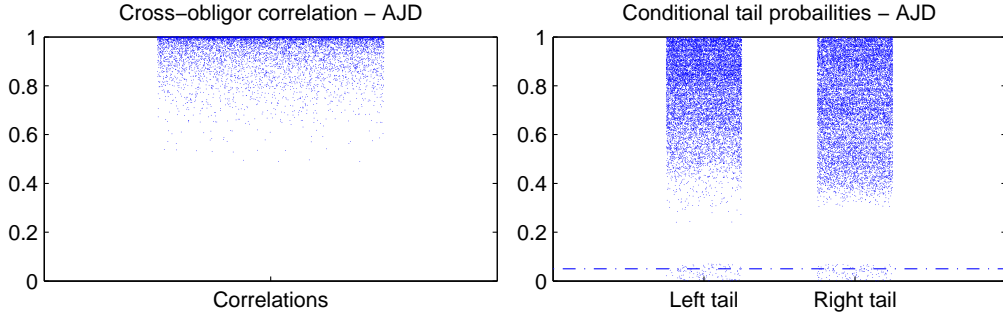


Figure 4.26: Left: Jitter plot of cross-obligor correlations. Right: Estimators, \hat{p}^- and \hat{p}^+ , for the conditional probability of having a large CDS spread move in an obligor given that there is a large CDS spread moves in other obligor. Each point represents the conditional tail probability between two obligors. Blue dotted lines at 5% level represents the estimator value for independent series. Data: Simulated spread returns from the affine jump-diffusion model.

	No. of Principal Components				
	1	2	3	4	5
% Explained	93.0%	7.0%	0.0%	0.0%	0.0%
% Cumulative	93.0%	100.0%	100.0%	100.0%	100.0%

Table 4.15: Percentage of variance that can be explained by the principal components. Data: simulated CDS speards based on affine jump-diffusion model.

4.3.6 Goodness-of-fit vs statistical properties

In the previous studies of the affine models, Feldhütter [49], Azizpour, Giesecke and Kim [6] conclude that the models fit well to the CDS and CDO tranche spread time series in which the errors between model and market spreads are sufficiently small. However, our simulations, using parameters estimated by Feldhütter [49], show that the goodness-of-fit does not necessarily imply the ability to reproduce the stylized properties.

Indeed, our results show that models can pass goodness-of-fit tests while having statistical properties which are qualitatively different from the data. In section 4.5, we will show that models which cannot capture the important stylized properties can lead to worse performance than other realistic models when they are applied to the risk management of CDS portfolios.

4.4 A heavy-tailed multivariate time series model for CDS spreads

When computing Value-at-Risk (VaR) for credit portfolios and initial margin for trading accounts, one needs a model for the loss distribution of credit derivatives. Based on the empirical properties observed in section 4.2, we propose a statistical model for CDS spreads.

4.4.1 A heavy-tailed multivariate AR-GARCH model

Our objective is to build a multivariate time series model for CDS spread returns, which satisfies the following properties, observed in section 4.2:

- Positive autocorrelations at small lags
- Volatility clustering and conditional heteroscedasticity
- Two-sided heavy-tailed distributions for both unconditional and conditional spread returns
- Heterogeneity of the tail indices for spread returns
- Large co-movements
- A heavy-tailed common factor that drives the parallel shift of CDS spreads

In order to capture positive autocorrelations and conditional heteroscedasticity, we model CDS spread returns as AR(1)-GARCH(1,1) processes where the spread return of, say obligor i , follows

$$r_t^i = C^i + \phi^i r_{t-1}^i + \epsilon_t^i, \quad (4.7)$$

$$\epsilon_t^i = \sigma_t^i Z_t^i \quad (4.8)$$

for $t = 0, \Delta t, 2\Delta t, \dots$ where (Z_t^i) is an i.i.d. sequence and σ_t^i is the conditional volatility which follows

$$(\sigma_t^i)^2 = K^i + G^i (\sigma_{t-1}^i)^2 + A^i (\epsilon_{t-1}^i)^2 \quad (4.9)$$

where $K^i > 0$, $G^i \geq 0$, $A^i \geq 0$, $G^i + A^i < 1$. We then assume the heavy-tailed conditional spread returns follow

$$Z_t^i = a^i V_t^0 + b^i V_t^i \quad (4.10)$$

where (V_t^0) and (V_t^1, \dots, V_t^n) are i.i.d. sequences which follow a Student t_{ν^0} distribution and a multivariate Student t distribution with degree of freedom $\nu^1 = \nu^i$ for all i respectively. In this case, Z_t^i , $i = 1, \dots, n$, share the same degree of freedom equal to $\min(\nu^0, \nu^1)$. Although this model restricts to the case of homogeneous tail index for conditional spread returns, the simple correlation structure allows efficient simulation to estimate the CDS portfolio loss distribution.

In the rest of this chapter, we call this model the *MAG* (**M**ultivariate **A**R-**GARCH**) model.

4.4.2 Parameter estimation

The MAG model can be estimated by maximum likelihood, but this approach has two main problems. First, if we maximize the joint likelihood function by considering all CDS time series simultaneously, we need to solve a high dimensional optimization problem which is not necessarily well-posed. Second, if an additional CDS time series is added to the data set, we need to repeat the maximum likelihood estimation again.

In order to overcome these problems, we consider a *quasi maximum likelihood estimation* which allows to break down the estimation into smaller optimization problems for each univariate series. Furthermore, we use CDX.NA.IG on-the-run index as our common risk factor (V_t^0) . This is consistent with our earlier analysis in section 4.2.9 that the first principal component factor is approximately an equally weighted CDS portfolio. The full estimation procedure is as follows:

1. For each obligor i , Z_t^i is assumed to have a Student t distribution. For each CDS spread series, we estimate the AR(1)-GARCH(1,1) coefficients in (4.7)-(4.9) together with the degree of freedom by maximizing the likelihood function. Let (\hat{Z}_t^i) be the standardized residuals for obligor i .

2. An AR(1)-GARCH(1,1) model with Student t distributed noise is fitted to the CDX.NA.IG index returns by maximum likelihood. The degree of freedom, ν^0 , of the noise is estimated together with the AR-GARCH coefficients. Let (\hat{V}_t^0) be the standardized residuals for the CDX.NA.IG index.
3. For each obligor i , (\hat{Z}_t^i) is regressed against (\hat{V}_t^0) by ordinary least squares (OLS) method with zero intercept coefficient. The estimator for a^i is set to be the slope coefficient of the regression. Let (\hat{Y}_t^i) be the residuals from the OLS regression.
4. Assume that (\hat{Y}_t^i) are i.i.d. samples of a scaled Student t distribution with degree of freedom $\tilde{\nu}^i$. $\tilde{\nu}^i$ is estimated by maximum likelihood.
5. Degree of freedom for the idiosyncratic risk factor V_t^i is set to be $\nu^i = \frac{1}{n} \sum_{j=1}^n \tilde{\nu}^j$ for all *i*. Estimator for b^i is set to be $\hat{b}^i = \sqrt{\text{var}(\hat{Y}^i)(\nu^i - 2)/\nu^i}$ and estimator for V_t^i is equal to $\hat{V}_t^i = \hat{Y}_t^i / \hat{b}^i$.
6. The correlation parameters for the multivariate t distribution of (V_t^1, \dots, V_t^n) is estimated by

$$\hat{\rho}_{i,j} = \sin\left(\frac{\pi}{2}\hat{\tau}_{i,j}\right), \quad (4.11)$$

where $\hat{\tau}_{i,j}$, $i, j = 1, \dots, n$ are the Kendall tau correlation coefficients of $(\hat{V}_t^i, \hat{V}_t^j)$.

In step 1, we assume that Z_t^i is a Student t variable instead of a weighted sum of two Student t variables. This allows us to consider each time series separately and reduce the high dimensional problem into several one dimensional problems. This approach leads to a quasi maximum likelihood estimation for the AR-GARCH coefficients but not an exact maximum likelihood estimation. Indeed, Newey and Steigerwald [86] show that estimators from quasi maximum likelihood estimation are consistent if either the conditional mean is identically zero, or the assumed and true error PDFs are symmetric about zero. Mathematical verification of consistency is beyond the scope of this chapter. Instead, we will backtest our model in section 4.5. We refer readers to chapter 5 of [62] for more details on quasi maximum likelihood.

In step 2, we consider the standardized residuals of the credit index returns from a AR(1)-GARCH(1,1) model as the common risk factor observations (\hat{V}_t^0). The reason is that we want to filter the positive autocorrelations and conditional heteroscedasticity in the index returns. It is not surprising that the credit index, which is an equally weighted portfolio of CDS, also exhibits similar stylized properties as in the constituent CDS series. Nevertheless, we will not further illustrate the stylized properties of the credit index.

Klüppelberg and Kuhn [64] show that the correlation estimator (4.11) is consistent and asymptotically normal. However, it does not guarantee that the resulting correlation matrix is positive definite. In those cases, we adjust the correlation matrix by using the eigenvalue shifting method proposed by Rousseeuw and Molenberghs [90]. In particular, we replace the negative eigenvalues of the correlation matrix by a small positive constant. Then, we scale the new matrix so that the diagonal values are equal to 1. We refer readers to [90] for details of this algorithm.

Figure 4.27 shows the confidence intervals for the degree of freedom of each OLS residual series (\hat{Y}_t^i), and the estimator for ν^1 , which is the average degree of freedom. Estimator for ν^1 appears to be roughly equal to the intersection of the confidence intervals.

Table 4.16 shows the estimated model parameters for three selected obligors. We observe that the degree of freedom for the common factor (index) is larger than the one for the idiosyncratic factors in both sample periods.

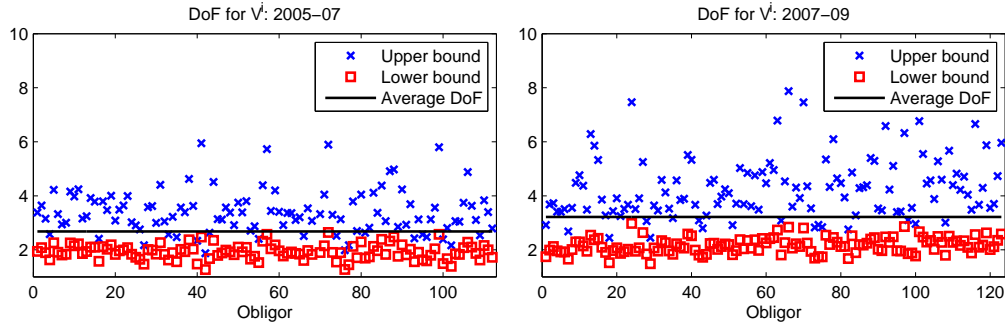


Figure 4.27: Upper and lower bounds of the 95% confidence intervals for the degree of freedom estimators of V_t^i . Black dotted line represents the average of the degree of freedom estimators across obligors.

	C	ϕ	K	G	A	a	b	ν^0	ν^i
2005-07									
Conoco Philips	0.00 (0.00)	-0.02 (0.04)	0.00 (0.00)	0.73 (0.08)	0.23 (0.11)	0.08 (0.02)	0.44 -	3.39 (0.51)	2.68 -
Eastman Chemical	0.00 (0.00)	0.14 (0.04)	0.00 (0.00)	0.67 (0.08)	0.29 (0.14)	0.13 (0.02)	0.43 -	3.39 (0.51)	2.68 -
First Energy	0.00 (0.00)	0.04 (0.04)	0.00 (0.00)	0.86 (0.03)	0.14 (0.04)	0.07 (0.03)	0.49 -	3.39 (0.51)	2.68 -
2007-09									
Conoco Philips	0.00 (0.00)	0.16 (0.04)	0.00 (0.00)	0.89 (0.05)	0.11 (0.07)	0.21 (0.03)	0.47 -	5.74 (1.11)	3.22 -
Eastman Chemical	0.00 (0.00)	0.19 (0.04)	0.00 (0.00)	0.81 (0.06)	0.15 (0.06)	0.38 (0.03)	0.49 -	5.74 (1.11)	3.22 -
First Energy	0.00 (0.00)	0.21 (0.04)	0.00 (0.00)	0.64 (0.08)	0.36 (0.14)	0.30 (0.03)	0.53 -	5.74 (1.11)	3.22 -

Table 4.16: Estimated parameters for the MAG model. Values in brackets are standard errors of the estimators.

4.4.3 Reproducing stylized properties of CDS spreads

The model estimated as above is observed to have the right qualitative properties in the sense that it matches well the stylized properties of CDS spreads listed in section 4.2.

We consider model parameters estimated from the 2007-09 sample and simulate CDS time series by using the MAG model. We illustrate univariate properties by using parameters of Eastman Chemical that are shown in Table 4.16. Figure 4.28, 4.29 and 4.30 show the autocorrelation functions, empirical extremograms, quantile plots and the tail indices³ of the CDS spread returns simulated from the MAG model.

Unlike the affine jump-diffusion model, the MAG model is able to reproduce the observed stylized properties: the simulated CDS spread returns exhibit positive serial dependence in spread returns, absolute spread returns and extreme spread returns, and they appear to have two-sided heavy-tailed distributions with tail indices in the range of $2 \sim 6$. Moreover, Figure 4.31 shows that the MAG model also reproduces realistic empirical probability of having co-movements in the CDS spreads.

³We also compute tail indices numerically by solving an integral equation for GARCH(1,1) model (see [38, 81]). The results are similar to the simulation study and they will not be shown in this chapter.

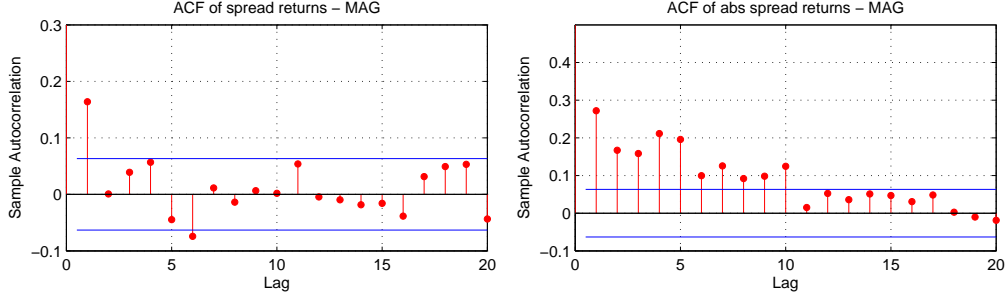


Figure 4.28: Sample autocorrelation function for simulated daily spread returns and absolute spread returns from the heavy-tailed multivariate AR-GARCH model (MAG).

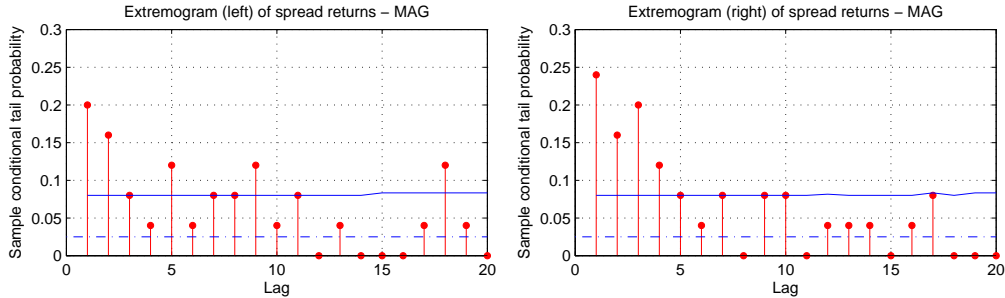


Figure 4.29: Empirical extremograms for simulated daily spread returns from the heavy-tailed multivariate AR-GARCH model (MAG). For the left tail estimates (resp. right tail estimates), threshold a_m is equal to 5% (resp. 95%) quantile of the sample. Blue line is the 95% confidence bound constructed from randomly permuted data series. Blue dotted line is equal to 5%, which is the theoretical value for an independent series.

4.5 Application: estimating loss distributions for CDS portfolios

Computation of the loss distributions, especially loss quantiles, for CDS portfolios is important in practice since it underlies risk measurement and the determination of margin requirements for the clearing of CDS contracts by central counterparties [24]. In this section, we use our heavy-tailed multivariate AR-GARCH model (MAG model) to estimate the loss quantiles for CDS portfolios, and compare its empirical performance with two other models.

We consider various examples of CDS portfolios with different long/short positions of various sizes. On each trading day, we estimate the 1% quantile for the daily loss, which corresponds the 99% 1-day Value-at-Risk (VaR), and compare these quantile levels to the realized daily loss across the sample. These VaR levels are not computed using a Gaussian model, which, as noted above,

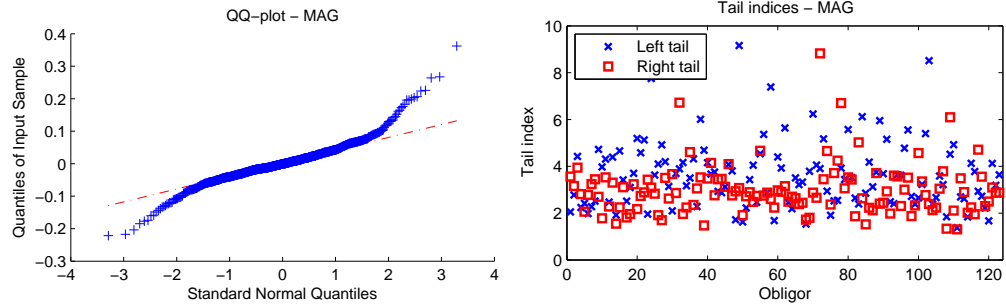


Figure 4.30: Quantile plots (left) and Hill estimators for the tail indices (right) of simulated CDS spread return from the heavy-tailed multivariate AR-GARCH model (MAG).

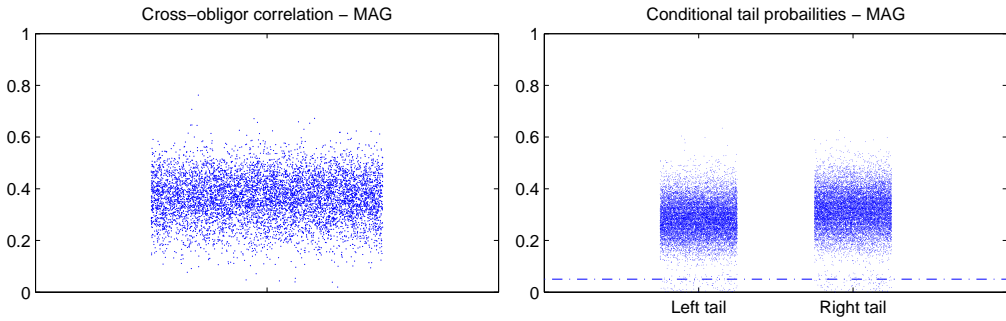


Figure 4.31: Left: Jitter plot of cross-obligor correlations. Right: Estimators, \hat{p}^- and \hat{p}^+ , for the conditional probability of having a large CDS spread move in an obligor given that there is a large move in the CDS spread of another obligor. Each point represents the conditional tail probability for a pair of obligors. Blue dotted lines at 5% level represents the estimator value for independent series. Data: Simulated spread returns from the heavy-tailed multivariate AR-GARCH model.

is not appropriate for modeling variations in CDS spreads, but using the heavy-tailed multifactor model described in section 4.4. If the model provides a good forecast of the quantiles of the loss distribution, then the realized loss will exceed the 99% VaR approximately 1% of the time. The proportion and timing of these exceedances allow to formally measure the accuracy of the model in predicting the tails of the portfolio loss distribution and to compare with other models.

4.5.1 Models for CDS portfolios

We compare three models in our empirical study: the affine jump-diffusion model [41], a random walk model proposed by Saita [91] and the MAG model that we proposed in section 4.4.

4.5.1.1 Affine jump-diffusion model

In section 4.3, we have shown that the affine jump-diffusion model is not able to reproduce the desired stylized properties, even though Feldhütter [49] and Azizpour et al [6] show that this model provides a good fit to the CDS and CDO data. We further examine this model by backtesting its performance on estimating the loss distributions for different CDS portfolios.

We estimate the model parameters by using a maximum likelihood method and principal component decomposition on the CDS spreads as follows:

1. We project daily changes of CDS spreads onto principal component factors.
2. We set the common risk factor values of the model equal to the first principal component factor values, and estimate the parameters describing the common risk factor by maximum likelihood method.
3. For each obligor, we estimate both statistical and risk-neutral parameters of the idiosyncratic risk factors from CDS spreads by maximum likelihood method.
4. We estimate risk-neutral parameters of the common risk factor by maximum likelihood method.

Details of the above procedure are given in Appendix 4.8. Using these model parameters, we estimate VaR by Monte Carlo simulation (see Appendix 4.7).

4.5.1.2 Random walk model

Saita [91] suggests that simple CDS spread returns follows a random walk

$$\frac{s_{t+\Delta t}^i - s_t^i}{s_t^i} = \sigma_{Z(i)} \sqrt{\Delta t} \left(\alpha_{Z(i)}^M N_t^M + \alpha_{Z(i)}^Z N_t^{Z(i)} + \sqrt{1 - (\alpha_{Z(i)}^Z)^2 + (\alpha_{Z(i)}^M)^2} N_t^i \right)$$

for $t = 0, \Delta t, 2\Delta t, \dots$ where $Z(i)$ is obligor i 's sector, $(N_t^M, N_t^{Z(i)}, N_t^i)$ are the market, sector and idiosyncratic factors which are independent among themselves as well as serially independent,

$(\alpha_{Z(i)}^M, \alpha_{Z(i)}^Z)$ are the factor loadings. For each time t , the factors are assumed to have zero means and unit variances. Obligors in the same sector are assumed to share the same spread volatility and factor loadings.

The spread return volatilities are estimated by

$$\hat{\sigma}_{Z(i)} = \sqrt{\frac{1}{n_Z} \sum_{t,i} \left(\frac{\Delta s_t^i}{s_t^i \sqrt{\Delta t}} \right)^2}$$

where n_Z is the number of terms in the summation which is over all data points in time and for all issuers that belong to sector Z . We estimate the loadings $(\alpha_{Z(i)}^M, \alpha_{Z(i)}^Z)$ by OLS regression across all obligors.

In this model, the distribution of spread returns is not directly specified. Instead, Saita [91] computes VaR as follows. Consider a CDS portfolio with notional values $\mathbf{w} = (w_1, \dots, w_n)$. Let $Spread01_t^i$ be the sensitivity of CDS i value with respect to 1 bp change in S_t^i , Ω be the estimated correlation matrix of the simple spread returns, and Σ be the diagonal matrix with diagonal element $\Sigma_{i,i}$ equal to the estimated volatility of the simple spread returns for obligor i . We define $R01_t^i = w_i S_t^i Spread01_t^i$ with $\mathbf{R01}_t = (R01_t^1, \dots, R01_t^n)$. Then, the portfolio volatility (standard deviation of daily portfolio P&L) is equal to

$$\sigma_{\mathbf{w}} = \sqrt{\Delta t \mathbf{R01}_t \Sigma \Omega \Sigma \mathbf{R01}_t^T}.$$

Then 99% VaR for portfolio \mathbf{w} is set to

$$VaR = \beta \sigma_{\mathbf{w}},$$

where β is a scaling parameter. We estimate β as in [91]:

1. Select a type of CDS portfolio, e.g. equally weighted with n CDS in protection seller's positions.
2. Randomly create 100 portfolios of the selected type.

3. Compute the historical P&L and model-implied volatility for each portfolios.

4. For a given β , compute the historical exceedance ratio for this portfolio type:

$$\frac{1}{100} \sum_{k=1}^{100} \frac{\text{Number of days where loss of portfolio } k \text{ is larger than } \beta\sigma_{w_k}}{\text{Total number of days}}, \quad (4.12)$$

where σ_{w_k} is the model-implied volatility of portfolio k .

5. If the historical exceedance ratio (4.12) is larger than 1%, we increase β . Similarly, if (4.12) is smaller than 1%, we decrease β .

6. Repeat step 4 – 5 until (4.12) is equal to 1%.

We repeat the estimation procedure of the scaling parameter β for each portfolio type.

4.5.1.3 Heavy-tailed multivariate AR-GARCH model

In section 4.4, we propose a heavy-tailed multivariate AR-GARCH model for the CDS spread returns. Since this model is built upon the observed stylized properties, it will be interesting to see whether it can also provide a good estimation for CDS portfolio loss distribution.

4.5.2 Backtesting

We evaluate the performance of the models in predicting loss quantiles for 9 types of CDS portfolios:

- Short-only: selling protection on 100, 40 or 10 obligors
- Long-only: buying protection on 100, 40 or 10 obligors
- Long-short: buying protection on 50, 20 or 5 obligors and selling protection on 50, 20 or 5 obligors

For each portfolio type, we consider 100 randomly chosen combinations of obligors and each position has the same notional value. Thus, we evaluate 900 CDS portfolios in total. In each sample period,

we start our evaluation on the 250th trading day so that we have sufficient amount of data for model calibration. This gives 324 and 285 evaluation days in 2005-07 and 2007-09 respectively.

4.5.2.1 Exceedance probabilities

Table 4.17 shows the percentage of days on which the portfolio loss exceeds the VaR estimates. In both 2005-07 and 2007-09, the affine jump diffusion model estimated using MCMC significantly overestimates the downside risk for short-only and long-short portfolios: there are no trading days that have losses exceed the VaR estimates for all short-only portfolios in 2005-07 and for almost all long-short portfolios in both periods. Moreover, the affine jump-diffusion model significantly underestimates the downside risk for the long-only portfolios. These observations are the results of upward jumps in the default intensity (4.6) in which the estimated jump sizes and frequencies appear to overestimate the potential losses for the short-only and long-short portfolios.

In 2005-07, the MAG model provide the best loss quantile prediction with exceedance probabilities almost equal to 1%, but the random walk model appears to overestimate the downside risk for all portfolio types. On average, the random walk model gives only 0.4% of the trading days that have losses exceed the VaR estimates, comparing to 1.0% given by the MAG model. In 2007-09, the MAG model still provides a good prediction of loss quantiles, especially for the long-short portfolios. However, the random walk model underestimates the downside risk of all portfolio types and gives, 2.6% of exceedances, compared to 1.0% for the MAG model.

In the Kupiec test [65], the exceedance probability for a portfolio is significantly different from 1% at 95% level if the number of exceedances is smaller than 1 or larger than 7 for the 2005-07 period which has 324 evaluation days, and small than 1 or larger than 6 for the 2007-09 period which has 285 evaluation days. Thus, the confidence interval for the number of exceedances are [1, 7] and [1, 6] respectively for 2005-07 and 2007-09.

Table 4.18 shows that the MAG model gives the fewest number of portfolios (11.3% and 2.4% in 2005-07 and 2007-09 respectively) whose number of exceedances is outside the Kupiec confidence

interval. The random walk model performs better than the the affine jump diffusion model in 2005-07, but the two models are comparable in 2007-09. Overall, we observe that the MAG model provides better loss quantile prediction than the two other models.

	2005-07			2007-09		
	AJD	RW	MAG	AJD	RW	MAG
Short 100	0.0%	0.0%	1.3%	1.2%	3.2%	0.6%
Short 40	0.0%	0.2%	1.7%	0.3%	3.2%	0.7%
Short 10	0.0%	0.5%	1.8%	0.1%	3.1%	1.0%
Long 100	15.5%	0.2%	0.2%	3.1%	1.7%	1.3%
Long 40	2.2%	0.3%	0.4%	1.3%	2.0%	1.2%
Long 10	1.7%	0.3%	0.6%	0.4%	2.0%	1.1%
Long 50 Short 50	0.0%	0.8%	0.9%	0.0%	3.1%	1.1%
Long 20 Short 20	0.0%	0.7%	1.0%	0.0%	2.8%	1.0%
Long 5 Short 5	0.1%	0.7%	1.2%	0.1%	2.6%	1.0%
Average	2.2%	0.4%	1.0%	0.7%	2.6%	1.0%

Table 4.17: Empirical exceedance probabilities: percentage of trading days which have losses larger than the 99% VaR. Portfolio type: protection sellers (short), protection buyers (long). Models: affine jump-diffusion model (AJD), random walk model (RW), heavy-tailed multivariate AR-GARCH model (MAG).

	2005-07			2007-09		
	AJD	RW	MAG	AJD	RW	MAG
Short 100	100.0%	100.0%	0.0%	1.0%	100.0%	0.0%
Short 40	100.0%	52.0%	5.0%	46.0%	99.0%	0.0%
Short 10	89.0%	17.0%	22.0%	84.0%	92.0%	1.0%
Long 100	100.0%	22.0%	23.0%	93.0%	2.0%	0.0%
Long 40	40.0%	36.0%	27.0%	11.0%	27.0%	0.0%
Long 10	49.0%	43.0%	13.0%	68.0%	31.0%	4.0%
Long 50 Short 50	100.0%	7.0%	1.0%	100.0%	81.0%	2.0%
Long 20 Short 20	100.0%	14.0%	1.0%	97.0%	70.0%	7.0%
Long 5 Short 5	77.0%	21.0%	10.0%	85.0%	59.0%	8.0%
Average	83.9%	34.7%	11.3%	65.0%	62.3%	2.4%

Table 4.18: Test for accuracy of loss quantile estimation: percentage of portfolios that have less than 1 or more than 7 (resp. less than 1 or more than 6) exceedances in 2005-07 (resp. 2007-09), i.e. which reject the null hypothesis that the exceedance probability is equal to 1% under the Kupiec test at 95% confidence level.

4.5.2.2 Clustering of exceedances

Figure 4.32 and 4.33 show, at each date, the total number of portfolios whose losses exceeded the VaR estimates. We group the portfolios into three categories: short-only, long-only and long-short.

Each category contains 300 different portfolios.

In 2005-07, exceedances of all portfolio types appear to be evenly distributed in time under both the random walk model and the MAG model. On the other hand, exceedances of the long-only portfolios cluster in the second half of 2007 under the affine jump-diffusion model. This is due to the fact that the CDS spread return distributions implied by the affine jump-diffusion model skew significantly to the right because of the upward jump components.

In 2007-09, exceedances of the short-only portfolios cluster in late 2008 under the random walk model. This period begins with the bankruptcy of Lehman Brothers, then followed by a series of market shocks lead to upward jumps in the CDS spreads. From Figure 4.34, we can see that the random walk model is slow in reacting to those market shocks. On the other hand, the MAG model appears to adjust quickly to the volatile market in the late 2008 and the number of short-only portfolios that have losses exceed the VaR estimates reduces quickly after Lehman's bankruptcy.

In order to further examine whether exceedances are serially correlated, we perform a Ljung-Box test on the exceedance sequence $(1_{\{L_t > VaR_t\}})$ for each portfolio where L_t is the portfolio loss at time t and VaR_t is the VaR estimate. As suggested by Berkowitz, Christoffersen and Pelletier [7], we carry out the test for the first five lags. Table 4.19 shows that the MAG model gives very few portfolios that have autocorrelated exceedances (4.6% and 7.2% in 2005-07 and 2007-09 respectively). On the other hand, the random walk model and the affine jump-diffusion model give a significantly larger number of portfolios that have autocorrelated exceedances, with 52.6% and 13.9% respectively in 2007-09. This confirms our earlier observations from Figure 4.32 and 4.33.

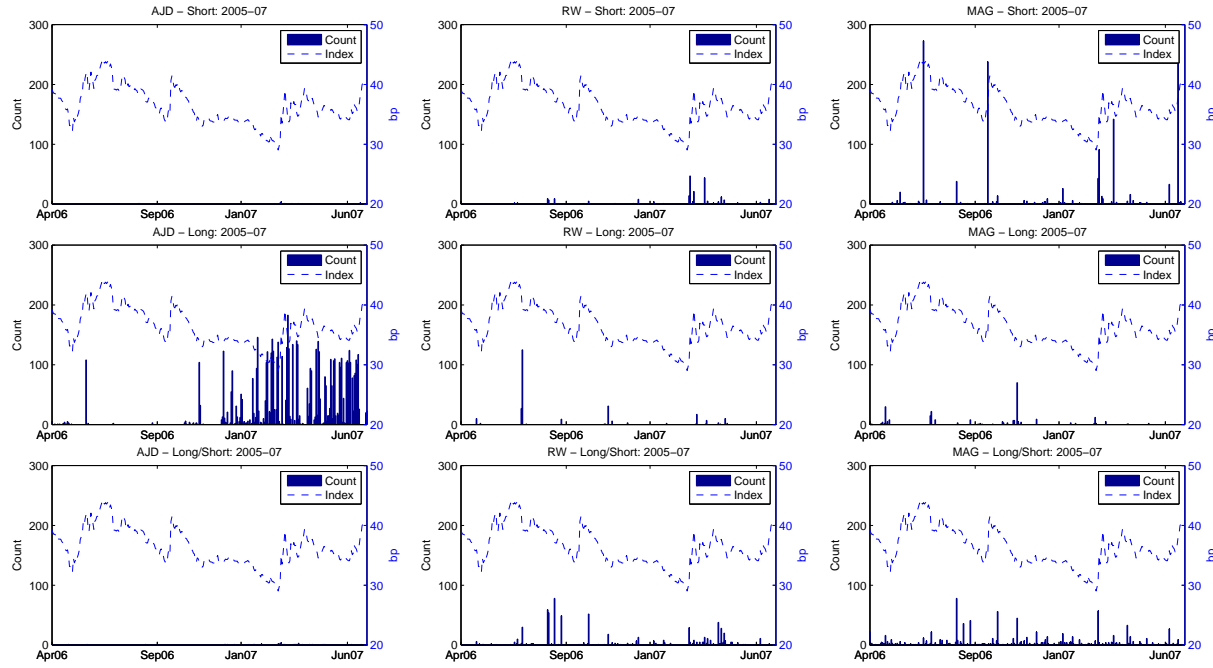


Figure 4.32: CDX.NA.IG on-the-run index and number of portfolios that have losses exceed 99% VaR in 2005-07. Portfolio types: protection sellers only (short), protection buyers only (long); half protection sellers half protection buyers (long-short).

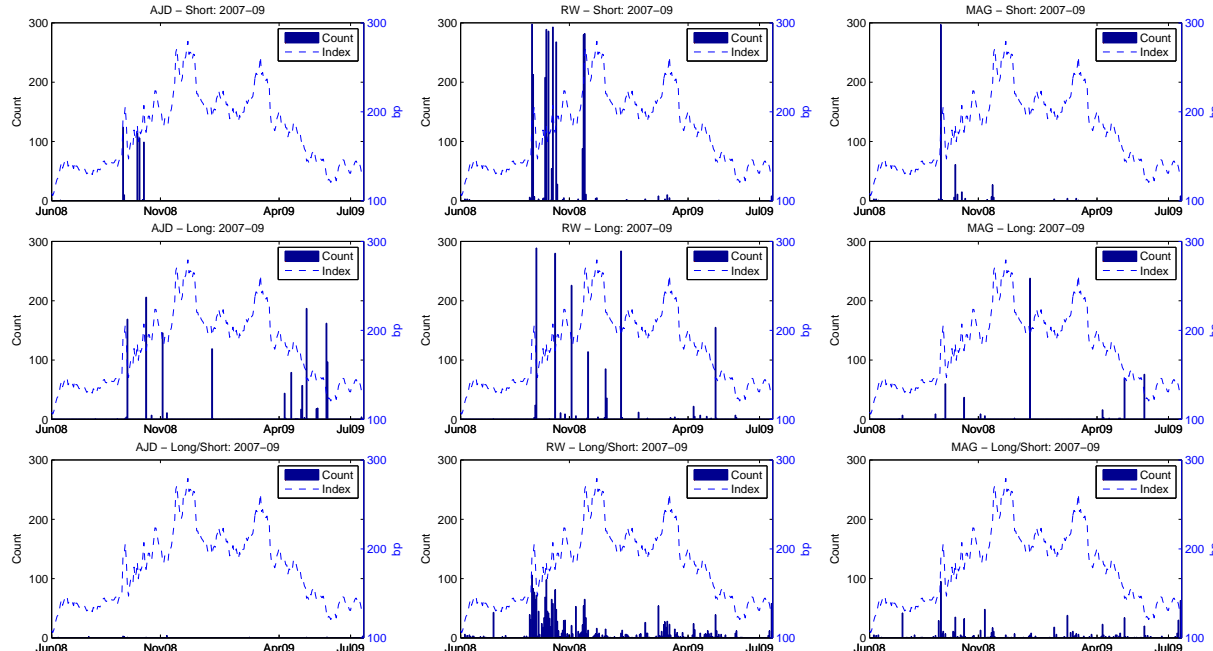


Figure 4.33: CDX.NA.IG on-the-run index and number of portfolios that have losses exceed 99% VaR in 2007-09. Portfolio types: protection sellers only (short), protection buyers only (long); half protection sellers half protection buyers (long-short).

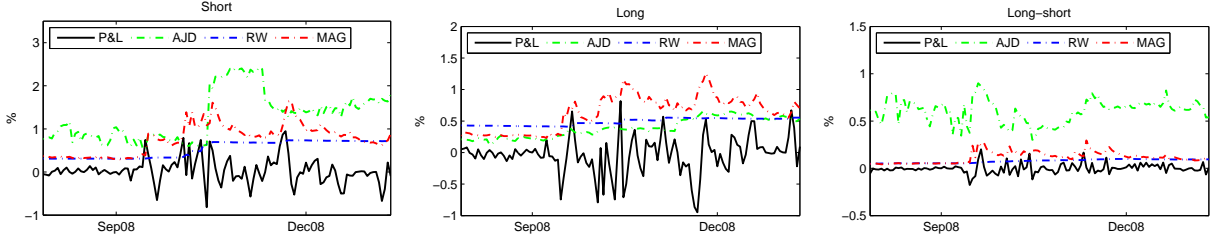


Figure 4.34: Daily P&L of a short-only, a long-only and a long-short portfolio, and the corresponding 99% VaR computed by the affine jump-diffusion model (AJD), the random walk model (RW) and the heavy-tailed multivariate AR-GARCH model (MAG) in 2008. Values are expressed as percentages of the total portfolio notional value.

	2005-07			2007-09		
	AJD	RW	MAG	AJD	RW	MAG
Short 100	0.0%	0.0%	0.0%	81.0%	100.0%	0.0%
Short 40	0.0%	3.0%	1.0%	18.0%	100.0%	1.0%
Short 10	2.0%	13.0%	11.0%	4.0%	98.0%	24.0%
Long 100	100.0%	0.0%	0.0%	6.0%	0.0%	0.0%
Long 40	60.0%	3.0%	2.0%	3.0%	1.0%	0.0%
Long 10	46.0%	2.0%	9.0%	13.0%	8.0%	5.0%
Long 50 Short 50	0.0%	21.0%	2.0%	0.0%	60.0%	11.0%
Long 20 Short 20	0.0%	17.0%	5.0%	0.0%	57.0%	15.0%
Long 5 Short 5	6.0%	18.0%	11.0%	0.0%	49.0%	9.0%
Average	23.8%	8.6%	4.6%	13.9%	52.6%	7.2%

Table 4.19: Test for autocorrelated exceedances: percentage of portfolios which reject the null hypothesis that the exceedance sequence ($1_{\{L_t > VaR_t\}}$) is serially uncorrelated, by using the Ljung-Box test at 95% confidence level.

4.5.2.3 Expected shortfall

Expected shortfall (ES) is defined as the expected loss given that the loss is larger than a given quantile (VaR). The *average relative shortfall deviation* (Table 4.20)

$$\frac{1}{N} \sum_{t: L_t > VaR_t} \frac{L_t - ES_t}{ES_t}, \quad (4.13)$$

where L_t is the portfolio loss at time t , VaR_t is the 99% VaR estimates, ES_t is the 99% expected shortfall estimates, and N is the number of trading days where the loss is larger than the VaR estimate of the previous day, measures how much the realized loss deviates from the expected

shortfall. If the model provides a good estimate for the loss distribution, we expect the shortfall deviation (4.13) to be close to zero.

In 2005-07, the random walk model gives the smallest (in absolute value) relative shortfall deviation on average at -1.7%. On the other hand, the MAG model overestimates the expected shortfall for all portfolio types with an average relative shortfall deviation of -17.2%. This shows that the MAG model is more on the safe side in terms of loss prediction during exceedances.

In 2007-09, the random walk model significantly underestimates expected shortfall where the relative shortfall deviation increases to 21.5%. This means that extreme losses appear to be more severe than anticipated by the random walk model. In this period, the MAG model give the best expected shortfall estimates with shortfall deviations equal to 2.2% on average.

In order to examine whether the sample expected shortfall is statistically different from the model expected shortfall, we follow McNeil, Frey and Embrechts [79] and assume that the loss process follows

$$L_t = \mu_t + \sigma_t Z_t,$$

where μ_t and σ_t are measurable at time $t - 1$, and (Z_t) is an i.i.d. sequence. Then, we define *expected shortfall residual* by

$$R_t = \frac{L_t - ES_t}{\sigma_t} 1_{L_t > VaR_t}, \quad (4.14)$$

where (R_t) is an i.i.d. sequence with zero mean. For each portfolio, we test whether the expected shortfall residual (4.14) has zero mean by computing the confidence intervals based on the bootstrap method [46, 79]. In order to have sufficient number of samples to obtain meaningful results⁴, we combine the observations in the two sample periods. We omit those time series that has none or only one exceedance.

Table 4.21 shows that, on average, the MAG model gives the fewest number of portfolios (41.6%)

⁴For each sample period with roughly 300 evaluation days, the typical number of nonzero expected shortfall residual observations is only 3, if the exceedance probability is 1%.

that can reject the hypothesis that the expected shortfall residual has zero mean, comparing to 47.9% of the affine jump-diffusion model and 45.2% of the random walk model.

	2005-07			2007-09		
	AJD	RW	MAG	AJD	RW	MAG
Short 100	-	-	-18.6%	-1.9%	27.4%	28.1%
Short 40	-	-13.1%	-21.8%	-6.0%	28.8%	21.3%
Short 10	-13.2%	-5.7%	-15.9%	17.6%	28.4%	7.1%
Long 100	-14.0%	-7.6%	-25.8%	29.3%	14.2%	-15.0%
Long 40	-10.6%	4.2%	-15.8%	6.7%	12.0%	-12.7%
Long 10	39.8%	0.8%	-13.3%	19.2%	10.2%	-8.3%
Long 50 Short 50	-	-0.8%	-20.1%	-	24.7%	-1.3%
Long 20 Short 20	-	3.9%	-15.2%	-24.8%	27.2%	1.6%
Long 5 Short 5	31.1%	4.4%	-7.9%	48.1%	20.6%	-1.2%
Average	6.6%	-1.7%	-17.2%	11.0%	21.5%	2.2%

Table 4.20: Average relative shortfall deviation (4.13) for CDS portfolios.

	AJD	RW	MAG
Short 100	19.6%	100.0%	0.0%
Short 40	41.7%	73.0%	18.0%
Short 10	50.0%	56.0%	24.0%
Long 100	98.0%	8.0%	100.0%
Long 40	28.0%	32.0%	87.8%
Long 10	59.7%	25.0%	50.0%
Long 50 Short 50	-	36.0%	41.0%
Long 20 Short 20	-	47.0%	22.2%
Long 5 Short 5	38.5%	30.0%	31.0%
Average	47.9%	45.2%	41.6%

Table 4.21: Test for accuracy of expected shortfall estimation: percentage of portfolios which reject the null hypothesis that expected shortfall residual (4.14) has zero mean at 95% confidence level. Data: 2005-09.

4.6 Moment generating function for affine jump diffusion process

Consider an affine jump diffusion process

$$dX_t = (\kappa_0 + \kappa_1 X_t)dt + \sigma \sqrt{X_t} dW_t + dJ_t$$

where (W_t) is a standard Brownian motion and (J_t) is a compound Poisson process with intensity ℓ and exponential jump size with mean μ under a risk-neutral measure \mathbb{Q} . The moment generating

function of the cumulative affine jump-diffusion process is equal to

$$E^{\mathbb{Q}} \left[\exp \left(q \int_t^{t+T} X_u du \right) \middle| \mathcal{F}_t \right] = \exp (\alpha(q, T) + \beta(q, T) X_t)$$

where

$$\begin{aligned} \alpha(q, T) &= \frac{2\kappa_0}{\sigma^2} \ln \left[\frac{2\gamma e^{(\gamma - \kappa_1)T/2}}{2\gamma + (\gamma - \kappa_1)(e^{\gamma T} - 1)} \right] - \frac{2q\ell\mu}{\gamma + \kappa_1 + 2q\mu} T \\ &\quad - \frac{2\ell\mu}{\sigma^2 + 2\mu\kappa_1 + 2q\mu^2} \ln \left[1 + \frac{[\gamma - \kappa_1 - 2q\mu](e^{\gamma T} - 1)}{2\gamma} \right], \\ \beta(q, T) &= \frac{2q(e^{\gamma T} - 1)}{2\gamma + (\gamma - \kappa_1)(e^{\gamma T} - 1)}, \\ \gamma &= \sqrt{\kappa_1^2 - 2q\sigma^2}, \end{aligned}$$

for $q < \frac{\kappa_1^2}{2\sigma^2}$.

Let τ^i be the random default time of an obligor i whose default intensity follows (4.4). Then, the survival probability under the affine jump-diffusion model is equal to

$$\begin{aligned} \mathbb{Q}(\tau^i > T | \mathcal{G}_t) &= 1_{\tau^i > t} E^{\mathbb{Q}} \left[e^{- \int_t^T \lambda_u^i du} \middle| \mathcal{F}_t \right] \\ &= 1_{\tau^i > t} E^{\mathbb{Q}} \left[e^{- \int_t^T X_u^i du} \middle| \mathcal{F}_t \right] E^{\mathbb{Q}} \left[e^{- a^i \int_t^T X_u^0 du} \middle| \mathcal{F}_t \right] \\ &= 1_{\tau^i > t} \exp (\alpha^i(-1, T) + \alpha^0(-a^i, T) + \beta^i(-1, T) X_t^i + \beta^0(-a^i, T) X_t^0) \end{aligned}$$

where (\mathcal{F}_t) is the filtration generated by $(W_t^{k, \mathbb{Q}})$ and (J_t^k) for $k = 0, i$ and (\mathcal{G}_t) is the filtration generating by all risk factors including the default time process, i.e. $\mathcal{G}_t = \mathcal{F}_t \vee \mathcal{H}_t$ where (\mathcal{H}_t) is the filtration generated by the default indicator process $(1_{\tau^i > t})$.

4.7 CDS spread simulation under affine jump-diffusion model

Let τ^i be the random default time of an obligor i . Assume that recovery rate R^i is deterministic. Given $\tau^i > t$, the fair CDS spread at time t is defined as

$$S_t^i = \frac{(1 - R^i) \sum_{k=1}^M B(t, T_k) \mathbb{Q}(T_{k-1} < \tau^i \leq T_k | \mathcal{G}_t)}{\sum_{k=1}^M (T_k - T_{k-1}) B(t, T_k) \mathbb{Q}(\tau^i > T_k | \mathcal{G}_t)} \quad (4.15)$$

where T_1, \dots, T_M are the payment dates and \mathcal{G}_t represents all the available market information up to time t . In this case, modeling the dynamic of the CDS spread is equivalent to modeling the dynamic of the conditional survival probabilities $\mathbb{Q}(\tau^i > T | \mathcal{G}_t)$.

Let $\Theta_i^{\mathbb{Q}} = (\kappa_0^i, \kappa_1^i, \sigma^i, \ell^{i,\mathbb{Q}}, \mu^{i,\mathbb{Q}}, a^i)$ and $\Theta_i^{\mathbb{P}} = (\kappa_0^i, \kappa_1^i, \sigma^i, \ell^{i,\mathbb{P}}, \mu^{i,\mathbb{P}})$, $\Theta_{i,j}^{\mathbb{Q}} = (\Theta_i^{\mathbb{Q}}, \Theta_j^{\mathbb{Q}})$, $\Theta_{i,j}^{\mathbb{P}} = (\Theta_i^{\mathbb{P}}, \Theta_j^{\mathbb{P}})$. From (4.15), we know that the CDS spreads under the affine jump-diffusion model can be written as

$$S_t^i = S^{ajd}(\Theta_{0,i}^{\mathbb{Q}}; t, X_t^0, X_t^i) \quad (4.16)$$

where

$$\begin{aligned} S^{ajd}(\Theta_{0,i}^{\mathbb{Q}}; t, x^0, x^i) &= \frac{D(\Theta_{0,i}^{\mathbb{Q}}; t, x^0, x^i)}{P(\Theta_{0,i}^{\mathbb{Q}}; t, x^0, x^i)}, \\ D(\Theta_{0,i}^{\mathbb{Q}}; t, x^0, x^i) &= (1 - R) \sum_{k=1}^M B(t, T_k) \left[\bar{F}(\Theta_{0,i}^{\mathbb{Q}}; t, T_{k-1}, x^0, x^i) - \bar{F}(\Theta_{0,i}^{\mathbb{Q}}; t, T_k, x^0, x^i) \right], \\ P(\Theta_{0,i}^{\mathbb{Q}}; t, x^0, x^i) &= \sum_{k=1}^M (T_k - T_{k-1}) B(t, T_k) \bar{F}(\Theta_{0,i}^{\mathbb{Q}}; t, T_k, x^0, x^i), \\ \bar{F}(\Theta_{0,i}^{\mathbb{Q}}; t, T, x^0, x^i) &= e^{\alpha^i(-1, T-t) + \alpha^0(-a^i, T-t) + \beta^i(-1, T-t)x^i + \beta^0(-a^i, T-t)x^0} \end{aligned}$$

for $x^0, x^i \geq 0$. Notice that the dynamic of the CDS spread process (S_t^i) is governed by the dynamic of the affine jump-diffusion processes (X_t^0) and (X_t^i) .

Recall that (X_t^k) follows (4.6) under \mathbb{P} . By time discretization, we write

$$\text{Under } \mathbb{P} : \quad X_{(j+1)\Delta t}^k = X_{j\Delta t}^k + (\kappa_0^k + \kappa_1^k X_{j\Delta t}^k) \Delta t + \sigma^k \sqrt{X_{j\Delta t}^k} \Delta W_j^{k,\mathbb{P}} + \Delta J_j^k \quad (4.17)$$

where Δt is the discretization step which is set to be 1 day, $(\Delta W_j^{k,\mathbb{P}})_{j=1, \dots, J}$ are i.i.d. $N(0, \sqrt{\Delta t}^2)$ normal random variables and $(\Delta J_j^k)_{j=1, \dots, J}$ are i.i.d. random variables where $\Delta J_j^k = 0$ with probability $1 - \ell^{k,\mathbb{P}} \Delta t$ and ΔJ_j^k is exponentially distributed with mean $\mu^{k,\mathbb{P}}$ with probability $\ell^{k,\mathbb{P}} \Delta t$.

Note that the dynamic of $(X_{j\Delta t}^k)_{j=1, \dots, J}$ depends on the parameters $\Theta_k^{\mathbb{P}}$.

We can simulate time series of CDS spreads for n obligors under the affine jump-diffusion models as follows:

1. Simulate time series $(X_{j\Delta t}^k)_{j=1,\dots,J}$ for $k = 0, \dots, n$ from (4.17).
2. For each time step j , compute CDS spread from (4.16).

4.8 Estimation of the affine jump-diffusion model from CDS spread time series

In this section, we describe a method based on principal component analysis for estimating the parameters of the affine jump-diffusion model from time series of CDS spreads. The method involves the following steps:

1. Decompose daily changes of CDS spreads into principal component factors.
2. Set $(x_{j\Delta t}^0)_{j=0,\dots,J}$ equal to the first principal component factor values and estimate $\Theta_0^{\mathbb{P}}$ by maximum likelihood method.
3. For each obligor i , estimate $(\Theta_i^{\mathbb{Q}}, \Theta_i^{\mathbb{P}})$ to the CDS spreads with the given values of $(x_{j\Delta t}^0)_{j=0,\dots,J}$ and $(\widehat{\Theta}_0^{\mathbb{P}}, \kappa_1^{0,\mathbb{Q}}, \ell^{0,\mathbb{Q}}, \mu^{0,\mathbb{Q}})$ by maximum likelihood method.
4. Calibrate $(\kappa_1^{0,\mathbb{Q}}, \ell^{0,\mathbb{Q}}, \mu^{0,\mathbb{Q}})$ by maximum likelihood method with given values of $(x_{j\Delta t}^0)_{j=0,\dots,J}$, $\widehat{\Theta}_0^{\mathbb{P}}$ and $(\widehat{\Theta}_i^{\mathbb{Q}}, \widehat{\Theta}_i^{\mathbb{P}})$, $i = 1, \dots, n$.
5. Repeat Step 3-4 until convergence.

Step 1: Decomposition of daily changes of CDS spreads

By the first order approximation of the Taylor series expansion, the pricing function (4.16) can be approximated by

$$S^{ajd}(\Theta_{0,i}^{\mathbb{Q}}; t, x^0, x^i) \approx S^{ajd}(\Theta_{0,i}^{\mathbb{Q}}; t, 0, 0) + \partial_{x^0} S^{ajd}(\Theta_{0,i}^{\mathbb{Q}}; t, 0, 0) x^0 + \partial_{x^i} S^{ajd}(\Theta_{0,i}^{\mathbb{Q}}; t, 0, 0) x^i \quad (4.18)$$

where the partial derivatives have the closed-form expression:

$$\partial_{x^0} S^{ajd}(\Theta_0^{\mathbb{Q}}; t, x^0, x^i) = \frac{\partial_{x^0} D(\Theta_0^{\mathbb{Q}}; t, x^0, x^i)}{P(\Theta_0^{\mathbb{Q}}; t, x^0, x^i)} - S^{ajd}(\Theta_0^{\mathbb{Q}}; t, x^0, x^i) \frac{\partial_{x^0} P(\Theta_0^{\mathbb{Q}}; t, x^0, x^i)}{P(\Theta_0^{\mathbb{Q}}; t, x^0, x^i)}, \quad (4.19)$$

$$\begin{aligned} \partial_{x^0} D(\Theta_0^{\mathbb{Q}}; t, x^0, x^i) &= (1 - R) \sum_{k=1}^M B(t, T_k) [\beta(-a^i, T_{k-1} - t) \bar{F}(\Theta_0^{\mathbb{Q}}; t, T_{k-1}, x^0, x^i) \\ &\quad - \beta(-a^i, T_k - t) \bar{F}(\Theta_0^{\mathbb{Q}}; t, T_k, x^0, x^i)], \end{aligned} \quad (4.20)$$

$$\partial_{x^0} P(\Theta_0^{\mathbb{Q}}; t, x^0, x^i) = \sum_{k=1}^M (T_k - T_{k-1}) B(t, T_k) \beta(-a^i, T_k - t) \bar{F}(\Theta_0^{\mathbb{Q}}; t, T_k, x^0, x^i), \quad (4.21)$$

and we have a similar expression for $\partial_{x^i} S^{ajd}(\Theta_0^{\mathbb{Q}}; t, x^0, x^i)$ by replacing a^i in (4.20) and (4.21) by 1.

Using this linear approximation, the change in CDS spreads under the affine jump-diffusion model is equal to

$$\Delta S_t^i \approx \partial_{x^0} S^{ajd}(\Theta_0^{\mathbb{Q}}; t, 0, 0) \Delta X_t^0 + \partial_{x^i} S^{ajd}(\Theta_0^{\mathbb{Q}}; t, 0, 0) \Delta X_t^i \quad (4.22)$$

where Δ is the difference operator with $\Delta S_t^i = S_t^i - S_{t-\Delta t}^i$.

There are three advantages of this approximation. First, this approximation is linear in the values of x^0 and x^i which will become handy when we want to decompose the CDS spreads into different linear factors. Second, the approximation is also strictly increasing in the variables x^0 and x^i , which preserves the property of the exact function. Finally, the minimum possible CDS spread under this approximation is the same as the one computed under the exact function.

However, this approximation also shows the problem of under-determination of the state variables x^0 and x^i : at each time t , we have $n + 1$ state variables to be determined, $(x_t^0, x_t^1, \dots, x_t^n)$, but we only observe n market variables, CDS spreads (s_t^1, \dots, s_t^n) . Because of the monotonicity and continuity of (4.16), a small increase in x_t^0 can be compensated by a small decrease in (x_t^1, \dots, x_t^n) and give the same CDS spreads before the changes. One solution is to consider additional CDS spreads with different maturities. However, CDS with maturities other than 5 years are not very liquid which gives poor estimation of the parameters. We solve this problem by decomposing the CDS spreads into different factors using the principal component method.

Consider the data matrix containing the daily changes in the CDS spreads of all obligors. Using an eigenvector decomposition we obtain

$$\Delta s_{j\Delta t}^i = c_1^i F_{j\Delta t}^1 + \sum_{k=2}^n c_k^i F_{j\Delta t}^k$$

where c_k^i is the factor loading of obligor i to factor k and F_t^k is the k^{th} principal component factor value at time t . By comparing to (4.22), we identify the common risk factor in the affine jump-diffusion model $(\Delta x_{j\Delta t}^0)_{j=1,\dots,J}$ with the first principal component

$$\partial_{x_0} S^{adj}(\Theta_{0,i}^{\mathbb{Q}}; t, 0, 0) = c_1^i, \quad (4.23)$$

$$\Delta x_{j\Delta t}^0 = F_{j\Delta t}^1 \quad \text{for } j = 1, \dots, J. \quad (4.24)$$

Step 2: Maximum likelihood estimation of $\Theta_0^{\mathbb{P}}$

Assume that x_0^0 is given. From (4.24), we obtain the observations of $(x_{j\Delta t}^0)_{j=1,\dots,J}$. Recall that (X_t^0) follows (4.6) under \mathbb{P} . By time discretization, we have (4.17). For a time step where there is no jump, i.e. $\Delta J_j^0 = 0$, $X_{(j+1)\Delta t}^0$ is normally distributed given the value of $X_{j\Delta t}^0$. If there is a jump, $X_{(j+1)\Delta t}^0$ is equal to the sum of a normal and an exponential random variable given the value of $X_{j\Delta t}^0$. Therefore, the density of $X_{(j+1)\Delta t}^0$ given $X_{j\Delta t}^0 = x_j$ is equal to

$$\begin{aligned} f(x_{j+1} | \Theta_0^{\mathbb{P}}, x_j) &= (1 - \ell^{0,\mathbb{P}} \Delta t) \frac{1}{\sigma^0 \sqrt{x_j \Delta t}} \phi \left(\frac{x_{j+1} - x_j - (\kappa_0^0 + \kappa_1^{0,\mathbb{P}} x_j) \Delta t}{\sigma^0 \sqrt{x_j \Delta t}} \right) \\ &\quad + \frac{\ell^{0,\mathbb{P}} \Delta t}{\mu^{0,\mathbb{P}}} \exp \left(\frac{x_j + (\kappa_0^0 + \kappa_1^{0,\mathbb{P}} x_j) \Delta t}{\mu^{0,\mathbb{P}}} + \frac{x_j \Delta t (\sigma^0)^2}{2(\mu^{0,\mathbb{P}})^2} - \frac{x_{j+1}}{\mu^{0,\mathbb{P}}} \right) \\ &\quad \times \Phi \left(\frac{x_{j+1} - x_j - (\kappa_0^0 + \kappa_1^{0,\mathbb{P}} x_j) \Delta t - x_j \Delta t (\sigma^0)^2 / \mu^{0,\mathbb{P}}}{\sqrt{x_j \Delta t} \sigma^0} \right) \end{aligned} \quad (4.25)$$

where $\phi(\cdot)$ and $\Phi(\cdot)$ are the density and cumulative distribution function of standard normal distribution respectively. Using this density function, we obtain estimators for x_0^0 and $\Theta_0^{\mathbb{P}}$ by maximizing the log-likelihood function:

$$\max_{\Theta_0^{\mathbb{P}}} \mathcal{L}^0(x_0^0, \Theta_0^{\mathbb{P}})$$

where

$$\mathcal{L}^0(x_0^0, \Theta_0^{\mathbb{P}}) = \sum_{j=1}^J \ln f(x_{j\Delta t}^0 | \Theta_0^{\mathbb{P}}, x_{(j-1)\Delta t}^0)$$

is the log-likelihood function.

Step 3: Maximum likelihood estimation of $\Theta_i^{\mathbb{P}}$ and $\Theta_i^{\mathbb{Q}}$

Consider the time series $(s_{j\Delta t}^i)_{j=0,\dots,J}$ of CDS spreads for obligor i . From Steps 1 and 2, we obtain a time series of risk factor values $(x_{j\Delta t}^0)_{j=0,\dots,J}$ and a parameter estimate $\widehat{\Theta}_0^{\mathbb{P}}$. Assume that we also know the parameters $(\kappa_1^{0,\mathbb{Q}}, \ell^{0,\mathbb{Q}}, \mu^{0,\mathbb{Q}})$. Then we estimate $(\Theta_i^{\mathbb{P}}, \Theta_i^{\mathbb{Q}})$ as follows.

As in Step 2, we discretize the process (X_t^i) under \mathbb{P} and compute the transition density (4.25) for $(X_{j\Delta t}^i)$. From (4.18), we can write the log-likelihood function as for $(x_{j\Delta t}^0)$ in Step 2. In addition, we account for the constraint (4.23) by adding a penalty term in the likelihood function:

$$\begin{aligned} \mathcal{L}^i(\Theta_i^{\mathbb{P}}, \Theta_i^{\mathbb{Q}}, \widehat{\Theta}_0^{\mathbb{P}}, \kappa_1^{0,\mathbb{Q}}, \ell^{0,\mathbb{Q}}, \mu^{0,\mathbb{Q}}, w) &= \sum_{j=1}^J \ln f(x_{j\Delta t}^i | \Theta_i^{\mathbb{P}}, \widehat{\Theta}_0^{\mathbb{P}}, \Theta_{0,i}^{\mathbb{Q}}, x_{(j-1)\Delta t}^i, x_{(j-1)\Delta t}^0) \\ &\quad - \ln \partial_{x^i} S^{ajd}(\Theta_{0,i}^{\mathbb{Q}}; t, 0, 0) \\ &\quad - w |1 - \partial_{x^0} S^{ajd}(\Theta_{0,i}^{\mathbb{Q}}; t, 0, 0) / c_1^i| \end{aligned} \quad (4.26)$$

where $f(\cdot|\cdot)$ is the transition density (4.25), w is the weight on the penalty with respect to (4.23) which will be set to 10^5 and

$$x_t^i = \left(s_t^i - S^{ajd}(\Theta_{0,i}^{\mathbb{Q}}; t, 0, 0) - \partial_{x^0} S^{ajd}(\Theta_{0,i}^{\mathbb{Q}}; t, 0, 0) x_t^0 \right) / \partial_{x^i} S^{ajd}(\Theta_{0,i}^{\mathbb{Q}}; t, 0, 0).$$

Then, we obtain the estimates for $(\Theta_i^{\mathbb{P}}, \Theta_i^{\mathbb{Q}})$ by solving

$$\max_{\Theta_i^{\mathbb{P}}, \Theta_i^{\mathbb{Q}}} \mathcal{L}^i(\Theta_i^{\mathbb{P}}, \Theta_i^{\mathbb{Q}}, \widehat{\Theta}_0^{\mathbb{P}}, \kappa_1^{0,\mathbb{Q}}, \ell^{0,\mathbb{Q}}, \mu^{0,\mathbb{Q}}, w).$$

We repeat this estimation for each obligor and obtain parameter estimates $(\widehat{\Theta}_i^{\mathbb{P}}, \widehat{\Theta}_i^{\mathbb{Q}})$ for $i = 1, \dots, n$.

Step 4: Maximum likelihood estimation of $(\kappa_1^{0,\mathbb{Q}}, \ell^{0,\mathbb{Q}}, \mu^{0,\mathbb{Q}})$

After obtaining $\widehat{\Theta}_0^{\mathbb{P}}$ and $(\widehat{\Theta}_i^{\mathbb{P}}, \widehat{\Theta}_i^{\mathbb{Q}})$ for $i = 1, \dots, n$, we estimate the remaining parameters $(\kappa_1^{0,\mathbb{Q}}, \ell^{0,\mathbb{Q}}, \mu^{0,\mathbb{Q}})$ which govern the \mathbb{Q} -dynamic of (X_t^0) by maximizing the likelihood function

$$\max_{\kappa_1^{0,\mathbb{Q}}, \ell^{0,\mathbb{Q}}, \mu^{0,\mathbb{Q}}} \sum_{i=1}^n \mathcal{L}^i(\widehat{\Theta}_i^{\mathbb{P}}, \widehat{\Theta}_i^{\mathbb{Q}}, \widehat{\Theta}_0^{\mathbb{P}}, \kappa_1^{0,\mathbb{Q}}, \ell^{0,\mathbb{Q}}, \mu^{0,\mathbb{Q}}, 0)$$

where $\mathcal{L}^i(\cdot)$ is the log-likelihood function (4.26). We set the penalty weight $w = 0$ to allow larger degree of freedom for the optimal solution.

Step 5: Iteration

In the final step, we iterate Step 3-4 until the solution converges. We find that it usually takes two to three iterations for convergence of the parameters within errors of 10^{-6} .

Bibliography

- [1] AIG and credit default swaps. Technical report, ISDA, November 2009.
- [2] Carol Alexander and Andreas Kaeck. Regime dependent determinants of credit default swap spreads. *Journal of Banking & Finance*, 32(6):1008–1021, 2008.
- [3] Thomas Almer, Thomas Heidorn, and Christian Schmaltz. The dynamics of short- and long-term CDS spreads of banks. Frankfurt School Working Paper Series 95, Frankfurt School of Finance & Management, 2008.
- [4] Ronald Anderson. What accounts for time variation in the price of default risk? Working paper, London School of Economics, 2008.
- [5] Matthias Arnsdorf and Igor Halperin. BSLP: Markovian bivariate spread-loss model for portfolio credit derivatives. *J. Comput. Finance*, 12(2):77–107, 2008.
- [6] Shahriar Azizpour, Kay Giesecke, and Baeho Kim. Premia for correlated default risk. Working paper, Stanford University, 2010.
- [7] Jeremy Berkowitz, Peter Christoffersen, and Denis Pelletier. Evaluating value-at-risk models with desk-level data. Manuscript, North Carolina State University, 2007.
- [8] Tomasz Bielecki, Stéphane Crépey, and Monique Jeanblanc. Up and down credit risk. *Quantitative Finance*, 10:1137–1151, 2010.
- [9] Tomasz Bielecki, Monique Jeanblanc, and Marek Rutkowski. Pricing and trading credit default swaps in a hazard process model. *Annals of Applied Probability*, 18(6):2495–2529, 2008.
- [10] Tomasz Bielecki, Monique Jeanblanc, and Marek Rutkowski. Hedging of credit default swaps in the CIR default intensity model. *Finance and Stochastics*, 2010.
- [11] Roberto Blanco, Simon Brennan, and Ian Marsh. An empirical analysis of the dynamic relation between investment-grade bonds and credit default swaps. *The Journal of Finance*, 60(5):2255–2281, 2005.
- [12] Paul T. Boggs, Paul D. Domich, and Janet E. Rogers. An interior point method for general large-scale quadratic programming problems. *Ann. Oper. Res.*, 62:419–437, 1996. Interior point methods in mathematical programming.

- [13] Tim Bollerslev, Ray Chou, and Kenneth Kroner. ARCH modeling in finance. *Journal of Econometrics*, 52(1-2):5–59, 1992.
- [14] Pierre Brémaud. *Point Processes and Queues*. Springer-Verlag, New York, 1981.
- [15] Damiano Brigo and Massimo Morini. Arbitrage-free pricing of credit index options. The no-armageddon-pricing measure and the role of correlation after the subprime crisis. Working paper, SSRN, 2008.
- [16] Damiano Brigo, Andrea Pallavicini, and Roberto Torresetti. Calibration of CDO tranches with the dynamical Generalized-Poisson loss model. *Risk*, May 2007.
- [17] Jessica Cariboni and Wim Schoutens. Jumps in intensity models: investigating the performance of Ornstein-Uhlenbeck processes in credit risk modeling. *Metrika*, 69:173–198, 2009.
- [18] Stephen Cecchetti, Jacob Gyntelberg, and Marc Hollanders. Central counterparties for over-the-counter derivatives. Quarterly review, BIS, September 2009.
- [19] Stuart Coles, Janet Heffernan, and Jonathan Tawn. Dependence measures for extreme value analyses. *Extremes*, 2(4):339–365, 1999.
- [20] Pierre Collin-Dufresne. A short introduction to correlation markets. *Journal of Financial Econometrics*, 7(1):12–29, 2009.
- [21] Pierre Collin-Dufresne, Robert Goldstein, and Spencer Martin. The determinants of credit spread changes. *Journal of Finance*, 56(6):2177–2207, 2001.
- [22] Rama Cont. Empirical properties of asset returns: stylized facts and statistical issues. *Quantitative Finance*, 1(2):223–236, 2001.
- [23] Rama Cont. Model uncertainty and its impact on the pricing of derivative instruments. *Math. Finance*, 16(3):519–547, 2006.
- [24] Rama Cont. Credit default swaps and financial stability. *Financial Stability Review*, 14:35–43, July 2010. Banque de France.
- [25] Rama Cont, Romain Deguest, and Yu Hang Kan. Default intensities implied by CDO spreads: inversion formula and model calibration. *SIAM J. Financial Math.*, 1:555–585, 2010.
- [26] Rama Cont and Yu Hang Kan. Dynamic hedging of portfolio credit derivatives. *SIAM J. Financial Math.*, 2:112–140, 2011.
- [27] Rama Cont and Yu Hang Kan. Statistical modeling of credit default swap portfolios. Working paper, Columbia University, 2011.
- [28] Rama Cont and Andreea Minca. Recovering portfolio default intensities implied by CDO tranches. *Mathematical Finance*, 2011. Forthcoming.
- [29] Rama Cont and Amal Moussa. Too interconnected to fail: contagion and systemic risk in financial networks. Working paper, Columbia University, 2010.

- [30] Rama Cont, Edson Bastos Santos, and Amal Moussa. Network structure and systemic risk in banking systems. Working paper, Columbia University, 2010.
- [31] Rama Cont and Ioana Savescu. Forward equations for portfolio credit derivatives. In R. Cont, editor, *Frontiers in Quantitative Finance: Credit Risk and Volatility Modeling*, chapter 11, pages 269–288. Wiley, 2008.
- [32] Rama Cont and Peter Tankov. Non-parametric calibration of jump-diffusion option pricing models. *Journal of Computational Finance*, 7(3):1–49, 2004.
- [33] Rama Cont, Peter Tankov, and Ekaterina Voltchkova. Hedging with options in presence of jumps. In F.E. Benth, G. Di Nunno, T. Lindstrom, B. Oksendal, and T. Zhang, editors, *Stochastic Analysis and Applications: the Abel Symposium 2005 in Honor of Kiyosi Ito*, pages 197–218. Springer, 2007.
- [34] Stéphane Crépey, Monique Jeanblanc, and Behnaz Zargari. Counterparty risk on a CDS in a model with joint defaults and stochastic spreads. Working paper, Université d’Evry Val d’Essonne, 2010.
- [35] Sanjiv Das, Darrell Duffie, Nikunj Kapadia, and Leandro Saita. Common failings: How corporate defaults are correlated. *The Journal of Finance*, 62(1):93–117, 2007.
- [36] Richard Davis and Thomas Mikosch. The extremogram: a correlogram for extreme events. *Bernoulli*, 15(4):977–1009, 2009.
- [37] Richard Davis, Thomas Mikosch, and Ivor Cribben. Towards estimating extremal serial dependence via the bootstrapped extremogram. Working paper, Columbia University, 2011.
- [38] Richard A. Davis and Thomas Mikosch. Extreme value theory for garch processes. In Thomas Mikosch, Jens-Peter Krei, Richard A. Davis, and Torben Gustav Andersen, editors, *Handbook of Financial Time Series*, pages 187–200. Springer Berlin Heidelberg, 2009.
- [39] Emanuel Derman. Markets and models. *Risk*, 14(7):48–50, 2001.
- [40] David A. Dickey and Wayne A. Fuller. Distribution of the estimators for autoregressive time series with a unit root. *J. Amer. Statist. Assoc.*, 74(366, part 1):427–431, 1979.
- [41] Darrell Duffie and Nicolae Gârleanu. Risk and valuation of collateralized debt obligations. *Financial Analysts Journal*, 57(1):41–59, 2001.
- [42] Darrell Duffie and Haoxiang Zhu. When does a central clearing counterparty reduce counterparty risk. Working paper, Stanford University, 2010.
- [43] Bruno Dupire. Pricing with a smile. *Risk*, 7(1):18–20, 1994.
- [44] Philippe Durand and Jean-Frédéric Jouanin. Some short elements on hedging credit derivatives. *ESAIM Probability and Statistics*, 11:23–34, 2007.
- [45] Andreas Eckner. Computational techniques for basic affine models of portfolio credit risk. *J. Comput. Finance*, 13(1):63–97, 2009.

- [46] Bradley Efron and Robert J. Tibshirani. *An Introduction to the Bootstrap*, volume 57 of *Monographs on Statistics and Applied Probability*. Chapman and Hall, New York, 1993.
- [47] Robert Engle. *ARCH: Selected Readings*. Oxford University Press, USA, 1995.
- [48] Eymen Errais, Kay Giesecke, and Lisa R. Goldberg. Affine point processes and portfolio credit risk. *SIAM J. Financial Math.*, 1:642–665, 2010.
- [49] Peter Feldhütter. An empirical investigation of an intensity-based model for pricing CDO tranches. Working paper, Copenhagen Business School, 2008.
- [50] Hans Föllmer and Dieter Sondermann. Hedging of nonredundant contingent claims. In *Contributions to Mathematical Economics*, pages 205–223. North-Holland, Amsterdam, 1986.
- [51] Rüdiger Frey and Jochen Backhaus. Dynamic hedging of synthetic CDO tranches with spread risk and default contagion. *J. Econom. Dynam. Control*, 34(4):710–724, 2010.
- [52] Raquel M. Gaspar and Thorsten Schmidt. CDOs in the light of the current crisis. In M. Jeanblanc and Ch. Gourieroux, editors, *Financial Risks: New Developments in Structured Products and Credit Derivatives*, chapter 4, pages 33–48. Economica, 2009.
- [53] Kay Giesecke, Lisa Goldberg, and Xiaowei Ding. A top-down approach to multi-name credit. *Operations Research*, Forthcoming, 2011.
- [54] Kay Giesecke and Baeho Kim. Estimating tranche spreads by loss process simulation. *Proceedings of the 2007 Winter Simulation Conference*, 2007.
- [55] Kay Giesecke and Jack Kim. Fixed-income portfolio selection. Working paper, Stanford University, 2009.
- [56] Lawrence Glosten, Ravi Jagannathan, and David Runkle. On the relation between the expected value and the volatility of the nominal excess return on stocks. *Journal of Finance*, 48(5):1779–1801, 1993.
- [57] Charles M. Goldie and Richard L. Smith. Slow variation with remainder: theory and applications. *Quart. J. Math. Oxford Ser. (2)*, 38(149):45–71, 1987.
- [58] Xin Guo, Robert Jarrow, and Haizhi Lin. Distressed debt prices and recovery rate estimation. *Review of Derivatives Research*, 11(3):171–204, 2008.
- [59] James D. Hamilton. *Time Series Analysis*. Princeton University Press, Princeton, NJ, 1994.
- [60] Alexander Herbertsson. Pricing synthetic CDO tranches in a model with default contagion: the matrix-analytic approach. *Journal of Credit Risk*, 4(4):3–35, 2008.
- [61] Bruce M. Hill. A simple general approach to inference about the tail of a distribution. *Ann. Statist.*, 3(5):1163–1174, 1975.
- [62] Eric Jondeau, Ser-Huang Poon, and Michael Rockinger. *Financial Modeling Under Non-Gaussian Distributions*. Springer Finance. Springer-Verlag London Ltd., London, 2007.

- [63] Yu Hang Kan and Claus Pedersen. The impact of margin interest on the valuation of credit default swaps. Working paper, Columbia University, 2011.
- [64] Claudia Klüppelberg and Gabriel Kuhn. Copula structure analysis. *Journal of the Royal Statistical Society: Series B (Statistical Methodology)*, 71(3):737–753, 2009.
- [65] Paul Kupiec. Techniques for verifying the accuracy of risk measurement models. *The Journal of Derivatives*, 3(2):73–84, 1995.
- [66] Denis Kwiatkowski, Peter Phillips, Peter Schmidt, and Yongcheol Shin. Testing the null hypothesis of stationarity against the alternative of a unit root: How sure are we that economic time series has a unit root? *Journal of Econometrics*, 54:159–178, 1992.
- [67] David Lando. On Cox processes and credit risky securities. *Review of Derivatives Research*, 2(2):99–120, 1998.
- [68] David Lando. *Credit Risk Modeling: Theory and Applications*. Princeton, 2004.
- [69] David Lando and Mads Stenbo Nielsen. Correlation in corporate defaults: Contagion or conditional independence? *Journal of Financial Intermediation*, 19(3):355–372, 2010.
- [70] Jean-Paul Laurent and Areski Cousin. An overview of factor modeling for CDO pricing. In R. Cont, editor, *Frontiers in Quantitative Finance: Credit Risk and Volatility Modeling*, chapter 10, pages 185–212. Wiley, 2008.
- [71] Jean-Paul Laurent, Areski Cousin, and Jean-David Fermanian. Hedging default risks of CDOs in Markovian contagion models. Working paper, April 2008.
- [72] Anthony W. Ledford and Jonathan A. Tawn. Modelling dependence within joint tail regions. *J. Roy. Statist. Soc. Ser. B*, 59(2):475–499, 1997.
- [73] Anthony W. Ledford and Jonathan A. Tawn. Concomitant tail behaviour for extremes. *Adv. in Appl. Probab.*, 30(1):197–215, 1998.
- [74] David X. Li. On default correlation: a copula function approach. *Journal of Fixed Income*, 9(4):43–54, 2000.
- [75] David X. Li. Base correlation. In Rama Cont, editor, *Encyclopedia of Quantitative Finance*. Wiley, 2010.
- [76] Alexander Lipton and Andrew Rennie, editors. *The Oxford Handbook of Credit Derivatives*. Oxford University Press, 2011.
- [77] Andrei V. Lopatin and Timur Misirpashaev. Two-dimensional Markovian model for dynamics of aggregate credit loss. In *Econometrics and Risk Management*, volume 22 of *Adv. Econom.*, pages 243–274. Emerald/JAI, Bingley, 2008.
- [78] Benoit Mandelbrot. The variation of certain speculative prices. *Journal of Business*, 36(4):392–417, 1963.

- [79] Alexander J. McNeil, Rüdiger Frey, and Paul Embrechts. *Quantitative Risk Management*. Princeton Series in Finance. Princeton University Press, Princeton, NJ, 2005. Concepts, techniques and tools.
- [80] Robert C. Merton. On the pricing of corporate debt: The risk structure of interest rates. *Journal of Finance*, 29(2):449–470, 1974.
- [81] Thomas Mikosch and Cătălin Stărică. Limit theory for the sample autocorrelations and extremes of a GARCH (1,1) process. *Ann. Statist.*, 28(5):1427–1451, 2000.
- [82] Sam Morgan and Allan Mortensen. CDO hedging anomalies in the base correlation approach. Technical report, Lehman Brothers, 2007.
- [83] Allan Mortensen. Semi-analytical valuation of basket credit derivatives in intensity-based models. *The Journal of Derivatives*, 13(4):8–26, 2006.
- [84] Thomas Møller. Risk-minimizing hedging strategies for insurance payment process. *Finance and Stochastics*, 5:419–446, 2001.
- [85] Matthias Neugebauer, Jeremy Carter, Richard Hrvatin, Tania Cunningham, and Rachel Hardee. Understanding and hedging risks in synthetic CDO tranches. Technical report, Fitch Ratings, August 2006.
- [86] Whitney K. Newey and Douglas G. Steigerwald. Asymptotic bias for quasi-maximum-likelihood estimators in conditional heteroskedasticity models. *Econometrica*, 65(3):587–599, 1997.
- [87] Peter Phillips and Pierre Perron. Time series regression with a unit root. *Biometrika*, 75:335–346, 1988.
- [88] Dima Rahman. Are banking systems increasingly fragile? Investigating financial institutions' CDS returns extreme co-movements. EconomiX Working Paper 2009-34, University of Paris West - Nanterre la Défense, 2009.
- [89] Sidney I. Resnick. *Heavy-tail Phenomena*. Springer Series in Operations Research and Financial Engineering. Springer, New York, 2007.
- [90] Peter Rousseeuw and Geert Molenberghs. Transformation of non-positive semidefinite correlation matrices. *Communications in Statistics - Theory and Methods*, 22(4):965–984, 1993.
- [91] Leandro Saita. A simple risk margin model for credit portfolios. Quarterly report, Barclays Capital, Q2 2010.
- [92] Philipp Schönbucher. *Credit Derivatives Pricing Models*. Wiley, 2003.
- [93] Philipp Schönbucher. Portfolio losses and the term structure of loss transition rates: a new methodology for the pricing of portfolio credit derivatives. Working paper, Department of Mathematics, ETH Zurich, 2005.

- [94] René Stulz. Credit default swaps and the credit crisis. *Journal of Economic Perspectives*, 24(1):73–92, 2010.
- [95] Robert J. Vanderbei. LOQO: an interior point code for quadratic programming. *Optim. Methods Softw.*, 11/12(1-4):451–484, 1999. Interior point methods.
- [96] Halbert White. A heteroskedasticity-consistent covariance matrix estimator and a direct test for heteroskedasticity. *Econometrica*, 48(4):817–838, 1980.